Purification of Recombinant Vaccinia Virus for Oncolytic and Immunotherapeutic Applications using Monolithic Column Technology

A thesis submitted to University College London
for the degree of Doctor of Engineering

by

David Isaac William Vincent

The Advanced Centre for Biochemical Engineering
Department of Biochemical Engineering
University College London
Gordon Street
London WC1H 0AH

I, David Vincent confirm that the work presented in this thesis is my own. Where information has been derived from other sources, I confirm that this has been indicated in the thesis.

Signed……Date……

Acknowledgements

I would like to thank my supervisor Dr Yuhong Zhou for her invaluable feedback and support over the course of this EngD. Without her continuous encouragement this work would likely never have been completed.

I would also like to thank my Advisor Prof. Ajoy Velayudhan for his help and guidance. Many a long discussion was had on the intricacies of vaccinia viral purification which were thought provoking, inspirational but also really good fun.

I would also like to express my gratitude to the staff and students at UCL. There are too many to mention everyone, but in particular I would like to thank Mrs Ludmila Ruban, Miss Dhushy Stanislaus and Dr Tarit Mukhopadhyay for their support, especially in setting up the vaccine lab in the department which I could benefit from in my final year. I would also like to thank Dr Patricia Perez Esteban for her support, friendship and bioprocess wisdom.

I would like to express my gratitude to BIA Separations and the EPSRC for sponsoring this work. Without this financial support this work would not have been possible. At BIA Separations I would especially like to thank Dr Aleš Štrancer, Dr Petra Kramberger, and Dr Rosana Hudej for their guidance and technical expertise.

At lot of this work was unexpectedly performed at Barts Cancer Institute, Queen Mary University of London. I would like to express my gratitude to the institute for being so accommodating, and especially like to thank Prof Yaohe Wang, Dr Ming Yuan, Dr Rathi Gangeswaren, Dr Chadwan Al-Yaghchi and Dr Jahangir Ahmed for their encouragement, assistance, and friendship.

Finally I would like to thank my family for sticking by me during the last 4+ years. I want to particularly thank my amazing wife Ruxandra for her love, support and guidance in all aspects of my life and work. During this work, my beautiful son was born, Joseph John Maurice Comisel-Vincent. Welcome to the world, I hope you find Daddy's work interesting and useful.

Also Angela you owe me £5.

Abstract

Vaccinia virus Lister strain, a large, structurally complex double stranded DNA pox virus, is being developed by a number of organisations around the world as an oncolytic and immunotherapeutic agent for the treatment of a broad range of cancers. Should these therapies prove to be efficacious in the clinic, large quantities of vaccinia virus will need to be produced at very high levels of purity as dosing requirements are expected to be as high as approximately $1x10^9$ pfu/dose.

In this thesis, the development of two convective interaction media (CIM) monolith capture steps for vaccinia virus with considerable purification factors is described; one uses cation exchange while the other uses hydrophobic interaction chromatography. The purification process development involved an extensive material characterisation study resulting in enhanced product understanding, a rapid resin screening study aimed at quickly identifying suitable resin chemistries, followed by process optimisation studies on the best performing monoliths.

After being challenged with crude infectious vaccinia harvest, CIM OH monoliths are shown to be able to recover up to 90% of the infectious virus loaded whilst removing up to 99% of the contaminating DNA (without nuclease treatment) and 100% of quantifiable protein. Binding capacities were shown to be in the order of $1x10^9$ pfu/mL. The high levels of both batch to batch and assay variability as well as the tendency of vaccinia virus to aggregate in the feed material, typical of viral processes especially when developed alongside un-optimised upstream conditions, are clearly demonstrated and the implications are explored. The results show that it can be challenging to draw robust conclusions on process performance. To minimise the effects of analytical

variability, a number of orthogonal analytical methods have been used to quantify and characterise viral particles. These include $TCID_{50}$, nanoparticle tracking analysis (NTA), tunable resistive pulse sensing (TRPS), transmission electron microscopy (TEM), scanning electron microscopy (SEM), and real-time PCR (qPCR). In order to put this into an industrial context, a comparative cost of goods analysis of monoliths and ultracentrifugation technologies for the purification of large viral particles is provided. This shows that both chromatography using monoliths and continuous flow ultracentrifugation can be economically viable, although both have limitations. The potential economic benefits of using a monolith-based process over an ultracentrifugation-based process are increased productivity, the ability to generate purer material and ease of scale-up.

CIM monoliths are unique stationary phases that offer efficient separation and high productivity owing to fast cycle times and high binding capacities. Both cation exchange (CIM SO3) and hydrophobic interaction (CIM OH) monoliths are effectual at removing the majority of contaminants in a single purification step that can easily be scaled up to 8 L bed volumes. CIM monoliths have the potential to be an attractive option for future manufacturing processes for oncolytic viral therapies. They are shown in this thesis to achieve a higher percentage recovery and better removal of DNA, protein and aggregate than any other technology described in the literature to date.

Impact Statement

The gene and immunotherapy field has picked up a lot in the last few years after some initial setbacks in the clinic. A number of *in vivo* and *ex vivo* viral constructs have recently entered clinical trials (Heo et al. 2013).

Vaccinia virus has shown promising efficacy in both animal models and late stage cancer patients for both solid tumours and models for metastasis (Garber 2006;Kirn and Thorne 2009;Tysome et al. 2009;Tysome et al. 2011). While challenges associated with oncolytic viral therapies do exist (Ferguson et al. 2012), there is a chance that vaccinia virus will need to be produced for direct injection into patients at a commercial scale. The scale of this production will of course depend on the efficacy of the trial, the indication, and the dose required. Clinical trials currently suggest that the total treatment dose requirement will need to be relatively high in order to achieve efficacy. It has been suggested that multiple treatments may be required each consisting of $1x10^9$ pfu per patient (Heo, Reid, Ruo, Breitbach, Rose, Bloomston, Cho, Lim, Chung, Kim, Burke, Lencioni, Hickman, Moon, Lee, Kim, Daneshmand, Dubois, Longpre, Ngo, Rooney, Bell, Rhee, Patt, Hwang, & Kirn 2013). This will not only increase the costs of production but may also result in the requirement for purer material as increasing the amount of viral particles per dose will also increase the amount of impurities per dose, which even at lower doses is already recognised as an issue (Wolff and Reichl 2011). It is clear that without effective, engineering led, process development and optimisation, production costs can become crippling, especially as vaccinia processes to date tend to be low yielding with cell productivity less than 100 pfu/cell (Liu et al. 2016).

The impact of this work inside academia will likely be twofold. Firstly, it will advance the levels of process knowledge and understanding of how vaccinia virus Lister strain interacts with charged and hydrophobic monolithic stationary phases. It will also enable

laboratories currently working with vaccinia virus Lister strain to produce material of a higher quality, in terms of purity, than previously possible in a single step. This will be especially relevant for groups currently relying on sucrose gradient ultracentrifugation or similar techniques. The wider medical community will indirectly benefit from this as the material supplied for pre-clinical and proof of concept studies will be more representative of that produced in late stage clinical and commercial processes.

From an industrial perspective, the impact of this work, at least in the short term, will be the addition of another purification tool in the vaccinia virus purification development toolbox. The reason why this is important is that vaccinia is a challenging virus to purify due to its large size and complexity, and therefore the number of purification options available is limited. The default unit operation used to purify vaccinia and other viruses is still ultracentrifugation. This work will add to the growing debate on whether this technology is still of value. It adds insight into the associated cost of goods for both technologies, suggests potential mechanisms involved in the separation of vaccinia using CIM monoliths, and presents encouraging results indicating the production of highly pure vaccinia virus material using chromatography.

Table of Contents

Table of Figures

Table of Tables

Abbreviations

RSD	Relative Standard Deviation
3D	Three Dimensional
Ad3	Adenovirus 3
AIEX	Anion Exchange Chromatography
BCA	Bicinchoninic Acid Assay
BCI	Bart Cancer Institute
BV	Baculovirus
CEV	Cell Associated Enveloped Virus
CIEX	Cation Exchange Chromatography
CIM	Convective Interaction Media
CMV	Cytomegalovirus
CO_2	Carbon Dioxide
CoGs	Cost of Goods
CPE	Cytopathic Effect
CV	Column Volume
DBC	Dynamic Binding Capacity
DEAE	Diethylaminoethanol
DLS	Dynamic Light Scattering
DMEM	Dulbecco's Modified Eagle's Medium
DNA	Deoxyribonucleic Acid
DoE	Design of Experiment
DSP	Downstream Processing
EDTA	Ethylenediaminetetraacetic Acid
EEV	Extracellular Enveloped Virus
EGFR	Epidermal Growth Factor Receptor
ELISA	Enzyme–Linked Immunosorbent Assay
EngD	Engineering Doctorate

FDA	Food and Drug Administration
fg	Femtogram
GE	General Electric
GFP	Green Fluorescence Protein
GM-CSF	Granulocyte-Macrophage Colony –Stimulating Factor
HETP	Height Equivalent to a Theoretical Plate
H5	Vaccinia Virus Promoter
HCP	Host Cell Protein
HETP	Height Equivalence to a Theoretical Plate
HIC	Hydrophobic Interaction Chromatography
HNSCC	Head and Neck Squamous Cell Carcinoma
HPLC	High Performance Liquid Chromatography
HRP	Horse Radish Peroxidase
ID	Internal Diameter
IEV	Intracellular Enveloped Virus
IFN	Interferon
IMV	Intracellular Mature Virus
kDa	Kilodalton
LLOQ	Lower Limit of Quantification
LMH	Litres per Meters Squared per Hour
M	Molar
MA	Membrane Adsorbers
mAb	Monoclonal Antibody
mg	Milligram
mM	Millimolar
MOA	Mechanism of Action
MOI	Multiplicity of Infection
MVA	Modified Vaccinia Ankara
NaCl	Sodium Chloride
NaOH	Sodium Hydroxide

$(NH_4)_2SO_4$	Ammonium Sulfate
NTA	Nanoparticle Tracking Analysis
NYCBOH	New York City Board of Health
NYVAC	Highly Attenuated Strain of Vaccinia Virus
pDNA	Plasmid Deoxyribonucleic Acid
pH	Power of Hydrogen
PVY	Potato Virus Y
QA	Quality Assurance
QC	Quality Control
QMUL	Queen Mary University of London
qPCR	Real-Time Polymerase Chain Reaction
R&D	Research and Development
RMSE	Root-Mean-Square-Error
RNA	Ribonucleic Acid
RPLC	Reverse Phase Liquid Chromatography
RT-PCR	Reverse Transcription Polymerase Chain Reaction
SC	Sulfated Cellulose
SDS-PAGE	Sodium Dodecyl Sulfate Polyacrylamide Gel Electrophoresis
SEC	Size Exclusion Chromatography
SEM	Scanning Electron Microscopy
TBE	Tris Borate EDTA
$TCID_{50}$	Tissue Culture Infectious Dose 50%
TEM	Transmission Electron Microscopy
TFF	Tangential Flow Filtration
ToMV	Tomato Mosaic Virus
TRPS	Tunable Resistive Pulse Sensing
UCL	University College London
UFDF	Ultra Filtration Diafiltration
UPLC	Ultra Performance Liquid Chromatography
USP	Upstream Processing

VACV	Vaccinia Virus
VGF	Vaccinia Growth Factor
VLP	Virus Like Particle
VVL15TK$^-$	Vaccinia Virus Lister Strain 15 Thymidine Kinase Deleted
WHO	World Health Organisation
WT	Wild Type

Table of Notations

a	Area available for mass transfer (m^2)
A	Eddy diffusion (m)
B	Longitudinal diffusion ($m^2\ s^{-1}$)
C	Resistance to mass transfer (s)
C	Concentration ($kg\ m^{-3}$)
C_{Ao}	Concentration of component A at boundary layer ($kg\ m^{-3}$)
C_{Ai}	Concentration of component A at interphase ($kg\ m^{-3}$)
D	Diffusion coefficient (-)
d_H	Hydrodynamic diameter of a particle (m)
D_L	Axial dispersion Coefficient ($m^2\ s^{-1}$)
D_p	Particle diffusivity ($m^2\ s^{-1}$)
J	Flux ($kg\ m^2\ s^{-1}$)
k	Mass transfer coefficient ($m\ s^{-1}$)
k'	Relative retention factor
K_d	Dissociation constant ($m^3\ kg^{-1}$)
k_f	Film mass transfer coefficient ($m\ s^{-1}$)
Na	Mass transfer rate ($kg\ s^{-1}$)
q	Concentration of solute bound to adsorbent ($kg\ m^{-3}$)
r_p	Particle radius (m)
SS	Sum of Squares
T	Temperature (K)
t	Time (s)
u	Velocity ($m\ s^{-1}$)
V	Volume (m^3)

ε_b	Bed porosity (-)
ε_p	Particle porosity (-)
μ	Viscosity (Pa s)

Chapter 1

Aims and Objectives of Study

The overall aim of this EngD project is to evaluate, understand, and work to reduce the current challenges faced by process scientists and engineers developing vaccinia virus constructs for vaccines and oncolytic therapies.

One such challenge is the scalability and productivity of presently used purification unit operations, arguably the most common being ultracentrifugation. It has been suggested that chromatography using monoliths could present an attractive alternative to ultracentrifugation namely owing to their high binding capacity, flow independent binding and resolution, and scalability stated by the manufacturers of commercially available monoliths.

The virus being used in this study is Barts Cancer Institute's back bone attenuated vaccinia viral construct containing a RFP reporter gene (VVL15TK^{-}RFP). The virus is currently being developed as an oncolytic virus against a range of cancers.

To start with, an extensive vaccinia virus stability study will be performed to determine whether there are certain conditions, such as variations in buffer salts, NaCl concentration or pH that might affect the stability (measured by infectivity) of the virus at room temperature over time.

Once this is ascertained, a process will be developed by screening different monolith chemistries for ability to bind and then elute the virus. As soon as a particular chemistry is found to reversibly bind the virus, a process of optimisation using both gradient elution and intelligent design of experiments (DoE) to develop stepwise elution schedules will be used. These strategies will help to determine windows of operation for

both binding, washing and eluting the column in order to maximise yield and purity of the final product.

The binding capacity of vaccinia virus onto CIM monoliths should be high. Previous work at BIA Separations used pure tomato mosaic viral preps (ToMV) with a known mass concentration to estimate the theoretical dynamic binding capacity of ToMV on CIM monoliths. The total particle concentration bound to the resin was estimated using the mass of a single viral particle (Matjaž Peterka et al. 2010). This was performed by running a DBC on a 0.34 mL monolith disk with a high concentration of pure virus material.

The theoretical binding capacity of vaccinia virus onto 6 µm channel monoliths has been estimated to be ~$1.15x10^{13}$ particles/mL of monolith. This is assuming the following (Mao et al. 2017).

- Surface area per gram of dry monolith (BET adsorption)= 2 m^2 (6 µm channel monoliths)
- Density is assumed to be 0.43 g/mL
- Vaccinia is 300x250 nm (total cross sectional area = $7.5x10^{-14}$ m^2
- The entire monolith surface area is available for adsorption and has been functionalised with either -OH or -SO_3 groups.
- Particles adsorb in ordered monolayers across the whole surface of the monolith

Analytical methods currently used for evaluating the total number of infectious virus particles has been described extensively in the literature as being an area requiring increased scrutiny and validation during process development (Darling et al. 1998). Current gold standards such as $TCID_{50}$ are time consuming, involve tedious preparation, and have been reported to give highly variable results (Stoffel et al. 2005). For this reason a combination of orthogonal analytical measurements including $TCID_{50}$,

nanoparticle tracking analysis (NTA), tunable resistive pulse sensing (TRPS), transmission electron microscopy (TEM), scanning electron microscopy (SEM), and real-time PCR (qPCR) will be used to characterise and quantify vaccinia virus particles. Bicinchoninic acid (BCA) assay will be used to quantify total protein and PicoGreen will be used to quantify double stranded DNA (dsDNA). Both total protein and DNA levels are identified as critical quality attributes (CQAs).

The final results chapter will consist of a process economics analysis that compares a defined monolith-based chromatography process and an ultracentrifugation process from an overall cost of goods perspective. The aim of this analysis is to further our understanding of where the major costs and process risks from each process option are likely to come from. Initial assumptions will need to be made but these will be tested in a sensitivity analysis and then discussed in detail. Once complete, the model will be able to be used for two potential purposes. The first one would be to assist in identifying drivers for process development in a chromatographic purification process scenario. The second purpose of this model would be to act as a decision tool to support later discussions with Barts Cancer Institute, who are developing vaccinia virus as an oncolytic therapy for a range of cancers, in order to manufacture some of their constructs for clinical development. An example of a question that this model aims to answer is "How well would a monolith process need to perform to ensure a cost benefit over an ultracentrifugation process?"

A section on process validation will be included that aims to show how the CQAs for vaccinia virus produced in a commercial setting for an oncolytic indication might be defined. The challenges associated with their characterisation from the point of view of safety and efficacy will be described and best practices discussed. The validation challenges involved in the production of monoliths will also be presented as it is

thought that these will be important considerations when validating a monolith chromatography step.

A number of challenges needed to be overcome over the course of this project. After conducting an internal risk assessment at UCL, Vaccinia virus was classified as requiring category 2 contwotainment. The department of Biochemical Engineering is organised into a number of labs and pilot facilities which are designed to be shared amongst all researchers and in some cases undergraduate and MSc students for the purposes of teaching. For this reason it was concluded that vaccinia virus would need to be handled in a specialist CAT II vaccine laboratory with dedicated equipment so as to reduce any risks of cross contamination. This was built and commissioned over the course of this project between 2012 and 2015, but it meant that a significant amount of work needed to be undertaken elsewhere. Some of the work was performed at BIA Separations in Slovenia. BIA Separations has access to chromatography equipment, however, didn't have the ability to perform non-plate based assays so analytical measurements such as Western blots, qPCR, and NTA could not be performed. Barts Cancer Institute did allow access to western blot facilities, however it was decided that this additional assay didn't add much clarity on how the system was performing as it is only semi-quantitative as well as fairly time consuming.

Virus analytics are generally accepted as being time consuming, and imprecise meaning that a bottleneck in terms of throughput as well as the ability to make conclusive decisions presented itself.

Time was spent establishing and partially optimising $TCID_{50}$, PicoGreen and BCA, as well as NTA, qPCR, TEM, and SEM as they became available towards the end of the project when labs at UCL became available.

Red florescence was used to confirm infectious titre (as a second read out during $TCID_{50}$ analysis).This also acted to increase the selectivity of the $TCID_{50}$ assay confirming the presence of vaccinia virus.

The aim of this project was to understand and work to reduce the challenges in vaccinia virus purification. A monoliths capture step was evaluated and shown to be a reasonable process option for manufacture at 100L scale.

Chapter 2

Introduction

2.1 Vaccinia Virus

2.1.1 Taxonomy, Classification, and Properties of Vaccinia Virus

The exact origin of vaccinia virus is not known. There are, however, a number of theories. One is that vaccinia virus was a form of orthopoxvirus that previously infected animals but is no longer endemic. Another suggestion is that it may have originated from horsepox virus as at least one strain of vaccinia virus (Ankara) was isolated from a horse (Antonio Alcami et al., 2010). Vaccinia is also said to be closely related to cowpox (Bourquain et al. 2013).

Vaccinia virus is a member of the *Poxviridae* family of viruses and is a large, complex, double stranded DNA-based poxvirus. The virus is described as "brick-shaped" with dimensions of approximately 300 x 250 nm (Michen and Graule 2010).

The *Poxviridae* family of viruses is split into two additional subclasses that infect vertebrates and insects; these are named *Chordopoxvirinae* and *Entomopoxvirinate* respectively. Vaccinia virus, which belongs to the subfamily *Chordopoxvirinae,* belongs to the genus *Orthopoxvirus* (Wittek 1994).

The mass of a typical vaccinia virus particle has been found experimentally by using microscale silicon cantilever resonators and atomic force microscopy to be of ~7.9 (+/-) 4.6 femtograms (fg) and ~12.4 (+/-) 1.3 fg (Johnson et al. 2006). This data was obtained from cantilevers of 6 µm x 4 µm and 21 µm x 9 µm respectively.

The isoelectric point (pI) of vaccinia virus Lister strain, which is likely to be an important consideration when developing adsorption-based processes, was found experimentally to range from 3.0, when using micro-electrophoesis with pure material, to 5.1, when using isoelectric focusing techniques with more crude material (Michen & Graule 2010). The pI of a protein is the pH in which the total net charge of the molecule is equal. This is documented as being determined by the superposition of the protonated and unprotonated functional groups. In the case of vaccinia, complexity is increased exponentially as there are multiple different proteins on the viral surface, each one with a different isoelectric point. As vaccinia virus is over an order of magnitude lager than a typical protein such as a monoclonal antibody (mAb) (~12nm), the location of charge densities on the viral surface will also have an effect on the adsorption characteristics of the virus, meaning that even if the overall net charge is negative at physiological pH a virus may still be able to adsorb to a cation exchange (CIEX) matrix.

2.1.2 Vaccinia Virus Life Cycle

The life cycle of vaccinia virus is complex, the mechanisms of which are of particular importance both clinically and from a process development perspective when developing oncolytic vectors.

Unusually for DNA-based virus, vaccinia replicates in the cytoplasm of a host cell, and once mature, is referred to as Intracellular Mature Virus (IMV). At this stage the virion is thought to be surrounded by a lipoprotein membrane (Townsley et al. 2005). As the IMV moves away from the viral factory, transported on microtubules, it is wrapped with a double membrane derived from the *trans*-Golgi apparatus and is given the name Intracellular Enveloped Virus (IEV). The IEV is then moved to the cell surface by

fusing with the cell membrane, becoming referred to as Cell Associated Enveloped Virus (CEV). This induces the formation of actin tails that act to propel the virus away from the cell surface. At this point the virus is known as Extracellular Enveloped Virus (EEV) (Smith et al. 2002).

The therapeutic benefits of the different viral forms are not well known. All viral forms are known to be infectious, but there is some speculation that vaccinia virions with a producer cell derived envelope (IEV,CEV, or EEV) might stimulate more of an innate immune response than IMV which in turn is thought to limit the number of infectious viral particles able to migrate to tumorigenic tissues (Ferguson, Lemoine, & Wang 2012).

2.1.3 Use of Vaccinia as a Smallpox Vaccine (1967-1980)

2.1.3.1 Background and History of Smallpox Vaccination

Edward Jenner is regarded worldwide as the initial promoter of vaccination after publishing his work entitled "An inquiry into the causes and effects of the variolae vaccinae" in 1798.

This work describes the use of cowpox, horsepox and attenuated smallpox to vaccinate against endemic smallpox, which at the end of the 18th century was recognised as a major public health threat (Baxby 1999).

The worldwide eradication of smallpox, which was declared by the World Health Organisation (WHO) in May 1980 (Fenner et al. 1988), is arguably the most famous use of vaccinia virus in the 20th century. It was a program launched in 1967 and run over 13 years, that aimed to eradicate smallpox from 31 countries around the world. According

to (Fenner, Henderson, Arita, Jezek, & Ladnyi 1988) it is estimated that ~300 million people were vaccinated each year.

2.1.3.2 Obstacles in the Development and Supply Chain of vaccinia virus as a smallpox vaccine

Due to the immense scale of the project, vaccinating such a large group of people from all over the word using an infectious virus, the WHO had to deal with a number of significant engineering challenges. The first was how to produce enough virus to meet the world's demand. The next challenge revolved around how to effectively distribute the vaccines to hot and hard to access places across the globe without it loosing infectivity.

In answer to the first obstacle, three main strategies of vaccine production were established. Virus was produced within endemic countries, donations were made directly to the WHO, subsequent to a resolution of the Twelfth World Health Assembly in 1959 (Fenner, Henderson, Arita, Jezek, & Ladnyi 1988), and virus was supplied directly to developing countries from bilateral aid organisations.

The second obstacle was tackled by the use of freeze-drying, a technique rediscovered by Shackell in 1909 (Meryman 1976). It was used in place of a liquid formulation for the New York City Board of Health (NYCBOH) strain of vaccinia virus, which was developed in part by Wyeth® as Dryvax® (J.Michael Lane 2003). The advantages of the freeze-dried virus preparations were that they had an increased shelf-life and could be distributed easily without losing infectivity (J.Michael Lane 2003).

2.1.3.3 Production of the Smallpox Vaccine (Vaccinia Virus)

During the eradication program vaccinia virus was generated from lymph collected from the skin of live animals, often calves and sheep, that had been infected with vaccinia (Monath et al. 2004). Purification was then performed by using sucrose gradient ultracentrifugation, which would typically give a percentage viral recovery of between 33% and 63% (Joklik 1962). While quality control measures were on the agenda of the WHO, they were not as developed as they are today. The manufacture of vaccinia virus in the form of Dryvax® by Wyeth® caused a number of undesirable side effects due to the presence of adventitious agents and other impurities (Monath, Caldwell, Mundt, Fusco, Johnson, Buller, Liu, Gardner, Downing, Blum, Kemp, Nichols, & Weltzin 2004). Adverse reactions included major cutaneous reactions such as vaccinial skin infection, particularly in patients with eczema, as well as acute myopericarditis (inflammation of the pericardium and heart) and encephalitis (inflammation of the brain). This was often seen in immunocompromised patients and patients with cardiac diseases. For this reason there has been a strong drive since this campaign to improve the safety of viruses and other therapeutic agents by developing well characterised and validated processes. Work has also focused on modifying existing strains to reduce virulence and pathogenicity (Tartaglia et al. 1992).

2.1.4 Use of vaccinia as an oncolytic and immunotherapy vector

2.1.4.1 Background to Oncolytic and immunotherapeutic viral therapies

An oncolytic virus is a virus that is known to infect, replicate in and lyse tumour cells preferentially to normal cells. Oncolytic viruses are also thought to be able to stimulate anti-tumour specific immune responses against certain antigens produced by cancer cells.

The immunogenicity of cancer cells (their ability to stimulate an adaptive immune response) varies between cancer types and also among individuals. It is thought likely by Pierre G. Coulie (Blankenstein et al. 2012) that all tumours cells present antigens that can be recognised and targeted by T-cells. However certain cancers, one example being melanomas, produce antigens that trigger a more elicit immune response than antigens specific to other cancer types. This allows for the development of more effective immunotherapies.

It has been postulated in the past that differences in immunogenicity of cancer cells has to do with their expression of self and non-self-antigens. Self-antigens are antigens that are normally produced by healthy cells in the body while non-self-antigens are antigens specifically produced by tumour cells. More recently, however, this theory has been challenged, and (Pradeu and Carosella 2006) describe an alternative. This is that it is not the difference in an antigen's origin that impacts its immunogenicity, but in fact differences in the molecular structure of the antigen's epitope. They put forward the view that epitope structures that are significantly different to those that the immune cells regularly interact with are more likely to elicit an immune response. This is potentially significant as a non-self-antigen may be able to fool the immune system by mimicking epitope structures of self-antigens.

A number of monoclonal antibodies acting as vaccines and immunomodulation agents against cancer have already been approved by the FDA, but it is widely accepted that combinatorial immunotherapies and more effective delivery platforms need to be found if the treatment of cancer by immunotherapy is going to be successful.

2.1.4.2 Recent Advances in Oncolytic Therapeutics

A number of viruses have been considered for their potential oncolytic applications. It has become relatively well known that viruses such as vaccinia (Hung et al. 2006), reovirus and Newcastle disease virus (McCart et al. 2001), as well as human papilloma virus (HPV) and Epstein-Barr virus (EBV) (Blankenstein, Coulie, Gilboa, & Jaffee 2012) can infect and replicate in tumour cells preferentially to normal cells. In addition, herpes simplex virus type 1 and adenovirus can be engineered to be less pathogenic to healthy human cells and more tumour specific, suggesting that they could be developed into successful oncolytic agents (Ferguson, Lemoine, & Wang 2012), although oncolytic adenovirus has a number of limitations, most notably being poor spread through tumour cells (Shayakhmetov et al. 2002).

The first oncolytic therapy, Oncorine, was licenced in China for the treatment of head and neck cancer in November 2005, and produced by Shanghai Sunway Biotech. This virus is a genetically modified recombinant human adenovirus 5 (AdV) (Garber 2006).

While this has been identified as a fantastic and encouraging result for the field, Ken Garber outlines that further work is needed in order to convince the rest of the developed world to invest in the same strategies in his review article “China Approves World’s First Oncolytic Virus Therapy For Cancer Treatment” (Garber 2006). It appears that the Chinese regulators based their approval on objective response rate

rather than overall patient survival. This was made difficult owing to the fact that a number of patients lived in rural places and were never revisited by doctors once initial responses were recorded. This is recognised as a "weakness in the clinical trial" by the company's president and plans to report survival rates in subsequent trails, as well as an intention to follow up with a number of patients from the AdV trail has been stated by Shanghai Sunway Biotech (Garber 2006).

More recently T-Vec or Imlygic® licenced by Amgen, Inc. became the first oncolytic viral therapy licenced in the US. T-Vec was derived from human herpes simplex virus type 1 and was licenced on 27th October 2015 by the US food and drugs administration (FDA) as an oncolytic virus for use in melanoma patients with injectable but non-resectable lesions in the skin and lymph nodes (Pol et al. 2016).

2.1.4.3 Obstacles to the Systemic Delivery of Oncolytic Viral Therapies

The delivery of oncolytic viruses by intravenous injection has a number of potential advantages. A viral therapy that can be injected intravenously has the potential of being able to reach distant metastasis as well as primary tumours. Intratumoural injection of oncolytic virus has shown some success in targeting solid tumours; however, it is well understood that death from cancer is often due to metastatic disease or recurrence, especially in distant hard to reach tumours, for example in the brain or pancreas (Ferguson, Lemoine, & Wang 2012).

One of the major challenges is that host defences limit the ability of viruses to infect tumour cells, particularly when injected intravenously. These include the activation of complement, neutralising antibodies and antiviral cytokines. There has also been reported uptake of virus by tissues and macrophages, all which limit the ability of the

virus to remain in the bloodstream and target distant metastasis (Ferguson, Lemoine, & Wang 2012;Wong et al. 2010). The limited ability of certain viruses to trigger a tumour-specific immune response can also be a limiting factor (Pol, Kroemer, & Galluzzi 2016). The limitations of systematic delivery of oncolytic viruses can be observed in Figure 2.1.

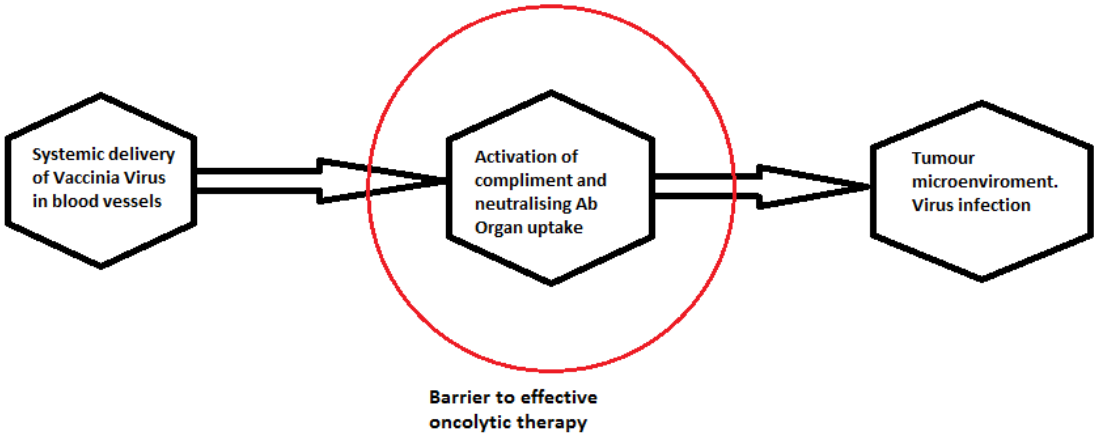

Figure 2.1: Illustration to show hurdles encountered by the systemic delivery of oncolytic viruses (Adapted from (Ferguson, Lemoine, & Wang 2012)). This shows that the action of blood vessels, neutralising antibodies, and uptake by organs can reduce the amount of virus available for uptake by tumour cells.

2.1.4.4 Clinical Applications of Vaccinia Virus

There are a number of reasons why vaccinia virus has been identified as a good candidate for oncolytic therapy (Kirn & Thorne 2009). One reason is that there is a lot of both laboratory and clinical data available on vaccinia virus biology and host response profiles to infection, following the use of multiple vaccinia virus strains during the smallpox eradication program. Commonly used strains for therapeutic use include the New York City Board of Health (NYCBOH), Lister, Copenhagen, Western Reserve,

Tian Tan, Modified Vaccinia Ankara (MVA), and NYVAC (derived from the Copenhagen strain) (Kirn & Thorne 2009). It should be noted that these vary in their oncolytic potential.

Another reason is that vaccinia has been shown to be very tumour selective, this is due in part to the fact that tumour cells produce less interferons (IFN) than normal cells in response to vaccinia virus infection (Luker et al. 2005). Vaccinia virus has also been shown to have a high host range and tissue tropism, allowing for broad spectrum tumour specificity (Tysome, Briat, Alusi, Cao, Gao, Yu, Wang, Yang, Dong, Wang, Deng, Francis, Timiryasova, Fodor, Lemoine, & Wang 2009).

Throughout the past decade, genetic engineering has been used to increase viral safety profiles and enhance clinical efficacy. One example of a genetic modification used in pre-clinical trials using the Western Reserve strain of vaccinia virus is the deletions in both the thymidine kinase (TK) and vaccinia growth factor (VGF) genes. This was found to activate the transcription factor E2F and the Epidermal growth factor receptor pathway (EGFR pathway), which in turn triggers the oncolytic effect (Kirn & Thorne 2009).

The virus was also engineered to express granulocyte-macrophage colony-stimulating factor (GM-CSF) which was shown to stimulate viral attack of foreign tumour cells. This reduced the potency of vaccinia virus in normal cells while increasing it in tumour cells (Thorne et al. 2007).

A different approach using the Lister stain of vaccinia virus for the treatment of pancreatic cancer is the insertion of a combined endostatin-angiostatin fusion gene (Scappaticci et al. 2001) which, when inserted in combination, has been shown to act synergistically to inhibit angiogenesis (Tysome, Briat, Alusi, Cao, Gao, Yu, Wang, Yang, Dong, Wang, Deng, Francis, Timiryasova, Fodor, Lemoine, & Wang 2009). This

approach has also been demonstrated in head and neck squamous cell carcinoma (HNSCC) models *in vitro* as well as *in vivo* (Tysome, Wang, Alusi, Briat, Gangeswaran, Wang, Bhakta, Fodor, Lemoine, & Wang 2011).

The potential therapeutic benefit of oncolytic viral vectors is undoubtedly very high. It is clear that a significant amount of work is still required in order to find viral strains with the right genetic modifications to deliver optimal therapeutic outcomes, but these medicines will also need to be affordable. This will require the development of commercially scalable and cost-effective processes early on in clinical development.

2.2 Options and Considerations When Developing Viral Bioprocesses

2.2.1 Introduction

In the early 20th century, from around 1900 until 1966, the smallpox vaccine (vaccinia virus) was produced from the lymph of calves and sheep. In the 1920's the concept of bacterially sterile cell culture preparations was starting to become better understood and legislated. The large number of vaccinia doses required for the eradication of smallpox, however, meant that the majority of vaccines were not able to be produced in sterile culture, even though the technology was available (Fenner, Henderson, Arita, Jezek, & Ladnyi 1988). The result was that viral preparations were often contaminated with bacteria and toxins that could not be completely removed by technologies such as ultracentrifugation. This increased the incidence of adventitious side effects.

2.2.2 Cell Culture and Primary Recovery

The majority of modern viral therapies including vaccines are now produced in either chicken eggs, or cell culture, with common cell lines being human, monkey, avian and insect cells. With the advancement of modern adherent cell culture technologies, egg-based manufacturing is usually not the preferred option. This is due to costs associated with scaling out, as well as environmental and animal welfare concerns. There are also risks to manufacturing resulting from avian flu and other diseases. Having said this, for the manufacturing of influenza vaccine, egg-based production is used for the majority of vaccines manufactured globally (Soema et al. 2015).

Many viral cell lines are adherent, and will only grow as monolayers on solid surfaces. Technologies currently used for culture of adherent cells with their pros and cons are listed in Table 2.1

Table 2.1 List of currently available technologies for expanding adherent cell lines with pros, cons as well as an example of commercially available systems (table not exhaustive)

Technology	Pros	Cons	Example
T-Flasks Roller - Bottles Cell stacks	- Good productivity - Easy to handle in small volumes - Flexible - Can recover cells easily - Do not require cell line development	- Limited scale up capacity - Not well controlled or automated - Hard to run in fed batch mode	Corning® Cell Culture Flasks
Packed Bed Bioreactors	- Scales up to $\geq$ 500 m^2 - Can be run in fed batch or perfusion mode - Fully intergraded controls - Does not require cell line development	- Poorly characterised small scale systems - Inherent variability in packed bed characteristics - Cannot recover cells easily	iCellis 500 (Pall Inc)
Hollow Fibre Bioreactor	- High surface area to volume ratio (100-200 cm^2/mL - Can be run at low sheer for longer process times - HF designed now well characterised in terms of porosity and uniformity - Well characterised small scale units - Can be run in Fed batch or perfusion - Fully intergraded controls	- Max surface area limited to 2.5 m^2 (lower than the iCellis) - Difficult to harvest cells (although easier than iCellis) - May require cell line development	FiberCell cartridges (FibreCell System Inc)
Micro carriers	- Easily scalable - Large surface area achievable - Fully integrated controls - Can run in fed-batch and perfusion reactors	- May require cell line development - Hard to recover cells - Possible productivity limitations	Cytodex GE Healthcare

For therapeutic areas such as some cancers, or genetic disorders affecting muscular tissues (an example being Duchenne Muscular Dystrophy), the amount of therapeutic virus needed to be produced is considerable. Some examples of technologies designed to scale up adhering cells are shown in Table 2.1; however, challenges to large scale production are a massive driver to adapt commonly used cell lines such as CV-1, Vero, or HEK293 cells to grow in suspension. The reasons for this are that adherent cell culture technologies will always be limited by scale, therefore affecting overall process productivity. It can also be very difficult with many technologies to recover the cells which, especially for purposes of in-line monitoring, makes robust process control and characterisation difficult. The major disadvantage of adapting an adherent cell line to grow in culture, however, is that it requires extensive cell line development which in turn requires time, resources and significant expertise.

Infectious viral particles in culture have been shown to be concentrated both inside the cell, therefore requiring cell lysis, and in the supernatant. Specific examples are vaccinia virus (Smith, Vanderplasschen, & Law 2002), which has a number of viral forms that are concentrated inside the cell, and murine leukaemia virus (MLV) (Aboud et al. 1982). As a rule of thumb, it is often seen that non-enveloped virus such as AAV are concentrated inside the cell, whereas enveloped viruses such as Lentivirus are concentrated in the supernatant (Segura et al. 2011). If the virus is concentrated in the supernatant, the main challenge becomes removing the cells whilst maintaining high yields of infectious virus. It can also be a challenge to remove host cell proteins, DNA, lipids, and other process-related impurities.

If the virus is located intracellularly, then cellular disruption is required in order to release the virus. Perhaps the most common laboratory scale method for cell disruption is multiple freeze thaw cycles of pelleted cells post centrifugation. At large scale,

however, this becomes impractical and expensive. Scalable methods include hypotonic shock, chemical lysis, ultra-sonication and mechanical disruption. Mechanical disruption by homogenisation is arguably the method of choice due to its ease of scalability and reproducibility (Monath, Caldwell, Mundt, Fusco, Johnson, Buller, Liu, Gardner, Downing, Blum, Kemp, Nichols, & Weltzin 2004). Changes in pressure and high shear forces can be produced and controlled to break open cells without damaging the viral particles, although this will likely depend on the viral size liability. An example of the use of homogenisation can be found in (Joklik 1962). Alternatives are agitation with glass beads as described in (Zwartouw et al. 1962).

In terms of cell removal, common methods include centrifugation and microfiltration. Flocculation, precipitation and aqueous two phase extraction, some of which will be described in more detail later in this chapter, have been attempted but are not common practice. Centrifugation is a common primary recovery unit operation in protein manufacturing due in part to its ease of scalability (Maybury et al. 2000). As many oncolytic and gene therapy products are currently produced at relatively small scale, microfiltration unit operations are discussed more in relation to viral primary recovery processes. Companies such as EMD Millipore and 3M have commercialised a range of depth filters which they have suggested can be used generically for viral bioprocesses. Application notes are available showing the use of depth filters as a primary recovery step for cell culture-based influenza vaccine processes (EMD Millipore 2014). Membrane filters of differing pore sizes can be run in both dead end and tangential flow filtration (TFF) mode. An example of membrane dead end filtration can be found when manufacturing cGMP lentiviral vectors (Ausubel et al. 2012). Examples of TFF filtration applications in viral primary recovery and as a viral concentration step can be found in Section 2.2.3.2.

2.2.3 Purification

2.2.3.1 Ultracentrifugation

The gold standard unit operation for the purification of viral particles is ultracentrifugation, used throughout the 20th century for the purification of multiple pox viruses (Zwartouw, Westwood, & Appleyard 1962). Ultracentrifugation can be broken down into two different modes (Segura, Kamen, & Garnier 2011). The first is equilibrium density ultracentrifugation, and the second is rate zonal ultracentrifugation. Equilibrium density ultracentrifugation uses a high density bed of sucrose, caesium chloride, (CsCl), iodixanol, Percoll®, or Nycodenz® to separate virus material based on its buoyant density. Rate zonal ultracentrifugation separates based on size and density. Density gradient ultracentrifugation works by loading virus either manually into a stationary ultracentrifugation tube containing a high density bed as described above, or continuously into the bottom of a packed rotating rota, the latter being more common at large scale. Rotational speeds can reach ≥ 40,000 rpm, with a resulting relative centrifugal force (RCF) of ≥ 100,000g, The duration of the process can last from many hours to even days, while particles move down the bed from an area of low concentration of media to an area of high concentration until the buoyant density of each particle reaches that of the media. Rate zonal ultracentrifugation on the other hand, while similar, can be performed more rapidly. A smaller, often more concentrated volume of virus is loaded onto the top of a gradient bed, which is again rotated at high speeds. While the virus will still band once it reaches its buoyant density if left to settle for long enough, the different particles present in the sample will travel down the bed at differing velocities depending on their size as well as (to a lesser extent) any differences in density and overall viscosity. In order to take advantage of this phenomenon, the ultracentrifuge is stopped prior to density equilibrium being reached, so that each

volume fraction can be analysed. This can be a high resolution technique used for viral purification due to the difference in size between virus particles and common impurities. However, as sample volume needs to be extremely small (~10% bed volume) scale up is challenging. At bench scale, typical bed volumes scale to ~250 mL. When using density gradient ultracentrifugation, vaccinia virus will often require around 12 hours (typically overnight) to band; smaller viral particles such as AAV can take up to 3 days. The operation is typically performed at 2-8°C to reduce the risk of viral inactivation.

The general disadvantages of density gradient ultracentrifugation are that the technique is very time consuming, requires skilled operators and is very labour intensive. At production scale it commonly takes two operators to setup and clean the system. This, coupled with the fact that in the past recovery of infectious viral particles was shown to be low, between 33% to 63% being fairly liberal estimates (Joklik 1962), demonstrates the need for a more optimal and scalable purification processes for viruses.

There are several companies that produce density gradient ultracentrifuges for production scale processing. A relevant example is Alfa Wassermann which manufactures a KII ultracentrifuge that has a maximum process capacity of 200 L (Alfa Wassermann 2013) (Figure 2.3).

Density gradient ultracentrifuges are not run in the same way from bench to manufacturing scales. Bench-scale ultracentrifuges are designed to be run in batch mode while larger manufacturing scale ultracentrifuges are often run in a semi-continuous mode. At bench-scale, an ultracentrifuge tube is filled with a packing matrix such as sucrose at differing concentrations from top to bottom. High concentrations are loaded into the tube first and then lower concentrations are added on top. This produces a sucrose concentration step gradient from the top to the bottom of the tube. Alternatively,

instead of sucrose, salts such as caesium chloride can also be used. These form linear concentration gradients when run under high centrifugal forces due to the high density of caesium salt (CsCl). In both cases, virus is loaded into the top headspace of the tube, which is then placed into the ultracentrifuge rotor and rotated at high g force (~RCF x 100,000).

Once the run is complete, the tubes are removed and harvested using a sterile needle which is used to pierce the bottom of the tube. Fractions are then removed and analysed for viral particles. This process is time consuming and prone to human error.

Semi-continuous ultracentrifugation works slightly differently to batch ultracentrifugation as shown in Figure 2.2.

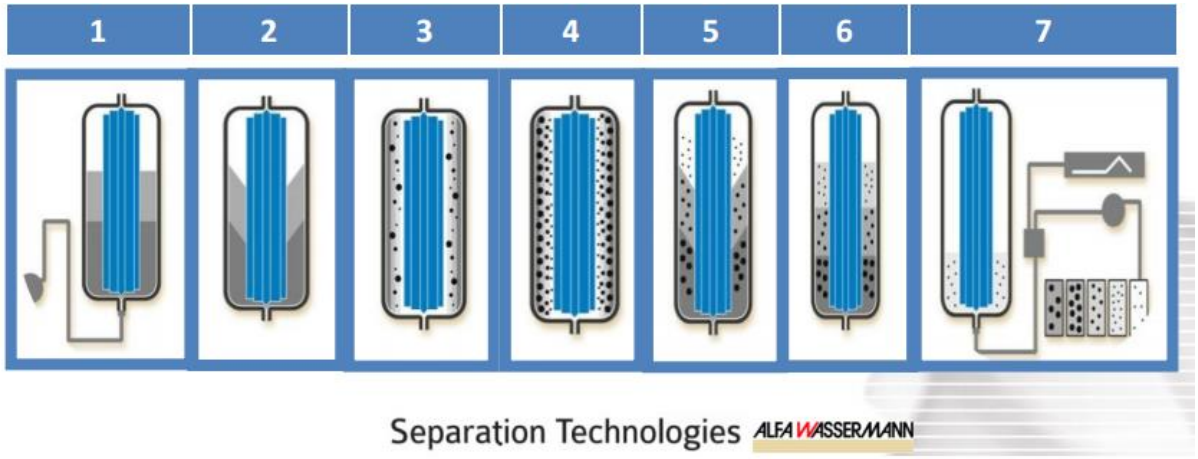

Figure 2.2 A graphical representation taken from (Sandra Merino 2015) to show how large scale ALFA WASSERMAN KII ultracentrifuges work.

Each step (1-7) as indicated in Figure 2.2 is listed below:

1. Ultracentrifugation gradient matrix is pumped into a stationary rotor (maximum volume 3.2 L)
2. Rotor is slowly accelerated and the bed aligns vertically on the walls.
3. Virus material is loaded into the bottom of the rota and particles are captured at the top of the bed – towards the middle of the rotor. Effluent flows out the top of the rota.
4. Viral particles move down the bed from the centre of the rota to the outer walls until their buoyant density is equal that of the media.
5. The rotor is decelerated until stationary.
6. The bed reforms horizontally but the gradient remains in place.
7. Fractions are pumped out the bottom of the rotor and passed through a UV cell to determine where virus has banded. Fractions can also be sampled for further analysis.

One of the major limitations of ultracentrifugation is volumetric throughput. Bench scale centrifuges are limited to a few hundred millilitres. Large scale ultracentrifuges can process more material, but this is still limited to a maximum of ~200L depending on the virus being purified. According to Alfa Wassermann this can be as low as 5 L for Hepatitis B, while in the case of influenza process volumes can reach up to 150 L. After a run the bed is collected in fractions between 15 and 500 mL. Each fraction is analysed for infectious virus particles. There have been some issues reported when using ultracentrifugation related to the removal of genomic DNA, which has a similar density to many viral particles. Alfa Wassermann suggests the use of benzonase if this is found to be the case; however, it should be noted that this is an expensive processing option as

nucleases and assays to test for their removal are costly and require validation. (Alfa Wassermann, 2013).

Another possible disadvantage of ultracentrifugation is that the machines can be difficult to clean as they need to be taken apart manually. It can take two operators, working together, several hours to clean and shut down a single system. This means that even if several machines are used in parallel in order to process a large volume of material, a bottleneck in terms of time and labour is experienced.

Ultracentrifuge rigs are also very expensive with prices greater than 300,000 USD for a process scale rig. Costs associated with ultracentrifugation will likely increase further when validation qualification and infrastructure requirements for GMP use are taken into account.

Figure 2.3 Picture of a KII Ultracentrifuge from Alfa Wassermann (Sandra Merino 2015).

There are a number of challenges to large scale ultracentrifugation making many industrialists keen to find alternatives. What is important to keep in mind, however, is that ultracentrifugation also has some advantages which can be difficult to find in other emerging technologies; these, together with some disadvantages, are summarised in Table 2.2.

Table 2.2 Advantages and disadvantages of ultracentrifugation

Advantages of Ultracentrifugation	**Disadvantages of Ultracentrifugation**
- Not reliant on changes in pH or salt concentrations to generate a separation. These can inactivate some viruses - Low sheer environment - Well tried and tested technique requiring little process development - Rotas can be steam sterilised - Some processes give high percentage recovery and purity	- High capital expenditure (CAPEX) and labour costs - Relatively low throughput - difficult to scale up - Can be very manual and laborious

2.2.3.2 Alternatives to ultracentrifugation

There are a number of scalable alternatives to ultracentrifugation. Comparison studies dating back to the 1980's have shown that many can outperform bench scale ultracentrifugation.

The issue is that in order to replace ultracentrifugation, in which significant investments have already been made, results from other technologies need to show significant

improvements in purity and yield as well as productivity. Techniques such as chromatography, aqueous two phase and precipitation are not straightforward to develop. Complex multifactorial experiments need to be performed in order to generate process knowledge and understanding. This is not the case with ultracentrifugation, or with TFF. Many factors that affect the separation efficiency of an ultracentrifuge cannot be modified; therefore relatively little process development is required. Experienced operators are needed to run manufacturing campaigns, and a significant amount of capital is required to purchase equipment, but once these are in place, there is often not much of a driver to switch technologies.

The main and most commonly developed alternatives to ultracentrifugation are summarised in Table 2.3.

Table 2.3 Alternatives unit operations to ultracentrifugation

Unit Operation	Viral purification applications	**References**
Tangential Flow Filtration (TFF)	- Both flat sheet (FS) and hollow fibre (HF) filters have been used to concentrate and purify viral feed streams and can be used to remove cells, cell debris, proteins, and DNA from crude lysate. - Relatively low molecular weight cut-off (small pore) filters are used to remove proteins and DNA. - Large pore diameter filters are typically used for the removal of cells and larger debris. - Filters are commonly manufactured using either polyethylene sulfone (PES) or regenerated cellulose (RC). - Nominal channel diameters range from <100KD to >0.45µm - One potential drawback is that shear forces need to be well controlled to prevent membrane fouling and viral degradation. This can be easier to control and measure when using HF filters rather than FS. - Flux vs TMP studies are required during process development in order to generate understand of critical process parameters (CPPs). - In general TFF is considered as a relatively low resolution technique, but easily scalable to large process volumes.	(Negrete et al. 2014;Wickramasinghe et al. 2005)
Gel Filtration	- Size exclusion chromatography also known as gel filtration (GF) has been shown to achieve higher yields than density gradient ultracentrifugation, although sometimes struggles to remove large contaminants such as genomic DNA. - Typical issues associated with GF often relates to volumetric throughput. Good separation requires low load volumes, typically ~2% of the total column volume. - Due to load volume restrictions GF is often found towards the end of the process once volume is reduced. - GF benefits by allowing isocratic elution often in physiological buffers such as PBS. - In general GF is regarding as high resolution, low volume technique.	(Andreadis et al. 1999;McGrath et al. 1978)
Precipitation	- Precipitation using PEG, ammonium sulfate and calcium phosphate has been used to aggregate viral particles allowing removal by low speed centrifugation. - Variable recovery of infectious viral particles has been reported in the literature likely due to changes in osmotic pressure. Reported for Retrovirus, but thought likely to affect other particles. - A combination of PEG 6000 followed by Sepharose Cl-4B (GF) has been reported to achieve a good recovery and purification efficiency of both extracellular and intracellular moloney murine leukemia virus. This was reported as being especially true for larger volumes as the PEG 6000 was able to pellet virus from bulk fluid prior to chromatography. - Potential issues regarding large scale manufacturing are solubilising viral pellets formed, and removal of co-precipitated impurities.	(Morenweiser 2005) (Aboud, Wolfson, Hassan, & Huleihel 1982)

Unit Operation	Viral purification applications	**References**
	- The mechanisms of viral precipitation are generally not well understood. This leads to challenges in process development.	
Aqueous Two Phase (ATPS)	- Aqueous two phase has been attempted with chemicals such as PEG, dextran and polyvinyl alcohol to separate virus material from cellular components, An example being a dextran-polyethylene glycol system successfully used to concentrate and purify HIV-1 along with external gp120 protein. - Scale up is generally considered possible using convention extraction equipment used in the chemical industry, however requires investment. - ATPS requires a lot of process development as phase equilibrium and protein partitioning is not well understood - Raw material costs (polymers) is also a concern.	(Morenweiser 2005) (HAMMAR and GILLJAM 1990) (Cunha and Aires-Barros 2000)
Chromatography	- Packed bed systems and continuous polymer monoliths and membrane sheets have been used successfully to purify a range of viral particles for clinical use. - Common types of chromatography used include Affinity (AF), Cation and Anion exchange, (IEX), Hydrophobic interaction, (HIC), Immobilised metal affinity (IMAC) as well as Pseudo-affinity and mixed modal resins. - Use of chromatography to purify viruses is discussed in more detail in Section 2.3.	(Cheng et al. 2001;Gagnon 2008;Wolff et al. 2010b)

New generation chromatography using membranes, fibres, and monoliths are perhaps the most widely published alternatives to ultracentrifugation for capture and purification of viral particles. Advances in resin design have paved the way to some very promising process designs with some impressive results. The next section of this introduction will concentrate on chromatographic history, theory, applications and results.

2.3 Chromatography

2.3.1 Overview

Chromatography was first developed by the Russian botanist M.S. Tswett, who has often been described as the father of modern chromatography. He published his first paper in 1903 on the separation of xanthophylls and chlorophyll on an inulin column. His second paper in 1906, on the insolubility of chlorophyll in petrol and ligroin, resulted in an early description of adsorption (Ettre and Sakodynskii 1993a;Ettre and Sakodynskii 1993b). Chromatography can, in general terms, be described as "a separation procedure for resolving mixtures and isolating components" by a process of "differential migration"(Doran 2005).

Chromatography has been used for the separation of a large number of biological agents from proteins, vitamins, and amino acids, to viruses, virus-like particles (VLPs) and plasmid DNA (pDNA).

A solvent otherwise known as the mobile phase, typically a liquid in liquid chromatography or a gas in gas chromatography, travels down a column and interacts with a stationary phase at different rates depending on its affinity for the matrix (Doran 2005). This is traditionally a solid support, although it can also be a liquid in liquid-liquid chromatography.

For most preparative bioprocess applications, the stationary phase consists of a solid inert compound. These structures are typically either porous beads, of ~40-100 µm, which have small micropores of around 100 nm on their surface, or solid porous materials with highly crosslinking channels. These channels can have very large diameters ranging from 0.4 to 100 µm, and are therefore often used for separation of

large macromolecules such as viruses and virus like particles (VLPs) or even cells (Dainiak et al. 2006).

Examples of typical bead materials, often used for protein purification, are highly cross linked agarose (MabSelect SuRe LX®, GE Healthcare Life Sciences), polystyrene divenyl benzene (POROS ® Applied Biosystems), polyacrylamide, (Bio-Gel, Bio-Rad), and hydrophilic cross-linked vinyl polymer (Toyopearlm TosoH Biosep).

There are a number of single rigid porous chromatographic structures on the market. The most common are membrane adsorbers and monoliths.

An example of a membrane that was commonly used in bioprocessing, although now discontinued, was ChromaSorb (EMD Millipore, Darmstadt, Germany) made from polyethylene. Another example is Sartobind® (Sartorius, Gottingen, Germany) which is made from stabilised reinforced cellulose. This product is available as a strong CIEX with sulphonic acid ligands, a strong anion exchange (AIEX) with quaternary ammonium ligands, and a HIC that uses a phenyl ligand. A salt tolerant addition, Sartobind STIC® designed for HCP, DNA and endotoxin removal is also available, and it consists of primary amine ligands. The other main membrane adsorbers on the market are Mustang filters (Pall, NYC, USA). from which Mustang S and Q are both made from polyethersulfone (PES) and come with sulphonic acid and quaternary ammonium ligands respectively.

Convective interaction media (CIM) monoliths are also single rigid open channel chromatographic structures commercially made at large scale from poly(glycidylmethacrylate-co-ethyleneglycoldimethacrylate, (BIA Separations, Ajdovscina, Slovenia). In general, charged, hydrophobic, affinity or active groups are chemically synthesised on the surface of the solid methacrylate support and interact with solutes via hydrophobic or electrostatic interactions, hydrogen bonding and/or Van

der Waals forces. The two modes of adsorption-based chromatography to be discussed in this thesis are preparative ion exchange and hydrophobic interaction chromatography.

2.3.1.1 Ion exchange chromatography (IEX)

In ion exchange chromatography adsorption is initiated by electrostatic interactions between a solute and the stationary phase. Ion exchange columns can be either positively charged, known as anion exchangers (AIEX), or negatively charged, known as cation exchangers (CIEX). Typical AIEX ligand chemistries include quaternary amine groups (QA) or diethylaminoethyl groups (DEAE). These chemistries represent strong and weak anion exchanges respectively. Primary amines are also common, although in preparative AIEX they are more often used for single use negative capture polishing steps, which are designed to capture residual impurities such as HCPs and DNA.

Common strong CIEX ligands are sulfate groups (SO_3) in the form of sulphonic acid or sulfopropyl groups. Weak CIEX ligands often consist of carboxymethyl groups (CM)

Separation is dependent on the difference in net charge between solute molecules, and the subsequent affinity of the solutes to the adsorbent. pH and ionic strength can be manipulated to bring about adsorption and elution depending on the isoelectric point of the solute of interest.

Increasing the salt concentration (often a neutral salt such as NaCl) allows smaller charge dense ions to compete with the often larger solute molecules for binding sites.

2.3.1.2 Hydrophobic interaction chromatography (HIC)

Hydrophobic interaction chromatography relies on the interaction between hydrophobic patches on the surface of a solute and the often non-polar ligands on the stationary phase. Butyl or phenyl groups are commonly used as preparative ligands, although hydroxyl and epoxy groups can also be used if a weaker interaction is desired. Adsorption is thought to be driven by an increase in entropy as a result of a reduction in the Gibbs free energy of the solute in solution. This occurs by increasing the concentration of kosmotropic salts such as ammonium sulfate in the load material. In addition to this, hydrophobic amino acids present close to the surfaces of proteins are thought to form surface hydrophobic cavities, due to the reduction in free water molecules. These cavities are then able to bind to hydrophobic ligands. A reduction in salt concentration and changes in pH are typically used to bring about elution, although organic solvents are sometimes required.

2.3.2 Practical considerations when developing viral chromatography steps

2.3.2.1 Trade-offs when evaluating process performance

A common trade-off needing to be considered when developing chromatographic processes for the majority of products is “recovery versus purity”.

In order to increase the optimum performance of a process, both the percentage recovery of the product of interest as well as the removal of impurities need to be maximised. It is here that process developers come across a common problem. When factors influencing process performance are varied, whether numerically or

categorically, optimum conditions favouring one response or the other are often found rather than both together. A compromise between the two responses thus becomes unavoidable. As a result, the relationship between each individual individual factor and overall process performance is often nonlinear. It is also common that areas of local optima can be found in a design space. This can be helpful in giving process developers more flexibility, especially when considering scale up challenges to achieving a certain criteria, since not all factors are as easy to accomplish at large scale as they are at bench scale, but can also make the determination of global optima difficult.

When developing processes for infectious viruses, the complexity of the problem increases further. Trade-offs relating to infectious viral processes need to take viral infectivity into account as well as total particle recovery. Conditions that are able to recover all viral particles loaded without any impurity contamination would only be acceptable if the viral particles recovered were infectious.

For this reason viral stability during processing and storage is of paramount importance and needs to be characterised. In order to do this, stability studies need to be performed over time at a range of temperatures and conditions that best represent those of a process.

Many viral particles are thought to be labile, although the exact mechanism of inactivation is not described in the literature in detail. Viral sample handling needs to be planned with stability data in mind. If viral infectivity crashes at room temperature for example, then samples will need to be put into controlled temperature storage as soon as possible after a fraction has been collected.

Sample handling needs to be consistent so that researches can rule out the possibility that any loss in infectivity is the result of a variation in the experimental protocol.

2.3.2.2 Resin screening considerations

Both ion exchange and hydrophobic interaction chromatography have been used to purify viral particles (Banjac et al. 2014;Gerster et al. 2013a;Opitz et al. 2008;Wolff et al. 2010a). What is interesting is that many viruses, especially enveloped viruses, have been shown to bind to both CIEX and AIEX at either side of their supposed isoelectric points (Banjac, Roethl, Gelhart, Kramberger, Jarc, Jarc, Strancar, Muster, & Peterka 2014;Wolff, Siewert, Lehmann, Hansen, Djurup, Faber, & REICHL 2010b). This has been demonstrated in protein separations in the past; however it appears to be particularly commonly in viral chromatography. This is perhaps due to the size and complex physicochemical properties of viral particles (Yamamoto and Ishihara 1999). For this reason, both strong and weak CIEX, AIEX, and HIC resins should be included in initial screening experiments.

There are a number of bottlenecks that need to be considered when setting up extensive screening experiments. Virus process development takes time, one of the major time bottlenecks being the infectivity assays. Assays can take anywhere from several days to several weeks to run; so unless high throughput screening technologies can be utilised, it is imperative to design experiments in a sequential manner in order to give as much information as possible per experiment. It can be difficult to generate enough virus material to perform extensive screening studies, thus experimental designs need to take this into account. The goals of screening studies in viral bioprocessing need to be clearly defined from the offset.

One of the attributes of using chromatography is that there are a lot of factors that can be manipulated in order to maximise the productivity and separation achievable. The

advantage of this is that there is a lot that can be done to optimise a separation process should this be required. Examples are changes in pH, salt concentration, type of buffer system in the load, wash and elution buffers, stationary phase and ligand chemistry, and type of matrix. The matrix could be a packed bed, monolith or membrane as previously mentioned.

When dealing with complex feed streams such as viruses, this can also be a disadvantage as to fully optimise, even a single step, can require a very large number of runs. In practical terms, it is impossible to screen every possible factor that might influence a separation. Therefore factors to be considered need to be prioritised based on previous experience, theoretical understanding and considerations, published literature, and often finite resources.

The use of multifactorial designs such as DoE and Simplex analysis can be useful, and have been used successfully in the past to find areas of optima within complex design spaces (Konstantinidis et al. 2016). Variability in viral analytics and time taken to analyse virus samples, however, make both of these approaches challenging.

The best process development techniques to utilise for viral separations will vary between laboratories and will not only depend on the product, but also on the situational constrains such as time available for process development, and equipment availability. For this reason a general statement on this topic is of limited use. A lytic virus such as vaccinia (which requires infectivity assays to determine viral titre, being developed in a laboratory with many other projects and with no high throughput capabilities), will need to consider DoE and intelligently designed one-factor-at-a-time approaches rather than high throughput screening (HTPD) and simplex analysis. On the other hand, a laboratory optimising an AAV separation, which requires qPCR as its major

quantitation assay, may well be able to utilise HTPD and Simplex methodologies as well as DoE if the resources are available.

Process developers need to take into account the amount of complexity inherent in the feed stream, time required to asses product concentration and impurity profiles, and assay variability.

As described later in this thesis, stability data, refined experimental design and the use of a large variety of orthogonal analytical methods can be used to generate reasonably robust conclusions on process performance. However, chromatographic process development is likely to be more time consuming and expensive compared to other techniques such as ultracentrifugation.

2.3.3 Use of chromatography for virus and other macromolecular separations

2.3.3.1 Membrane adsorbers and packed bed columns

Membrane adsorbers have been used to purify viruses and other large macromolecules. They have some of the same advantages as monoliths in terms of mass transfer and flow independent adsorption; however, the achievable resolution is not as high due to a shorter bed length and a less interlinking channel structure.

Figure 2.4 is an illustration of the comparative strengths and weaknesses of membrane adsorbers (MA), monoliths and packed bed columns for viral separations. As it can be seen in Figure 2.4, membrane adsorbers benefit from high capacity and flow rate, but limited resolution. Packed bed columns can achieve high resolution, but need to be run

at lower flow rates and cannot achieve as a high capacity as membranes or monoliths. Monoliths benefit from being able to run at high flow rates without compromising capacity or resolution.

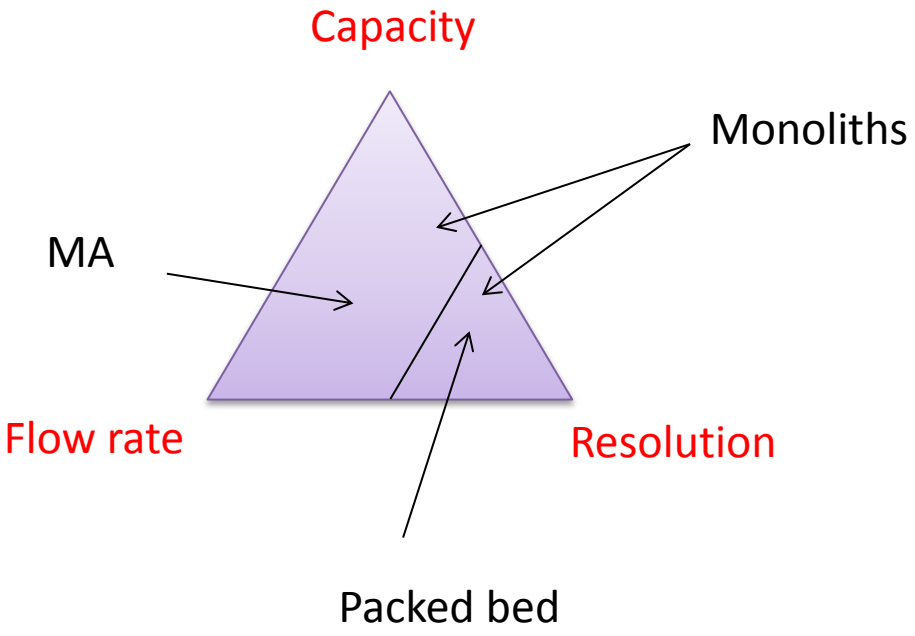

Figure 2.4 Visual comparison between packed bed, membrane adsorbers and monolith chromatography, adapted from (Ales Strancar 2011).

There have been a number of studies that have used membrane adsorbers to purify viruses such as vaccinia, influenza, retroviral vectors, adenovirus and others (Peixoto et al. 2008;Wolff and Reichl 2008;Wolff, Siewert, Hansen, Faber, & Reichl 2010a).

(Wolff, Siewert, Hansen, Faber, & Reichl 2010a) describe the use of pseudo-affinity membrane adsorbers (MA) combined with HIC resins from the ToyoScreen HIC mix pack (Tosoh Biosciences GmbH, Stuttgart, Germany) to purify modified vaccinia

ankara (MVA) virus with the aim to reduce DNA levels to ≤ 10 ng per dose (as required by the WHO 1998). A combination of two membrane adsorbers were used, one with sulfated cellulose (SC) and the other with heparin ligands. A protein present on IMV (A27L) is known to bind to heparin (Chiu et al. 2007) making this an attractive candidate as a pseudo affinity ligand. It was found that both strategies worked; HIC combined with SC-MA and Heparin-MA gave similar total virus particle yields of approximately 60 %. Both were able to reduce HCP levels to lower limit of quantification (LLOQ), and final DNA levels were comparable and as low as 10ng/dose.

It was concluded that nuclease treatment would still be required to robustly reduce DNA to specified levels; however, as the amount of DNA was reduced significantly compared to other technologies such as ultracentrifugation, the amount of nuclease treatment could also be reduced, resulting in a more cost effective process.

SC-MA has also been utilised for MDCK cell culture derived influenza virus capture. H1N1 and H3N2 were both purified as described by (Opitz, Zimmermann, Lehmann, Genzel, Lubben, REICHL, & Wolff 2008). In this study, commercially available CIEX-MA and column-based cellufine sulfate were compared to SC-MA. SC-MA showed higher infectious virus recovery as well as increased DNA removal when compared to both technologies. High flow rates (15 mL/min) coupled with a higher binding capacity (13 µg HA/cm^2) were achieved in comparison to column-based cellufine sulfate chromatography, also resulting in an added process productivity benefit over this technique.

It is clear from both studies that pseudo-affinity-based membrane adsorbers are an attractive option for capture and polish of large enveloped viruses. It should be noted

that neither of these supports are available as catalogue items from Sartorius. But the technology shows potential and clearly has advantages over packed bed chromatography. There is still room for development to increase vaccinia virus yield from 60 % and remove more DNA to achieve concentrations below 10 ng DNA/dose, however; if GMP compliant columns are available then pseudo-affinity membrane adsorbers might be an attractive process option.

2.4 Monoliths

2.4.1 History and Overview

There are now several types of monolithic materials on the market. Originally monoliths were made from N,N'–methylenebisacrylamide; however, this was replaced with piperazine diacrylamide and methacrylamide when it was found that these compounds allowed for higher flow velocities (Svec 2008). Process scale commercial monoliths are now made from poly(glycidylmethacrylate-co-ethyleneglycoldimethacrylate) or Styrene-divinylbenzene (CIM® BIA separations, Ajdovscina, Slovenia), and currently BIA Separations are the only company that can make up to 8000 mL columns (Ales Strancar 2011).

Larger scale columns are currently in R&D phases, as manufacturing hurdles are encountered during the polymerisation reaction due to the heat released across the structure, potentially causing structural distortion if not kept within a certain range. The polymerisation reaction which combines glycidyl methacrylate and ethylene dimethacrylate in a free radical bulk polymerisation reaction with benzoyl peroxide as an initiator has an activation energy $E_{a,app}$ *of* 81.5 kJ/mol with a heat of reaction (ΔH_r) of 190 J/g (Mihelic et al. 2001).

All monolith columns produced by BIA Separations from 1 mL up to 8000 mL are run in radial rather than axial flow as this reduces their footprint whilst maintaining a minimum bed length required to ensure a low pressure drop (ΔP). Smaller commercially available columns from 0.1 mL to 0.34 mL are run in axial flow as this is mechanically easier to fabricate at small scale, owing to their smaller cross sectional area to bed length ratio. As a result of this difference in area to bed length ratio, it is advised by the manufacturer to perform scale up studies using 1 mL columns as a minimum.

Other manufacturers of monoliths are BioRad (Hercules, CA, USA) who have produced polyacrylamide UNO columns. These are advertised for their high resolution at high flow rates for protein separation. Merck have produced a silica-based monolith called Chromolith, but have concentrated on the analytical ability of the columns taking advantage of their high number of theoretical plates compared to packed bead resins of an equivalent bed length. GE Healthcare has produced monobeads, which are made from polyvinyl alcohol and polystyrene-coated. These can be packed into traditional chromatography columns and are marketed for their high resolution and flow rate capabilities.

2.4.2 Theoretical Considerations when using Monoliths

Purification of large macromolecules such as viruses, VLPs and pDNA, is typically restricted by very low dynamic binding capacities (DBC) when using conventional packed bed chromatography. For this reason chromatography has not conventionally been the first method of choice for macromolecular separation.

Vaccinia virus, which is one of the largest known viruses, has an approximate diameter of 300 nm. The pore opening on the surface of commercially available chromatography

media tends to be around 100 nm in diameter. Most viruses, therefore, can only bind to the outer surface of these beads and so cannot utilise the full surface area available.

Packed bed columns are designed for the purification of relatively small molecules such as therapeutic proteins, mAbs and peptides. These molecules can easily diffuse into the micropores on the surface of typical bead-based resins, so the surface area available for adsorption is very large and hence not a limiting factor. Manufacturers can further optimise capacity as well as increase the number of theoretical plates of their resins by reducing bead diameter and increasing ligand density. Efficiency is directly related to particle diameter and is described by the number of theoretical plates or equilibrium stages in a column per meter. The height of each theoretical plate (HETP) measured in meters can be determined by the equation below,

$$HETP = A + \frac{B}{u} + C.u \qquad 2\text{-}1$$

where A is eddy diffusion (m), B is longitudinal diffusion ($m^2\ s^{-1}$), C is the resistance to mass transfer (s), and u is linear velocity ($m\ s^{-1}$).

This expression can also be expanded for process IEX chromatography as described in (Jungbauer 2005;Lettner et al. 1995).

$$\boldsymbol{HETP = \frac{2\varepsilon_b D_L}{u} + \frac{2u}{1-\varepsilon_b}\left[\frac{k'}{1+k'}\right]^2\left[\frac{r_p}{3k_f} + \frac{r_p^2}{15\varepsilon_p D_p}\right]} \qquad 2\text{-}2$$

where ε_b is bed porosity, ε_p is particle porosity, D_L is the axial dispersion coefficient ($m^2\ s^{-1}$), D_p is the particle diffusivity ($m^2\ s^{-1}$), k' is relative retention factor, r_p is particle radius (m), and k_f is the particle film mass transfer coefficient ($m\ s^{-1}$).

Due to mechanical constrains, limitations do exist regarding scale up of packed bed columns (Jungbauer and Hahn 2008). High back pressures due to bed compression towards the centre of a packed bed, as well as areas of non-linear flow distribution, particularly at the column walls, can occur if the column diameter is increased above a certain point. This is not thought to be a serious limiting factor for protein separations in terms of productivity, due to the high binding capacities now achievable with commercially available resins, 40-100 g/L in some cases. If packed bed columns were to be used for viral separations, however, especially for high dose applications, column size may become a bottleneck as capacity will be significantly lower, potentially by orders of magnitude.

When considering the purification of viruses monoliths are becoming extremely useful tools (Jungbauer & Hahn 2008). Monoliths have excellent mass transfer properties, as reviewed and demonstrated by a number of authors including (Gritti et al. 2003;Hahn et al. 2002;Jungbauer & Hahn 2008;Zou et al. 2002). However controversy exists as to whether the observed mass transfer characteristics are due to the open pore structure and subsequent convective flow or the small size of particles used in the polymerisation process (Hahn, Panzer, Hansen, Mollerup, & Jungbauer 2002). The generation of an open pore structure seen in CIM monoliths is due to the polymerisation process; small particles ~1 μm in diameter agglomerate into a single, rigid polymeric homogeneous structure called poly(glycidylmethacrylate-co-ethyleneglycoldimethacrylate). While the overall surface area of monoliths is smaller than that of a conventional packed bed chromatography column, the surface area available to large macromolecules for adsorption is much higher. The three dimensional structure of monoliths has been described as similar to membranes, which have in turn been described as very thin monoliths (Ales Strancar 2011). They are highly porous and contain a vast amount of cross-linking. This allows them to exhibit very low back pressures at high flow rates,

even at process scale. The HETP and dynamic binding capacity observed are almost completely unaffected by velocity; therefore monoliths can in theory give very fast, efficient separation of large macromolecules.

As Illustrated in Figure 2.5 the velocity profile in monolithic structures is important when discussing their performance in comparison to packed bed chromatography and especially membrane adsorbers.

Figure 2.5 An illustration to show the cross linking wide channel structure, and almost flat velocity profile achievable using monoliths. The red arrows represent directional flow and their size represents relative velocity. This picture was adapted from (Gagnon 2008).

A phenomenon known as eddy diffusion and axial dispersion occurs between the beads of packed bed chromatography columns, causing band broadening and reduced performance due to inter-particulate mixing. The velocity profile through a monolith on the other hand is incredibly flat and relatively constant across the whole structure. This

eliminates eddy diffusion and axial dispersion, and hence, minimises band broadening as there is no mixing occurring within the column. Mass transfer in monoliths, is therefore not limited by diffusion like in a packed bed column.

$$N_A = ka\ \Delta\ C_A = ka\ (C_{Ao} - C_{Ai}) \qquad 2\text{-}3$$

where N_A is the rate of mass transfer (kg s^{-1}), k is the mass transfer coefficient (m s^{-1}), a is the area available for mass transfer (m^2) $\Delta\ C_A$ is the change in concentration of component A between the phase boundary and the interface as described by ($C_{Ao} - C_{Ai}$). C_{Ao} is the concentration at the phase boundary of component A (kg m^{-3}) and C_{Ai} is the concentration at the interphase of component A (kg m^{-3}).

In a packed bed column, which is limited by diffusion, this equation can be rewritten as

$$N_A = k_L\ a\ (C_{Ao} - C_{Ai}) \qquad 2\text{-}4$$

where k_L is the liquid-phase mass transfer coefficient (m s^{-1}).

The main resistances to mass transfer in a packed bed column are shown in Figure 2.6 for reference.

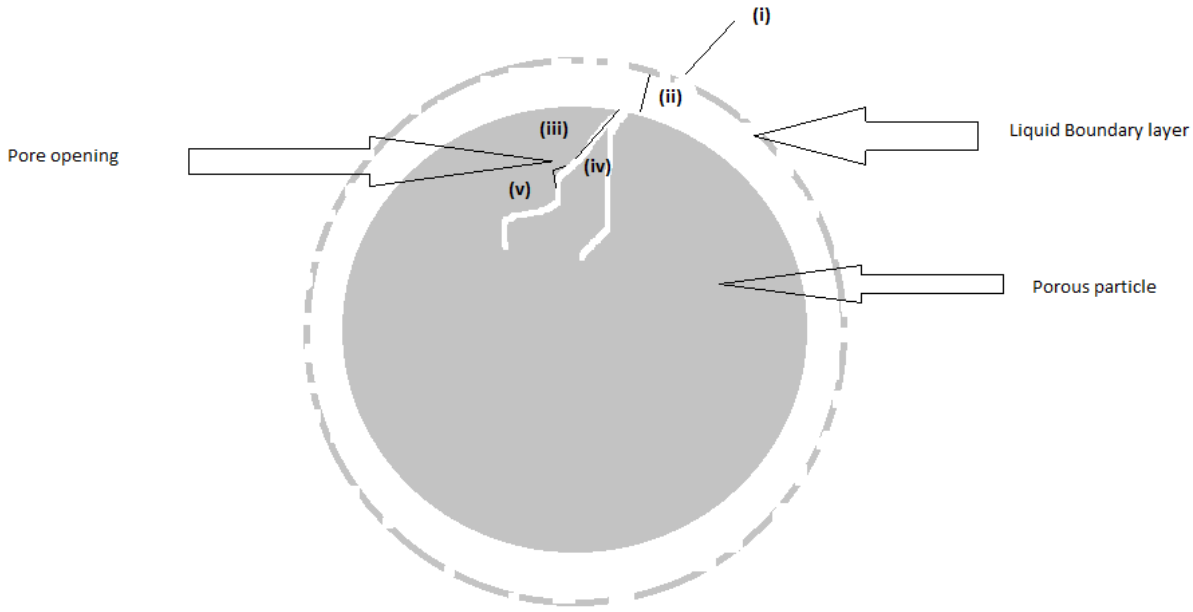

i) Convective mass transfer from bulk liquid to boundary layer

ii) Diffusion across liquid boundary layer

iii) Diffusion into micropore

iv) Adsorption at solid liquid interface

v) Surface diffusion

Figure 2.6 An illustration showing the resistances to mass transfer involved in the adsorption of a solute molecule to a ligand within a micropore of a resin bead in a packed bed system adapted from (Bak et al. 2007).

A typical adsorption isotherm for a short bed monolith is highly favourable and often fits with Langmuir isotherms, as shown in Equation 2-5.

$$q = \frac{q_{max}\, c}{K_D + c} \qquad 2\text{-}5$$

where q_{max} is the maximum solute binding capacity (kg m^{-3}), K_D is the dissociation constant (m^3 kg^{-1}), c is the concentration of solute in the mobile phase (kg m^{-3}), and q is the concentration of solute bound to the adsorbent (kg m^{-3}).

The generation of adsorption isotherms is challenging when using infectious virus as a starting material. This is due to the complex nature of the analytics. Viral quantification assays tend to be incredibly variable with percentage coefficients of variance of >30% routinely. This is a challenge when making any process development decisions, but when attempting to create isotherms to describe adsorption equilibrium for modelling applications a higher degree of certainty is required. Efforts to model mass transfer properties of monoliths have therefore been performed using model proteins such as BSA, lysosyme and IgG (Hahn, Panzer, Hansen, Mollerup, & Jungbauer 2002), which can be quantified easily using UV absorption-based techniques.

As previously described, monolith porosity is very high ($\varepsilon > 0.5$). In practical terms this makes it possible to operate monoliths at high flow rates without significant pressure drops which, coupled with high binding capacities for large macromolecules, results in significant advances in productivity compared to packed bed chromatography. CIM monoliths from BIA Separations can be operated at >10 column volumes (CVs)/min at small scale (1 mL) and ~ 1 CV/min at large scale (8000 mL). In comparison, the majority of packed bed columns are run at between ~0.2 – 0.5 CV/min.

2.4.3 Purification of large complex macromolecular entities using CIM monoliths

2.4.3.1 Introduction

Monoliths have been used for a large range of applications, such as the capture and purification of viruses, VLPs, and bacteriophage, which are discussed in this section. Besides this, literature from BIA Separations shows that CIM monoliths have also been used for purifying transfection grade pDNA, IgG, IgM, His-tagged proteins, and His-containing proteins (BIA separations 2010).

2.4.3.2 Virus purification using monoliths

In this section the following will be reviewed:

- Vaccinia virus
- Tomato mosaic virus
- Potato virus Y
- ΔNS1-Influenza A + B virus
- Baculovirus
- Adeno-associated virus (AAV)
- Lentivirus
- Adenovirus type 3 dodecahedric virus-like particles
- VLPs generated in Saccharomyces *cerevisiae*
- Staphylococcus *aureus* bacteriophages
- Bacteriophases, Lambda, T7, and M13

Following a review of the literature, there has been some recent work on MVA purification using CIM monoliths, but authors have indicated severe challenges in removing DNA to the required specifications of 10 ng/dose (Yang 2013). The authors suspected a strong association between MVA and genomic DNA, which appeared to prevent viral enrichment during IEX or HIC chromatography. What is interesting is

that this interaction appeared to be reversed after the addition of certain chaotropic agents. 250 mM NaBr and 150mM KCl were added to CR.pIX avian cell culture infected with MVA prior to lysis. Diatomaceous earth was then added post lysis and incubated for 20 minutes at room temperature before being removed by filtration using 0.2 µm glass fibre disks. Subsequent IEX monolith chromatography was able to yield a concentration of DNA/dose (assuming a relatively low dose of $1x10^8$ plaque-forming units (pfu)) of 2 fold above the acceptable levels for clinical applications (Jordan et al. 2015a). The percentage yield of infectious virus achieved is not available. This work clearly outlines the challenges and complexity of removing contaminating DNA from viral feed streams and indicates a clear unmet need to develop a process capable of removing DNA and other impurities in order to develop vaccinia virus at the required levels of purity in an economically feasible way. This will become particularly urgent if clinical trials currently involving the development of vaccinia virus for oncolytic applications are successful.

A study by (Kramberger et al. 2004) used CIM quaternary amine (QA) monolith disks to concentrate tomato mosaic virus (ToMV) by several orders of magnitude. This technique was intended to be, and hence optimised, for the concentration of ToMV in irrigation waters, which are typically well below the limits of detection by standard ELISA quantification assays. It was shown that even low concentrations of virus in irrigation water can infect plants and cause losses to crops, particularly in a greenhouse environment. The method development focused around viral concentration, with the main optimisation criteria being percentage yield. This was so that the total amount of virus eluted from the column could then be measured for a given volume of water so as to determine the relative concentration of virus in the water system. The yield achieved from CIM QA monoliths after two parallel experiments was 90% and 89% by ELISA, respectively. Virus was eluted in 1.5 M NaCl in sodium acetate buffer pH 5.5.

ToMV was also purified using CIM QA monoliths as described by (Kramberger et al. 2007) for the development of a preliminary quantification technique to replace ELISA and reverse transcriptase PCR (RT-PCR) technologies, which are labour intensive and take a long time to complete. The study describes the generation of a standard curve by loading five samples on the CIM QA monoliths at different concentrations of between 0.1 mg/mL and 0.43 mg/mL. The virus was eluted from the column using a linear gradient between 0-1.5 M NaCl in sodium acetate buffer, and the corresponding peak height was measured by UV absorbance at a wavelength of 280 nm. This data was then used to generate a standard curve for the assessment of unknown virus concentrations using the same method.

At preparative scale CIM QA was able to purify ToMV removing >99% of the contaminating DNA and all quantifiable protein. The percentage viral recovery was shown to be as high as 90%. Virus was elution between 0-1.5 M NaCl in sodium acetate buffer using a multi-stepwise elution schedule. This is comparable to conventional ultracentrifugation-based purification of ToMV; however, the authors point out that the process can be shortened from 5 days to 2 hours when using monoliths.

More recently, CIM QA 0.34 mL monoliths disks were used to purify Potato virus Y (PVY) produced from inoculated leaves from *N tobacum cv* White Burley and both leaves and stems from Solanum *tuberosum cv* Pentland plants in a study by (Rupar et al. 2013). This was the first time that a filamentous virus had been purified using monoliths and showed a number of purification challenges due to its size, shape and flexibility. The dimensions of PVY are 700 nm x 11 nm. Impurities originating from the plant cell lysate material such as cell wall components, pigments, poly-phenols and a variety of host cell plant proteins and organelles posed challenges to purification due to their variety and complexity. PVY is also known to aggregate, causing reduced yields during

purification. As with all infectious viruses, PVY presents an analytical challenge with regards to the quantification of infectious virus particles and contaminants. To combat this, the authors used a number of different analytical techniques in order to build a complete picture of process performance. Transmission electron microscopy was used to measure viral integrity, RT-PCR was used to measure PVY RNA, SDS-PAGE and a 260 nm/280 nm UV absorbance ratio was used to estimate viral purity. In the presence of 0.5-1M urea, which was added to the load to prevent protein-induced aggregation, 99.9% of plant nucleic acids were removed as well as all quantifiable protein. Up to 50% of the viral RNA loaded was recovered across the elution factions, which after inspection using TEM contained integral PVY. The infectivity of the recovered virus was tested by infecting healthy *N. tobacum* plants with purified PVY, and it was found that infectivity was not significantly affected by CIM monoliths. Elution was performed in two parts, first a stepwise elution was run from 0.1 - 0.25 M NaCl and then a linear gradient was run between 0.25–1 M NaCl over 100 column volumes with Tris buffer containing EDTA.

Ion exchange CIM monoliths have been used to purify Vero cell derived ΔNS1 live replication deficient influenza virus A and B (Banjac, Roethl, Gelhart, Kramberger, Jarc, Jarc, Strancar, Muster, & Peterka 2014). ΔNS1-H3N2, ΔNS1-H1N1, ΔNS1-H5N1, and ΔNS1-Influenza B were all tested. ΔNS1-Influenza A virus strains were found to adsorb to both strong and weak AIEX monoliths, DEAE and QA respectively, as well as strong CIEX CIMSO3 monoliths all at neutral pH. Interestingly, this was not the case for ΔNS1 Influenza B virus which did not adsorb to CIMSO3. The dynamic binding capacity measured for ΔNS1-H1N1 was $1.9x10^{10}$ pfu/mL on CIM QA monoliths, $1x10^{10}$ pfu/mL on CIM DEAE, and $8.9x10^{8}$ pfu/mL on CIMSO3. After scale up to 8 mL CIMQA monoliths, process reproducibility was tested on all viruses. Average infectious virus recovery was between 70.8% ± 32.3% and 87.9% ± 30.8%. Percentage

removal of contaminating protein was between 93.3% ± 0.4% and 98.6% ± 0.2% and of DNA between 76.4% and 99.9%. All viruses were eluted in HEPES buffer in 500 mM NaCl pH 7.5.

A study by (Gerster et al. 2013b) mentions the use of Benzonase (Merck KgA, Darmstadt Germany) to reduce DNA load challenge going onto CIM monoliths. The study deals with the development of CIM QA monoliths to purify infectious baculovirus produced by *Spodoptera frugiperda* cells (Sf-9) using a stepwise elution schedule. It also illustrates the potential use of epoxy monoliths for the removal of lipids from the feed stream run in flow through mode. The percentage recovery of infectious virus was shown to be highly dependent on the age of the load and its composition; DNA concentration, levels of aggregation, and ratio of infectious to inactivated virus. The recovery of infectious virus in the main elution pool was between 20% and >99%. The total protein removal was reported to be between 92% and 99%, and DNA removal between 52% and 62%. Virus was initially eluted over a linear NaCl gradient between 0.2–1 M, however, this was later redesigned and virus was eluted using a multi-stepwise elution schedule. This paper stresses the difficulty to report a full picture due to the complex nature of the system, but does use a range of orthogonal assays in an attempt to generate process understanding. These studies illustrate the reduced time needed to purify large amounts of virus using monoliths compared to ultracentrifugation, and the authors suggested that further scalability studies would be worthwhile in order to develop a viable large scale process.

A range of recombinant Adeno-Associated Virus serotypes (rAAV) have been successfully purified using CIM QA monoliths. AAV1 capture using CIM QA monoliths has been shown to yield between 40% and 72% prior to affinity-based AVB-Sepharose (GE Healthcare, Uppsala, Sweden) as a second step (Wang et al. 2009).

Virus was eluted using a stepwise elution schedule in Tris buffer containing 260 mM NaCl. In a separate article, separation of full and empty AAV8 capsids using CIM QA monoliths was performed on 0.34 mL disks (Lock et al. 2012). Virus was eluted over shallow gradients from 80-115 mM NaCl over 20 column volumes. Two peaks were reported over the elution, the first containing empty capsids, these are vectors lacking a genome, and the second containing up to 99% full, genome containing capsids. Results were confirmed both by negatively staining TEM, which showed empty capsids with an electron dense core, and qPCR. This was originally developed as an analytical technique, however, BIA Separations now market CIM QA as both an analytical tool to estimate full/empty ratios and as a preparative method to remove empty capsids from purified AAV material.

CIM DEAE weak AIEX monoliths have been used to purify HIV-1-derived lentiviral vectors (LVs) (Bandeira et al. 2012). LV is known to be very unstable. This is likely due to the degradation of its envelope surrounding the capsid causing loss of infectivity. This often occurs over typical processing conditions during both ultracentrifugation and chromatography using membrane adsorbers, which have been shown to recover ~30% of infectious LV. CIM DEAE achieved a recovery of up to 80% and removed up to 88.8% of contaminating DNA prior to the addition of Benzonase. After Benzonase treatment the whole process was shown to remove 99.9% of contaminating DNA, with an overall infectious LV recovery of 36%. This included losses over depth filtration, chromatography using CIM DEAE, ultrafiltration, and size exclusion chromatography as a final polishing step. LV was eluted in Tris buffer using a stepwise elution schedule at 0.65 M NaCl. A pre-elution wash step contained 0.1 M NaCl was also employed to remove contaminating protein.

In the examples shown above, the main recurring challenge has been to remove genomic DNA from viral feed streams. The main reason why DNA is a problem is that many viral processes require cell lysis. This means that high concentrations of cellular DNA are present in the harvest prior to purification. The exact amount will depend on the cell density and type of primary recovery steps being used. CIM monoliths have shown the ability to efficiently adsorb infectious virus material. Over 50% of virus material loaded is commonly eluted without significant loss in infectivity, and DNA and protein can be removed to an acceptable level with the addition Benzonase. One of the main attributes that will likely drive the industry away from ultracentrifugation is productivity, as many authors have reported significant gains in terms of time when using monoliths with comparable or improved purity and yield. There is clearly more work to be done to improve process performance with monoliths; however, as often shown in the literature, it is currently difficult to draw conclusions due to analytical challenges.

2.4.3.3 Virus like Particle VLP purification using monoliths

CIM monoliths have been successfully used to purify a number of VLPs from partially purified and crude cell lysate. Work by (Urbas et al. 2011) has shown that CIMac QA columns, which are 0.1 mL analytical monoliths supplied by BIA Separations, are able to purify recombinant adenovirus type 3 dodecahedric virus-like particles (Ad3 VLP) expressed in a baculovirus / insect Sf21 cell systems. The recovery of biologically active VLP achieved by CIMac QA monoliths was shown to be 52%, with levels of host cell DNA removal greater than 99%. The monolith process also allowed the purification to be reduced from 5 days, when using ultracentrifugation, to 1 day when using

monoliths. VLPs were eluted between 0-1 M NaCl initially using a linear gradient, and then latter using a multi-stepwise elution schedule in Tris buffer containing EDTA and glycerol. While CIMac columns are primarily used for quantification, this work demonstrated that they can also be used to screen and optimise preparative purification processes.

Work done as part of an EngD collaboration between University College London and BIA Separations as described by (Burden et al. 2012) uses CIM OH monolith to purify VLPs produced in Saccharomyces *cerevisiae*. This study is another good illustration of the potential of monoliths to purify large macromolecules as an alternative to either ultracentrifugation or conventional packed bed chromatography. The author describes problems associated with lipid contamination in the feed stream and outlines a methodology for the removal of lipids prior to the purification process, which was shown to double the DBC and increase the life time of the monolith column. Amberlite / XAD-4 beads were used to remove 70% of the lipids, whilst recovering 80% of the VLP. This increased the CIM OH DBC from 0.11 mg/mL to 0.25 mg/mL. In comparison to Butyl-S Sepharose 6 FF, CIM OH monoliths achieved a DBC of approximately 3-4 fold higher. The recovery of VLP was comparable, 85% from CIM OH and 90% from Butyl-S Sepharose 6 FF. CIM OH load buffer contained 1 M Ammonium sulfate, while Butyl-S Sepharose 6 FF only required 0.6 M. Elution was achieved by a stepwise schedule in phosphate buffer from both columns without ammonium sulfate.

2.4.3.4 Bacteriophage purification using monoliths

A study by (Kramberger et al. 2010) focuses on the purification of Staphylococcus *aureus* bacteriophage (phages) VDX-10 using CIM QA monoliths. This was developed as a one-step purification process, and was scaled up from 0.34 mL CIM QA disks to an 8 mL column. Viable phage recoveries were recorded between 54% and 65%, DNA removal was between 99.4% and 99.8%, and total protein removal was between 90% and 91%. Phage was initially eluted in a linear gradient between 0-1M NaCl over 100 columns volumes. When the process was scaled up, a step wise elution schedule was used at 0.6 M NaCl.

In a separate study (Smrekar et al. 2011) three different phages, T7, lambda and M13 were purified using CIM QA monolith disks. The binding capacity of M13 was found to be very high, $4.5x10^{13}$ pfu/mL. T7 and Lambda phages both showed lower capacities closer to $1x10^{13}$ pfu/mL. All three phages were eluted in a linear gradient between 0-1M NaCl over 20 column volumes with 100% recovery of all phages recorded. Lamda phage, however, required the addition of 0.2 M NaCl in the load in order to reach 100% recovery and maximum DBC.

In conclusion, commercially available CIM monoliths are able to remove impressive amounts of host cell DNA and protein from viral feed streams without compromising viral infectivity. Monoliths offer significant advantages in terms of productivity over traditional unit operations like ultracentrifugation, although differences in infectious virus recovery and purity between the two technologies depend on the virus in question. For example, the percentage recovery of Baculovirus has been reported to be less than 1% following ultracentrifugation (Chen et al. 2009), while human respiratory syncytial virus can reach infectious recoveries of 69% according to (Gias et al. 2008).

The next section will focus on viral analytics, which is a massive challenge and bottleneck in process development. For chromatography to become indispensable for the purification of virus material, conclusions drawn during process development regarding process performance need to be accurate. This is currently not possible in many cases as viral analytics are too variable, and no one assay is able to tell the whole story.

2.5 Virus Bioprocess Analytics

2.5.1 High Level Analytical challenges faced during virus bioprocessing

There are a number of reasons why viral analytics can be a challenge. Prior to the commencement of process development, a precise understanding of exactly what the starting material is and what impurities are present is crucial. The answer to these questions, however, is complex. Many assays are needed in order to generate a realistic approximation of viral titre as questions relating to the number of infectious viral particles, number of transducing units, number of whole, integral viral particles, number of empty viral particles, number of full viral particles, and number of full particles containing the correct genetic material all need to be answered depending on the virus in question. All of these assays add layers of complexity and all of this information needs to be put together in order to generate robust conclusions.

To complicate this further, viruses, unlike most proteins, are generally expressed intracellularly. This means that cells need to be lysed in order to release the virus into the supernatant. Some viruses are lytic, meaning they can be left to lyse the cells themselves, others require chemical or mechanical treatment in order to lyse the cells. During this process, cellular components such as host cell DNA, proteins, and lipids, if

using mammalian, insect or avian expression systems, or cell wall components, pigments, and poly-phenols if using plant cells (Rupar, Ravnikar, Tusek-Znidaric, Kramberger, Glais, & Gutierrez-Aguirre 2013), are released into the supernatant along with the virus. Assays need to be developed that are able to quantify all of these contaminants, especially if they are considered to be critical quality attributes (CQAs).

One of the major contaminants in viral therapies is dsDNA. According to the WHO, Technical report series, No 926, 2004, (World Health Organisation 2004) a smallpox vaccine needs to have less than 10 ng of cellular DNA per dose.

The Host Cell Protein concentration in a final drug substance is often defined as a CQA, however, typical specifications for viral therapies in terms of mass of HCP per viral dose is not as specifically defined as it is for dsDNA.

The reason for this is that acceptability criteria for HCPs will often depend on the production cell line used, specific HCP populations known to be present, and any clinical safety data available. The regulators typically suggest an open dialog with manufactures and require evidence of HCP removal across the process using sensitive and qualified assays. A justification for in-house acceptability criteria is then put forward by the manufacturer.

According to International Conference on Harmonization (ICH) guidelines Q6B: “For host-cell proteins, a sensitive assay (e.g., immunoassay, capable of detecting a wide range of protein impurities) is generally utilized. In the case of an immunoassay, a polyclonal antibody (pAb) used in the test is generated by immunization with a preparation of a production cell minus the product-coding gene, fusion partners, or other appropriate cell lines.(…) “Clearance studies, which could include spiking experiments at the laboratory scale, to demonstrate the removal of cell substrate-derived impurities

such as nucleic acids and host cell proteins may sometimes be used to eliminate the need for establishing acceptance criteria for these impurities".

The FDA and EMA have similar wording each requiring the use of sensitive and GMP qualified assays to monitor HCPs according to ICH guidelines. According to (F.Wang et al. 2015) the actual speciation of HCPs is determined on a case by case basis but is often between 1 and 100 ng/mg of protein. It should be noted that this range in specification is likely taken from the biopharma sector, and therefore relevant for products such as a mAbs and therapeutic protein rather than ATMPs.

1-100 ng/mg does not translate well to viral vectors as 1 mg of vaccinia would be approximately $5x10^{12}$ viral particles; this is assuming the mass of 1 vaccinia virus particle is 5 fg. A dose of vaccinia virus is likely to be around $1x10^{9}$ infectious particles per injection so if the specifications were set to 100 ng/mg of virus then the total mass of HCPs per vaccinia dose would need to be 0.02 ng. This is unlikely to be achievable.

For this study total protein has been recorded across each unit operation and shown to be reduced to LLOQ levels based on the BCA assay. An immunoassay such as an ELISA would be more appropriate for a GMP compliant process to show protein removal, however, it was decided that data from the BCA assay would be good enough to generate process knowledge and understanding while working with vaccinia at UCL. The main reason for this was cost and availability.

When conducting process development of viral vectors for gene therapy applications in industry both PicoGreen and BCA assays are routinely used to test in process samples to show removal of dsDNA and total protein. This is particularly true during early phase development. More specific ELISA assays are then developed, qualified and used for product release testing and as required for in process control following dialog with the regulators.

2.5.2 Current analytical methods used in virus bioprocessing

It is relatively straightforward to get a measure of the total number of particles, assuming equipment availability, in a pure viral sample. Harvest samples are very difficult to analyse without specific assays such as ELISAs as the majority of particles are not viral. Dynamic light scattering (DLS) using a Zetasizer, and Nanoparticle Tracking Analysis (NTA) using a NanoSight, both supplied by Malvern Instruments (Malvern Instruments, Worcestershire, UK), can be used to generate particle size distribution data. DLS is not able to reliably estimate the concentration of particles especially in polydisperse samples due to bias caused by large particle in the solution. NTA does not suffer from this issue as the instrument measures individual particles separately. Neither of these techniques are specific to viral particles. Both the DLS and NanoSight measure the movement of particles and calculate size based on Brownian motion.

NTA works as follows:

A laser is passed into a chamber containing the sample in suspension at between $1x10^6$ and $1x10^9$ particles/mL. The particles scatter the laser beam which is detected by a video camera mounted on top of a microscope permanently set at 20x magnification. The camera records frames of the particles moving under Brownian motion at lengths of time determined by the operator. The particles are then tracked and the hydrodynamic diameter is calculated based on specified temperature and viscosity inputs according to the Stokes Einstein equation shown below.

$$d_H = \frac{kT}{3\pi\mu D} \qquad 2\text{-}6$$

where d_H is the hydrodynamic radius of a particle (m), k is the Boltzman constant (J/K), T is temp (K), μ is viscosity (Pa.s) and D is the diffusion coefficient (m^2s^{-1}).

Tunable Resistive Pulse Sensing (TRPS) equipment supplied from IZON (IZON Oxford, UK) is an alternative system that uses impedance measurements rather than Brownian motion to estimate particle size. A voltage is placed across a tuneable nanopore at constant pressure, and a measurement is made by recording the resistive pulse generated as a particle traverses through. As particles traverse they block the flow of ions through the nanopore and the resulting voltage impedance is measured. The magnitude of the resistance pulse in proportional to the particle size and velocity. TRPS can also measure the zeta potential of individual particles in a sample. This is calculated from the electrophoretic mobility according to the Smoluchowski equation. As the magnitude of the resistive peak is independent of the zeta potential the size and zeta potential can be measured simultaneously for each particle traversing the nanopore.

Flow cytometry, specifically the Virus Counter 3100 from Virocyt (Virocyt CO USA) is a fourth option, this system using general nucleic acid and protein stains to tag viral particles containing both DNA and protein. Particles are then passed through a laser probe region one by one and those emitting florescence from both stains are counted as integral viral particles.

All four systems described above will approximate the total particle concentration in a sample, but each has a very low specificity. What this means in practice is that all four assays will overestimate total virus concentration in a sample, even if only taking into account particles within the specific size range corresponding to the virus. This will be especially true when analysing impure samples.

In order to quantify total particle concentrations more specifically, ELISAs are commonly used. ELISAs use antibodies to bind to conformational epitopes on viral surfaces. Conjugated antibodies are then used to generate a colour change that can be

detected by absorbance plate readers. A common example (AAV2 Titration ELISA, Progen Biotechnik GmbH, Heidelberg, Germany) uses a biotin-conjugated antibody to generate a colour change when streptavidin and a substrate are added.

In order to quantify infectious titre, infectivity assays need to be performed. Examples are Tissue culture infectious dose (TCID50) assays and plaque assays. Transduction assays can also be used, although only for virus that can transduce cells in culture. These assays are cell-based and require trained personal to perform, often taking 5-6 days to obtain a reading. One of the most challenging aspects, however, is the variability commonly seen between replicates. This is routinely above 30% (RSD), but can be as high as an order of magnitude.

The use of a large variety of orthogonal analytical methods to help build a quantitative picture of the system in question is currently thought to be the best option when analysing virus material. This is generally accepted as best practice amongst industry professionals and academics within the field. As previously mentioned, there is no one assay that can provide all the information.

The following table, while not exhaustive, gives a detailed overview of some of the more commonly used techniques for analysing virus material.

Table 2.4 Commonly used analytical methods for the quantification of viral CQAs

Assay	Application	Advantages	Limitations
Quantification of total viral particles and related impurities			
Analytical Chromatography	- Total viral particle quantification	- Fast - Sensitive - Fairly high precision	- Requires base line resolution - Relatively low specificity unless affinity-based - Indirect measure of viral particles / based on standard curve
ELISA (direct or sandwich)	- Total viral particle quantification	- Sensitive - Specific - Fairly high precision	- Indirect measure of viral particles / based on standard curve - Fairly time consuming - Expensive
Electron Microscopy	- Visualisation of virus integrity morphology and polydispersity	- Very high resolution - Generates a visual image	- Expensive - Requires significant expertise - Prone to artefacts
Dynamic light scattering (DLS)	- Particle size distribution / aggregation profile - Quantification of total particles	- Very Fast - Sensitive	- Low resolution - Struggles with polydisperse samples - Non-specific

Assay	Application	Advantages	Limitations
NanoSight (NTA)	- Particles size distribution / aggregation profile - Quantification of total particles	- Very Fast - Relatively high resolution - Generates a visual image	- Non-specific
qPCR ddPCR RT-PCR	- Quantification of total viral genomes	- Fast - Specific - Sensitive - (ddPCR generates absolute quantification) - Fairly high precision	- Indirect measure of viral particles - Requires complex pre-treatment of sample to remove residual viral DNA
Viral counter InDevR	- Quantification total particles (some comparisons made to infectious titre)	- Fast - May give infectivity data	- Expensive equipment - Low specificity
Quantification of infectious viral particles			
Infectivity assays (eg $TCID_{50}$ Plaque Assays	- Quantification of infectious viral particles	- Specific (Infectious virus)	- Time consuming - High variability - Laborious - Requires experienced operators
Cell-based reporter gene assays	- Quantification of infectious replication	- Specific (Infectious replication competent/ transducing units)	- Time consuming - High variability - Requires experienced operators

Assay	Application	Advantages	Limitations
/transduction assays	competent virus Or - Quantification of transducing units		
Quantification of process related impurities			
Protein Absorbance Assays BCA (or similar)	- Quantification of total protein	- Fast - Sensitive - Fairly high precision	- Non-specific - Relatively high LLOQ
RP HPLC	- Quantification of lipids	- Sensitive - Fast - Can give high resolution especially if coupled with mass spec (LC/MS) - Fairly high precision	- Requires base line resolution - Relatively low specificity
DNA Florescence Assays (PicoGreen)	- Quantification of total dsDNA (ssDNA also available)	- Sensitive - Fast - Fairly high precision	- Non-specific - Reagent may be able to detect encapsulated viral DNA
HCP (ELISA)	- Quantification of host cell protein (HCP)	- Sensitive - Specific - Fairly high precision	- Indirect measure - Fairly time consuming - Expensive

2.5.3 Quantification of viral infectivity

Common assays utilised for the quantification of infectious virus particles are often slow, laborious and prone to high variability and human error. The most common is the plaque assay redeveloped from an early method designed to quantify bacteriophage in 1952 by Renato Dulbecco (Flint et al. 2004). The plaque assay works by incubating adhering cells with a virus preparation and allowing it to be absorbed by the cells. The inoculum is then replaced with a gel that prevents viral infection of other cells once the infected cells on the plate are lysed. Circular zones are then formed around infected cells called plaques, which are assumed to be the result of infection from one virus particle. There are a number of variations of the plaque assay including the Fluorescent-Focus assay and the Infectious Centre Assay.

The Fluorescent-Focus assay is very similar to the plaque assay but rather than adding a gel, such as agar, cells are permeabilised with a solvent, such as acetone, and incubated with an antibody against a specific viral protein. A second antibody with an attached fluorescent marker is then added, which recognises the first. Infected cells can then be examined using a fluorescence microscope. This technique is often used for viruses that are not able to kill and lyse cells. The Infectious Centre assay on the other hand is utilised to determine the number of cells in a culture that are infected with virus. It works by growing the cells and allowing viruses to propagate for a short period of time before taking an aliquot of the cell suspension and re-infecting known dilutions of the harvested cells onto fresh adhering cells which are covered in a gel in the same way as when performing a plaque assay. The number of resulting plaques formed is then a measure of how many cells in the original sample were infected with the virus.

The $TCID_{50}$ assay, derived from a statistical method for deriving 50% end points by (Reed and Muench 1938), works in a similar way to the plaque assay, however, does not require the addition of a gel to quantify infection. Instead it relies on the identification of cytopathic effect (CPE) when the cells are observed under a microscope after the infection has taken place. Serial dilutions of the initial virus sample are performed in a 96 well plate containing a monolayer of adhering cells in each well. Plates are then incubated for 5-6 days, depending on the virus, at 37 °C and 5% CO_2.

There has been a lot of work in recent years to develop fast and effective reporter gene assays for the quantification of infectious virus particles. The application of such assays can be within a clinical setting, for example used for diagnostic testing, or can be a process analytical technology (PAT) for virus bioprocessing. There are a number of examples in the literature of reporter gene assays being used for virus replication detection. A study by (Lutz et al. 2005) shows the use of both green fluorescence protein (GFP) and firefly luciferase reporter genes to detect replication of Influenza virus A in 293T cells. RNA polymerase I promoter/terminator cassettes expressing RNA transcripts of either GFP or luciferase flanked by untranslated regions of the influenza A were constructed and transfected into 293T cells. It was shown that after infection with Influenza A the cells started expressing the reporter gene within 6-24 hours. The study used two different methods to detect expression of each protein, GFP was detected using a dual laser excitation FACSCalibur flow cytometer (Becton Dickinson, San Jose, CA, USA), whilst luciferase activity was measured in 293T cell lysate using the Luciferase Assay System (Promega, Madison, WI, USA).

Reporter genes have typically been cloned into the backbone of viruses themselves rather than into cell lines used for titre estimation. An example of how this has been done is given in (Cosma et al. 2004). While this approach has been shown to work,

there are some associated safety concerns. Viruses are known to drop large genes, if a replicating virus was to drop a reporter gene in a patient cells it is unknown whether this might be incorporated in the cellular DNA, and what the effects might be. This risk is that residual DNA might contain oncogenes or infectious agents (Yang 2013).

To get around this issue there are a number of examples of virus induced cell-based reported gene assays where genes are expressed in cell lines under the control of viral promoters that express the gene of interest during infection. A study by (Levy et al. 2010) has used a strong poxvirus promoter 7.5-kDa-STR upstream of luciferase cloned into a pGL4.10 vector and transfected into HeLa cells. The study also used green fluorescence protein (GFP) for live cells assays. When virus infects the cell the promoter sequence is activated by viral transcription factors that are able to pass though the nuclear membrane. Infection causes translation and expression of the reporter gene by the cell.

2.6 Summary

It is clear that vaccinia and other oncolytic viruses hold immense potential to enhance the lives of global populations. Many companies are working with vaccinia and other oncolytic viral vectors to achieve desirable patient outcomes, which could significantly enhance survival rates for patients with difficult and hard to reach tumours. If this potential is to be brought forward to a commercial setting, however, then affordable, safe and well validated manufacturing regimes need to be established.

Vaccinia virus purification remains a challenge. While some work on vaccinia and other large infectious virus particles has shown that monoliths and membrane adsorbers are able to outperform unit operations such as ultracentrifugation in terms of productivity, work to remove DNA and other contaminants whilst demonstrating a robust recovery of

infectious particles is still limited and needs to be understood and developed further. Companies have already made significant investments in ultracentrifugation. Ultracentrifugation is a tried and tested technique requiring very little process optimisation. Recovery and purity of infections virus generated from most ultracentrifugation processes is reasonably high and is acceptable for clinical applications. As a result of this, the industry is cautious not to completely move away from ultracentrifugation. Chromatography does have some significant advantages. There are significantly more factors that can be optimised in order to generate superior process performance. This makes it likely that chromatography will be able to outperform ultracentrifugation. The problem is that as a result of the large number of factors available for optimisation, chromatography requires a lot of process development time, resources and expertise. This is made even more problematical due to analytical challenges associated with estimating total and infectious virus, as robust conclusions on process performance are difficult to generate. A large number of orthogonal assays are needed in order to build up a picture of how a viral process is performing.

Chapter 3

Materials and Methods

3.1 Introduction

All experimental methods undertaken during this work have been explained in a single Materials and Methods section. This chapter is not intended to act as a list of standard operating procedures (SOPs), but has been written in order to allow a reader to be able to repeat any experimental procedure described in this thesis with appropriate training and access to relevant manufacturer's instructions.

3.2 Preparation of vaccinia virus load material

3.2.1 Viral production

Vaccinia virus was produced in *Cercopithecus aethiops* Kidney (CV-1) cells (ATCC) and cultured in Corning® 175cm^2 cell culture flasks (Corning, NY, USA) in an incubator at 37^{0}C, 5% CO_2. Flasks were seeded at a cell density of 1x10^6 cells/flask, measured by a haemocytometer. (All cell counts were measured in duplicate).

The media used was Dulbecco's Modified Eagle's Medium (DMEM), high glucose (4500 mg/500 mL) containing Sodium pyruvate (110 mg/500 mL), and 4 mM L-Glutamine. 5% Foetal bovine serum (FBS) was sterile filtered through a 0.22 µm sterile Millex® syringe filter (Merck Millipore, MA, USA) and added to the media along with 1% penicillin/streptomycin purchased from (Sigma-Aldrich St Louis, MO).

25 mL of DMEM was used as a standard volume for all T175 flasks used.

Cells were infected with vaccinia once they were ~80% confluent. Confluence was measured by eye; a single T175 flask was then trypsinised and the total number of cells counting using a haemocytometer. The resulting count was used to determine the total number of viral particles required per batch.

The multiplicity of infection (MOI) was set to 0.01 pfu/cell. The total number of cells present per batch before infection was calculated as the total number of cells in a single T175 flask multiplied by all 30 flasks per batch.

3.2.2 Primary recovery

Cells were harvested 72 hours post infection using a Corning Cell Scraper purchased from (Sigma-Aldrich St Louis, MO). The resulting cell suspension was centrifuged at 1500 rpm for 5 minutes to pellet the cells and remove the supernatant. The supernatant contains viral forms with an extra envelope derived from the cell membrane. Pelleted cells were re-suspended in DMEM media containing 5% FBS and freeze thawed three times to lyse cells and release virus.

Material was re-centrifuged at 2000 rpm for 5 minutes to remove cell lysate, collected, and stored at -80^{0}C until further processing.

It should be noted that the resulting material was freeze thawed 4 times, aliquots of 1 mL were taken at final thaw in order not to continually freeze and thaw the bulk material prior to chromatographic or filtration experiments.

The size of a single batch of material was kept constant at 30x T175 flasks and yielded ~$3x10^{10}$ infectious virus particles. The final concentration of material, herein referred to as "harvest material" was $1.57x10^{9}$ pfu/mL on average.

3.2.3 Preparation of chromatography load material

Harvest material was diluted 1:5 with equilibration buffer in order to achieve appropriate salt and pH conditions for adsorption. Diluted material was then passed through a 0.8 µm cellulose acetate syringe Minisart filter (Sartorius Stedim Biotech, Sartorius AG, Goettingen, Germany) before being sampled and loaded onto the column.

The 0.8µm filter was put in place to protect the column from potentially fouling materials such as large debris or viral aggregates. A process flow diagram is shown in Figure 3.1.

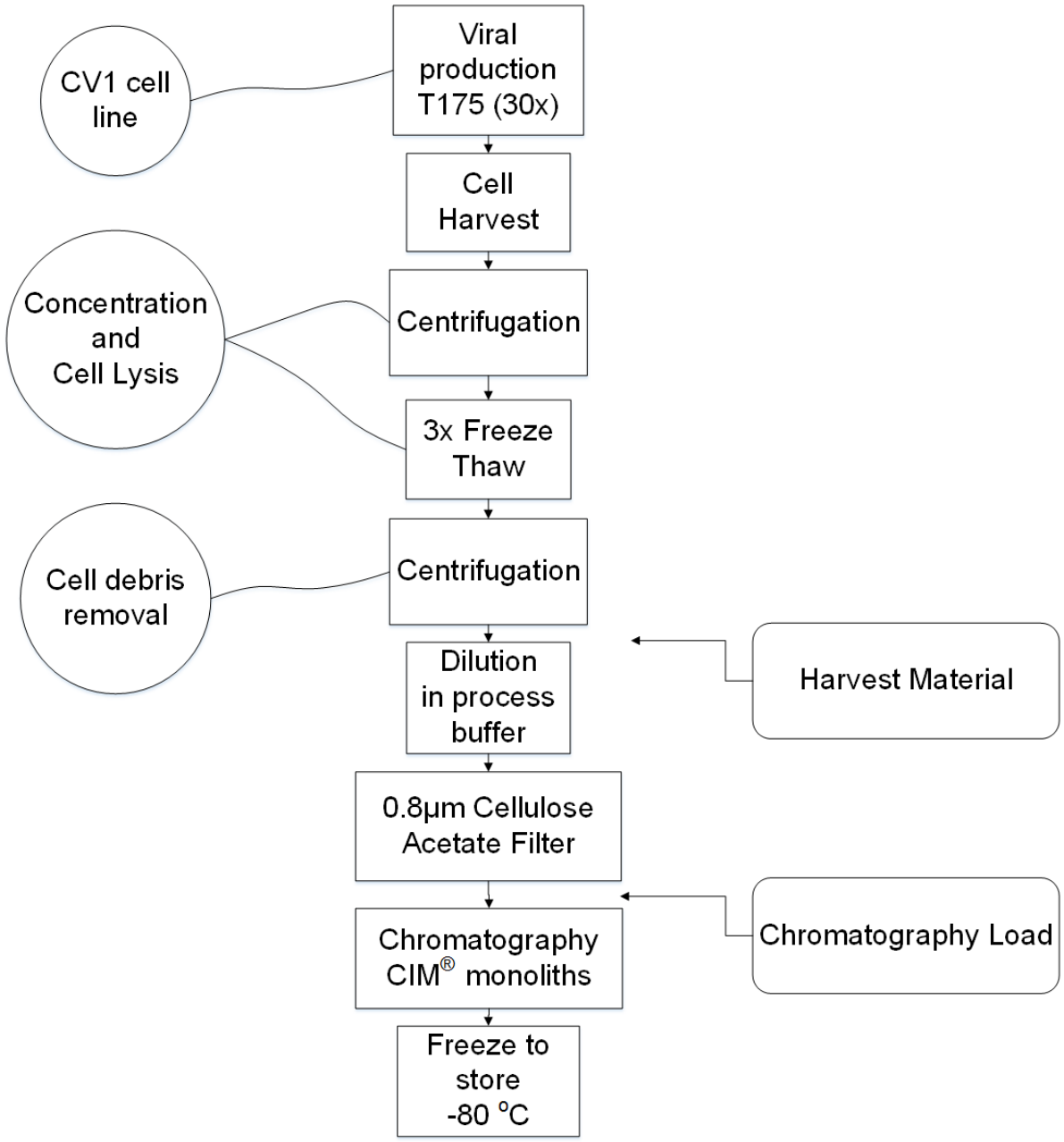

Figure 3.1 Process flow diagram showing method used to produce vaccinia virus throughout this work.

3.2.4 Chromatographic systems used

A number of different chromatography systems were used during this work. Initial studies were performed using an AKTA Explorer (GE Healthcare, Uppsala Sweden). Due to resource limitations, all CIM SO3 stepwise elution optimisation runs were performed using a Pharmacia P-6000 FPLC pump connected to a Pharmacia conductivity monitor. As a UV monitor was not available, elution fractions were collected in fixed volumes and analysed for infectious virus, DNA, and total protein concentration offline. An image of this setup is shown in Figure 3.2.

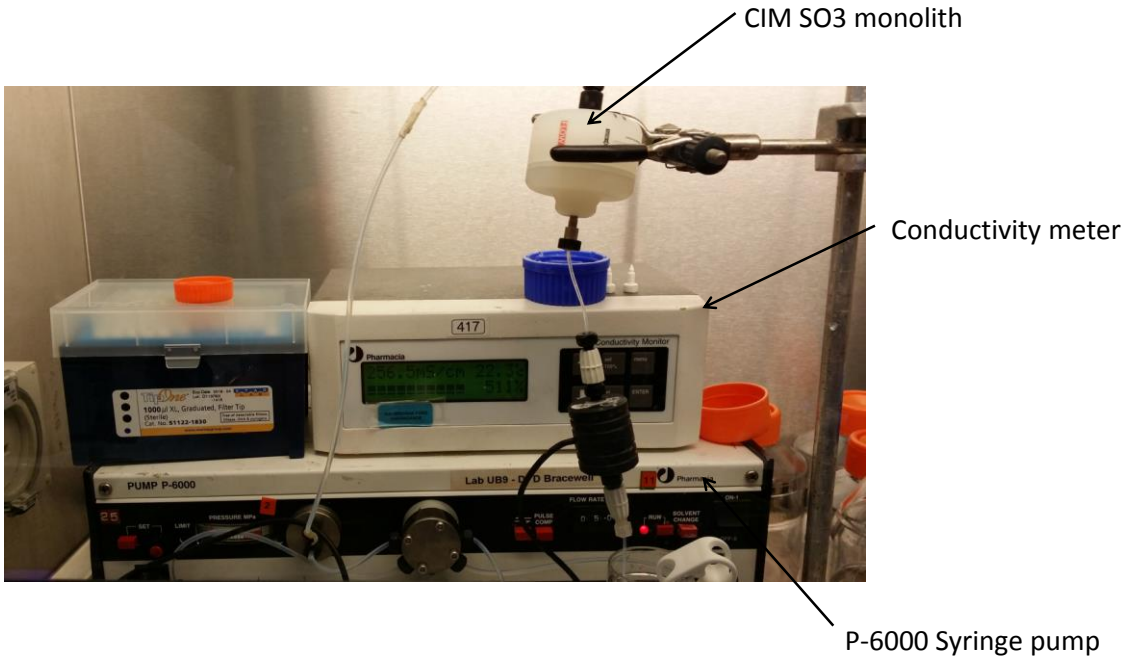

Figure 3.2 Chromatography system setup used for CIM SO3 stepwise elution optimisation runs.

CIM OH optimisation experiments were performed using an AKTA Pure (GE Healthcare, Uppsala, Sweden) with all fractions collected using a F9-R fraction collector. All monolith columns were run at 5 column volumes (CV)/min (195 cm/h) to ensure scalability and all fractions were collected and stored at -80 ^{0}C prior to processing.

As vaccinia virus requires BSL II containment all chromatography experiments were performed in dedicated CAT II laboratories in closed systems inside a biosafety level II cabinet.

The chromatography method used for running each monolith chemistry is shown in Figure 3.3.

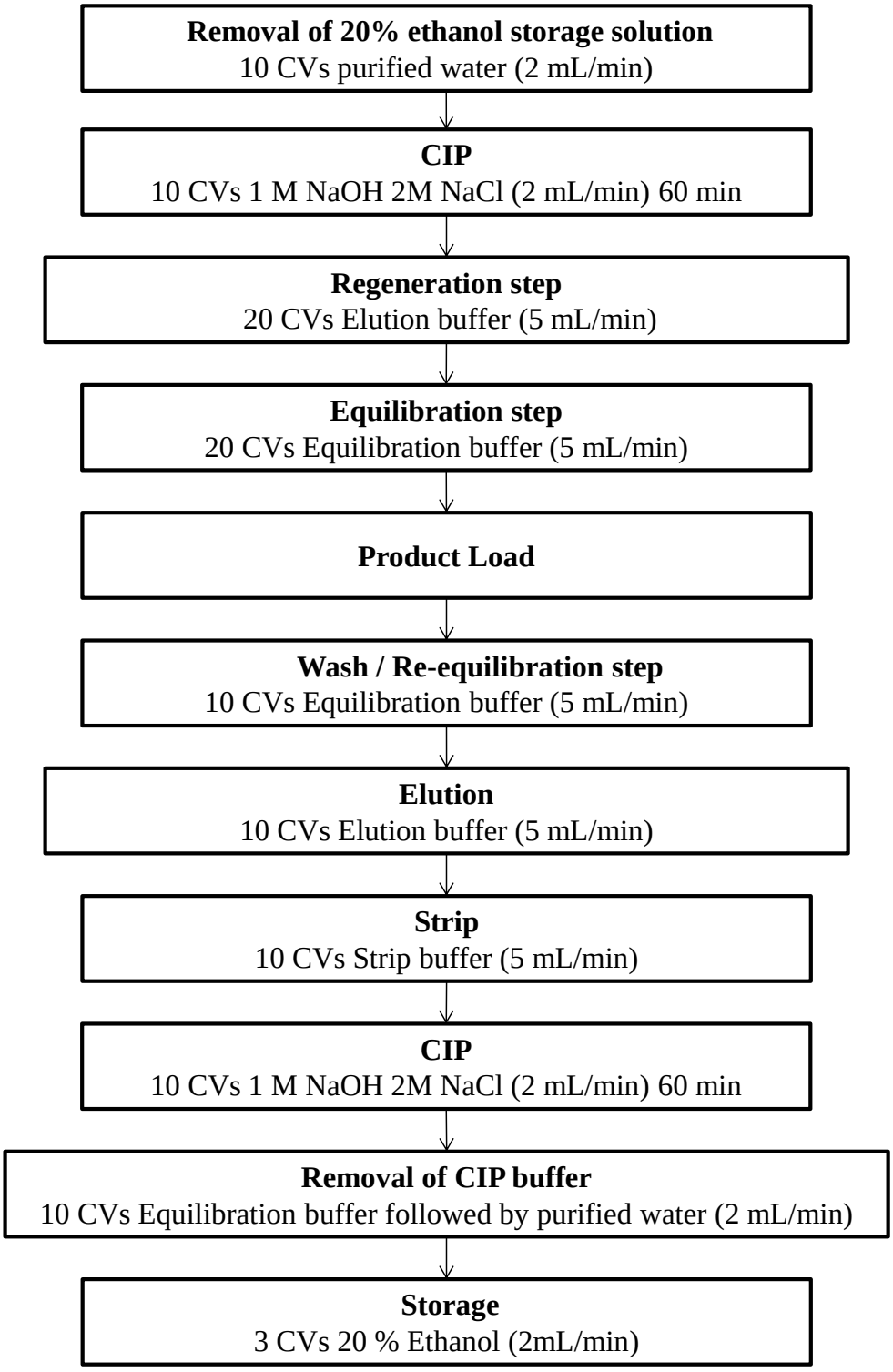

Figure 3.3 Chromatography run setup used for CIM monolith stepwise elution runs

3.2.5 Monolith chemistries used

Four different commercially available Convective Interaction Media™ (CIM) 1 mL monoliths (BIA Separations GmbH, Villach, Austria) were evaluated as potential capture steps for vaccinia virus, each with a nominal channel diameter of ~6 µm.

The chemistries evaluated are listed below;

- CIM SO3-1mL columns, strong cation exchangers due the presence of sulfate groups, negatively charged between pH 2-13
- CIM QA-1mL columns, strong anion exchanges, positively charged between pH 2-13 due the presence of quaternary amine groups
- CIM DEAE-1mL columns, weak anion exchangers due the presence of diethylamine groups positively charged between pH 3-9
- CIM OH-1mL columns, weak hydrophobic columns due to the presence of hydroxyl groups. These are generated by the hydrolysis of epoxy groups. Hydroxyl groups are negatively charged and are very hydrophilic

Monoliths were equilibrated with >20 CV of elution buffer, followed by >20 CV of equilibration buffer after a 60 min sanitisation in 1 M NaOH 2 M NaCl. Wash and elution fractions were both collected in 5 CV fractions throughout. All buffers were sterile filtered prior to use using 0.25 µm membrane filters run in dead end mode at constant pressure.

3.3 Buffer preparation

All buffers where purchased from Sigma – Aldrich unless otherwise stated.

Sodium phosphate monobasic monohydrate (NaH2PO4.H_2O) was purchased as a powder and has a molecular mass of 137.99 g/mol.

HEPES (4-(2-Hydroxyethyl)piperazine-1-ethanesulfonic acid) was purchased in powder form and has a molecular mass of 238.3 g/mol.

The titrant used to pH HEPES and NaH_2PO_4 buffers was NaOH. This was also purchased as a solid and has a molecular mass of 40 g/mol.

Tris base (2-Amino-2-(hydroxymethyl)-1,3-propanediol) was purchased as a powder and has a molecular mass of 121.14 g/mol. Titrant used was HCL ACS reagent, 37% purchased in liquid form with a molecular mass of 36.46 g/mol.

NaCl was purchased as a powder and has a molecular mass of 58.44 g/mol.

Benzonase® was purchased from Merk & Co Kenilworth, NJ, USA

Buffer used to dilute samples containing ammonium sulfate was:

10 mM Tris 2 mM magnesium chloride pH 8.

3.4 Analytics

3.4.1 Quantification of infectious titre

$TCID_{50}$ was the method of choice for the quantification of infectious vaccinia virus particles, and was calculated using the Reed and Muench method (reed and Muench 1938) and expressed in pfu/mL.

The logarithm of the $TCID_{50}$ was calculated as follows:

$$\log TCID_{50} = Log\left(dilution\ factor\ about\ 50\% - \left(\frac{\%\ infected\ cells\ above\ 50\%}{\%\ infected\ cells\ below\ 50\%}\right)\right) \quad (3\text{-}1)$$

This expression is a function of the dilution factor used in each row, and the percentage of infected wells at that dilution factor. The $TCID_{50}$ can be directly found from this expression and this is then multiplied by the volume of diluted virus material added per well in a 96-well plate format in order to generate a $TCID_{50}$/mL value.

In order to then estimate the pfu/mL in a sample of a known $TCID_{50}$, the Poisson distribution is used as follows:

If we take the expression

$$P(0) = e(-m) \quad (3\text{-}2)$$

where p(0) is the proportion of uninfected wells, and m is the mean number of infectious units/volume. If we assume that the conditions for virus infection and

replication are the same in a plaque assay and a $TCID_{50}$ plate then for any number expressed as $TCID_{50}$, the following expression would be correct.

$$P(0) = 0.5 \tag{3-3}$$

This would then mean that,

$$e(-m) = 0.5 \tag{3-4}$$

Therefore,

$$m = -In\ 0.5 = 0.693147 \tag{3-5}$$

A value of 0.69 has been used in all infectivity calculations in this thesis to estimate pfu/mL as follows.

$$\frac{TCID_{50}}{mL}\ x\ 0.69 = \frac{pfu}{mL} \tag{3-6}$$

The $TCID_{50}$ was performed by dispensing 10-fold sample dilutions down a 96-well plate onto CV-1 cells seeding at a density of 8000 cells/well. The plates were then incubated at 37 ^{0}C, 5% CO_2 for 6 days and read by visually inspecting for cytopathic effect (CPE) using a Leica DMIL LED bright field microscope (Leica Microsystems Inc, IL USA) as well as visually inspecting for red fluorescence protein (RFP). An RFP

gene had previously been inserted into the backbone of the virus under investigation; this was driven by a vaccinia virus (H5) promoter. $TCID_{50}$ generated from inspecting for CPR and RFP were equivalent as H5 is a stable promoter and vaccinia is unlikely to drop genes the size of RFP (approx. 401 bp).

3.4.2 Quantification of total viral genomes by qPCR

Relative total intact virus particles were measured using quantitative real time polymerase chain reaction, (qPCR) with Custom TaqMan® QSY® probes (Thermo Fisher Scientific Inc. Waltham, MA, US) which contains a QSY® quencher and FAM® dye.

The virus sample was diluted 1:10 in 20mM Tris buffer 2mM MgCl pH 8 and treated with 350 units of Benzonase® for 4 h at 37^0C. Samples were then incubated at 90^0C for 1 hour in order to inactivate the nuclease and partially lyse the virus. Viral DNA was then purified using the DNeasy Blood and Tissue kit (Cat# 69504 + 69506) (Qiagen, Venlo, Limburg, Netherlands) in accordance with the manufacturer's instructions. The protocol used was for non-nucleated blood.

The total qPCR reaction volume was set to 50µL per reaction, 20 µl of template DNA was used. Forward and reverse primer concentrations per reaction were 900nM and probe concentration was 200nM.

Sequence data was as follows:

Probe: 6-FAM-ATTTTAGAACAGAAATACCC-MGB

Primers: Sense 5'-AACCATAGAAGCCAACGAATCC-3'

Antisense 5'-TGAGACATACAAGGGTGGTGAAGT-3'

A standard curve was generated using chromatography load material purified DNA.

qPCR recovery data is relative to the concentration of DNA in the chromatography load samples.

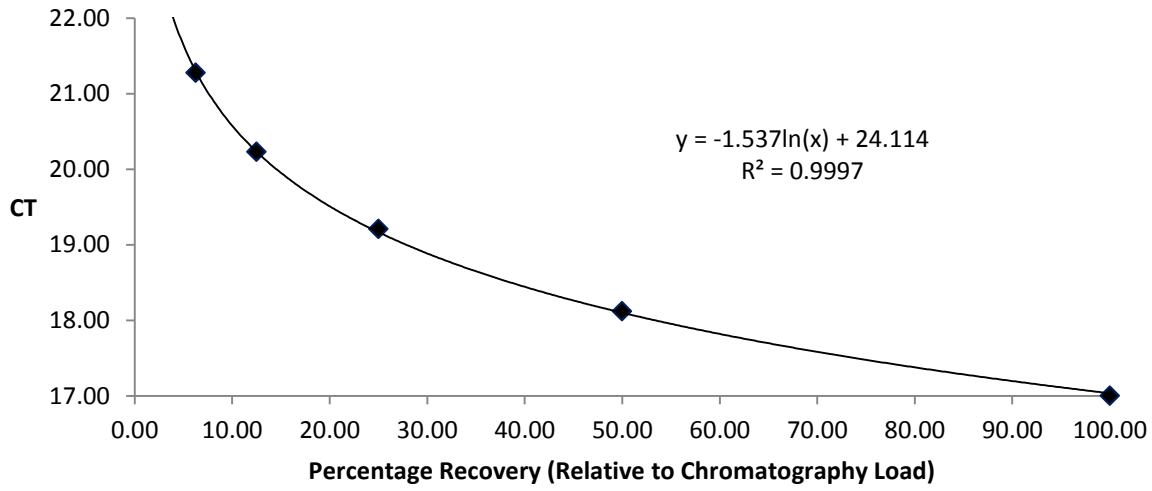

Figure 3.4 qPCR standard curve generated from using chromatography load material

3.4.3 Quantification of total protein

The bicinchoninic (BCA) protein assay (Thermo Fisher Scientific Inc. Waltham, MA, US) was used to assay total protein. Samples were analysed in accordance with the manufacturer's instructions.

This assay works on 2 key principles. The first is the chelation of copper with protein in alkaline conditions in the presence of sodium potassium tartrate known as the biuret reaction. This results in the formation of a light blue complex. During this reaction Cu^{2+} ions are reduced to Cu^{+}. In the second reaction, two molecules of BCA form a complex with each monovalent cation to from a purple complex which strongly absorbs light at 262 nm. As the levels of Cu^{2+} reduction is proportional to the levels of protein in the

sample, a linear standard curve can be generated and used to estimate protein concentrations of unknown samples.

Bovine serum albumin (BSA) was used as a standard for both the generation of a standard curve, between 0 and 2000 µg/mL, and for spiking samples with known quantities of protein to demonstrate the reliability of the assay. The diluent used was 50 mM sodium phosphate (NaH_2PO_4) pH 7.0 and all samples were diluted at least 4 times to ensure appropriate buffer conditions and appropriate protein concentration. All samples were measured in duplicate. The lower limit of quantification (LLOQ) is 20 µg/mL. 40 µg of BSA standard was used to estimate spike recovery.

Micro BCA was used when LLOQ was reached using BCA. Samples were analysed according to manufacturer's instructions. A standard curve was generated between 0 and 200 µg/mL, LLOQ is 2 µg/mL.

3.4.4 Visualisation of total protein by SDS-PAGE

3.4.4.1 SDS – PAGE

Non-reducing SDS-PAGE was used to visualise the total protein in selected chromatography fractions. 10µl of each fraction was diluted in NuPage MES loading buffer containing SDS. Precast NuPage Tris-Bis gels where used with MES running buffer in an XCell SureLock Mini gel tank and run at 100V for 40 min. The protein ladder used was the thermo scientific page ruler plus pre-stained protein ladder. All materials were purchased from Thermo Fisher Scientific (Thermo Fisher Scientific Inc. Waltham, MA, US).

Gels were initially strained with SimplyBlue SafeStain, which is a safe Coomassie G-250 stain for proteins; however protein bands in the elution were too low in concentration to be visible. A silver staining protocol was therefore used.

3.4.4.2 Silver staining protocol

1. Gels were fixed in 500mL of 40% methanol, 10% Acetic acid, in MilliQ for 1 h.
2. Washed in MilliQ 3x for 5min each.
3. Incubated in sensitizing buffer consisting of 5% (w/v) of sodium thiosulfate, 17g sodium acetate and 75mL of ethanol in 250mL with water (MilliQ) for 30 min.
4. Washed in MilliQ 3x for 5min each.
5. Silver stained in 2.5% (w/v) silver nitrate in 250mL of MilliQ for 20min.
6. Washed in MilliQ for 45 s.
7. Developed in sodium carbonate (12.5g) with 200 µL of formaldehyde in 500 mL of MilliQ until bands appears in elution fraction.
8. Stopped in EDTA-Na_2 (3.65g) in 250 mL of MilliQ for 20min.
9. Washed in MilliQ 3x for 5 min each.
10. Preserved in 5% Acetic acid at 2-8^{o}C until imaging.

3.4.5 Quantification of total dsDNA

The dsDNA quantification was done using the Quant-iT^{TM} PicoGreen$^{®}$ dsDNA reagent from Molecular Probes Inc. (Cat. # P7581, Eugene, OR, US). Samples were analysed in accordance with the manufacturer's instructions. Lambda DNA (Cat. # D1501, Promega Corporation, Madison, WI) was used as a standard for both the generation of a

standard curve, between 0 and 2000 ng/mL, and for spiking samples with known quantities of DNA to demonstrate the reliability of the assay. The diluent used for all dilutions was Tris EDTA (TE) and all samples were diluted at least 4 times (and up to 200x) to ensure appropriate buffer conditions such as removal of salt and appropriate DNA concentration. All samples were measured in duplicate. The lower limit of quantification (LLOQ) is 250 pg/mL. 40 µg of λ DNA standard was used to estimate spike recovery.

PicoGreen® is a proprietary asymmetrical cyanine dye, similar to SYBR Green I (Blotta et al. 2005). The dye binds specifically to dsDNA has an excitation wavelength of 485nm and emission wavelength of 530 nm.

3.4.6 Calculation of total protein and total DNA purification factor

A purification factor is a useful way to show the level of clearance of process related impurities such as DNA and total protein in relation to the product. This was calculated according to the equation below.

$$PF = \frac{(C_{DNA} x\, V_{Load})/dose}{(C_{DNA} x\, V_{Elution})/dose} \quad (3\text{-}7)$$

where a dose is assumed to be $1x10^9$ pfu and PF is purification factor. C_{DNA} is the concentration of DNA in ng/mL and V_{Load} is the volume of the load in mLs and $V_{Elution}$ is the volume in the elution in mLs. The PF for total protein was calculated in the same way in each case by substituting concentration of DNA for the concentration of total protein.

3.4.7 Quantification of total particles

3.4.7.1 Nanoparticle tracking analysis (NTA)

NTA (Malvern Instruments Ltd, Malvern, UK) was used to analyse viral particle distribution and total particle concentration. A NanoSight LM10 model was used in all experiments.

The camera level was set to 11 and the screen gain was set to 1. During processing of the video frames, the detection threshold was set either 3 or 5 (stated in figures). Each sample was analysed 5 times and the mean concentration was processed in all evaluations.

Samples were first diluted to within the dynamic range of the assay ($1x10^6$ – $1x10^9$ pfu/mL) using phosphate buffer without salt at pH 7. Dilutions made were typically between 10 and 100. Using a 1 mL syringe the sample was then loaded into the LM10 chamber and progressed manually after every reading. In order to prevent any additional dilution in the LM10 chamber, the optical flat was cleaned and dried between all runs using water and compressed air.

3.4.7.2 Tunable Resistive Pulse Sensing (TRPS)

The qNano, produced by (IZON, Oxford, UK) was used to measure chromatography load and elution fractions in order to determine levels of polydispersity as well as to determine an approximate Zeta potential.

The system was calibrated with 200 nm ceramic beads (ID # CPC 200) in 300 mM NaCl diluted 1000 times.

30-40 µL of virus sample was diluted 1000 times in PBS and loading into the top of the qNano using a p200 pipette. TRPS can measure the concentration of particles between concentrations of $1x10^5$ – $1x10^{12}$ particles/mL.

3.4.8 Visualisation of virus and contaminants using electron microscopy

3.4.8.1 Transmission electron microscopy (TEM)

Virus was fixed with 0.5% glutaraldehyde before being loaded onto carbon coated copper grids. 20 µL droplets were left to partially dry at room temperature, washed with deionised water, and then stained with 2% uranium acetate solution. Grids were prepared in triplicate, and loaded into a Jeol 1010 transition electron microscope (with digital image capture).

3.4.8.2 Scanning electron microscopy (SEM)

Virus was fixed and loaded onto carbon coated copper grids in the same way as is described in Section 3.4.8.1. For SEM analysis grids were not negatively stained with uranium acetate. Once dry, grids where coated with gold palladium using a Gatan high

resolution gold beam coater. Grids were loaded into a Jeol 7401 high resolution field emission scanning electron microscope.

3.4.9 Statistical analysis

Throughout this work infectious virus concentration, total particle concentration and residual DNA and protein concentration measurements were performed in either duplicate or triplicate. In order to calculate error in these measurements relative standard deviation (RSD) was calculated as follows:

The STDEV.S function in excel was used to calculate sample standard deviation, and the sample relative standard deviation. This was under the assumption that the assay measurements taken did not represent the entire population. The following equation is used to calculate sample standard deviation.

$$s = \sqrt{\frac{1}{n-1} \sum_{i=0}^{n} (x_i - \bar{x})^2} \tag{3-8}$$

where n is the total number of replicates for a single sample, x_i is the value of each replicate and $\bar{x}$ is the mean of all the replicates.

The RSD was then calculated as follows.

$$RSD = \frac{s}{\bar{x}} \times 100 \tag{3-9}$$

Multivariate analysis was run using SAS JMP in order to test for correlations between multiple variables. The built in analysis tool uses the Pearson product moment correlation coefficient as a measure of the linear relationship between two variables (SAS JMP 12 2017a).

$$r = \frac{\sum(X-\bar{X})(Y-\bar{Y})}{\sqrt{\sum(X-\bar{X})^2}\sqrt{(Y-\bar{Y})^2}} \quad 3\text{-}10$$

This can be simplified and written as

$$r = \frac{SP_{XY}}{\sqrt{SS_X\, SS_Y}} \quad 3\text{-}11$$

where SP_{XY} is the sum of products, SS_X and SS_Y are the sum of squares for each variable.

DoE was used to model the effects of pH and salt concentration for CIM SO3 monoliths. The R^2 values presented in the analysis shows how much the variation in response values can be attributed to the model (Rouiller et al. 2012). The R^2 values were calculated as follows:

$$R^2 = \left(\frac{SS_{model}}{SS_{total}}\right) \quad 3\text{-}12$$

where SS_{total}, or total sum of squares, is the sum of the squared difference between the response values and the sample mean. This is the total variation in the response values. The $SS_{model,}$ or model sum of squares, is the difference between SS_{total} and the SS_{error}. It represents the variability explained by the model. SS_{error} is the error sum of squares and represents the sum of the squared differences between the fitted values and the actual values. This represents the variability unexplained by the fitted model (SAS JMP 12 2017b).

Throughout this thesis, the adjusted R^2 has been used, which adjusts the R^2 value for the number of parameters in the model. The Adjusted R^2

$$R^2Adj = 1 - \frac{Mean\ Square\ (Error)}{SS_{total}/DF_{total}} \quad 3\text{-}13$$

where DF_{total} is the degrees of freedom for the model and the error. The mean square for error is the sum of squares divided by its associated DF. It represents an estimate of population variance.

In a fitted model the residuals, or difference between the predicted responses, Y_{model} , and the measured observations, x_i, is calculated in JMP using the root mean square error (RMSE). This should be a low as possible.

$$RMSE = \sqrt{\frac{\sum_{i=0}^{n}(Y_{obs}-Y_{model})^2}{n}} \qquad 3\text{-}14$$

3.5 Sample handling

Sample handling is a very important part of virus bioprocessing.

Vaccinia virus stability will be discussed in some detail in Chapter 4. From the offset of experimentation, it was decided that all samples should be treated in as close to the same way as possible so as not to introduce any variability in virus infectivity as a result of handling.

During every experiment, samples were taken of each fraction or stage needing to be recorded. Samples were then aliquoted into smaller volumes for each assay needing to be performed and all samples were left on the bench at room temperature until all experimental samples had been taken. All samples from an individual experiment, such as a chromatography run, were then frozen together at -80 ^{0}C until required.

Chapter 4

Material Characterisation

4.1 Introduction

Initial material characterisation is a very important first step when developing viral bioprocesses. Upstream processes are inherently variable thus an understanding of how much batch to batch variability is likely and why it occurs is crucial if its effects on the downstream process are to be understood.

In many viral processes infectivity is a major critical quality attribute (CQA). Significant amounts of process knowledge and understanding need to come from infectivity assays, which, as discussed in the previous chapter, can have an error range of up to an order of magnitude. This makes it difficult to accept trends taken at face value unless the experiments can be repeated and trends identified many times. Often, due to time and material constraints, this is simply not possible without the availability of optimised high throughput processes and accompanying analytics.

One way to combat this is to identify trends by using more than one analytical technique. These techniques need to be orthogonally coupled with infectivity data in order to generate a "picture" of what is happening in the system under evaluation. What is often challenging is that each technique provides a specific angle of insight into the often complex system, so they can often be misleading when individually evaluated.

In this chapter, characterisation of the viral harvest and chromatography load material will be discussed in detail. The stage in the process in which this material is generated is

indicated in Figure 3.1, a process flow diagram is shown from cell culture to chromatographic capture.

4.2 Harvest titre and residual impurity variability

In an attempt to understand batch to batch variability in vaccinia virus harvest material the infectious titre, DNA concentration, and total protein concentration were measured across a number of batches. Figure 4.1 shows the raw data generated. The distribution in infectious titre is Gaussian and has a mean value of $1.57x10^9$ pfu/mL. Infectious virus was measured across 11 batches, DNA concentration measured across n=6 batches and protein concentration measured across n=3 batches. The distribution incorporates the variability in the analytics as well as inherent variability in the cell culture and primary recovery processes. Figure 4.2 reiterates these points, showing the range in the infectious viral titre, DNA, and total protein concentrations recorded in the harvest material.

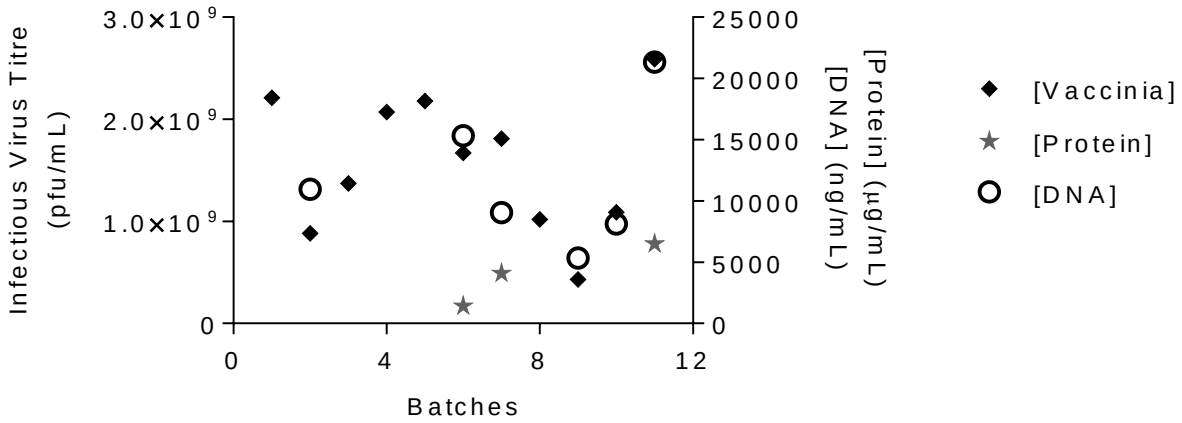

Figure 4.1 Variability in infectious titre, DNA, and Protein concentration in vaccinia virus harvest material post freeze thaw and centrifugation measured across 11 batches.

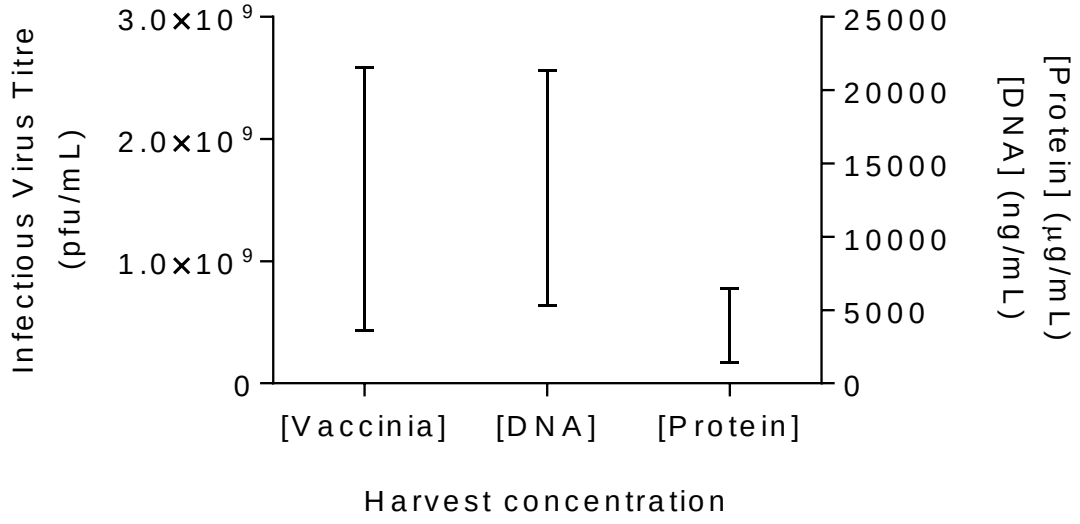

Figure 4.2 Infectious titre, DNA, and total protein concentration range in the harvest material. (Vaccinia titre was measured across n=11 batches, DNA concentration measured across n=6 batches and protein concentration measured across n=3 batches.

When taking a closer look at the data in Figure 4.1, there appears to be a correlation in the concentrations of infectious virus and the total DNA in the harvest material. This trend is also shown in Figure 4.3 after running a multivariate analysis on the raw data. The blue shaded area shows a 95% density eclipse assuming a bivariate normal distribution between each pair of variables. The red line and shaded area shows the fitted regression line and a 95% confidence interval for the fitted regression. The correlation between the virus and DNA concentration is shown to have an r value of 0.8614. The value summarises the strength of the linear relationship between each pair of responses. The correlation between DNA and protein (r = 0.4029) and infectious virus and protein (r = 0.6106) is less significant. The R value is calculated using the Pearsons product moment correlation coefficient as shown in Equation 3-10.

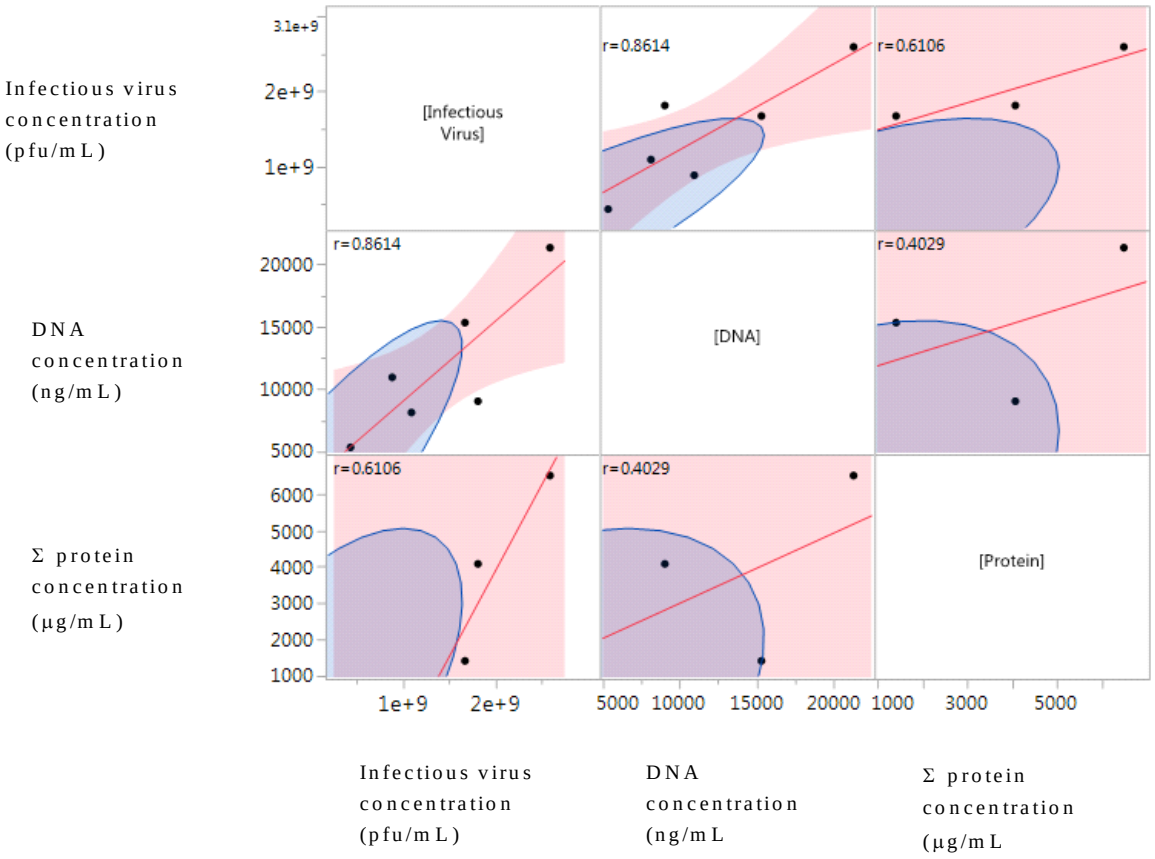

Figure 4.3 Scatterplot matrix showing correlations between variations in concentration of virus, DNA and protein in vaccinia harvest material.

It is possible that this may be linked to the number of cells per batch at the point of infection varying from batch to batch, due to the methods used to estimate the total number of cells per flask. It has been suggested in the literature when discussing indirect measurements for determining cell expansion efficiency that glucose, lactate or DNA concentration may be useful when dealing with cell culture systems in which direct measurements of cell concentration are challenging, such as in hollow fibre bioreactors (Wung et al. 2014). The reason this methodology was not evaluated in this case, was that significant optimisation would have been required as well as an increased amount of manual handling. Cell counting was performed either by using a TC20^{TM} automated cell counter (Bio-Rad Laboratories, CA, USA) or a haemocytometer. The

total number of cells in a single T175 flask was then assumed to be the same across all flasks seeded at the same cell density (of ~$1x10^6$ cells/flask). The total number of cells per batch prior to infection was then calculated as the number of cells in a single T175 flask multiplied by the total number of flasks used. Batches of cells were infected with vaccinia once they became ~80% confluent.

4.3 Determination of vaccinia harvest Zeta Potential

The zeta potential of the viral harvest material was measured using a QNano devise designed by (IZON, Oxford, UK). The Zeta potential of each particle is calculated from the electrophoretic mobility using the Smoluchowski equation. The data is shown in Figure 4.4, and suggests that the majority of particles have a negative zeta potential of approximately -30mV. Similar to NTA the QNano is not able to measure particles of larger than 1µm depending in the nanopore used. This data is in agreement with literature values for vaccinia virus in terms of its isoelectric point, which is between 4 and 5 (Michen & Graule 2010).

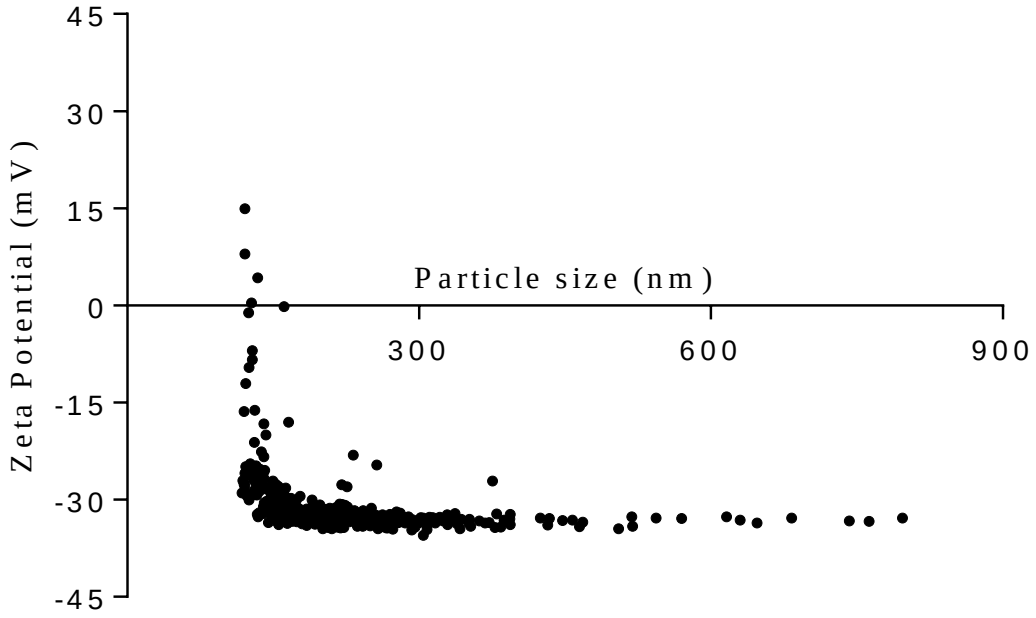

Figure 4.4 Zeta potentials of vaccinia harvest measured using the QNano showing calculated zeta potential values for individual particles. Average value shown to be -32 mV.

4.4 Virus stability

Initially stability studies were performed in order to identify critical process parameters that might have an impact on the recovery of infectious virus during chromatography. The first study shown in Figure 4.5.A was designed to test whether vaccinia harvest material was stable at room temperature, as typical downstream unit operations are conducted without thermoregulation. A 1 mL aliquot of vaccinia harvest was left inside a biosafety level two (BSLII) cabinet and assayed for infectious virus every hour.

The mean data shows an initial drop in the number of infectious particles, although the assay shows high variability in initial measurements. After the first 2 hours, the infectivity remains constant. After running an ordinary one-way ANOVA assuming a Gaussian distribution, no significance was found if a P value cut of 0.05 is used. (P

value = 0.0605, R^2 = 0.5233) On this basis, it was concluded that vaccinia harvest is likely to be relatively stable at room temperature.

The second experiment shown in Figure 4.5.B was designed to test whether increasing the salt concentration would have an impact on the infectivity of the chromatography load material. 50 mM sodium phosphate buffer was made up at pH 7 ranging from 0 to 2M NaCl. Samples were incubated for 2 hours and then assayed for infectious virus. The rational for analysing viral stability in different salt concentrations was that typical load and elution buffers used for IEX and HIC chromatography vary in both concentration and type of salts required. It was decided that any understanding of the edges of failure in terms of loss in infectivity was important.

The concentration of infectious virus is at its highest without NaCl. When 0.25 M NaCl is added, the total number of infectious viral particles decreases by almost 30%; however, as the concentration of NaCl further increases, from 0.25-2 M, the concentration remains constant.

As a control and comparator, the stability of virus in cell culture media (DMEM) containing 5% FBS and hydrophobic interaction chromatography load buffer containing ammonium sulfate was also tested. Samples diluted in media (DMEM) were assayed at t=0 h and t=2 h and the concentration was not found to increase significantly. Given this, it can be inferred that vaccinia virus infectivity, both in media and sodium phosphate without NaCl, is relatively unaffected over a 2 h incubation at room temperature. There does appear to be an initial drop in infectivity in sodium phosphate buffer containing NaCl at concentrations typically seen in chromatographic separations. However, due to assay variability being as high as it is, this difference was not found to be statistically significant (P = 0.2030, R^2 = 0.4314).

A

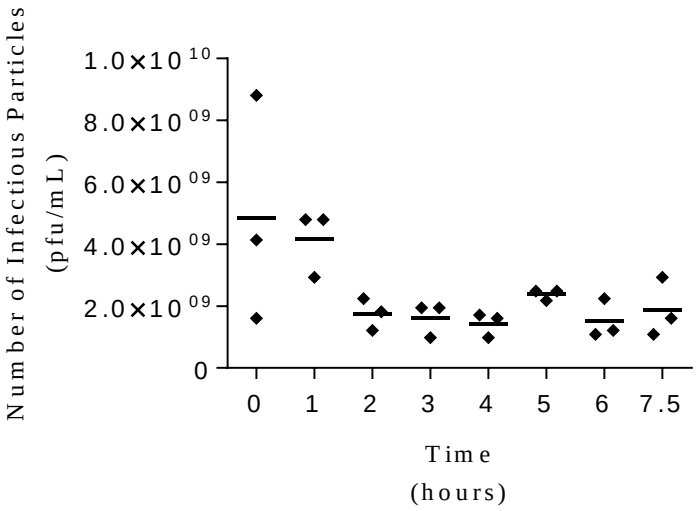

B

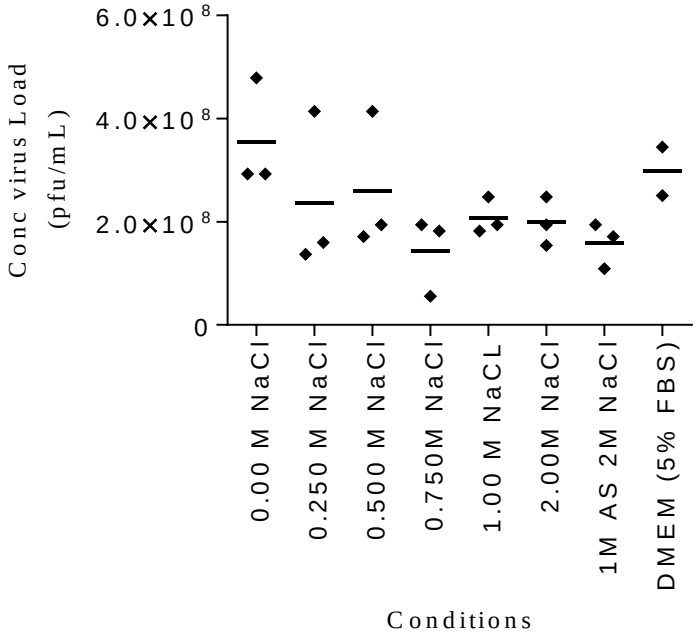

Figure 4.5 A) Vaccinia virus harvest stability time trail at room temperature. B) Vaccinia stability study with increasing NaCl concentration in phosphate buffer pH 7 at room temperature. Points refer to raw $TCID_{50}$ replicate values (n=3), mean values shown as a horizontal line for each condition.

A design of experiments (DoE) was then performed in order to analyse the combined effects of both NaCl and pH on virus stability, again at room temperature, over a 2 hour period, in 25 mM sodium phosphate buffer. Given the inherent variability in the $TCID_{50}$ measurements, fitting correlations to the data is challenging. The ANOVA showed a significant individual P value for effects due to NaCl concentration (P = 0.0048). The P value for effects due to pH was relatively low, but above the 0.05 cut often used to demonstrate significance (P=0.0541). However, after fitting a partial least squared model to the dataset the adjusted R^2 value was only 0.31, and the residuals were high, the RMSE was $1.453x10^9$.

The data is shown in Figure 4.6. Each triplicate $TCID_{50}$ reading is shown as a 3D histogram rather than the modelled data being shown as a response surface plot. There appears to be an apparent increase in stability as pH and NaCl concentration increases. It should be noted that the material used was purified by density gradient ultracentrifugation prior to analysis and so would have contained less DNA and host cell protein. This was due to material availability.

Compared to the data in Figure 4.5 this result does seem to suggest a slightly different trend in terms of the effects of NaCl concentration on infectious virus stability; however, in both cases the variability is around 30%. Under close inspection, this variability appears even higher at high NaCl concentration and pH. While the material in the DoE appears slightly more stable as NaCl and pH increase, the control samples left in DMEM media remained fairly constant at $8.16x10^9$ and $1.41x10^{10}$ pfu/mL respectively. This shows that the sample diluted in sodium phosphate buffer without NaCl recovered only 5% of the infectious particles after 2 hours at low pH.

As aforementioned, robust conclusions are difficult to generate when dealing with highly variable datasets. When considering future chromatographic development it

seems fair to assume that increasing the NaCl concentration will unlikely cause vaccinia infectivity to drop significantly. This makes both ion exchange and hydrophobic interaction chromatography possible candidates when screening different chemistries. As expected, low pH seems to have a negative effect on infectivity. Therefore, when optimising loading and elution conditions higher pH values have generally been used.

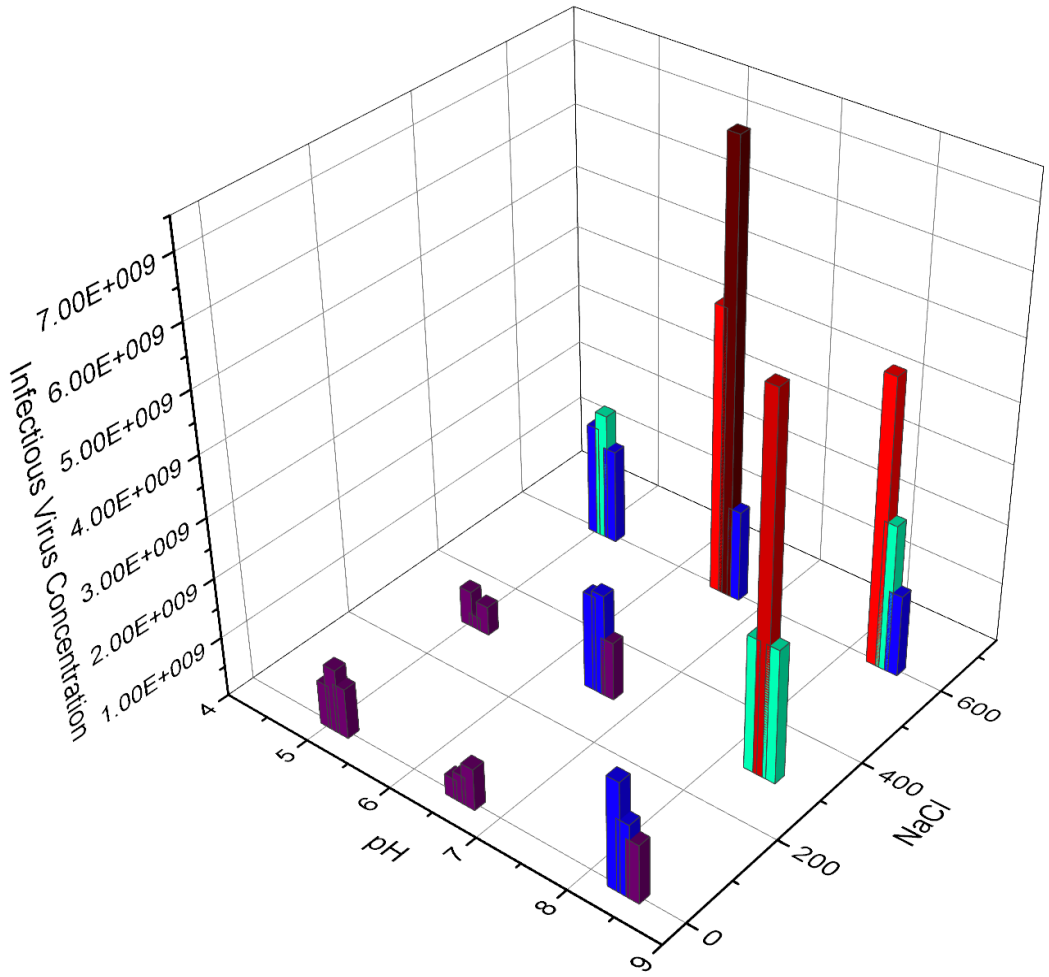

Figure 4.6 3D histogram showing raw data values from vaccinia virus stability factorial design. Virus was purified using 2 consecutive sucrose density gradient ultracentrifugation runs prior to analysis. Study was performed at room temperature over a 2 hour period in 25mM Sodium phosphate buffer. Replicate values (n=3) have been jittered by shifting the pH by 0.1 units. A control was run in DMEM media containing 5% FBS at the beginning, t=0, and after 2 hours t=1, the concentration of the control samples were 8.16×10^{9} and 1.41×10^{10}, respectively.

4.5 Physical characterisation

While infectivity and residual impurity levels are vital to obtain in order to understand process outputs such as efficiency and productivity, not to mention being required for final product release, physical characterisation is also important.

There are a number of techniques available that have either been designed or implemented to study viral integrity, morphology and characteristics such as levels of polydispersity. In this study vaccinia was analysed using transmission and scanning electron microscopy as well as NTA in order to investigate levels of aggregation.

While it is unknown whether viral aggregates need to be considered as a critical quality attribute, it is considered possible that vaccinia aggregation may have an effect on process yield. Data from the literature also suggests that viral aggregation can influence infectivity measurements (Floyd and Sharp 1979). For these reasons it was decided that possible process parameters that could cause or prevent aggregation should be evaluated.

4.5.1 Size distribution using nanoparticle tracking analysis (NTA)

The size distribution of the chromatography load material overlaid with a null prep sample as measured using a NanoSight (Malvern Instruments Ltd, Malvern, UK) is shown in Figure 4.7. The null prep contained uninfected cell lysate prepared in the same way as the virus load. Both samples were diluted in 50mM sodium phosphate buffer pH 7 (1:30) prior to analysis to ensure that the concentration of particles was within the correct working range for the instrument as specified by the manufacturer, (between $1x10^6 – 1x10^9$ particles per mL).

A bimodal distribution is evident in both the load and the null prep samples. Both peaks can be seen to overlay (Figure 4.7) but are at a lower concentration in the null prep than in the virus load. It is speculated that host cell components and degraded viral particles make up the first peak in the load fraction. Vaccinia virus is around 300nm in diameter, which approximately corresponds to the size range of the second peaks. It is likely, therefore, that this population in the load sample contains intact viral particles. The fact that there is a second peak in the null prep sample leads us to the conclusion that there are particles of a similar size range to vaccinia generated during the primary recovery step. Based on this observation, it is expected that the NTA will overestimate the number of virus particles in the load fraction. Similarly, it would likely underestimate the recovery of virus across the column, assuming that a proportion of 300 nm particles derived from the host cell will be removed during chromatography.

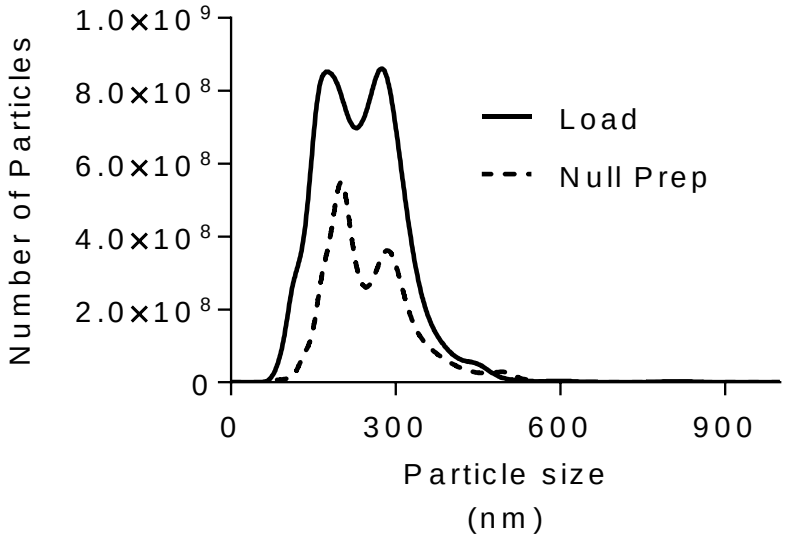

Figure 4.7 Average size distribution data (n=5, 1min tracks, detection threshold 3). Load is vaccinia virus harvest material post dilution post filtration. Null prep is harvest material post dilution post filtration without virus, up and down stream steps treated in the same way throughout.

The effects of high and low salt concentration on particle size distribution were then tested, again using NTA. As this thesis is focusing on the development of a chromatographic process, it was decided to use IEX and HIC load buffers in the evaluation.

Figure 4.8 shows the size distribution of the chromatography load material when diluted in cation exchange (CIEX) load buffer, 50mM sodium phosphate pH 7, and HIC load buffer 50mM sodium phosphate 1M ammonium sulfate 2M NaCl pH 7. The results show that buffer containing ammonium sulfate causes an increase in polydispersity. NTA is unable to identify particles larger than 1000 nm, which may result in some inaccuracy. However, it appears that the profile when diluted in high salt shifts to the right, suggesting self-association of particles in the sample. There also appears to be a slight increase in the number of particles at approximately 150 nm. The reason for this is not clear, however, it is speculated to be due to the aggregation of smaller particles such as fragments of DNA or proteins in the load that has previously been below the dynamic size range of the instrument. As it is unknown from looking at this data whether it is the virus material, contaminants, or a combination of both that are aggregating, the experiment was repeated and analysed using electron microscopy in order to gain more information.

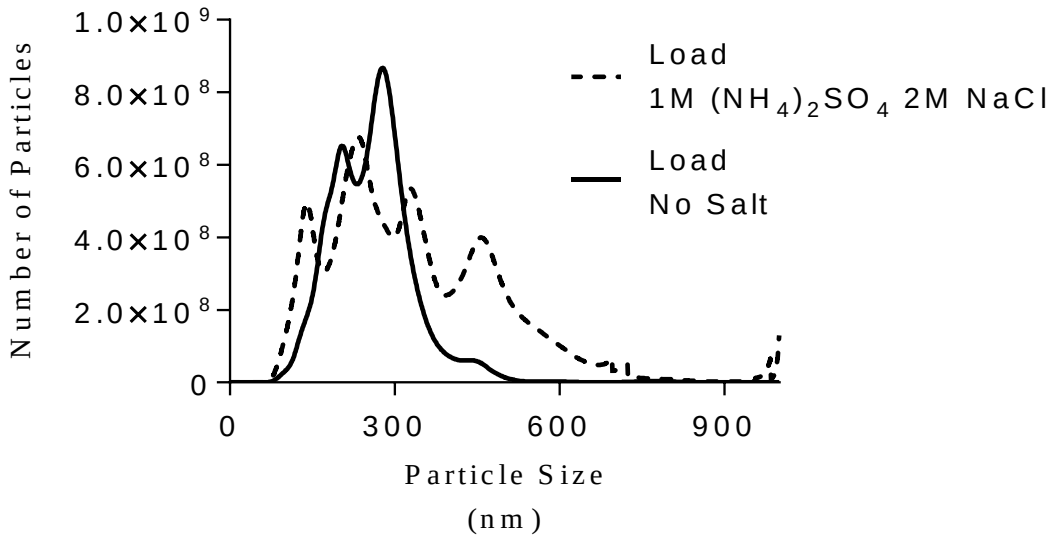

Figure 4.8 Effects of diluent salt concentration on particle size distribution. (n=5, 1min tracks, detection threshold 5) Harvest material post dilution post filtration was diluted 1:30 times in 50mM NaH_2PO_4 pH7 and 50mM NaH_2PO_4 1M $(NH_4)_2SO_4$ 2M NaCl pH7 respectively.

4.5.2 Visualisation of intact particles and evaluation of visible impurities

Information in the literature does agree with initial findings from NTA data. It suggests vaccinia virus is prone to aggregate, especially in impure preparations (Kim and Sharp 1966).

Data generated using transmission and scanning electron microscopy was compared in order to visualise the extent of virus aggregation in DMEM media containing 5% FBS, IEX loading buffer, and as previously mentioned HIC loading buffer conditions. This was then compared to the NTA data previously discussed.

Images generated from electron microscopy are not quantitative. They represent an extremely small fraction of a sample and require a partial drying and staining or gold

coating step depending on the methodology used. Images can therefore only be used to aid in our understanding of more quantitative measurements.

Images generated from impure preps of vaccinia virus in both DMEM and sodium phosphate buffer without salt, appear to show relatively high levels of aggregation, as shown in Figure 4.9 and Figure 4.10. Viral clusters were evident across all grids analysed (n=3 for each sample). Stability data in Figure 4.5.B indicates that virus is relatively stable under both of these conditions. Data in Figure 4.5.A indicates that variability in infectivity is higher at t=0 h than at later time points. This may be due to aggregation. Floyd and Sharp showed that aggregation can impact on infectivity of both polio and reoviruses, (Floyd & Sharp 1979). If aggregation is time dependant, this may explain this initial variation.

A TEM image, at high NaCl and ammonium sulfate concentration can be seen in Figure 4.11. Virus is shown to be positively stained; perhaps due to the size of the clusters formed, nevertheless a large amount of aggregation is clearly visible. When compared to Figure 4.9, which is at the same magnification of 15,000x, the level of aggregation looks significantly higher. As it is difficult to make out individual particles, the sample was also analysed using SEM. This data can be seen in Figure 4.12 and Figure 4.13. Particles of a similar size to vaccinia virus can be seen in Figure 4.12 to form extremely large complexes. The aggregates formed are larger than 6 µm across and appear to be made of many virus like particles. It is speculated that these aggregates in reality are made up of other contaminants as well as vaccinia. This hypothesis is partially backed up in Figure 4.13. A smaller virus aggregate appears to be associated with another material. The image shows two proposed vaccinia particles with an associated structure possible resembling DNA complexed with positively charged histone proteins. It is speculated that this may represent heterochromatin as the structure appears to resemble

the “beads on a string” model often used to describe the complex between DNA and histone proteins. It is well documented in the literature as discussed (Wolff & Reichl 2008) that the removal of DNA from viral feed streams is challenging. These observations, may partially explain why this is the case. DNA is likely to be difficult to remove as a result of the complexes it forms with virus particles. This view was also put forward and addressed in (Jordan et al. 2015).

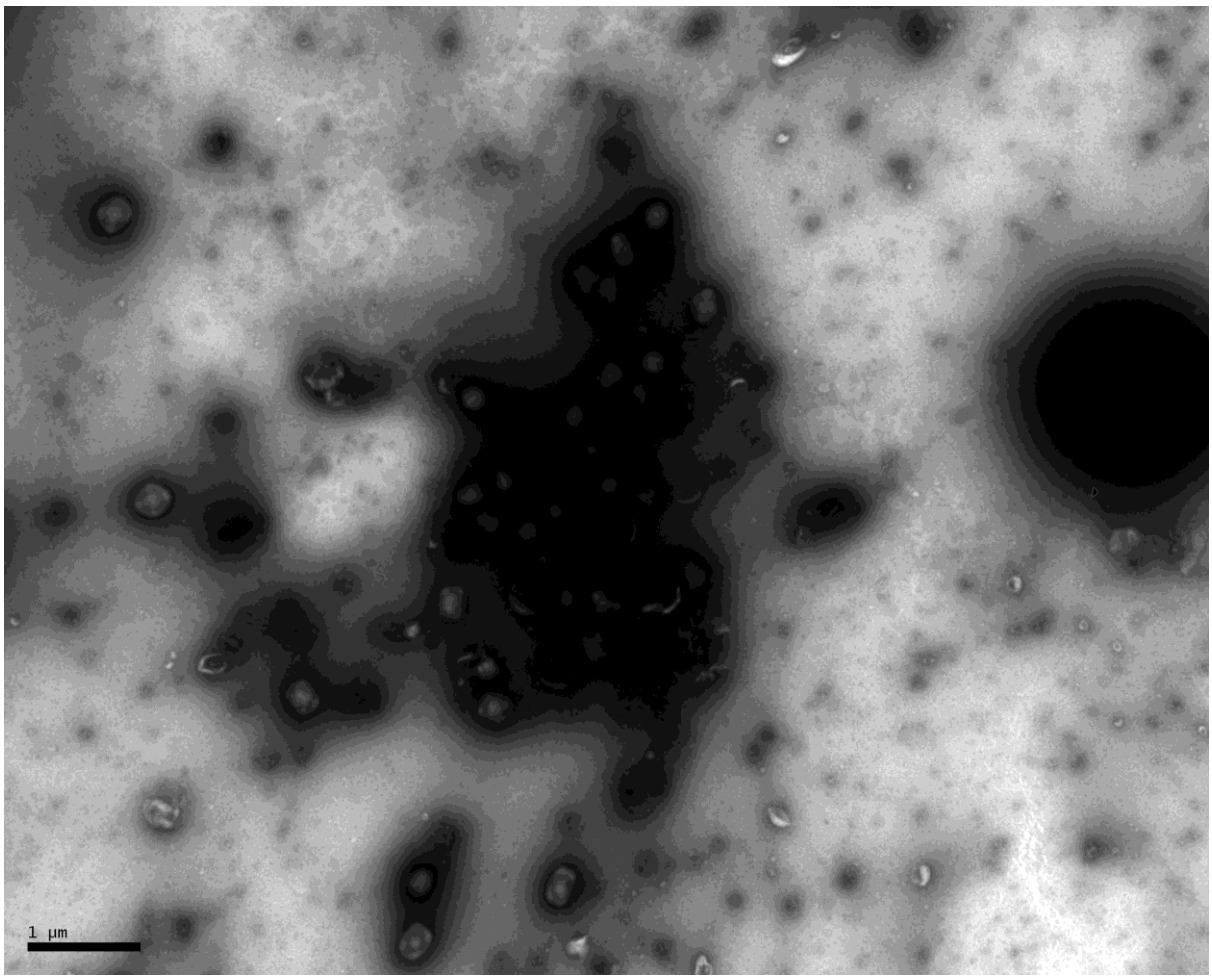

Figure 4.9 Vaccinia virus harvest material in DMEM 5% FBS 15000x magnification, scale bar reads 1µm

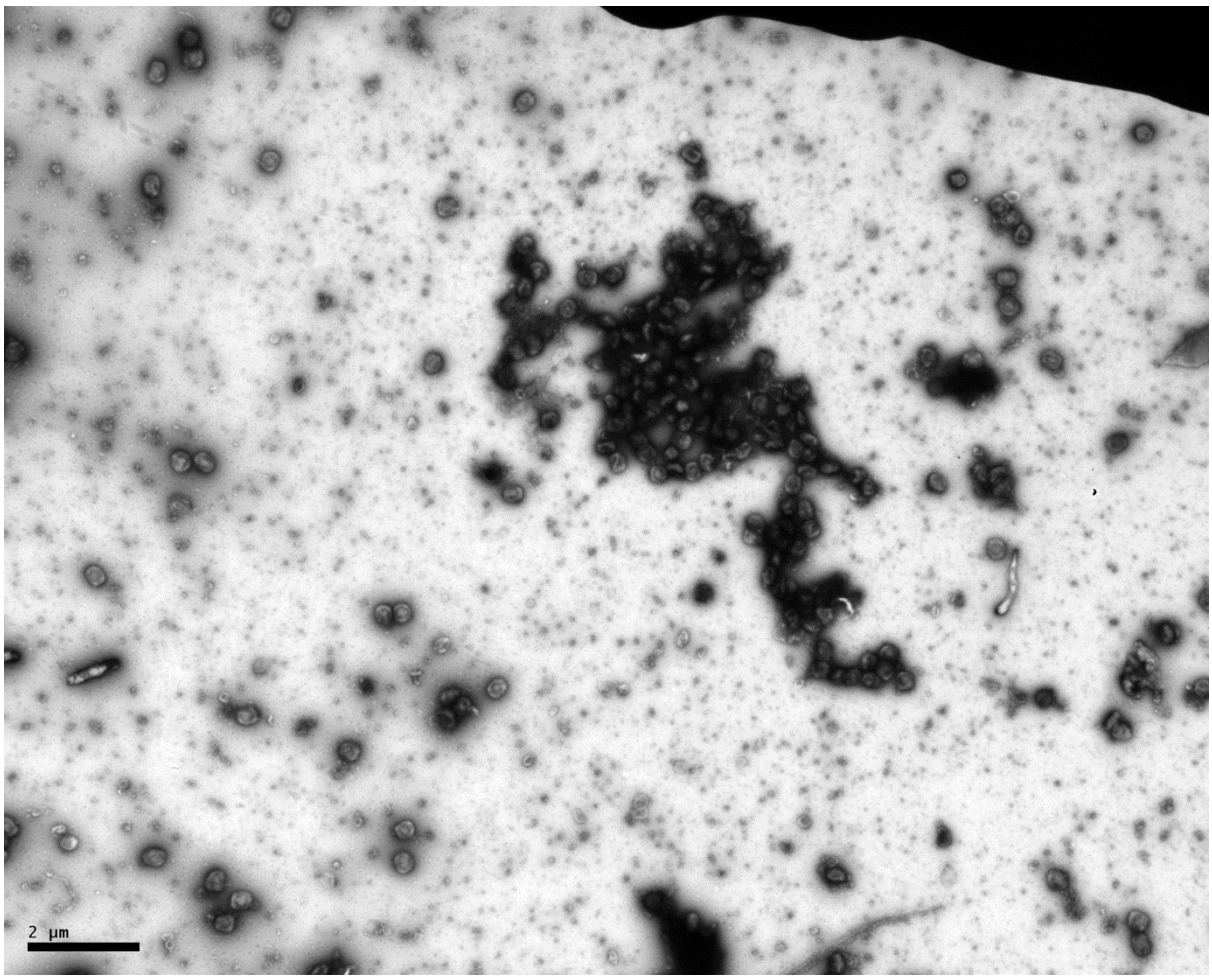

Figure 4.10 Vaccinia harvest diluted in CIEX load buffer 8000x magnification, scale bar reads 2µm.

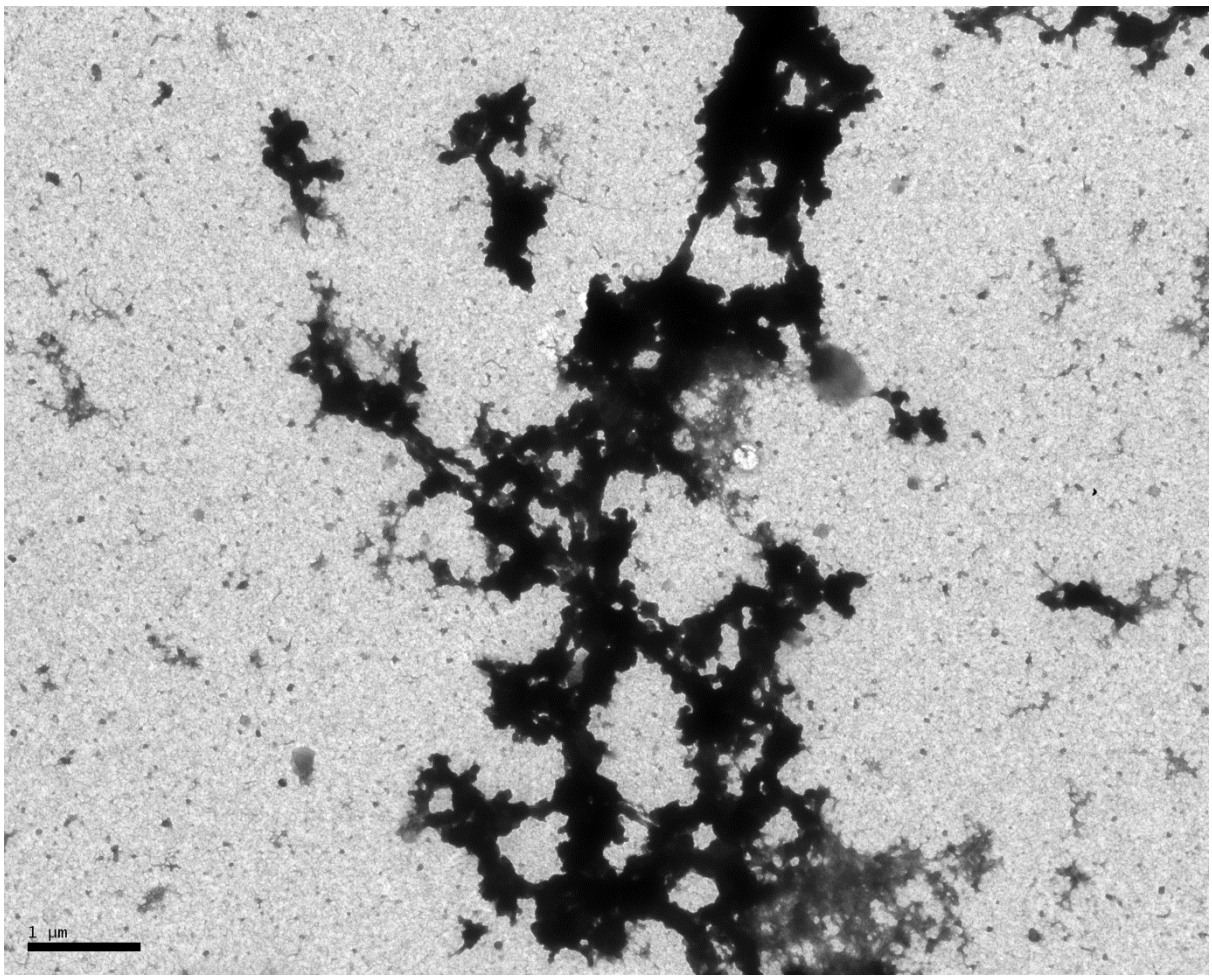

Figure 4.11 TEM micrograph of Vaccinia harvest in HIC load buffer 15000x magnification, scale bar reads 1µm

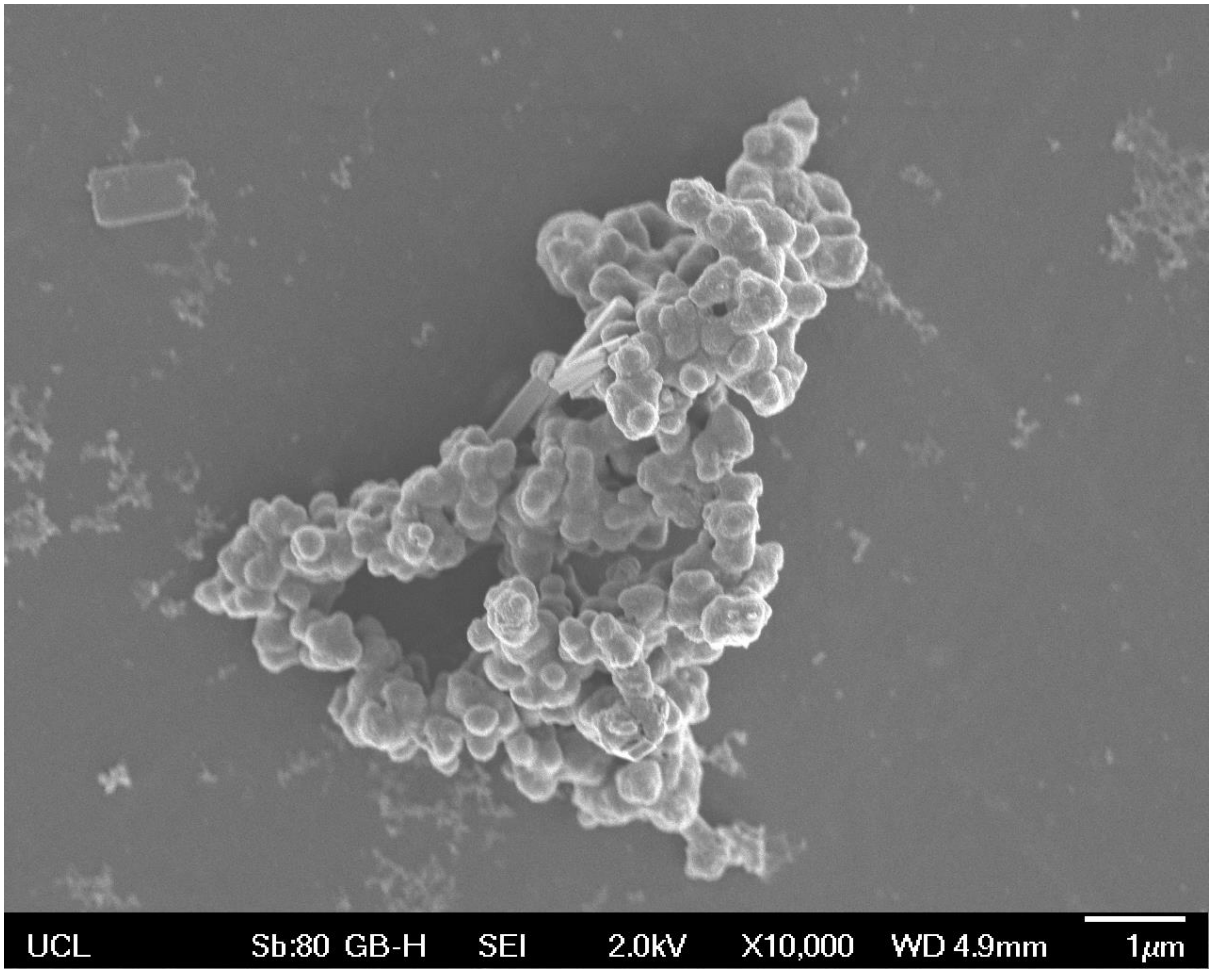

Figure 4.12 SEM micrograph of vaccinia virus material diluted in HIC load buffer 10000x magnification, scale bar reads 1µm Image shows an extremely large aggregated molecules potentially made up of many associated vaccinia virus particles. Rod-like structures are thought to be ammonium sulphate crystals.

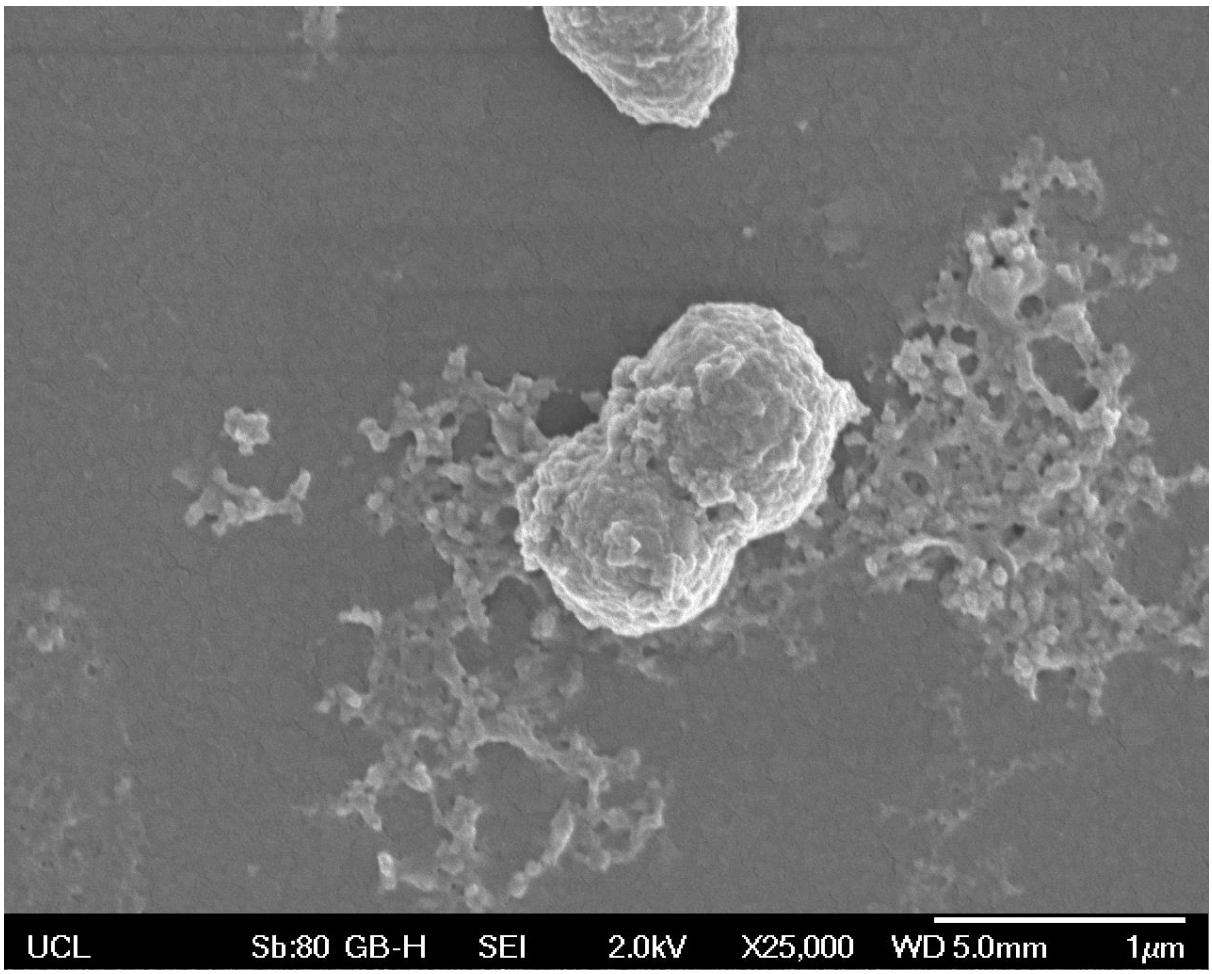

Figure 4.13 SEM micrograph of vaccinia virus material diluted in HIC load buffer, 25000x magnification, scale bar reads 1µm

4.6 Conclusions

Batch to batch variation in infectious viral titre as well as residual impurity concentration has been investigated in this chapter along with virus stability, morphology, and aggregation.

The use of a variety of orthogonal analytical methods has allowed a number of conclusions to be drawn that are important to take into account when developing downstream unit operations. These conclusions are that:

- Vaccinia virus infectivity is relatively unaffected by elevating NaCl and ammonium sulfate concentrations, but appears to drop off over time at room temperature, especially at low pH.
- High levels of aggregation have been identified in impure viral preparations, especially at elevated ammonium sulfate concentration.
- High batch to batch variability in infectious titre and residual DNA and protein concentrations identified, possibly due to variation in the total number of cells prior to infection per batch as well as variability in the $TCID_{50}$ assay.

A full characterisation of viral starting material is a never ending process. What is important is to generate enough product knowledge and understanding to be able to generate and work to understand mass and particle balances generated during process development activities. Without this information troubleshooting activities become impaired, and the generation of robust conclusions on process performance, ultimately contributing to patient safety, is impossible.

Chapter 5

Ion Exchange Chromatography Process Development

5.1 Introduction

As described in Section 2.4.3, ion exchange (IEX) monolith chromatography, and especially anion exchange (AIEX), has been demonstrated in the literature as being capable of capturing and purifying infectious viral particles, virus like particles (VLPs) and other large macromolecular entities. The design of an efficient adsorption-based separation process for vaccinia virus, however, is complicated by its large size and complex physicochemical properties. Enveloped viruses in general are also known to be fairly labile, which has further complicated the development of chromatographic separations. An important constraint is to prevent loss in infectivity post purification. The large size of vaccinia virus excluded many popular IEX adsorbents and attention has been focused on large pore adsorbents. In this chapter, the process development of vaccinia virus using three commercially available ion exchange monoliths for initial capture and purification will be described. The aim was to generate a capture step able to bind and elute infectious vaccinia virus from crude lysate removing double stranded DNA (dsDNA) and proteins. The plan was to start with a screening study designed to test a selection of IEX chemistries, CIM QA, CIM DEAE, and CIM SO3 (each with a nominal channel diameter of 6 μm). The chemistries were chosen based on previously published data on the use of CIM monoliths to purify viruses described in Section

2.4.3.2. It was decided that the most promising chemistry would then be taken forward to start optimising load and elution strategies.

5.2 IEX Monolith Screening Study

Initial screening studies were primarily designed firstly to determine which IEX CIM monolith chemistries vaccinia was able to adsorb to at neutral or weakly basic pH, and then secondly to determine if there were any major differences in viral recovery or impurity removal capabilities from any of the monoliths. Approximately $1x10^{10}$ pfu of virus (10 mL fractions) were diluted 1:5 in IEX load buffer, as shown in Table 5.1, and passed through a 0.8µm cellulose acetate syringe filter, as described in Figure 3.1, before being loaded onto each column. The rationale for choosing the conditions outlined are listed below:

1. Typically low pH is used to remove infectious viruses from biological products (WHO 2004). It was thought that loading vaccinia at low pH would likely cause unacceptable losses in infectivity.
2. Cell culture pH is around neutral (pH 7) therefore it was thought sensible to test both CIM SO3 and CIM QA at pH 7. The rationale here is that vaccinia is likely to be stable at physiological pH.
3. CIM DEAE was run at pH 8.5 as the capacity was speculated to be lower than that of CIM QA at pH 7. HEPES was used in place of Tris for CIM QA when run at pH 7
4. CIM QA was then also tested at pH 8.5 in order to compare directly with CIM DEAE.
5. Tris has a pK_a of 8.07 and is therefore cationic at neutral pH. pH 7 is also at the bottom of its buffering capacity. Sodium Phosphate was used in place of Tris for CIM SO3.

Table 5.1 DNA and total protein purification factors recorded during initial screening studies on CIM SO3, CIM QA, and CIM DEAE. Buffer systems used are as shown, a concentration of 50 mM was used in each case. Equilibration buffer did not contain NaCl. Elution buffer contained 1.5 M NaCl. Purification factors calculated according to Equation 3-7.

Monolith Chemistry	Buffer System (used for equilibration, wash, and elution)	Protein Purification Factor	DNA Purification Factor
SO3	Sodium phosphate pH 7	7.63	0.58
QA	Tris pH 8.5	2.09	0.18
QA	HEPES pH 7	2.18	0.40
DEAE	Tris pH 8.5	2.99	0.16

1 mL radial monolith columns were used in all experiments. The volumetric flow rate used was 5 mL/min (linear velocity = 195.08 cm/h). A process flow diagram indicating each unit operation from cell culture to chromatographic capture is shown in Figure 3.1. Representative chromatograms for each chemistry are shown in Figure 5.1. UV absorbance at 280 nm and conductivity values shown in mS/cm are presented for CIM SO3, CIM QA and CIM DEAE monoliths.

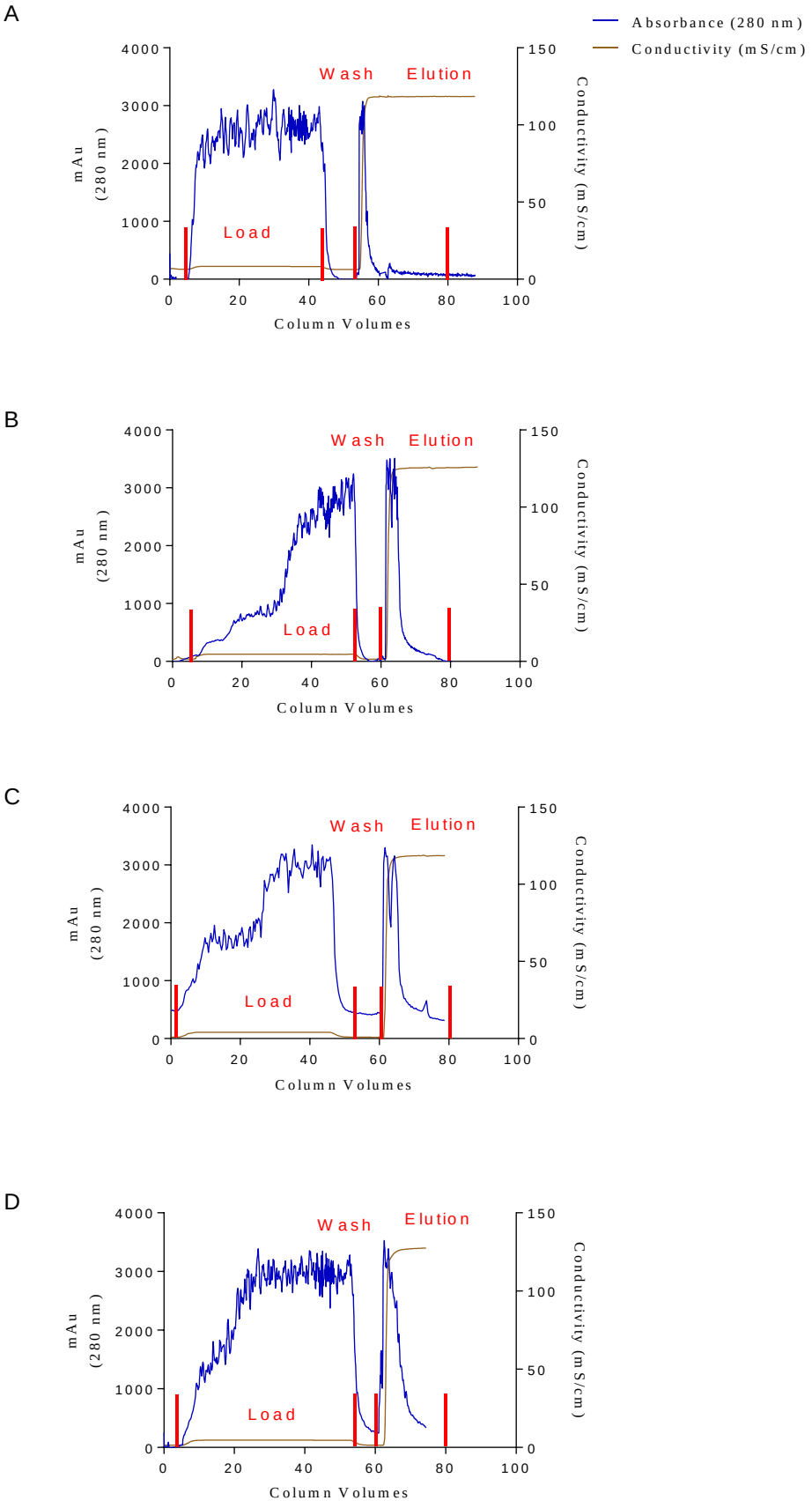

Figure 5.1 Representative chromatograms from CIM S03 in Sodium Phosphate pH 7.0 (A), CIM QA in Tris pH 8.5 (B), CIM QA in HEPES pH 7.0 (C), and CIM DEAE in Tris pH 8.5 (D).

A

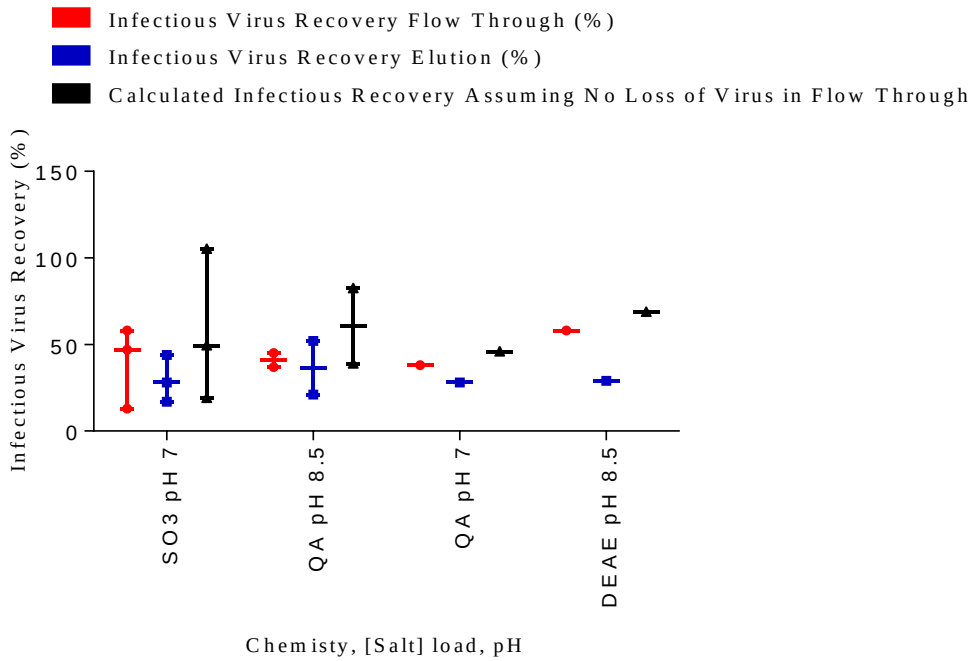

B

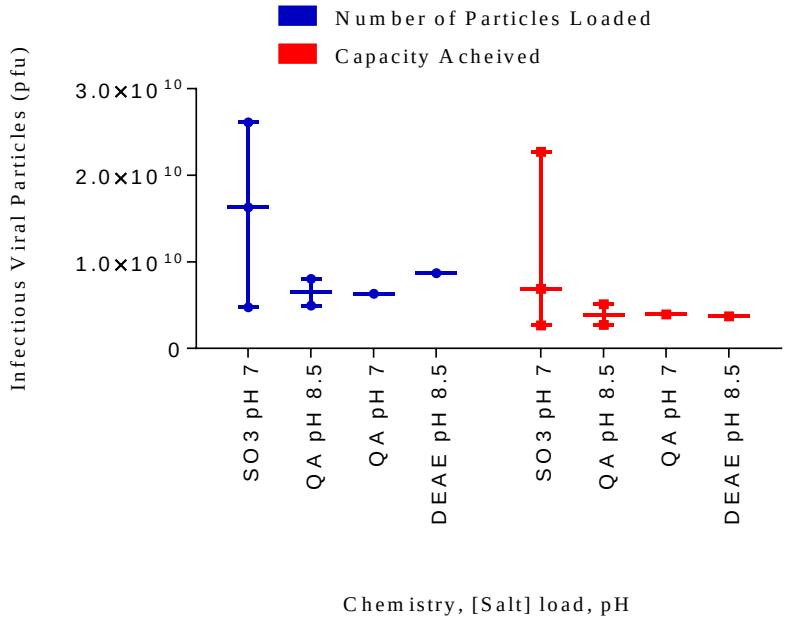

Figure 5.2 A) Box and whiskers plot (median & range) showing infectious vaccinia recovery data from CIM SO3, CIM QA, and CIM DEAE at pH 7 and pH 8.5. Red plots show the percentage of infections virus in the flow through fraction relative to the load, blue plots shows percentage of infectious virus in the elution fraction relative to the load, and black plots show the percentage infectious virus in the elution minus the total number of particles lost in the flow through relative to the load. B) Box and whiskers plot (median & range) showing the number of viral particles loaded vs the capacity achieved on CIM SO3, CIM QA, and CIM DEAE.

After analysing the results, the vaccinia virus concentrations in each stream are shown in Figure 5.2, it can be seen that vaccinia is able to adsorb to both AIEX and CIEX monoliths even though it has a zeta potential of approximately -32 mV (Figure 4.4), and an isoelectric point of between 4 and 5 (Michen & Graule 2010). After a review of the literature it was found that viral adsorption onto IEX resins at both sides of their given isoelectric point has been reported for a number of viruses before (Banjac, Roethl, Gelhart, Kramberger, Jarc, Jarc, Strancar, Muster, & Peterka 2014;Wolff & Reichl 2011;Wolff, Siewert, Lehmann, Hansen, Djurup, Faber, & REICHL 2010b); however, a definitive conclusion as to why it occurs so commonly has not been reached. As with proteins, it is likely that viruses are sufficiently heterogeneous to form electrostatic interactions on the "wrong" side of their isoelectric point (Yamamoto & Ishihara 1999); however, complex interactions between charged viral particles and contaminating impurities of opposite charge may also play a role, especially in crude feed streams.

The recovery of virus in the elution fractions for all IEX monoliths is shown to be comparable indicating that the capacity of each column is similar. However, infectious virus was also found in the flow through fractions, indicating that the columns may have been overloaded (Figure 5.2A).

Residual impurity removal data is shown in Table 5.1. DNA purification factors can be seen to be less than 1, indicating that the net recovery of infectious virus was lower than the recovery of DNA relative to the load for each chemistry. Protein purification factors, on the other hand, show some encouraging results. The AIEX monoliths (CIM QA and CIM DEAE) are able to achieve a protein purification factor of between 2 and 3, while the CIEX monolith (CIM SO3) achieved a protein purification factor of 7.63. This suggests that the majority of proteins in the load are acidic. The experiments were not designed to test for removal of residual DNA or protein, as the elution buffer NaCl

concentrations used were too high (1.5 M). This concentration was picked in order to maximise the recovery of infectious virus.

Following on from the screening studies on IEX monoliths there are a number of conclusions that can be drawn prior to moving on to the next stage in process development.

1. DNA removal will likely be dependent on resolution being achievable in the elution fraction.
2. Protein removal will likely by easier to achieve than DNA removal, as some base-line clearance is seen even without elution buffer optimisation. This is especially true for CIM SO3, as the majority of proteins loaded are recovered in the flow through fraction and so do not bind to the column.
3. Vaccinia virus is able to adsorb to both CIEX and AIEX monoliths at neutral pH.
4. Binding capacity and percentage recovery of infectious virus is similar across all chemistries tested.
5. AIEX monoliths, especially CIM QA, appear to show a double breakthrough in absorbance during the load (as seen in Figure 5.1.B & C). It is unlikely that this phenomenon is due to vaccinia breakthrough, as it does not occur in any of the CIM SO3 chromatograms. It is thought possible that it may be DNA and/or protein as both adsorb to AIEX. The fact that QA is a stronger AIEX than DEAE would also support this theory, since the double breakthrough occurs earlier in DEAE suggesting a lower capacity.

It was decided at this point that only two chemistries would be taken to the next stage of process development due to resource limitations. CIM SO3 was chosen as the main candidate because of its potential to remove protein. More than 60% of the total protein loaded onto CIM SO3 monoliths during the screening study was recovered in the flow through fractions. It was speculated that this would allow elution step design to focus on DNA removal and infectious yield. Based on the data from the screening study, it was not possible to fairly distinguish between CIM QA and CIM DEAE as both showed comparable recovery of infectious particles and achievable capacity as well as removal of DNA and protein. As only one could be taken forwards, however, it was decided that CIM DEAE would be put aside and CIM QA would be developed further. Due to the presence of infectious virus in the flow through fractions from both CIM SO3 and CIM QA it was decided that a dynamic binding capacity study (DBC) needed to be performed. A DBC was completed on CIM SO3 (Figure 5.4D Run 1) and showed breakthrough at approximately $3x10^9$ pfu/mL of monolith. This was taken as an approximate binding capacity for both CIM SO3 and CIM QA monoliths, based on the capacities achieved in the screening studies (Figure 5.2B). The DNA and total protein concentration in the virus load material, prior to running the DBC study, was ~1000 ng/mL and ~700 µg/mL, respectively.

5.3 Evaluation of DNA and Protein Elution Profiles from CIM SO3 and CIM QA Monoliths

A linear gradient elution was run on CIM SO3 as it can be seen in Figure 5.3.A and B and CIM QA monoliths (Figure 5.3.C). The gradient was run over 20 CVs between 0-1.5M NaCl in 50 mM sodium phosphate and 50 mM Tris for CIM SO3 and CIM QA, respectively. Both columns were challenged with approximately $3x10^9$ infectious viral particles. 90% of the virus loaded adsorbed to each chemistry, with only 5-10 % of the infectious virus found in the flow through fractions. The CIM SO3 chromatograms (Figure 5.3.A and Figure 5.3.B) show that the majority of infectious virus is eluted before the DNA. 40% of the DNA in the load is adsorbed to the column, and greater than 90% is removed with a 50% recovery of infectious virus in the first 10CVs. Virus starts to elute after 2 CVs, which corresponds to approximately 150 mM NaCl. DNA is then co-eluted with a smaller viral peak after 10 CVs, corresponding to approximately 750 mM NaCl.

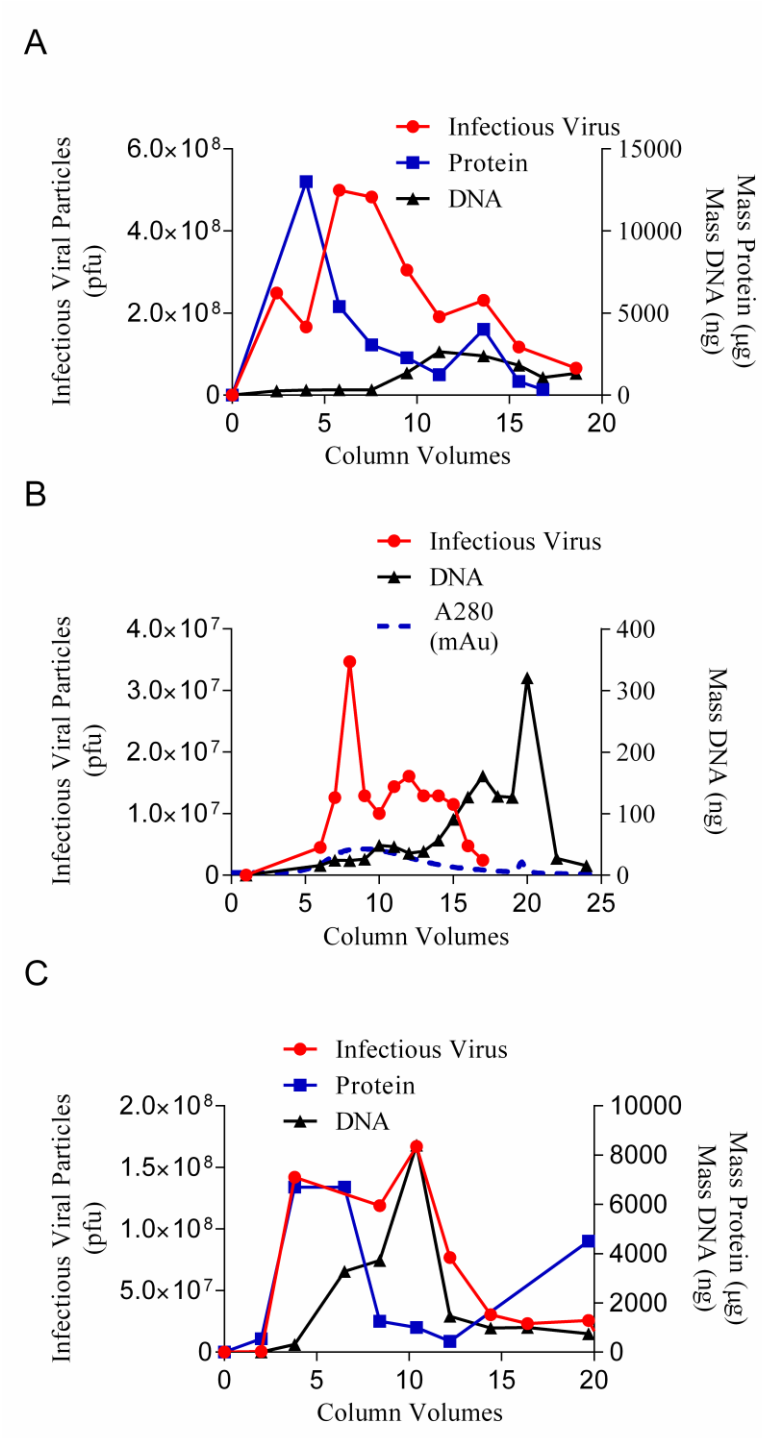

Figure 5.3 Data shows the infectious viral particles (pfu) mass of protein (µg) and mass of DNA (ng) in elution fractions A) Linear gradient elution run on CIM SO3 monolith loaded to approximately $3x10^9$ pfu/mL run over 20 CV. B) Linear gradient elution run on CIM SO3 monolith loaded to approximately $3x10^8$ pfu/mL and run over 25 CV. Conditions for CIM SO3 Buffer A: 50mM sodium phosphate pH7, Buffer B: 50mM sodium phosphate 1.5M NaCl pH 7. C) Linear gradient elution run on CIM QA monolith loaded to approx. $3x10^9$ pfu/mL monolith run over 20CV between 0 and 1.5M NaCl. Condition for CIM QA Loading Buffer: 50mM Tris pH 8.5. Elution Buffer: 50mM Tris 1.5M NaCl pH 8.5

The results indicate that CIM SO3 monoliths are able to resolve most of the virus from the adsorbed DNA. CIM QA is not able to achieve this without heavy losses in virus yield, as DNA co-elutes with the main infectious viral peak as seen in Figure 5.3.C. As DNA was identified as a critical quality attribute (CQA), it was decided that the CIM SO3 linear gradient should be repeated but that the column should be challenged with an order of magnitude less infectious virus (approximately $3x10^8$ viral particles per mL of monolith) and eluted over a longer gradient (25 CVs rather than 20 CVs) in order to maximise the resolution achievable, The results can be observed in Figure 5.3.B. It shows the same trend and percentage removal of DNA across the elution peak as illustrated in Figure 5.3.A.

The reason why virus and DNA co-elute towards the end of the gradient is unclear. It has been speculated that this may be due to a complex interaction between the virus and DNA molecules. SEM images of CIM OH fractions, presented in Figure 6.9, show virus associated with long DNA-like structures resembling “beads on a string”. It has been speculated that this structure may represent heterochromatin, which, due to the positive charge of the histone complexes, might enhance the interaction between the virus and the monolith. Other groups have also experienced difficulty in separating vaccinia virus and DNA, and experimented by adding chaotropes to disrupt potential viral-DNA complexes prior to nuclease treatment (Jordan, Weimer, Iarusso, Bernhardt, Lohr, & Sandig 2015b).

A positive charge may also come from viral coat proteins even though the overall charge across the surface is negative. It has been suggested, based on work with influenza virus, which is also able to adsorb to CIM QA and CIM SO3 monoliths, that buffer condition dependent variation in charge distribution across the viral surface may

give viral vectors enough net charge to bind to both cationic and anionic chemistries (Banjac, Roethl, Gelhart, Kramberger, Jarc, Jarc, Strancar, Muster, & Peterka 2014).

Another possibility might be the presence of a cationic bridging molecule in the feed stream that adsorbs to the stationary phase and is able to retain enough positive charge to interact with the virus, DNA, and any viral-DNA complexes present. Based on the screening studies, there is protein in the flow through fraction from both the CIEX and AIEX monoliths, suggesting that while the majority of host cell proteins in the load are acidic, there are also basic proteins present. The issue with this hypothesis is that it is difficult to envisage a species of host cell protein that would be able to retain enough net charge while bound to CIM SO3 to hold a large viruses like vaccinia on the surface.

What is evident from the data in Figure 5.3 is that DNA is more retained at high NaCl concentration than the majority of infectious viral particles. This indicates that either DNA on its own, or DNA complexed with other particles in the feed stream, forms a stronger interaction with the column than the infectious viral particles on their own.

It is clear that complex mechanisms underlie the retention of vaccinia on these resins. In the current context of developing a robust separation, it was decided at this point to design a stepwise elution scheme for CIM SO3 as this resin appeared to be able to separate infectious virus from contaminating DNA and protein.

5.4 Development of a stepwise elution schedule for CIM SO3

A central composite screening DoE was initially performed in order to sift through factors affecting the removal of DNA whilst maximising the recovery of infectious virus in the elution. Factors tested were sodium chloride concentration and pH. The load

challenge in each case was approximately $3x10^9$ pfu/mL of monolith. Based on the gradient elution results shown in Figure 5.3, ranges tested in the DoE were set between 250-750 mM NaCl pH 6-8 in sodium phosphate buffer. Initially only the corners of the design space and centre points were tested, however, as there was a large amount of noise in the $TCID_{50}$ measurements, face centred and internal augmented points were run in order to generate more information, specifically on infectious virus recovery.

Figure 5.4.A & B shows the effects of NaCl and pH on the removal of DNA and recovery of infectious virus in the elution pool. DNA purification factors are used here to show the effects of any trade-off between DNA removal and virus recovery. Modelled data showing the effects of NaCl concentration and pH on the removal of DNA is portrayed in Figure 5.4.C. The black solid lines show the modelled data points while the blue dotted lines indicate a 95 % confidence interval. The red dotted lines show the points on the graph where the recovery of infectious virus was shown in Figure 5.4.B to be at its highest.

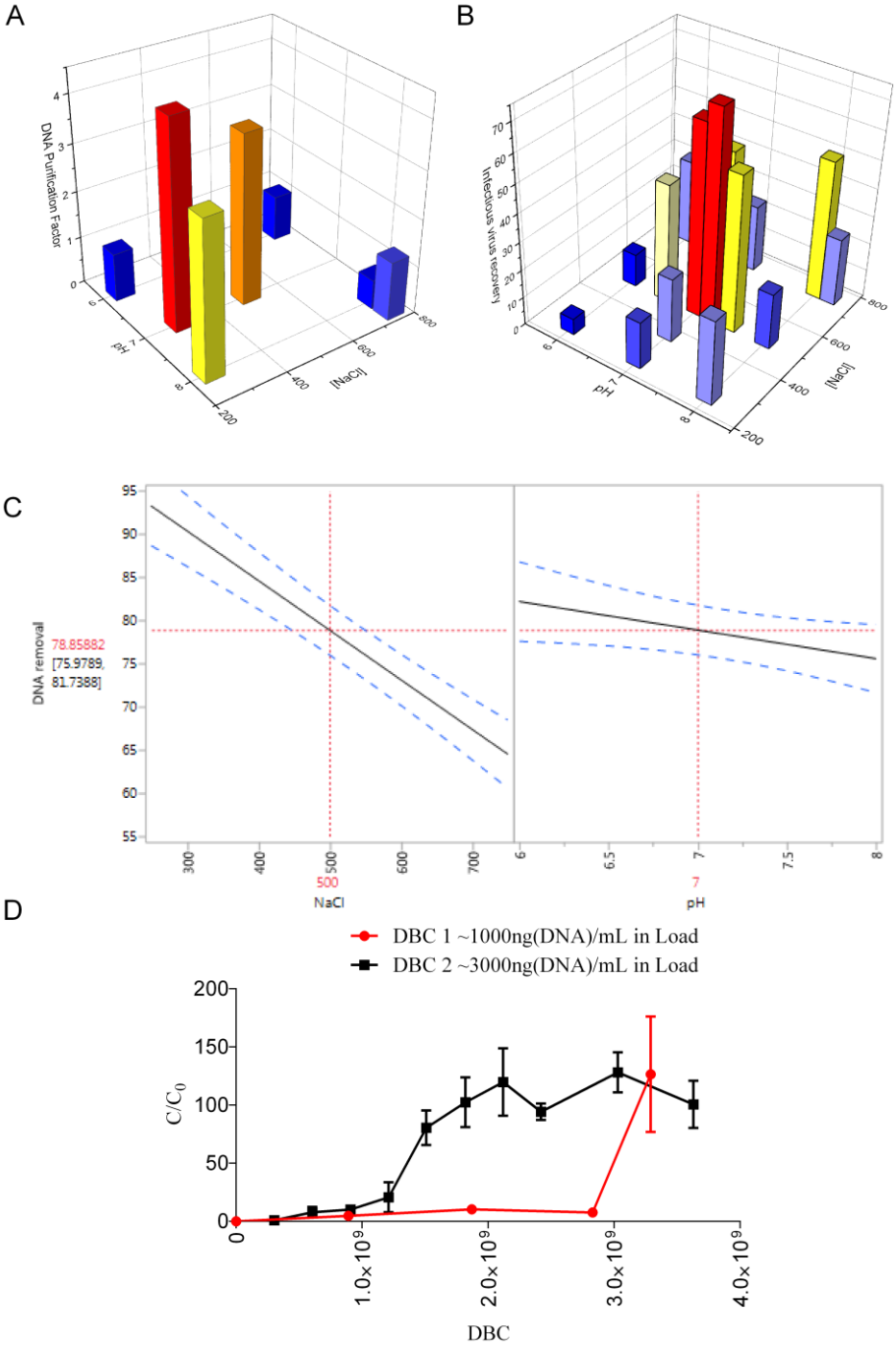

Figure 5.4 Data generated from CIM SO3 monoliths. A) 3D histogram illustrating the effects of NaCl concentration and pH on DNA purification factors measured from each run across a DoE central composite design. Raw data rather than modelled points are shown. B) 3D histogram showing the effects of NaCl concentration and pH on infectious viral recovery from each run across a DoE central composite design. Face centred and internal axial points are also shown as raw data rather than modelled points. C) DoE prediction profiler showing the modelled effects of NaCl concentration and pH on the removal of DNA from the load. (NaCl concentration leverage, P = 0.0007, pH leverage, P = 0.0451, Adjusted R^2 = 0.98) (n = 2). All $TCID_{50}$ measurements were performed in triplicate, DNA and protein values measured in dublicate, mean values shown. D) Two dynamic binding capacity (DBC) runs on CIM SO3 with ~1000 ng and ~3000 ng of DNA/mL in the load.

JMP Pro12 (SAS Cary NC USA) was initially used to model the data, and fitted a quadratic function suggesting curvature in infectious virus recovery due to sodium chloride concentration. The DoE suggested that 500 mM sodium chloride would give the highest recovery from CIM SO3; however, due to the levels of inherent variability in the $TCID_{50}$ measurements, the adjusted R^2 for the model fit was only 0.23. The model P-Value was fairly small at 0.0476 indicating significance in the model fit for curvature due to NaCl concentration, however, due to the size of the residuals (RMSE = 18.6) it was decided that conclusions on optimal CIM SO3 elution conditions should not be drawn from the model. The raw data was therefore plotted without the regression as a 3D histogram. An optimum salt concentration required to elute infectious virus would suggest a potential trade-off, perhaps between the number of viral particles desorbed from the column, and the stability of vaccinia in the elution buffers. When referring back to the stability data discussed in Chapter 4, there does appear to be some reduction in infectivity in 50 mM sodium phosphate as NaCl concentration is increased from 0-0.75 M. However, the statistical significance of this data is low making it difficult to generate a conclusion. This is likely due to $TCID_{50}$ assay variability. Although the variation between replicates in Figure 5.4.B is high, there appears to be a general increase in infectious virus recovery as NaCl concentration in the elution buffer increases. An alternative hypothesis to an optimal recovery at 500 mM NaCl may therefore be that the recovery in actual fact plateaus between 500-750 mM NaCl, especially as pH increases from 7 to 8 (Figure 5.4.B).

As expected, the recovery of DNA in the elution fraction from the CIM SO3 increases as the NaCl concentration and pH are increased. This supports the conclusions generated from the linear gradient elution data from CIM SO3 in the previous section. DNA is eluted from the column at approximately 750 mM NaCl while virus elutes at between 150 and 350 mM NaCl.

The trade-off in terms of DNA removal is that a relatively high salt concentration of or around 500 mM NaCl is required to recover between 68% and 84% of the infectious virus from the column, which leads to a relatively low 80% removal of DNA relative to the load. To confirm this, a lower NaCl concentration of 300 mM NaCl was tested at pH 7. The results showed that 92% of the DNA was removed but the recovery of infectious virus was only 35 % resulting in a DNA purification factor of 4. A summary of this data is tabulated in Table 5.2 and shows the effects of decreasing NaCl concentration on percentage virus recovery and DNA removal. Some effect due to increasing pH can also be seen to increase virus recovery and reduce DNA removal.

Table 5.2 Overview of the data generated from CIM SO3 DoE showing effects of decreasing NaCl concentration on recovery and DNA removal and therefore purification factor. Data in bold represents the conformation run described above designed to maximise the DNA purification factor. *represents averaged data points.

Elution condition	Percentage virus recovery (Elution)	Percent DNA removal (Elution)	DNA purification factor	Percent protein removal (Elution)	Protein purification factor
750mM NaCl pH 6	31 %	69 %	1.0	90 %	3.0
750mM NaCl pH 8	*38 %	*60 %	*0.9	*81 %	*2.3
500mM NaCl pH 7	68 %	80 %	3.6	85 %	4.5
300mM NaCl pH 7	**35 %**	**92 %**	**4.3**	**92 %**	**4**
250mM NaCl pH 6	6.0 %	94 %	1.0	80 %	0.3
250mM NaCl pH 8	30 %	90 %	3.2	81 %	3.4

In terms of protein removal, this appears to occur mostly during the adsorption step as between approximately 60 – 90% of the protein loaded is recovered in the flow through fraction, and so does not bind to the column. Data from Figure 5.3 suggests that the majority of protein bound elutes at around 300 mM NaCl either co-eluting or eluting just before the main infectious viral peak. The DoE suggests that, unless the virus is eluted at low NaCl and low pH protein removal remains relatively constant across the

design space (Table 5.2). The reason the purification factor is so low when CIM SO3 is eluted at 250 mM NaCl pH 6 is that virus recovery is only 6%. In an attempt to visualise the removal of impurities, especially viral aggregates, transmission electron microscopy (TEM) was used at low magnification (8000x) to visualise CIM SO3 load and elution samples. The run analysed was eluted at 300mM NaCl at pH 7. This data is shown in Figure 5.5. A large viral aggregate is clearly seen in Figure 5.5.A as well as other debris and impurities. It is unclear what the origins of these impurities are. The approximate concentration of DNA and total protein in the load for this sample was 1364 ng/mL and 337 µg/mL, respectively. The micrograph in Figure 5.5.B shows less aggregation, single vaccinia particles can be seen homogenously dispersed across the grid. Both images are representative of all grids analysed (n=3) and are shown at a magnification of 8000x.

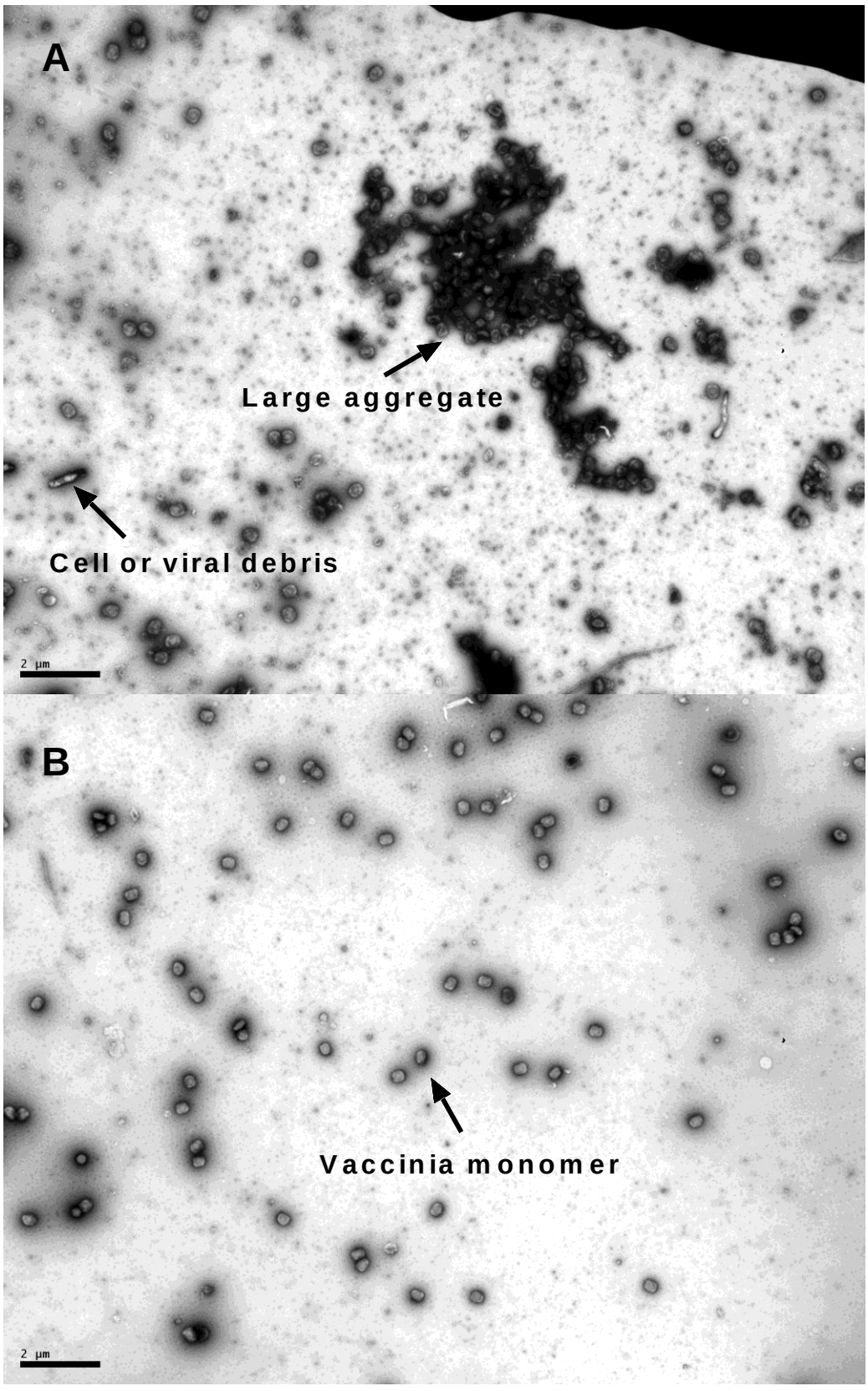

Figure 5.5 TEM micrographs of A) CIM SO3 load annotated to show contaminating viral aggregate and debris B) SO3 eluate annotated to show vaccinia monomer. Virus was eluted in 50 mM sodium phosphate 300mM NaCl pH 7.

Another observation from the DoE was that there were more infectious viral particles recovered in the flow through fractions than expected. The numbers were variable, but averaged 44% (RSD = 62%). Throughout the DoE the columns were all loaded to their measured DBC, ($3x10^9$ pfu/mL). A single batch of material was used for the initial 6 runs, and a second batch was used for the augmented and axial points. As this result was unexpected, the DBC study on CIM SO3 run previously was repeated with the same batch of material as used for the initial DoE, and the results were overlaid with the original DBC curve. This can be seen in Figure 5.4.D. There is what appears to be a significant difference in the breakthrough curves between the two runs. The binding capacity of the initial batch of material was approximately $3x10^9$ pfu/mL of monolith, whilst that of the second run was three times lower, at approximately $1x10^9$ pfu/mL.

There is a chance that this variability is due to the error in the $TCID_{50}$; however, the coefficient of variance in the assay, as previously mentioned, is only found to be approximately 30%, which may not explain the whole discrepancy in terms of error in C/Co or percentage breakthrough. The difference in virus concentration in the flow through when comparing 0% and 100% breakthrough is greater than an order of magnitude; therefore it was speculated that the difference is due to, at least in part, the variability in the load material. Residual impurity concentrations were analysed in the two batches, and the main difference appeared to be the DNA concentration. In the first DBC run, the DNA concentration in the load was calculated to be approximately 1,000 ng/mL, while the second batch had a DNA concentration of approximately 3,000 ng/mL. This observation supports the above stated hypothesis that DNA is complexed with histone proteins resulting in competition for binding sites with the virus. Similar effects on CIM monoliths have been cited in the literature; however, they were explained as resulting from lipid fouling (Burden, Jin, Podgornik, & Bracewell 2012). It is unknown why the batches vary so much in DNA concentration. One possibility is that

there is variation in the total number of cells present in a single batch of cells prior to viral infection. As stated previously a single batch consists of 30x T175 flasks. Previous work on influenza virus (Banjac, Roethl, Gelhart, Kramberger, Jarc, Jarc, Strancar, Muster, & Peterka 2014) has also reported large variation in DNA concentration in the virus harvest material, suggesting a resulting effect on the reproducibility of virus yield. As mentioned elsewhere, this combination of variability in feedstock and assay complicates process development considerably. However, this is typical of infectious viral processes.

In summary, the difference in the binding capacities (Figure 5.4.D) explains the increased recovery in the flow through, and therefore the overall lower recovery in the elution fractions observed. The trade-off between the recovery of infectious virus, and the recovery of DNA in the elution appears to limit the purification factor achievable in CIM SO3 monoliths under the conditions tested to around 4. Interestingly, even when the load was reduced to $1x10^9$ pfu/mL, the purification factor was not improved.

5.5 Evaluation of CIM SO3 as a suitable capture step for vaccinia virus

CIM SO3 does appear to be able to resolve most of the infectious viral particles from the contaminating DNA and protein in the load. It is not, however, able to remove enough DNA to achieve the required specifications for DNA removal specified by the WHO. It is assumed that this will remain at 10ng DNA/dose (World Health Organization 1998), and that vaccinia will be required at a dose of approximately $1x10^9$ pfu/dose.

5.5.1 Evaluation into the suitability of Benzonase® as a pre-chromatographic treatment step.

Benzonase® produced by (Merk KGaA, Darmstadt, Germany) is a CGMP compliant genetically engineered endonuclease, designed to digest DNA from biological feed streams. The disadvantage of using Benzonase® is that it is expensive, and its removal has to be validated. It is, however, the only effective biochemical method of removing DNA and RNA that is licenced for manufacturing use.

In order to evaluate the suitability of Benzonase® for the use in the manufacture of vaccinia virus, an experimental protocol was designed to test different pre-treatment conditions with and without Benzonase® prior to CIM SO3 capture. The rationale here was to evaluate the effectiveness of different nuclease treatment schedules at removing DNA contamination. The idea was that this data could then be compared with an assumed process relying on two orthogonal monolith steps but without Benzonase®. The data in Table 5.3 shows the pre-treatment conditions used in each experiment. DNA purification factors are given, along with percentage DNA removal and percentage infectious virus recovery. The mass of DNA per dose in the elution is also shown, assuming a required dose of $1x10^9$ pfu (Heo, Reid, Ruo, Breitbach, Rose, Bloomston, Cho, Lim, Chung, Kim, Burke, Lencioni, Hickman, Moon, Lee, Kim, Daneshmand, Dubois, Longpre, Ngo, Rooney, Bell, Rhee, Patt, Hwang, & Kirn 2013), along with the number of uses each monolith has had including the experiment in question. Monoliths were loaded to a capacity of $1x10^9$ pfu/mL (5 mL) and eluted using a stepwise elution schedule in 50mM sodium phosphate 500mM NaCl pH 7 as shown in Figure 3.3. The same batch of virus was used in all experiment. DNA concentration in the harvest control runs showed variability of less than 10% (RSD 9.75%).

Table 5.3 Benzonase study showing experimental conditions including incubation time and temperature, DNA purification factor (PF) % DNA removal in the elution fraction, measured DNA per dose, % recovery of infectious virus, and number column reuses are shown. Concentration of Benzonase used in all experiments was 150 U/mL. Harvest material was all from same batch and thawed at 37 °C. No additional Mg^{2+} Ions were added to harvest material prior to treatment with Benzonase. DMEM contains 0.81mM Magnesium Sulfate ($MgS0_4$). RT = Room Temperature. Control = Run performed without Benzonase®

Conditions	Total DNA Harvest (ng) (post-treatment)	DNA PF Elution	% DNA Removal Elution	DNA/dose Elution ($1x10^9$ pfu)	% Infectious Virus Recovery Elution	Number of Reuses
Benzonase ® 1 hr RT	9703	1.56	88	5399	19	6
Control 1 hr RT	19614	0.98	86	8442	14	8
Benzonase ® 6 hr 4-8 °C	8525	1.83	87	3537	24	3
Control 6 hr 4-8 °C	23857	0.96	93	13383	6	5
Control New column, No incubation	21781	2.83	70	3974	84	1

What is immediately obvious when analysing the data in Table 5.3 is that Benzonase® does not remove the entire mass of DNA present in feed stream. It in fact removes approximately half of it. This phenomenon has previously been noted in the literature by other groups working with vaccinia virus (Jordan, Weimer, Iarusso, Bernhardt, Lohr, & Sandig 2015b), and has been suggested to be the result of complexes formed between the virus and contaminating DNA molecules. The data in this thesis shows that vaccinia forms large aggregates, especially in high salt conditions. It is perhaps reasonable to speculate, therefore, that Benzonase® would be unable to get close enough to the DNA,

especially if located towards the centre of a large aggregate molecule, to be able to hydrolyse it.

5.5.2 Evaluation of CIM SO3 robustness

The data in Table 5.3 also shows a reduced recovery of infectious virus from CIM SO3 when eluted at 500 mM NaCl when compared to data generated when optimising the stepwise elution (Figure 5.4). It was originally thought that this could be the result of variation in DNA concentration in the load, however, there does not appear to be a trend when analysing the data in Table 5.3. As previously stated the RSD between the control runs in terms of DNA concentration was 9.75 %. The optimisation runs, as well as the Benzonase® control run, were performed on new columns suggesting that a residual foulant may have built up during the column lifetime. It was speculated that this may have changed the surface chemistry of the monolith sufficiently to affect the retention of virus on the column. As it is difficult to analyse the foulant layer itself, an experiment was designed with a column that had already been used twice, in an attempt to repeat the low recovery of infectious virus and then to regenerate the monolith performance using a variety of CIP strategies. The results can be seen in Table 5.4.

Table 5.4 experimental CIP buffers used in an attempt to regenerate a CIM SO3 monoliths. Number of particles loaded, elution buffer conditions and batch of material used for each run was constant. Percentage infectious virus in the flow through fraction was less than 1% for each run. Note elution peak was collected from 100-100 mAu (Optical Path length 0.2 cm) CIP conditions shown for each run were performed on the run before, as so where the last CIP conditions seen by the column prior to loading. ➔ means followed by.

	CIP conditions performed on previous run	**Infectious virus % Recovery in 500 mM NaCl**	**Infectious virus % Recovery in 2 M NaCl**	**Number of reuses**
Run 1 Normal CIP	1M NaOH 2M NaCl 1hr incubation	27	34	3
Run 2 Experimental CIP	80% IPA 15 min incubation	21	6	4
Run 3 Experimental CIP	Trypsin (5 min inc.) ➔ 2M NaCl ➔ 1M NaOH (1hr inc.)	16	14	5
Run 4 Normal CIP	1M NaOH 2M NaCl 1hr incubation	27	19	6

It should be noted that the elution peak was collected from 100 mAu on its leading edge to 100 mAu on its tailing edge rather than using a 10 mL fixed volume elution as mentioned previously. This variance in the method does not appear to have affected the results. The recovery data matches that observed during the Benzonase® experiments. The recovery of infectious virus was lower when eluted at 500 mM NaCl than had been observed with fresh columns during the optimisation runs. The use of standard CIP conditions recommended by BIA Separations, 1M NaOH 2M NaCl, as well as 80%

IPA, and Trypsin do not appear to reverse this effect. What is interesting is that when the columns were further washed with 50 mM sodium phosphate 2 M sodium chloride pH 7 up to 34% of the infectious virus loaded was eluted as a separate peak; this was only observed after BIA Separations recommended CIP buffers where used.

The data suggests that the affinity of infectious virus to the SO3 monolith may increase when a column has been used previously. It also appears that a higher salt concentration is required to elute the virus, suggesting that the mechanism of adsorption is still electrostatic.

Without more data it is not possible to conclusively state that the columns are unable to be reused, but this data is sufficient to warrant later costing analysis to include number of monolith reuses into the sensitivity analysis shown in Section 7.4.2.

NTA data from run 1 (Table 5.4) is shown in Figure 5.6. 5 mL of virus ($1x10^9$ pfu) was loaded onto the column, the flow through was collected with the equilibration step in 15 mL, the elution was collected in 1-3 mL, and strip was collected in 5 mL. The CIM SO3 load polydispersity appears similar to previous measurements, although smaller diameter particles appear more variable. This is likely as the measurement was taken at a detection threshold of 5 rather than 3 in order to better analyse the larger (300 nm) particles in solution. Detection threshold is the minimum intensity value of an image in order for it to qualify as a particle and therefore be tracked and analysed by the software. It is clear that the elution fraction has a significantly smaller number of particles then the load. This was expected based on the analysis of the load and null prep samples shown in Figure 4.7. What is surprising is the area of each 250-350 nm peak in both the load and elution samples relative to the other peaks in the same sample. It appears that the smaller peak in the elution fraction is larger than the smaller peak in

the load fraction relative to the larger species in each distribution. It also appears that the larger, likely virus containing peak in the elution fraction has shifted to the left by approximately 10-20 nm. If it can be assumed that the smaller species in the load is an impurity, which is a reasonable assumption being that it is half the size of the virus, then this data would suggest that the purification factor of this impurity would be less than 1. In conclusion, the elution fraction appears to contain a relatively large population of particles of approximately 150 nm. It is not clear what this population consists of, although either a protein DNA aggregate or degrading virus particles seem the most likely. Another observation that can be made is that the number of particles in the load outnumbers the particles in the flow through, elution and strip fractions. This suggests that material is still bound to the column after the elution, which supports the argument in Section 5.5.2 that proposes that a foulant is adsorbing to the column and reducing yield after multiple injections.

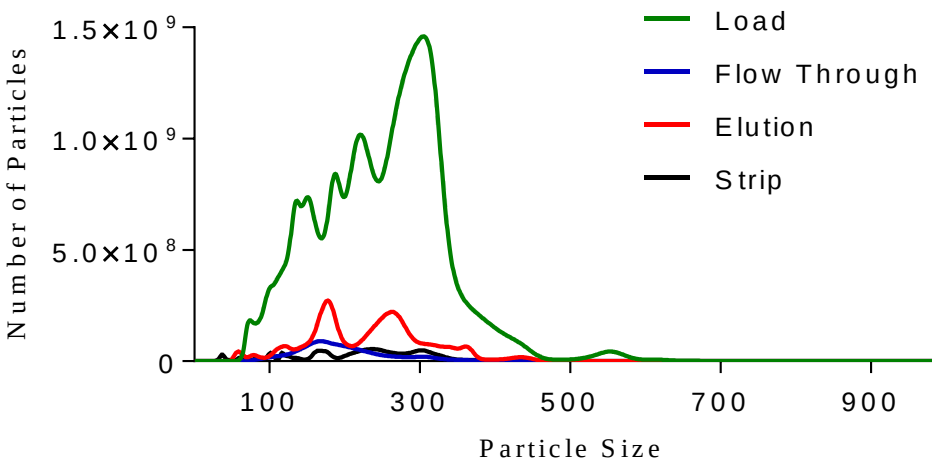

Figure 5.6 NTA data showing size distribution of SO3 load, flow through, elution and strip fractions. CIM SO3 monolith had been used 3 times; NTA data is showing mean values from 5 tracking experiments, Data from run 1 (Table 5.4)

5.6 An illustrative description of vaccinia virus adsorption on CIM SO3 monoliths

It has been shown in this chapter that vaccinia virus is able to adsorb to CIM SO3 monoliths at 2 pH units above its isoelectric point.

Both the gradient and stepwise elution runs show that the DNA adsorbed to the monolith elutes at a higher NaCl concentration than the majority of the infectious viral particles. There are two hypotheses that might explain this:

Hypothesis 1 is that the DNA is complexed with a strong cationic molecule which is able to interact with the monolith.

Hypothesis 2 is that the DNA is able to associate with large viral aggregate molecules that have a higher affinity to the CIM SO3 stationary phase than smaller individual viral particles.

5.6.1 Hypothesis 1

It is known that the majority of the DNA in the load does not adsorb to the column as it was recovered in the flow through fractions collected during the CIM SO3 runs. It has been speculated, based on SEM images taken of both the DNA in the load and the flow through, that the DNA present is complexed with particles similar in size and morphology to histone proteins. As histone proteins are positively charged, this would explain why DNA is able to bind to the stationary phase and may also explain why DNA is able to form a bridge between the virus and the monolith.

5.6.2 Hypothesis 2

In the second hypothesis, DNA is able to associate with large viral particles. There is a chance that a positive charge could come from the virus itself, but if this were true, and DNA was binding to positively charged regions on the viral surface, then it might be assumed that either the virus and DNA would co-elute, or the DNA would elute first. The reason for this assumption is that increases in the ionic strength of the mobile phase during the elution step would likely break the electrostatic interactions between either the virus and DNA, eluting DNA, or the virus and the column, eluting both DNA and virus. The fact that this does not happen suggests that the DNA is able to be retained without the majority of the infectious virus present. For this to be the case, DNA must either have a strong positive charge and so be able to adsorb directly to the CIM SO3 or be associated with large viral aggregates, likely made up of infectious and non-infectious viral particles that do not break apart when NaCl is introduced and elute later in the gradient.

Information in the literature on histone protein interactions (Rippe et al. 2008) is interesting. It shows that histone proteins, in the absence of DNA form aggregates which are stabilised at high salt (2 M NaCl). As the ionic strength decreases to physiological levels (100-150mM NaCl) the histone complexes begin to disassociate and at low ionic strength, histone proteins become soluble and unfold. *In vitro* reconstruction of nucleosomes is achieved by slowly reducing the salt concentration from 2 M to physiological ionic strength. This allows assembly of the nucleosome particles in an ordered manner and prevents histone-DNA aggregation. During CIEX experiments this would not have occurred and it seam conceivable that DNA-histone aggregates may have been formed in the harvest that were then able to interact with viral particles or aggregates and facilitate adsorption onto CIM SO3. In addition to this,

previous work performed on histone purification using CIEX chromatography shows that histone proteins bind to SP ligands at 0.2M NaCl and require between 0.8 and 2 M NaCl to elute (Rodriguez-Collazo et al. 2009). Histone proteins are amongst the most basic proteins known with an isoelectric point of around 11 as discussed in (Chung et al. 1978).

While more supporting experiments need to be performed, the results generated when vaccinia was treated with Benzonase® endonuclease also support this theory. Benzonase® is not able to degrade all of the DNA in the load suggesting that large aggregates are present. This has been confirmed by TEM, as shown in Figure 4.10. It has also been shown, by SEM, that DNA is able to associate with vaccinia, suggesting that it may be responsible for the inter-particle interactions. This will be described in more detail in Chapter 6.

An attempt at illustrating these molecules and their associated affinity to the CIM SO3 is shown in Figure 5.7. The removal of viral aggregates in the CIM SO3 elution at 300 mM NaCl supports the theory that the affinity of individual vaccinia particles for the CIM SO3 stationary phase is lower than that of large aggregates. The increased affinity of the DNA, potential complexed with positively charged histone proteins is supported by the linear gradient elution runs Figure 5.3 and the DoE Figure 5.4.A-C.

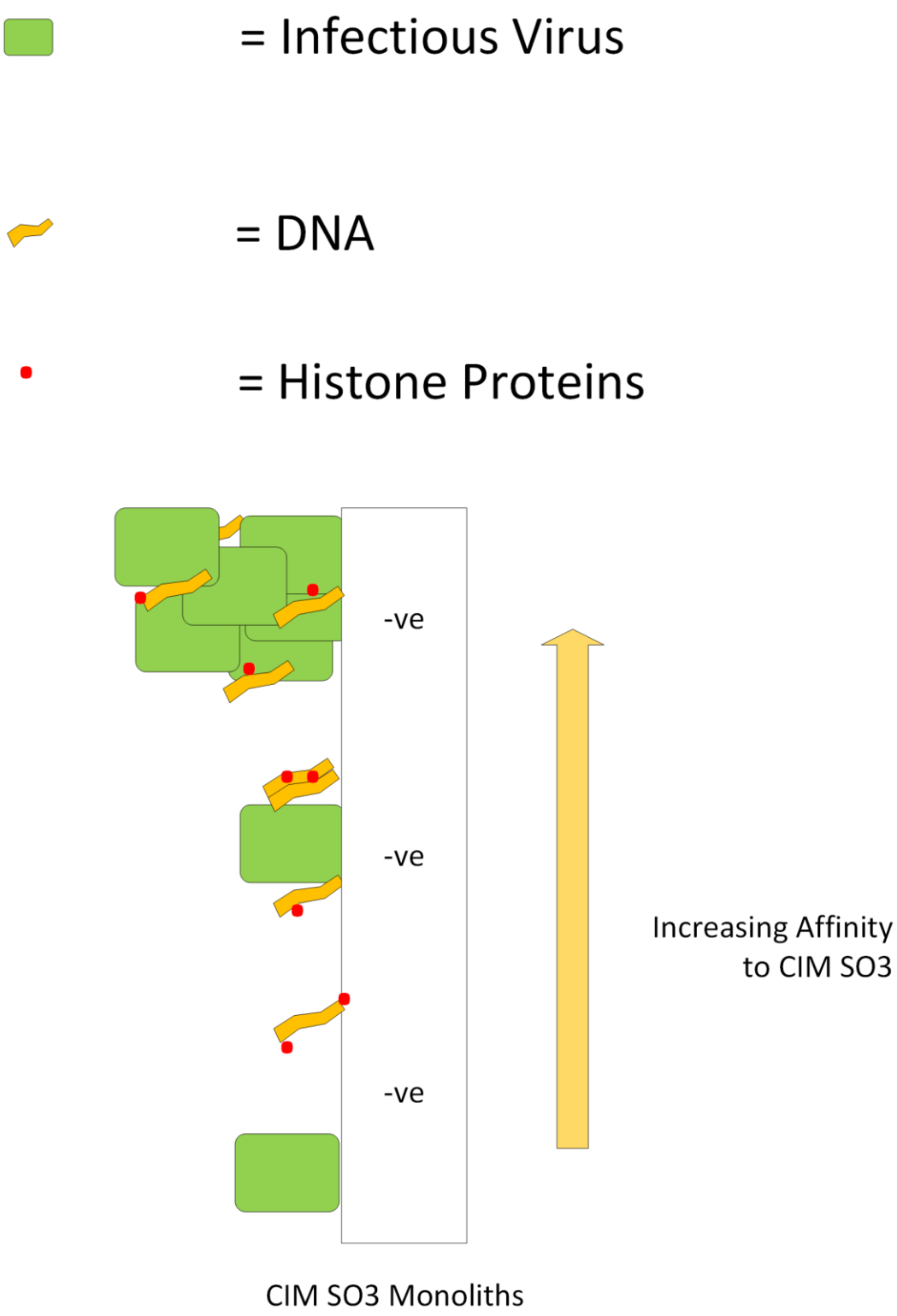

Figure 5.7 Schematic to show proposed binding affinity of vaccinia virus and Vaccinia-DNA complexes on CIM S03 Monoliths.

5.7 Conclusion

This chapter has illustrated that Vaccinia virus has some unusual properties in that it is able to bind to both CIEX and AIEX monoliths. From the initial linear gradient elution runs performed, CIM SO3 appears to be able to separate a large proportion of DNA from crude vaccinia viral harvest. DNA appears to adsorb more strongly to the column than viral particles, suggesting the presence of a strongly cationic molecule in the feed that is able to form a bridge between the anionic stationary phase and the DNA.

When using a stepwise elution schedule, the unit operation is still able to separate virus from DNA. However, as DNA binds more strongly than the virus a pre-elution wash step cannot be used to remove DNA. A trade-off appears to occur in terms of the recovery of infectious virus and subsequent removal of DNA as an increased NaCl concentration increases the recovery of both infectious virus and DNA. Greater than 50 % recovery is achievable at NaCl concentrations around 500 mM, however 20% of the total DNA loaded is co-eluted at this molarity. Lower salt concentrations (300 mM NaCl) reduce the levels of eluted DNA to around 10%, but this also reduces the recovery of infectious virus to around 35%. The resulting DNA purification factor appears to remain at around 4. According to TEM data, 300mM NaCl is able to remove large viral aggregates present in the CIM SO3 load. This data is qualitative rather than quantitative but is useful of note especially if levels of virus aggregation are defined as a critical qualities attribute. CIM SO3 monoliths appear to require more NaCl to elute vaccinia after they have been used more than once. This potentially supports the hypothesis that histone driven DNA – viral aggregation occurs that increases the affinity of virus adsorption onto the SO3 ligand. With this in mind, the most efficient application of CIM SO3 is likely to be as a single use capture step, vaccinia would be loaded at low salt and eluted at around 500 mM NaCl in order to maximise recovery

and remove the majority of contaminating DNA. A second step would then need to be performed to remove the residual DNA and protein to levels acceptable for clinical application.

Benzonase® is able to reduce the levels of DNA in the load, but not by enough to remove all contaminating DNA without the need for another step. This conclusion is supported by previous work on vaccinia virus.

At this stage in process development, it was concluded that no further studies would be done with CIM SO3 monoliths until other systems were considered. There are some theoretical advantages of using a HIC system, and as vaccinia is shown to be reasonably stable in high salt, in terms of infectivity, CIM OH monoliths were evaluated next.

Chapter 6

Hydrophobic Interaction Chromatography Process Development

6.1 Introduction

CIM OH monoliths are produced by the hydrolysis of epoxy ligands on the polymethacrylate monolith surface to produce a high density of hydroxyl groups. This makes CIM OH monoliths hydrophilic and negatively charged. The high salt levels usually needed in hydrophobic interaction chromatography (HIC) can damage labile viruses. Nevertheless standard HIC resins with phenyl and butyl groups have been used previously in both virus and VLP capture and intermediate polishing steps (Burden, Jin, Podgornik, & Bracewell 2012;Jordan, Weimer, Iarusso, Bernhardt, Lohr, & Sandig 2015b;Wolff, Siewert, Hansen, Faber, & Reichl 2010a). It is more common today to use ion exchange (IEX) monoliths to purify viruses, (Banjac, Roethl, Gelhart, Kramberger, Jarc, Jarc, Strancar, Muster, & Peterka 2014;Gerster, Kopecky, Hammerschmidt, Klausberger, Krammer, Grabherr, Mersich, Urbas, Kramberger, Paril, Schreiner, Nobauer, Razzazi-Fazeli, & Jungbauer 2013;Kramberger, Petrovic, Strancar, & Ravnikar 2004;Kramberger, Peterka, Boben, Ravnikar, & Strancar 2007;Kramberger, Honour, Herman, Smrekar, & Peterka 2010;Rupar, Ravnikar, Tusek-Znidaric, Kramberger, Glais, & Gutierrez-Aguirre 2013) although the low hydrophobicity of CIM OH coupled with the relatively high salt tolerance of vaccinia virus (Figure 4.5) may reduce or minimise losses in infectivity. CIM OH could also be able to offer unique

selectivity, especially for DNA clearance, and is therefore considered here for vaccinia purification.

6.2 CIM OH monolith screening study

In order to evaluate the suitability of CIM OH monoliths as an initial capture and purification step for vaccinia virus, a number of decisions needed to be made from the outset, prior to the generation of any data, and based on previous experience and information in the literature. It was decided to start by running initial bind-and-elute experiments at neutral or weakly basic pH in sodium phosphate buffer. The reason for this was that it was speculated that a lower pH would reduce the stability of vaccinia virus as well as potentially increase the binding affinity of the virus to the monolith and so reduce the recovery in the elution. The mobile phase modulator used to drive adsorption was ammonium sulfate due to its high ionic strength and kosmotropic nature. 1 mL monoliths were used in all experiments. Chromatography run setup is shown in Figure 3.3. A process flow diagram detailing how vaccinia was produced can be seen is shown in Figure 3.1.

Three experiments were performed using the following loading condition: vaccinia harvest was diluted in 50 mM sodium phosphate pH 7 in both 1 and 2 M ammonium sulfate, and pH 8.5 in 2 M ammonium sulfate. Rather than initially optimising a diafiltration step, vaccinia was diluted 1:5 with each chosen load buffer in order to bring the pH and conductivity close to that of the buffer used. Table 6.1 shows the recorded conductivity and pH for each buffer and diluted load fraction. As the binding capacity of CIM OH was unknown at this point, a binding capacity of $\leq 1x10^{10}$ pfu of virus was assumed, and so $1x10^{10}$ pfu of viral harvest material was diluted in load buffer, filtered,

and loaded into each column. Viral harvest, chromatography load, flow through and elution fractions were collected in order to generate a mass balance. The columns were eluted at the same pH as the load, but without ammonium sulfate in the buffer. The strip buffer consisted of pure water and the column was cleaned with 1 M NaOH 2 M NaCl.

Table 6.1 Equilibration buffer and diluted viral load material conductivity and pH conditions. Conductivity meter was uncalibrated, so it was used as a reference only. The Chromatography system was not equipped with a pH meter. (N/T- not tested). AS stands for ammonium sulfate.

Equilibration buffer / Load conditions		Conductivity (mS/cm)	pH
1 M AS pH 7	Buffer	143.17	7.00 +/- 0.09
1 M AS pH 7	Load	122.70	N/T
2 M AS pH 7	Buffer	231.52	7.00 +/- 0.09
2 M AS pH 7	Load	205.78	N/T
2 M AS pH 8.5	Buffer	N/T	8.5 +/- 0.09
2 M AS pH 8.5	Load	200.40	N/T

The results of the screening study are presented in Figure 6.1.A and show the recovery of infectious virus in the flow through and elution fractions, as well as the calculated recovery assuming no loss in the flow through fraction. This additional analysis was performed in order to illustrate the total number of infectious particles unaccounted for, as infectious particle balances rarely close. The best explanation for why this occurs is that infectious particles are either inactivated during the unit operation, or remain on the column after the elution and strip steps and are likely hydrolysed when washed with NaOH during the CIP step. The data appears to show that in 1 M ammonium sulfate the

virus is unable to bind strongly to the column, because around 60% of the infectious particles loaded are recovered in the flow through fraction. As a result, only around 40% of particles adsorbed are recovered in the elution. It should be noted that the relative standard deviation (RSD) in the infectivity assay is approximately +/- 30%.

A

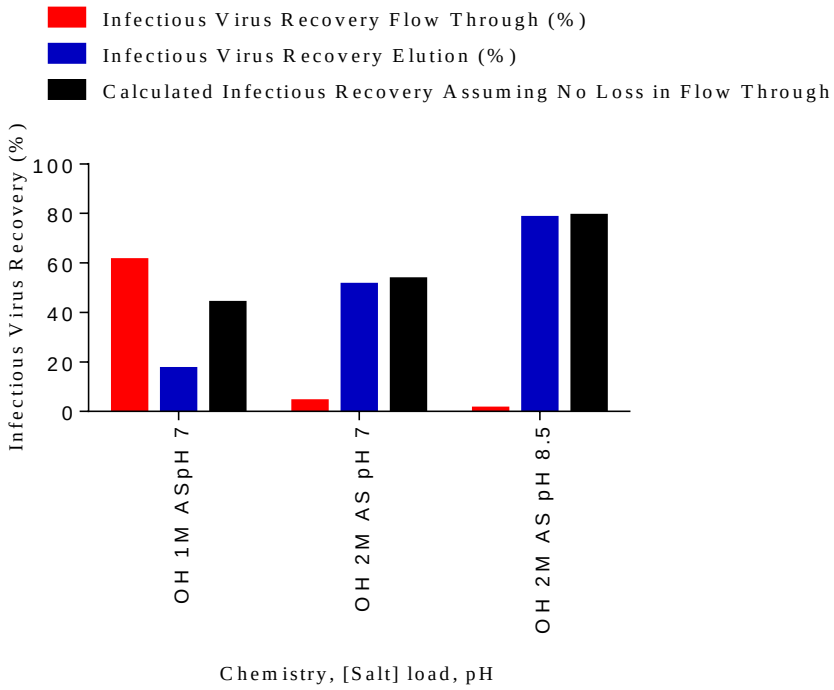

B

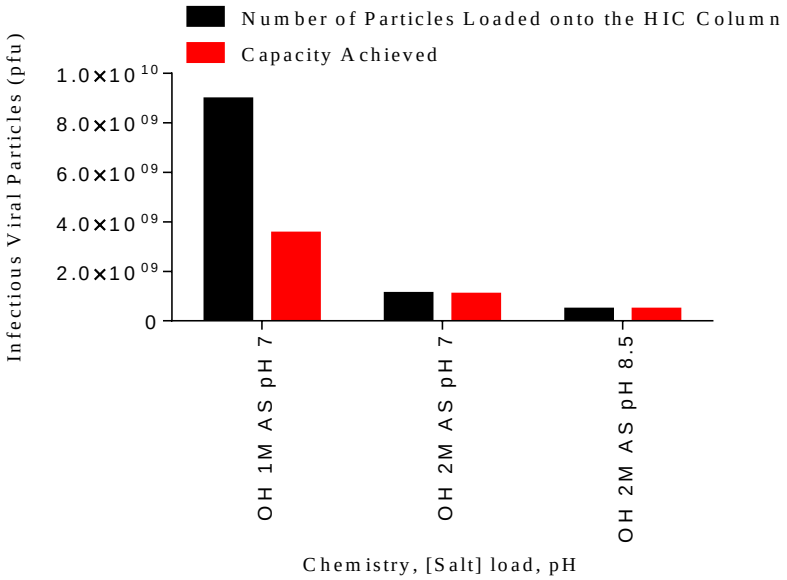

Figure 6.1 A) Histogram showing vaccinia virus loaded in 1 and 2 M ammonium sulfate at pH 7 and 2M ammonium sulfate at pH 8.5. Red bars show the percentage of infections virus in the flow through fraction relative to the load, blue bars shows percentage of infectious virus in the elution fraction relative to the load, and black bars show the percentage infectious virus in the elution minus the total number of particles lost in the flow through. B) Histogram showing the number of viral particles loaded vs the capacity achieved on CIM OH.

In 2 M ammonium sulfate virus is present in very low amounts in the flow through with approximately 50-80% recovered in the elution fraction. At first glance this appears promising, however, after a more careful look at the data it was discovered that the virus recovery across the 0.8µm pre-filter when loaded in 2M ammonium sulfate was only 6%. This is graphically represented in Figure 6.1.B and is shown in Table 6.2. The number of virus particles in the harvest (pre filtration) and load fractions are shown for each of the three runs along with the estimated capacities achieved on CIM OH along with the estimated percentage recovery achieved across the pre-filter and in the CIM OH elution. It can be seen that the number of particles loaded when the experiment was run at 1 M ammonium sulfate is significantly higher than when run at 2 M ammonium sulfate. It also shows a higher capacity achieved when run at 1 M ammonium sulfate. The low capacity at 2 M ammonium sulfate is thought to be the result of the low load challenge due to the low recovery of virus across the pre-filter. The higher recovery across the pre-filter when run at 1 M ammonium sulfate explains the higher load challenge on the column. The increased number of infectious virus particles in the flow through for this run suggests that the column may have been overloaded. Chromatograms for runs with 1 M and 2 M ammonium sulfate pH 7 are shown in Figure 6.2.

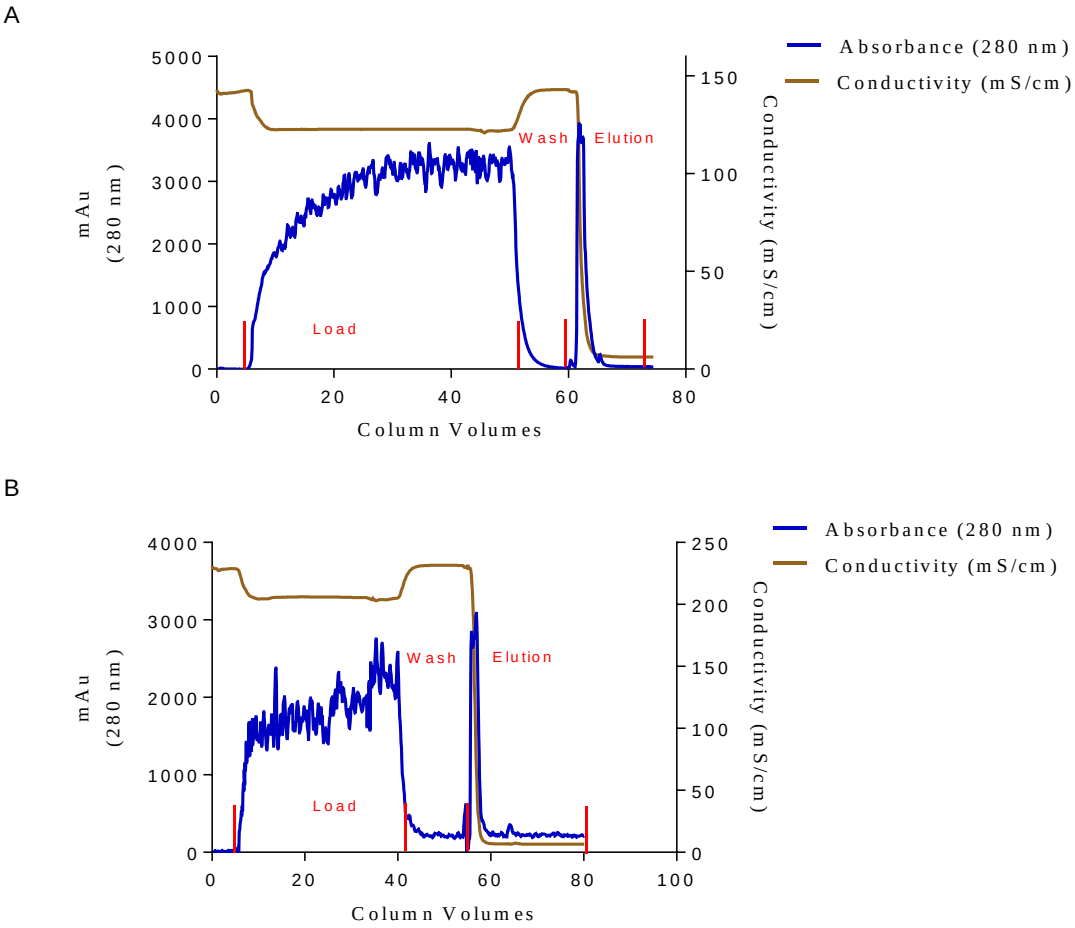

Figure 6.2 A) Chromatogram for 1 M AS pH 7 run B) Chromatogram for 2 M AS pH 7

Table 6.2 Summary of CIM OH screening study. The number of virus particles in the harvest and post 0.8µm filtration is shown along with percentage recovery of virus across the filter and the column. Capacity achieved is calculated by number of particles in the load minus the number of particles in the flow through. (* = Indicates that a new batch of material with a lower tire was used for 2 M AS run at pH 8.5). N/T = not tested.

Load conditions	Number of viral particles in harvest (pre 0.8 µm filter) (pfu)	Percentage recovery across 0.8 µm filter	Number of virus particles loaded (post 0.8 µm filter) (pfu)	Capacity achieved (pfu/mL)	Number of viral particles in elution (pfu)	Recovery in elution relative to harvest	Recovery in elution relative to load	Recovery in elution relative to capacity achieved	DNA purification factor	Protein purification factor
1M AS pH 7	$2.48x10^{10}$	36%	$8.94x10^{9}$	$3.51x10^{9}$	$1.53x10^{9}$	6%	17%	44%	3.71	3.00
2M AS pH 7	$1.56x10^{10}$	7.0%	$1.08x10^{9}$	$1.04x10^{9}$	$5.52x10^{9}$	4%	51%	53%	1.72	2.35
*2M AS pH 8.5	$2.09x10^{9}$	21%	$4.38x10^{8}$	$4.35x10^{8}$	$3.43x10^{9}$	16%	78%	79%	3.31	N/T

The elution buffer conditions tested during the screening experiments were not designed to test the ability of CIM OH to remove DNA or total protein, but to examine whether virus was able to bind and be eluted from the column without losing infectivity. Interestingly however, DNA and total protein purification factors calculated during these runs show promising results, as shown in Table 6.2. This is comparable to purification factors achieved for CIM SO3 after elution step optimisation. CIM SO3 achieves a DNA and protein purification factor of approximately 4 when eluted in 300 mM NaCl. The majority of DNA and contaminating protein is not able to bind to CIM OH. This explains why relatively high purification factors are achievable without elution buffer optimisation.

6.3 OH load buffer optimisation

In order to evaluate HIC as a potential capture and polishing step for vaccinia virus, an experiment had to be designed to address pre-column filterability.

It was hypothesised that the low recovery across the 0.8µm filter was a result of viral aggregation in the presence of kosmotropic salts in the HIC load buffer. Experiments were designed in order to confirm this, and were aimed at increasing the recovery across the filter by modifying the load buffer conditions.

The filters used in all studies were surfactant free cellulose acetate (SFCA) 0.8µm syringe filters manufactured by Sartorius (Gottingen, Germany). Cellulose acetate membranes are hydrophilic, and, in theory, ideally suited for pressure driven filtration due to low protein adsorption properties.

In order to increase filterability, a study was designed to test the effects of ammonium sulfate and NaCl concentration on both the pre-column filterability of the virus, and its ability to then adsorb efficiently to CIM OH. The conditions tested are shown in (Table 6.3).

Table 6.3 CIM OH load buffer optimisation study showing different NaCl and $(NH_4)_2SO_4$ concentrations tested. Run 1 (bold) was taken from screening experiments.

Run	[NaCl] (M)	$[(NH_4)_2SO_4]$ (M)
1	**0**	**2**
2	1	1.5
3	2	1
4	3	0.5
5	4	0

Ammonium sulfate concentration was reduced by 0.5 M per run (from 1.5 M to 0 M), while the sodium chloride concentration was increased by 1 M per run (from 1 M to 4 M). A volume of 2.3 mL of virus with a titre of approximately $1x10^9$ pfu/mL was diluted 1:5 in load buffer and was loaded onto the (filter-column) units as described in Table 6.3. The results, as can be seen in Figure 6.3.A, show the recovery of infectious virus in the 0.8µm filtrate relative to the harvest, and the flow through and elution fractions relative to the load.

Figure 6.3.B shows the DNA and total protein purification factors achieved in the elution fractions for each run. Table 6.4 also shows a summary of this data set and

includes the number of infectious particles recovered pre and post filtration as well as in the flow through and elution fractions. The data suggests that as the ammonium sulfate is reduced, the filterability of the material increases. This is evident by the increase in recovery across the 0.8µm filter. The recovery when loaded in 4 M NaCl, without ammonium sulfate, and when loaded without any salt (shown in Figure 6.4) are similar. This suggests that NaCl does not strongly affect filterability.

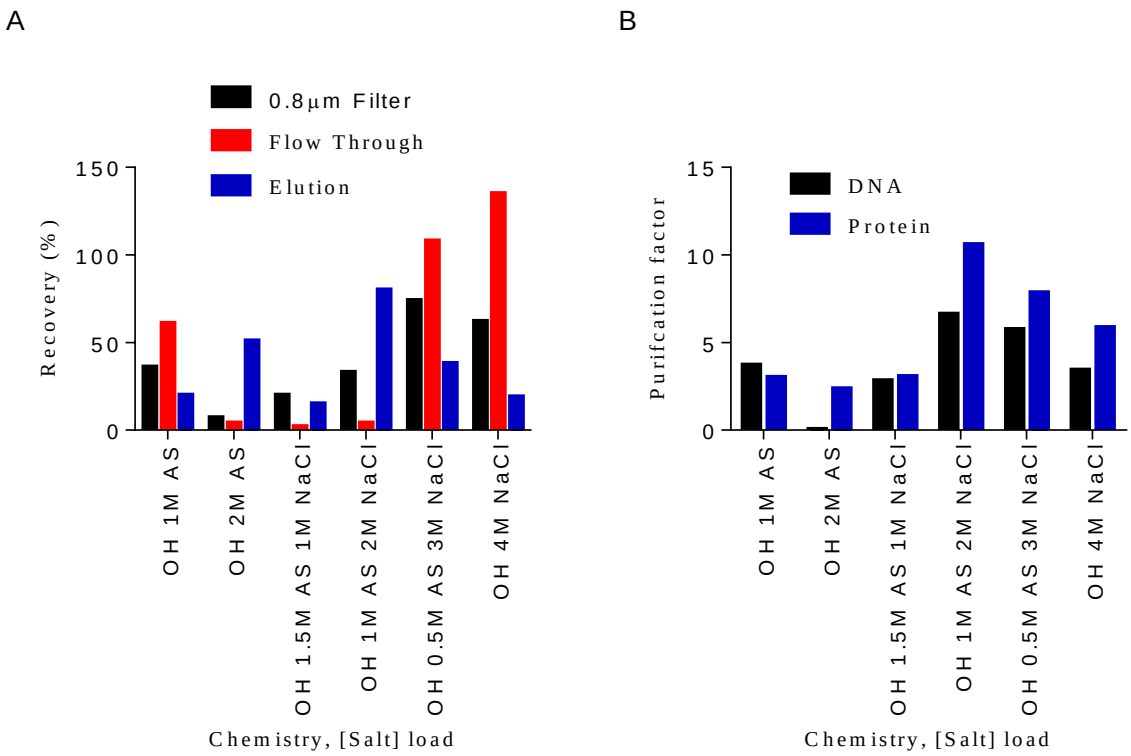

Figure 6.3 A) CIM OH load optimisation study showing the percentage recovery of infectious virus across the 0.8µm filtration step relative to the harvest, and the recovery of infectious virus in the flow though and elution fractions relative to the load. B) Purification factors achieved for DNA and total protein. Elution buffers used for all experiments were 50mM sodium phosphate pH 7. ~2x10^9 pfu of vaccinia was filtered, and all virus in the filtrate was loaded onto the columns. (AS = Ammonium sulfate).

Table 6.4 CIM OH buffer optimisation study showing the number of infectious virus particles present before and after dilution and 0.8 µm filtration, in the flow through and elution fractions. The percentage recovery of infections virus in the flow through and elution fractions, and the DNA and protein purification factors in the elution fractions for each condition tested. Rows in bold represent original data from screening study (different batch of virus, higher load volume (10mL). Buffer optimisation study came from a single batch of virus, 2.3 mL virus was diluted and loaded onto filter-column system.

Conditions	Number of particles (Harvest)	Number of particles (Post 0.8 µm Filter)	Number of particles (Flow Through)	Number of particles (Elution)	Percentage recovery (Flow Through)	Percentage recovery (Elution)	DNA purification factor (Elution)	Protein purification factor (Elution)
1 M AS pH 7	**$2.48x10^{10}$**	**$8.94x10^{9}$**	**$5.43x10^{9}$**	**$1.53x10^{9}$**	**61.0**	**20.0**	**3.71**	**3.01**
2 M AS pH 7	**$1.56x10^{10}$**	**$1.08x10^{9}$**	**$4.38x10^{7}$**	**$5.52x10^{8}$**	**4.00**	**51.0**	**0.05**	**2.35**
1.5 M AS 1 M NaCl pH 7	$4.80x10^{9}$	$9.63x10^{8}$	$1.93x10^{7}$	$1.46x10^{8}$	2.00	15.0	2.82	3.06
1 M AS 2 M NaCl pH 7	$4.58x10^{9}$	$1.53x10^{9}$	$6.59x10^{7}$	$1.22x10^{9}$	4.00	80.0	6.62	10.6
0.5 M AS 3 M NaCl pH 7	$3.46x10^{9}$	$2.56x10^{9}$	$2.75x10^{9}$	$9.62x10^{8}$	108	38.0	5.74	7.84
0.0 M AS 4 M NaCl pH 7	$3.78x10^{9}$	$2.36x10^{9}$	$3.19x10^{9}$	$4.60x10^{8}$	135	19.0	3.42	5.85

The trade-off is that as the ammonium sulfate concentration decreases, the adsorption efficiency of virus onto the CIM OH also decreases. This is shown by an increase in recovery in the flow through fraction, which is dramatic for ammonium sulfate concentrations of 0.5 M and below. The same relationship is also evident in the DNA and total protein purification factors achieved in the elution fractions from each run. This is the case as purification factor is a function of both viral recovery and DNA/protein removal as described in Equation 3-7. It can be seen that the total particle balance is greater than 100% when low concentrations of ammonium sulfate are used in the load buffer. This is most likely due to the variability in the analytics.

Based on the data in Figure 6.3 it was concluded that the best load buffer condition tested was 50 mM sodium phosphate 2 M sodium chloride 1 M ammonium sulfate pH 7. *This will from now on be referred to as optimised HIC load buffer.*

In order to test the robustness of this conclusion, the percentage recovery of virus across the filter in different load buffers was tested with and without salt, and in optimised HIC load buffer as shown in Figure 6.4. Box and whisker plots are shown together with the raw data values for each condition tested. The box represents the interquartile range with the median shown in the centre. The whiskers show the range.

The plot illustrates that when vaccinia is filtered in optimised HIC load buffer a reasonably robust recovery of infectious virus is achieved. This recovery is approximately 35%. The recovery when loaded with 2 M ammonium sulfate was unacceptably low at around 6%. Interestingly, when run without salt the filtration recovery is higher, but also more variable. This may be due to more dynamic aggregation patterns without the presence of ammonium sulfate as a mobile phase

modulator acting to promote aggregation. This would likely affect the $TCID_{50}$ as the number of particles per unit volume would likely be more stable.

Figure 6.4 also shows the filtration recovery of virus in 2 M ammonium sulfate at pH 8.5 after high g centrifugation. All other fractions were centrifuged at a relative centrifugal force (RCF) of 440, however this sample was centrifuged at 771 to test whether removing more debris prior to dilution in HIC load buffer would prevent filtration fouling. This experiment was only performed once, and the data showed no change in the infectious viral recovery.

In future work, an evaluation of alternative filters would be recommended as described in Section 9.2. This work was focused on the development of a chromatographic separation, so while not perfect, a median recovery of 35% was taken as an acceptable pre-filtration recovery and the optimised HIC load buffer conditions were taken forward for the development of a capture step for vaccinia virus.

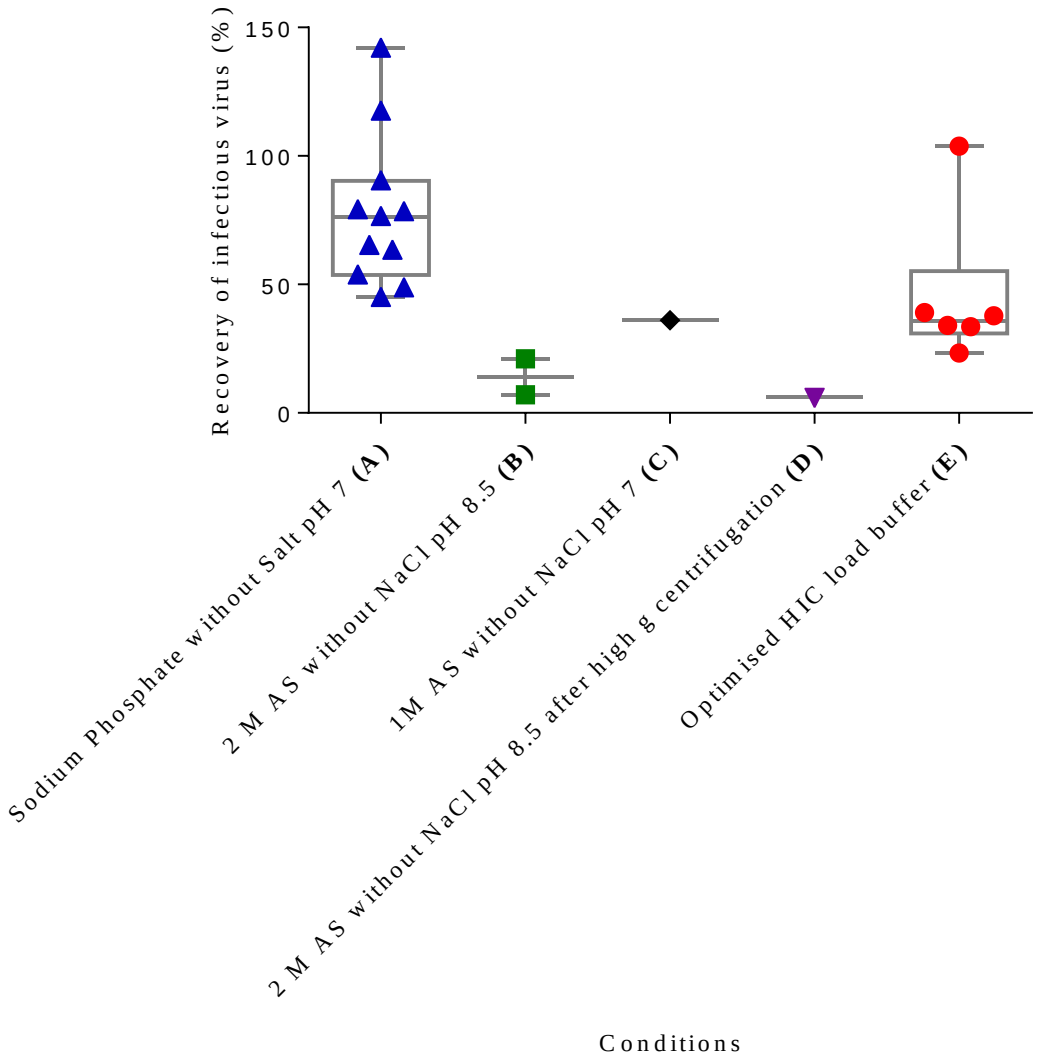

Figure 6.4 Replicate data showing filterability expressed as percentage recovery of virus across the filter in different load buffers. (High g centrifugation was attempted to remove cell debris at an RCF of ~771 for 5 min; normal centrifugation conditions consisted of an RCF of ~440 for 5 min) (AS = Ammonium sulfate)

6.4 Evaluation of dynamic binding capacity

Binding capacity studies were performed in optimised HIC load buffer at pH 7 and pH 8 as shown in Figure 6.5. The load material at pH 7 was calculated to be $1.42x10^8$ pfu/mL and at pH 8 to be $1.66x10^8$ pfu/mL. While the exact breakthrough curve is hard to plot with certainty due to the error in the $TCID_{50,}$ it is clear that initial breakthrough occurs at approximately the same time in each experiment, corresponding to $1x10^9$ pfu/mL of monolith. The slope of the breakthrough curve appears to be fairly shallow suggesting that adsorption is relatively inefficient. Further work needs to be carried out to understand the exact mechanism of adsorption; however, the data in Figure 6.9 suggests that aggregation in the presence of ammonium sulfate may be reversible, dynamic and variable depending on the diluent used. It is likely that the relative affinity of viral aggregates to the CIM OH stationary phase is dependent on the hydrodynamic diameter of the particles. If the aggregation profile and therefore the average particle diameters keeps changing, then this could lead to different adsorption kinetics for each aggregate particle.

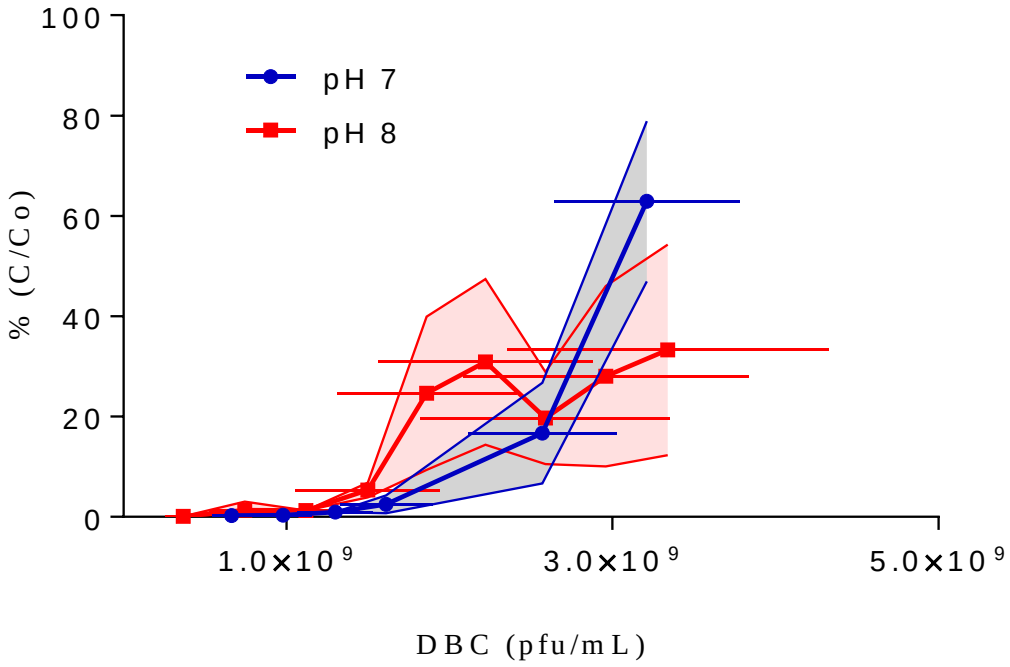

Figure 6.5 CIM OH DBC run in optimised HIC load buffer at pH 7 and pH 8. Error bars show error in $TCID_{50}$ data and are generated from 1 DBC study at each pH measured in triplicate, error bars show 1 SD. Y-error bars are shown as shaded areas and X-error bars are shown as horizontal lines.

6.5 CIM OH step wise elution design

A linear gradient elution was run over 25 CVs and fractionated in order to evaluate when infectious virus particles of 250-350 nm, DNA and total protein eluted from the column. Buffer A consisted of optimised HIC load buffer and buffer B was the same elution buffer as used in the early screening studies, 50mM sodium phosphate pH 7. The results are shown in Figure 6.6.A. DNA appears to elute first after around 10 CVs, followed by the virus towards the end of the gradient. This data suggested that it might be possible to remove DNA in a pre-elution wash step by decreasing the salt concentration enough to elute the DNA without eluting the virus. In order to test this hypothesis and make the process more commercially viable a stepwise elution schedule

needed to be developed. Two runs were therefore performed, the first at pH 7 and the second at pH 8; virus was eluted over 25 column volumes using a multi-step elution schedule. This consisted of reducing the ammonium sulfate and NaCl concentrations by 20% every 5 column volumes by increasing the percentage of buffer B. Each of the elution steps is shown in Table 6.5.

Table 6.5 CIM OH Multi-Stepwise elution schedule design showing percentage buffer A and percentage buffer B for each step (Each step was 5 CVs) Row in bold (step 4) shows buffer molarity in which the majority of infectious virus was eluted.

Step	Percentage buffer A Equilibration buffer (Optimised HIC load buffer pH 7-8)	Percentage buffer B Elution buffer (50 mM sodium phosphate pH 7-8)	Approximate molarity of elution fraction
1	80	20	0.8 M AS 1.6 M NaCl
2	60	40	0.6 M AS 1.2 M NaCl
3	40	60	0.4 M AS 0.8 M NaCl
4	**20**	**80**	**0.2 M AS 0.4 M NaCl**
5	0	100	0.0 M AS 0.0 M NaCl

The corresponding chromatograms are shown in Figure 6.6 B and C. Virus in each elution pool was analysed using $TCID_{50}$ and NTA. The chromatograms show that both measurements agree in terms of where the virus is being eluted from the columns, although as expected, the NTA overestimates the total number of virus particles in each fraction.

Figure 6.6C shows that loading at pH 8 gives a slightly better removal of DNA than at pH 7 therefore the 3rd and 4th steps when run at pH 7 were increased from 5 CVs to 10 CVs in an attempt to maximise DNA removal in the 3rd fraction and maximise virus yield in the 4th. The resulting chromatogram is shown in Figure 6.6D. It appears when analysing the chromatogram that this worked, however, the raw data in Table 6.6 shows that a lower overall removal of DNA relative to the load was achieved. This is due to a higher concentration of DNA in the starting material when compared to the initial experiments run at pH 7. All CIM OH runs where performed twice.

A

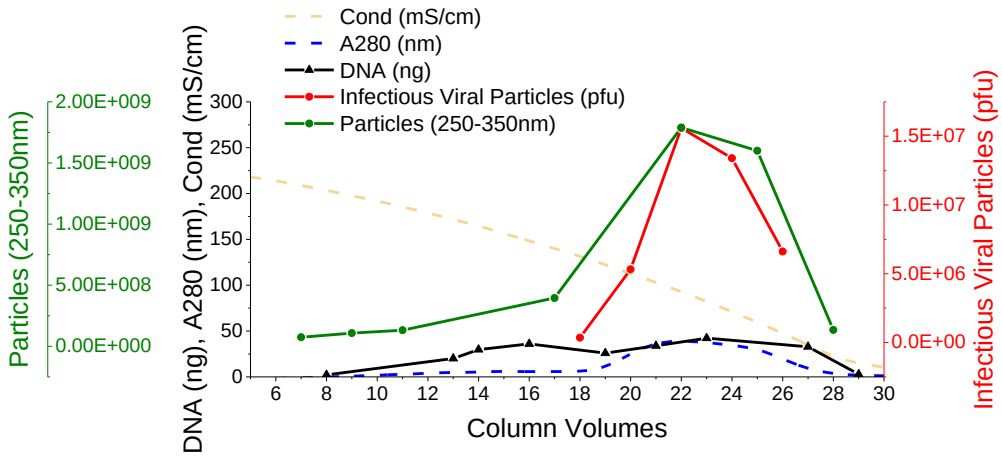
Cond (mS/cm)
A280 (nm)
DNA (ng)
Infectious Viral Particles (pfu)
Particles (250-350nm)
Particles (250-350nm)
DNA (ng), A280 (nm), Cond (mS/cm)
Infectious Viral Particles (pfu)
Column Volumes

B

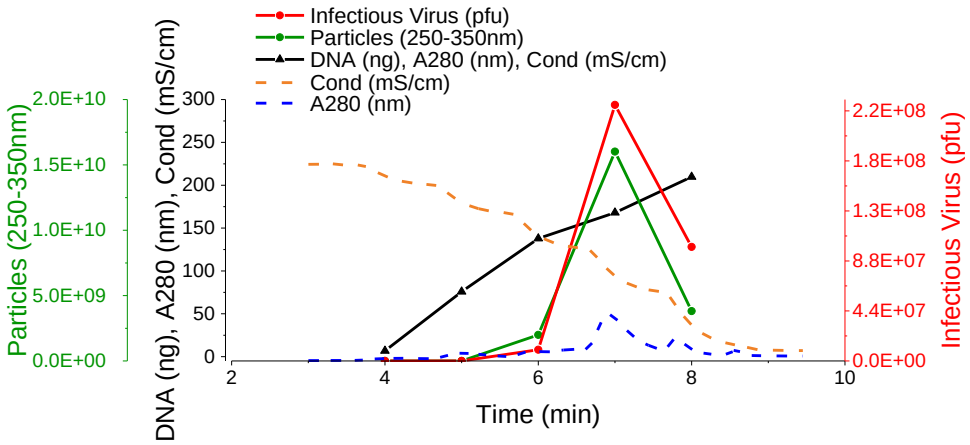
Infectious Virus (pfu)
Particles (250-350nm)
DNA (ng), A280 (nm), Cond (mS/cm)
Cond (mS/cm)
A280 (nm)
Particles (250-350nm)
DNA (ng), A280 (nm), Cond (mS/cm)
Infectious Virus (pfu)
Time (min)

C

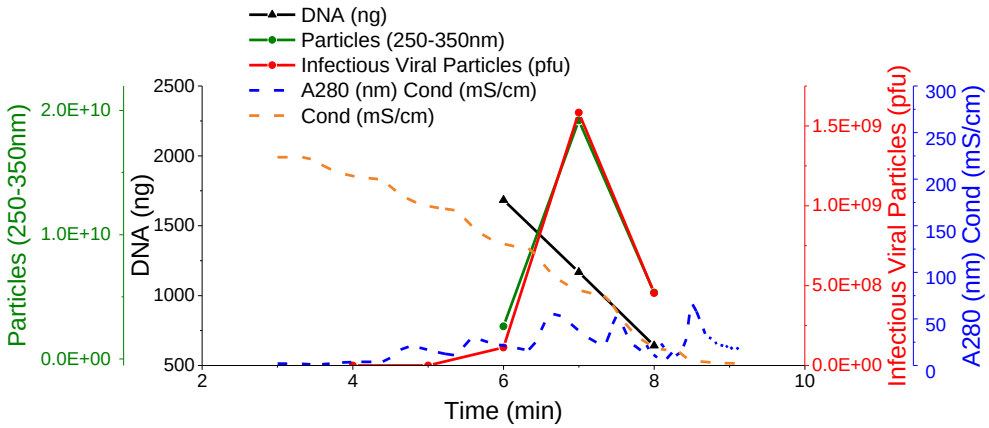
DNA (ng)
Particles (250-350nm)
Infectious Viral Particles (pfu)
A280 (nm) Cond (mS/cm)
Cond (mS/cm)
Particles (250-350nm)
DNA (ng)
Infectious Viral Particles (pfu)
A280 (nm) Cond (mS/cm)
Time (min)

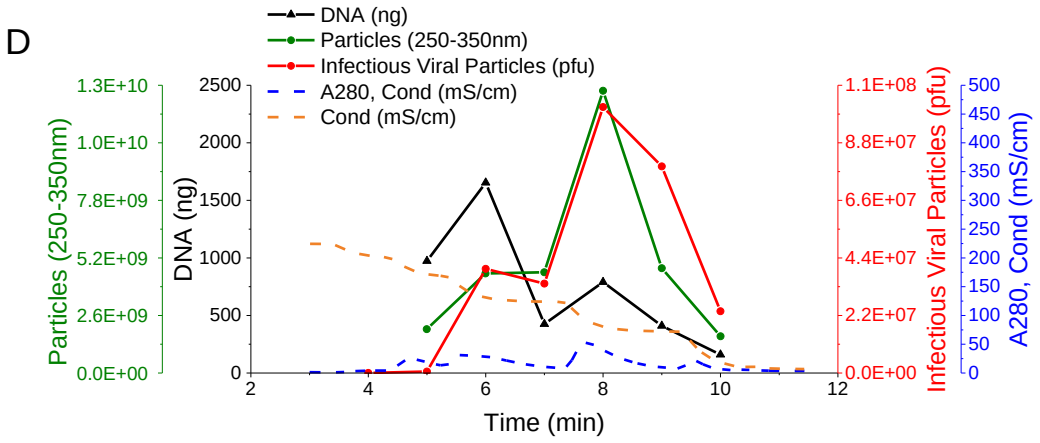

Figure 6.6 CIM OH Linear and stepwise elution schedules A) Linear gradient elution over 25 CVs B) multi-stepwise elution schedule run at pH 7 C) multi-stepwise elution schedule run at pH 8 (DNA and particle data only collected across elution peak 3 rather then 5 data points plotted) D) multi-stepwise elution schedule run with additional column volumes for 3rd and 4th steps pH 7.

Data in Table 6.6 shows that the total protein concentrations in all fractions were below the limits of quantification. This was the case when analysed with both BCA and micro BCA protein assays. It is understood that micro BCA, while having an LLOQ of 2 µg/mL, is incompatible with ammonium sulate. The regular BCA assay has an LLOQ of 20 µg/mL, so for this reason an SDS page gel, shown in Figure 6.7, was run in order to visualise the protein present in the elution. After staining with SimpleBlue™ SafeStain (Life Technologies, Carlsbad, CA, USA) there were no visible bands, therefore the gel shown was silver stained. 10 µL of each fraction under non-reducing conditions was loaded into each well. The gel shows that protein is present in the elution fractions at pH 7 and pH 8, however, at very low concentration. The majority of protein is collected in the flow through fraction. A null prep sample, which was filtered cell lysate without virus, was run as a control (lane 10). This appears to have a similar protein profile to the load material, suggesting that the majority of protein in the sample was contamination from the host cell.

Table 6.6 CIM OH multi-stepwise elution scheduals run at pH 7 and pH 8 (N/T = not tested) LLOQ = lower limit of quantification. % R = percentage recovery

*** = CIM OH run with elution fractions 3 and 4 increased from 5 to 10 CV's.**

**** = CIM OH run without 1st and 2nd elution fractions and with 3 and 4 increased from 5 to 10 CVs.**

Conditions tested	0.8 µm Filter (% R)	Number of particles loaded (pfu)	Mass of DNA loaded (ng)	Flow Through $TCID_{50}$ (% R)	Elution $TCID_{50}$ (% R)	Elution NTA (% R)	Elution qPCR (% R)	Elution DNA Removal (%)	DNA purification factor	Elution Protein
pH 7 Run 1	104	$6.62x10^8$	7200	0.16	92	35	N/T	97	21	LLOQ
pH 7 Run 2	38	$5.35x10^8$	6100	0.08	42	55	N/T	97	15	LLOQ
pH 7 Run 3*	39	$5.07x10^8$	23000	0.58	36	25	25	95	7	LLOQ
pH 7 Run 4**	34	$1.12x10^9$	25000	0.46	50	37	44	94	8	LLOQ
pH 8 Run 1	32	$1.75x10^9$	29000	0.42	90	39	N/T	96	22	LLOQ
pH 8 Run 2	34	$1.08x10^8$	18000	0.15	91	10	12	99	88	LLOQ

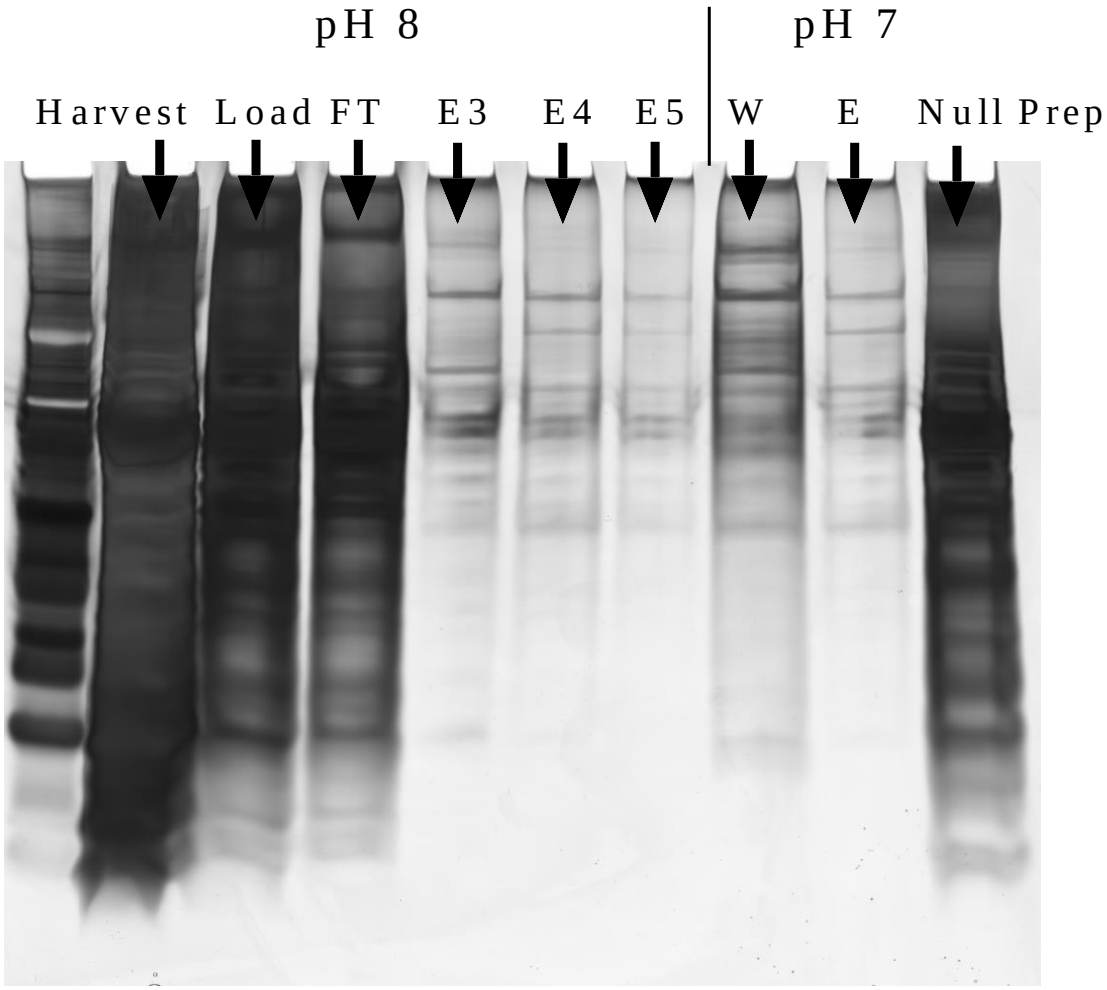

Figure 6.7 Non reduced SDS page gel after silver staining. Fractions are from CIM OH harvest, load, flow though, wash, and elution fractions run at pH 7 (Figure 6.6.B) and pH 8 (Figure 6.6.C). Null Prep fraction was prepared in the same way as chromatography load material but did not contain virus material. FT = flow through, E=elution.

NTA size distribution data for load and elution fractions analysed from CIM OH runs at pH 7 and pH 8 are shown in Figure 6.8. The load material originates from the same source, although has been diluted 1:5 in optimised HIC load buffer at pH 7 (A) and pH 8 (B). The elution fractions from each run are less polydisperse than the load material, and appear comparable in terms of particle size profile. The load fractions show considerable differences which may be related to the change in pH; however, it is also likely to be indicative of the high levels of variability seen in the starting material. What is encouraging is that the variable polydispersity in the upstream does not appear to affect the levels of polydispersity in the CIM OH elution fraction.

A

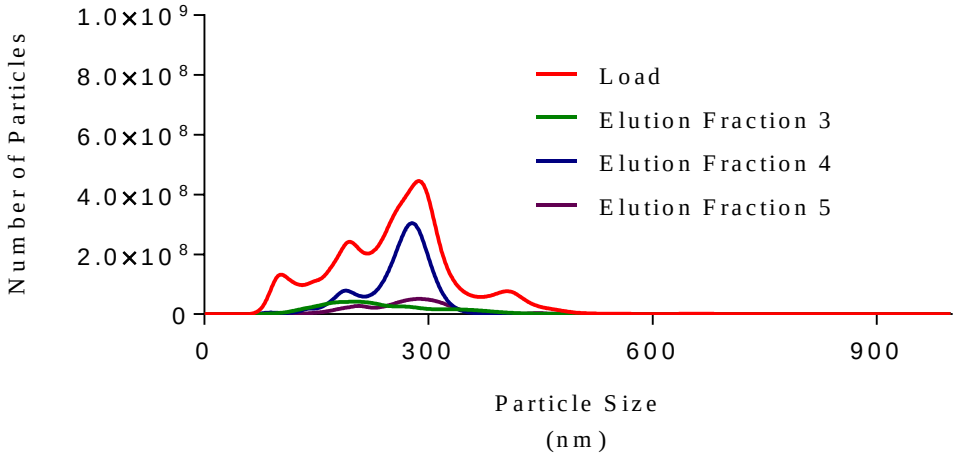

B

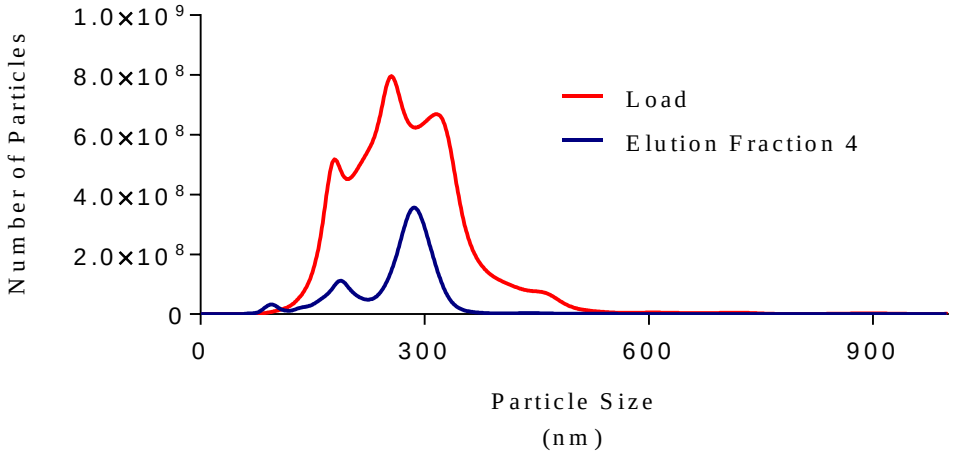

Figure 6.8 Size distribution of CIM OH stepwise elution schedule load and elution fractions. A) data includes elution fractions 3, 4 and 5 pH 7 B) data show load and elution pH 8. N=5 for all samples, curves represent mean values.

6.6 Evaluation of robustness and process variability

The ability of CIM OH to remove contaminating DNA from the viral load material varies depending on the total mass of DNA in the load. However, it is shown to be as high as 99% resulting in a total mass of DNA/dose of less than 10 ng (depending on the dose specified). A second chromatographic step would likely be necessary if vaccinia was required at high dose. When compared to sulfated cellulose membrane absorbers (SC-MA) evaluated in the literature, (Wolff, Siewert, Hansen, Faber, & Reichl 2010a;Wolff, Siewert, Lehmann, Hansen, Djurup, Faber, & Reichl 2010b) CIM OH monoliths appear to have a lower binding capacity than SC-MA, which has shown to adsorb up to $6.42x10^9$ pfu of MVA per capsule. Each capsule tested was 75 cm^2. A direct comparison is difficult to make as the cell line, vaccinia strain and analytical measurements were all different, however, it appears that a higher percentage recovery of infectious virus was achieved using CIM OH. The authors measured virus recovery from SC-MA using an in-house ELISA, and achieved a recovery of 75%. The total infectious recovery across the whole process was reported to be approximately 34% although a pre-column filtration step was not included in the process stream and this was after a second chromatography step. Infectious recovery from CIM OH is variable but as high as 90%. CIM OH and SC-MA show comparable removal of total protein, which is below the lower limit of quantification (LLOQ) of the BCA assay used in both studies. Total DNA removal was slightly higher using CIM OH, although still comparable to SC-MA. The best result shown for SC-MA was a removal of 98% of the total DNA loaded while CIM OH removed up to 99%. This corresponds to an impressive purification factor of 88.

The data in Table 6.6 shows that the DNA and total protein removal capability of CIM OH is fairly consistent at both pH 7 and pH 8. The recovery of infectious virus, while variable, appears to be above 66% on average. The median infectious viral recovery when comparing all the runs at both pH values is 70%, while the mean recovery is 67%.

The limited qPCR-based recovery data (only 3 data points are available, Table 6.6) is in close agreement with the recovery data generated using the NTA. The qPCR protocol was designed to quantify intact viral particles by adding a nuclease treatment step to remove free viral DNA from the sample prior to analysis. More data is required to make accurate conclusions; however, these results may indicate that CIM OH is able to remove intact but non-infectious virus particles from the feed stream.

Figure 6.9 shows SEM images of the CIM OH load, flow through and elution fractions. Viral aggregation in the presence of ammonium sulfate can clearly be seen in the CIM OH load. Particles larger than 6 µm were present across all grids analysed. A large number of other particles, appearing to be associated with the virus, are present in Figure 6.9B. We speculate that this is DNA, as the particles resemble "beads on a string" which is often used to describe heterochromatin. The "beads" are nucleosomes which consist of DNA wrapped around eight histone proteins known as a histone octamers. This hypothesis is supported by CIM OH mass balance data, as 60-80% of the DNA loaded onto the columns is recovered in the flow through fraction. The associated particles in the SEM images are shown again in Figure 6.9.C to be present at a seemingly high concentration in the flow through fraction. They do not appear to be present in the elution.

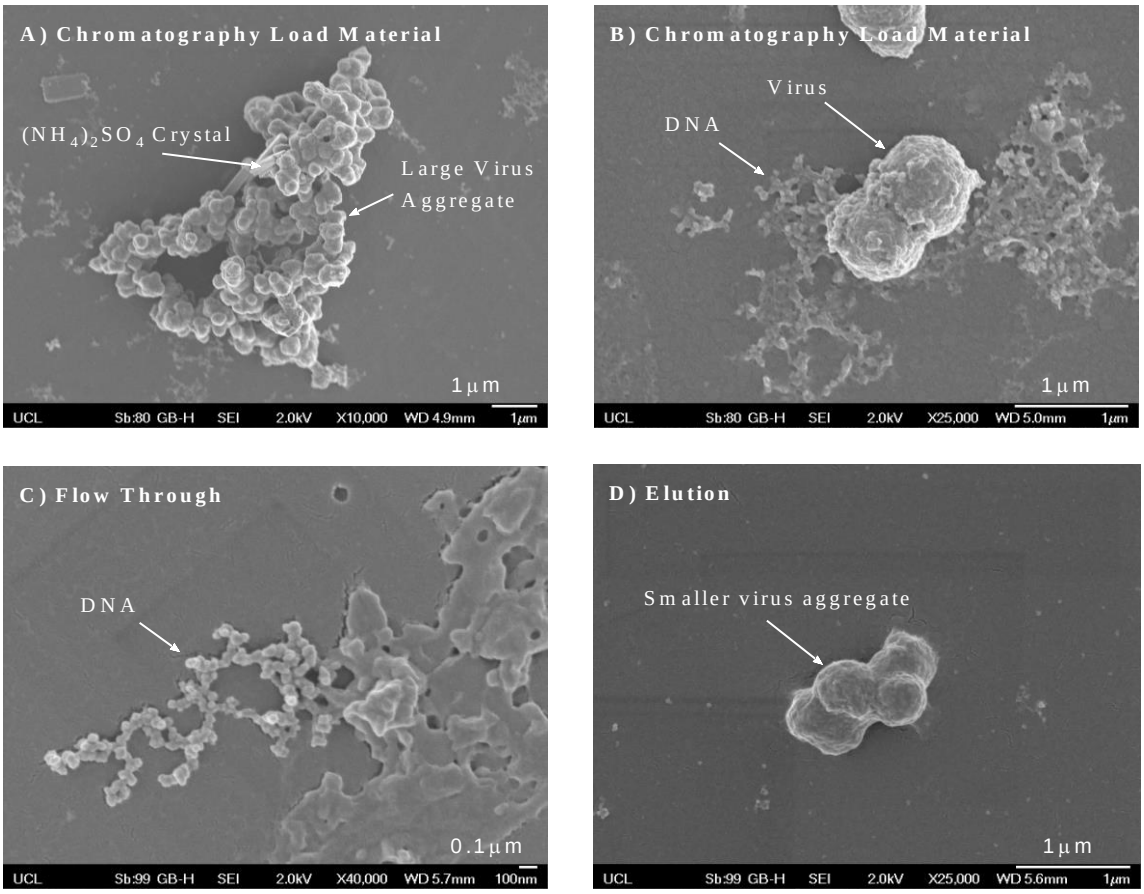

Figure 6.9 A) large virus aggregate in CIMOH load (post filtration) >6µm in diameter B) Potential Viral-DNA complex in CIM OH Load (post filtration) C) DNA type structure with associated protein in CIM OH flow though fraction D) smaller virus aggregate (approx. 1µm) with less DNA association in CIM OH.

An illustration, based on the data available on CIM OH is shown in Figure 6.10. The image is attempting to simplify a complex system, but shows how the NTA and qPCR data may be able to agree on a low yield of total particles, while the infectivity assay shows relatively high but variable infectious viral recovery. The NTA is identifying particles of between 250 nm and 350 nm. The recovery appears to be less than 50%. Large viral aggregates do not appear to be present, although particles above 1000 nm are above the limit of quantification for the instrument. The fact that the NTA and qPCR agree in terms of percentage recovery is interesting. This may be due to large viral aggregates present in the load material binding to the column and then being

broken down and recovered in the elution fraction. These particles wouldn't be detectable in the load by the NTA, as they would be larger than 350 nm, but would be detectable by qPCR as this is able to detect all encapsulated viral genomes. The particles would then be detectable by both assays in the elution. This theory only works if the majority of non-viral, host cell derived particles, of a similar size to vaccinia are removed prior to elution. However, data from BCA, PicoGreen and SEM suggest this may be the case. These assays show that that the concentration of contaminants in the elution is low. If this were not the case the NTA would yield a higher recovery than the qPCR as it is a non-specific step. Microscopy data suggests significantly less aggregation in the elution relative to the load, however, as only small sections of a sample can be analysed, many more images would be required in order to generate statistical significance, but this is still supportive data. $TCID_{50}$ is shown to yield a variable but high recovery of infectious virus. It is not known whether a single infectious viral particle can infect a cell if aggregated with other non-infectious particles. It is speculated, however, that in a dynamic system this may be a high source of variability. This question has been raised before, (Floyd & Sharp 1979;Kim & Sharp 1966) and it was concluded that aggregates are able to infect cells, however, how many cells an aggregate is able to infect and how the specific composition of the aggregate affects the infectivity is still unknown. What is worthy of note, is that aggregated vaccinia particles appear to be more resistant to UV radiation then single particles that have been sonic-treated to remove aggregates (Galasso and Sharp 1965). Based on the data presented in this thesis, aggregation in the presence of ammonium sulfate can be reversed by the addition of sodium phosphate without salt, as was shown in Figure 4.8.

Based on the NTA and $TCID_{50}$ data, the approximate total particle to infectious unit ratio (P:I ratio) in the CIM OH load is 100:1. In the elution this is reduced to 10:1. This

suggests that the CIM OH column is able to remove approximately 90% of the non-infectious particles from the load.

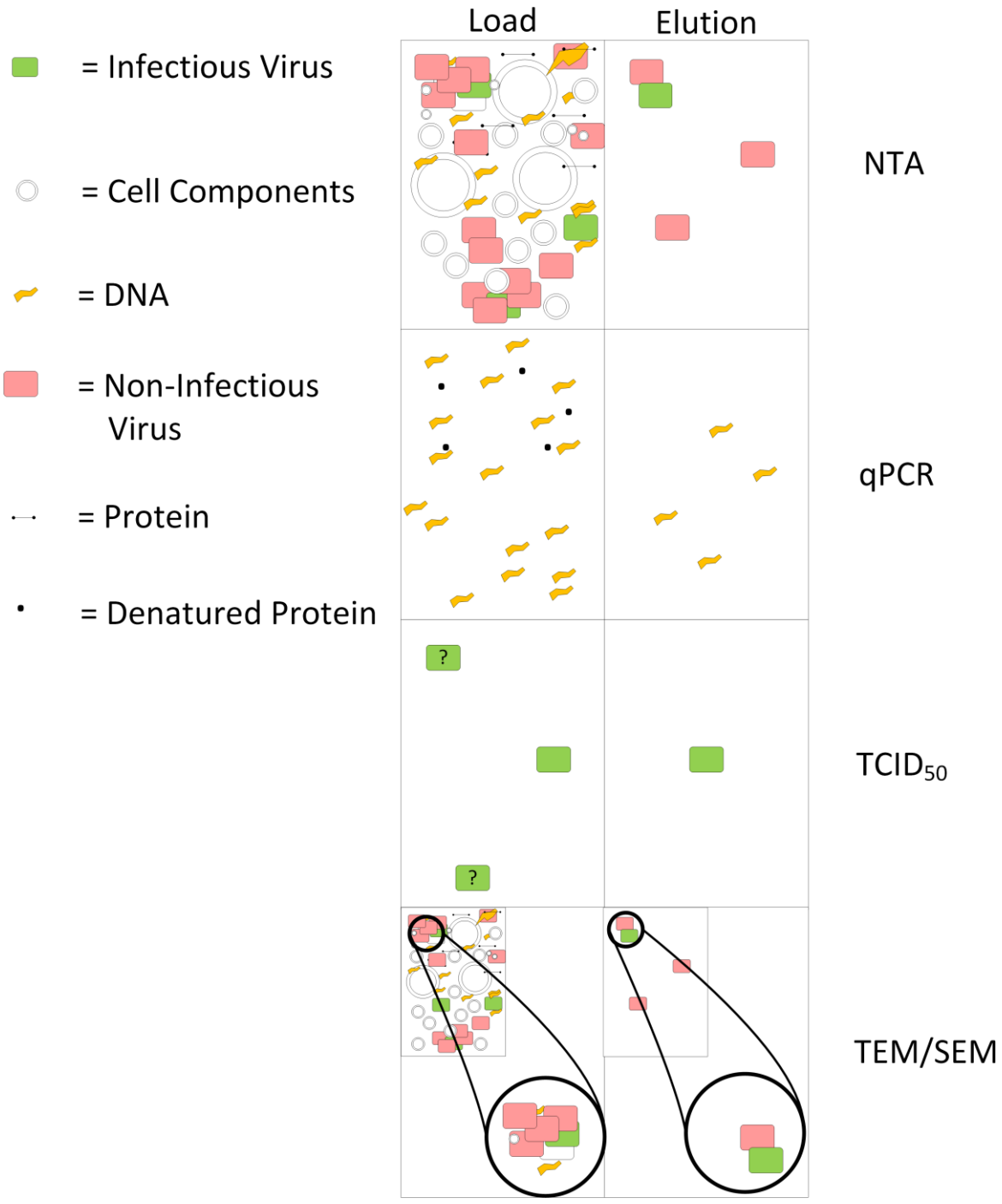

Figure 6.10 An illustration to show proposed feed stream complexity and purification output based on data from CIM OH. NTA is assumed to be able to count any particle of close to 300nm (red and green rectangle (viral particles), and circles (cell components)), qPCR will count all intact virus particles regardless of whether infectious or not, $TCID_{50}$ will only be able to count infectious virus particles, it is unknown whether infectious particles within an aggregate is able to infect a cell. TEM show an extremely small snap shot of the system.

6.7 Conclusions

CIM OH monoliths have proven to be an effective capture and polish step for vaccinia virus lister strain. The total protein concentration in the elution fractions were reduced to below LLOQ levels of the BCA assays used in this study. More specific host cell protein (HCP) ELISAs will be needed to confirm the results prior to clinical application, but the outcome of this study is encouraging. CIM OH monoliths are also able to remove an impressive amount of DNA without the use of Benzonase®. At pH 8 up to 99% of the DNA loaded was removed and infectious virus recovery in the elution was approximately 90%. This corresponded to a purification factor of 88. This purification factor is significantly higher than that achieved with CIM SO3. It was found that when developing a capture step for CIM S03 monoliths, a trade-off existed between the recovery of infectious virus and the recovery of DNA. This meant that the DNA purification factor was limited to 4.3. To illustrate this, in order to remove 92% of the DNA only 35% of the infectious virus loaded onto the monolith was recovered in the elution. CIM SO3 monoliths were also not able to remove as much total protein. When eluted with 300 mM NaCl a maximum of 92% of the total protein loaded was removed. This corresponded to a total protein purification factor of 4.

A potential downside of using CIM OH as a capture step is the loss of virus across the pre-column filtration step. The filtration step is necessary to prevent monolith fouling which can result in high backpressures. The recovery across the 0.8 µm filter in optimised HIC load buffer was found to be approximately 35%. This was increased from 6% by decreasing the levels of ammonium sulfate in the load buffer. In comparison the recovery across the same filter when loaded in CIM SO3 load buffer (50 mM sodium phosphate pH 7) is around 60 – 70%. This will need to be addressed in future work. 35% recovery, while reasonable for the purpose of developing a capture

step, would make the whole process extremely expensive in terms of overall cost per dose.

While there are many challenges associated with the development of viral processes, two stand out as being the most significant. The first is the complexity and incredible variability of the starting material in terms of infectious titre, concentration of DNA and protein, and levels of polydispersity in relation to particle size. The second is the poor quality of the available analytical assays. No single assay is able to tell the "whole story" in terms of virus concentration and many have a routine intra-sample variability greater than 30%. Both CIM SO3 and, in particular, CIM OH appear to be able to adsorb a relatively large number of viral particles, approximately $1x10^9$ pfu/mL of monolith. Both chemistries have demonstrated the ability to remove the majority of contaminants, both removing over 90% of DNA and Protein, and recovering a reasonably large percentage of infectious virus, up to 50% from CIM SO3 and up to 90% from CIM OH.

By employing a number of orthogonal analytical methods, simplified illustrations of each chromatographic system have been generated. These models are data driven and comparable to previous work. In order to increase the levels of certainty on the conclusions drawn, more replicates and an even greater variety of analytical measurements need to be performed. Resource limitations prevented these from being possible during this study; however, future work will need to include them.

Chapter 7

An Economic Evaluation of Monolith-based processes and Comparison to Parallel Technologies

7.1 Introduction

This chapter aims to compare monolith chromatography with ultracentrifugation for the purification of vaccinia virus feed streams. This comparison is designed to firstly, assess the feasibility of the industry moving away from ultracentrifugation. Secondly, it aims to identify the critical parameters that will need to be focused on during future process development of vaccinia virus in order to generate viable commercial processes. As described in Chapter 2, there are advantages and disadvantages to both ultracentrifugation and chromatography; hence in order to make decisions both of these need to be addressed. To assist with this process, a decision tool in the form of a cost of goods (CoG) model, built using BioSolve Process Enterprise Version 7 (Biopharm Services, Chesham, Bucks, UK) was used. The data used in the model is based on the chromatographic data generated during this EngD research project as well as published literature on the purification of vaccinia virus using large-scale ultracentrifugation. Process flow diagrams for the proposed ultracentrifugation and CIM monolith-based processes are show in Figure 7.1 (Section 7.3.2).

Purification using small and large pore TFF filters has also been used previously to purify influenza virus (Wickramasinghe, Kalbfuß, Zimmermann, Thom, & Reichl

2005), however, this has not been focused on in this chapter as question marks arise over this unit operation's ability to remove enough contaminates for high dose applications (Greenberg and Kennedy 2008;Monath, Caldwell, Mundt, Fusco, Johnson, Buller, Liu, Gardner, Downing, Blum, Kemp, Nichols, & Weltzin 2004).

7.2 Model Design and Setup

7.2.1 Cost breakdown

BioSolve Process Enterprise version 7 (Biopharm Services, Chesham, Bucks, UK) was used as a platform to build the whole process model. Cost data was taken from BioSolve's own data base unless otherwise stated. Exact unit prices for cGMP monoliths cannot be disclosed. This information is considered proprietary by BIA Separations; however, an up-to-date price list supplied BIA Separations was used in building this model.

The cost of goods breakdown considered in this study is shown in Table 7.1

Table 7.1 Breakdown of costs and their associated components

Grouped Costs	Components
Capital	General equipment
	Process equipment
	Cost of works
Materials + QC	
	Media
	Buffers
	Direct Raw Materials
	Bought WFI
	CIP
	QC tests
Consumables	
	Monoliths Columns
	Bags
	Filters
	Other
Labour	
	Process
	Quality
	Indirect
Other	
	Insurance/other
	Waste management
	Maintenance
	Utilities

7.2.2 Key equations and model rules

During small scale studies in T175 flasks CV-1, cell productivity was measured at approximately 100 pfu/cell. It is unknown whether this would scale up when producing vaccinia virus using microcarriers in stirred tank reactors, however, as a starting point, this value was carried through.

The following equation was used to estimate viral titre:

$$Titre = Mc\ x\ Md\ x\ Cm\ x\ VPc \quad (7\text{-}1)$$

where *Mc* is microcarrier surface area in cm^2/g, *Md* is microcarrier seeding density in g/L, *Cm* is the average number of cells per microcarrier in cells/cm^2 and *VPc* is the total viral particles produced per cell in pfu/cell.

cGMP compliant monoliths are available in three sizes, 0.08 L, 0.8 L and 8 L. In order to determine the size of monolith capsule required the following rule was applied.

$$IF\left(\frac{P_L}{DBC\ V_c\ N}\right) => 1 \ldots .\text{use larger column } ELSE\ use\ current\ size. \quad (7\text{-}2)$$

where P_L is the number of vaccinia particles in the feed stream in pfu, *DBC* is the dynamic binding capacity of CIM monoliths, which is set to 1 x 10^{12} pfu/L, V_c is the monolith volume in L, and *N* is number of cycles allowed (set manually).

This rule starts with the smallest monolith which is 0.08 L and will work up each available size until it gets to the largest of 8 L.

Labour costs are broken down into direct hours, solution preparation, and cleaning. Process operator and supervisors also incur indirect costs to the total.

$$\sum \boldsymbol{Labour\ cost} \quad (7\text{-}3)$$
$$= ((direct\ hours\ \times remuneration\ per\ worker) + unit\ operation\ solution\ prep\ costs + unit\ operation\ cleaning\ costs) + indirect\ costs$$

where indirect costs are made up of logistics, engineering and 'other' costs and are assumed by BioSolve to be 38% of the total production operator and supervisors direct costs.

Other costs, shown in Table 7.1, are made up of insurance, waste management, maintenance and utility costs.

Insurance, utilities and maintenance are calculated as a percentage of the total facility costs, as being 1%, 3% and 5% respectively.

Waste management is broken down into non-contaminated and contaminated, aqueous and plastic waste. The associated disposal costs of each are shown in the appendix.

As shown in Figure 7.1 later in this chapter, both the ultracentrifugation and monolith-based processes included two TFF steps.

The surface area of the filter is determined using the following equation.

$$A = \frac{V_p T}{J_p} \qquad 7\text{-}4$$

where V_p is permeate volume in L, J_p is flux in L m^{-1} h^{-1} and T is process time in h.

Total capital costs are made up of the components shown in Table 7.1. This number is assumed to be borrowed upfront. The capital cost per batch and per dose are then calculated from the estimate of capital costs per year. Annual capital is the amount needing to be paid back to the loan provider and is calculated using the following equation.

$$Annual\ capital = \frac{PR}{1-(1+R)^{-N}} \qquad 7\text{-}5$$

where P is the total capital cost, R is the fixed periodic interest rate, assumed to be 12% per year and N is the number of years required to pay back the loan. This is assumed to be 10 years.

7.3 Model Implementation

7.3.1 Key Assumptions

The base case assumptions made in the model are shown in Table 7.2.

Table 7.2 Ultracentrifugation and CIM Monolithic base case assumptions

	KII Ultracentrifugation	Monolith
Capacity	20 L/cycle	$1x10^{12}$ pfu/L
Flow rate	0.2 L/min	1 CV/min
Hold time 1st purification unit operation	12 hr	0 hr
Hold time 2nd Purification unit operation	1 hr	0 hr
Number of reuses	Infinite (cannot be cycled)	20 cycles
Percentage Virus Recovery	60%	60%
Bioreactor Volume	100 L	100 L

The capacity achievable on a KII ultracentrifuge using a K3 rota is reported by the manufacturer as being up to 200 L (Alfa Wassermann 2013). Previous work reported in the literature has shown that approximately 20 L of vaccinia broth can be processed with an RK-centrifuge in an RK3 rota with percentage recovery of approximately 60%

(Hilfenhaus et al. 1976b). The RK system is now obsolete, but the equivalent rota is available from Alfa Wassermann and has since been scaled up. It is likely that volumes greater than 20 L can be processed in the new rota as its volume has been increased from 1.6 L to 3.2 L. It is also assumed, based on data in the same publication, that two ultracentrifugation steps will be required. Virus material is pumped into the rota and then left for a set period of time for virus to band in the sucrose bed. In the base case scenario, the first banding occurs in 12 hours while the second takes 1 hour. Smaller viruses can take several days to band; therefore a maximum of 50 hours for each (ultracentrifugation) unit operation has been used in the comparative analysis section of this chapter (Figure 7.5).

Based on work with CIM SO3 and CIM OH monoliths, a dynamic binding capacity of $1x10^{12}$ pfu/L is a reasonable assumption for large-scale vaccinia processes. This assumes that the 1 mL monoliths scale linearly. As large-scale monoliths can be run up to a maximum velocity of 1 CV/min, this flow rate has been fixed for all sensitivity and scenario analyses. The percentage recovery of infectious virus was shown to be above 60% from both CIM SO3 and CIM OH, therefore the base case infectious recovery was fixed at 60%. The production volume was set to 100 L. In reality this would depend on the therapeutic application, the efficacy of the therapy and the market demand. As these are unknown it was decided to indiscriminately set a limit and keep this constant during all comparative studies. A table of main costs is shown in Table 7.3. Key personnel remuneration costs are show in Table 7.4.

Table 7.3 Lists of key process costs. The "General process" costs category comprises costs specific (referring) to unit operations that are the same regardless of the purification strategy. This includes upstream, primary recovery and final formulation costs. * Monolith costs are confidential so have been approximated.

Process	Step	Unit cost
General process	100 L bioreactor	200,000 USD
	Depth filters	300 USD/m^2
	UFDF filters	3000 USD/m^2
	Bags	
	• 20L	420 USD
	• 50L	450 USD
	• 100L	520 USD
	• 200L	660 USD
	Media serum free (DMEM/F12)	3.31 USD/L
	Buffers (DPBS)	0.73 USD/L
	In vitro virus assay (infectivity)	13,000 USD/assay
Monolith chromatography process	Chromatography rig	220,000 USD
	Monoliths*	
	• 0.08 L	~5,000 USD
	• 0.8 L	~10,000 USD
	• 8 L	~30,000 USD
Ultracentrifugation process	Ultracentrifuge	350,000 USD

Table 7.4 Personnel remuneration costs per year (BioSolve Process Enterprise)

Personnel	Remuneration (USD/Year)
QC	74,400
QA	97,650
Supervisors	100,750
Operators	62,000

A list of more general process assumptions made in relation to both monolith and ultracentrifugation processes are listed below.

- Each process is able to generate material to the required regulatory standards in terms of purity.
- Ultracentrifuges are not cycled. Ultracentrifugation cycling occurs when a single system is run multiple times in order to process the whole batch. If an ultracentrifuge reaches capacity and additional material requires purification, the batch will be split and run in multiple machines in parallel. The reason behind this assumption is given in Section 7.3.2 Process Flow and Facility Design.

- Infectivity analysis (*in vitro)* is required after every unit operation. If a batch is split in two, each new feed stream is analysed independently before being pooled back together.

- A new facility will be built with new equipment. Capex will be spread across a 10 year duration in which it will lose 90% of its value.

- Treatment requirements are five injections of $1x10^9$ pfu/injection. This makes the total treatment requirements of $5x10^9$ pfu per patient. A dose is assumed to be the total $5x10^9$ particles.

- The bioreactor volume is fixed to 100 L in all scenarios unless otherwise stated. It was assumed that the treatment was for Head and Neck cancer which had an incidence of 58,293 patients in the UK between 2010-2013 (Public Health England 2015). The base case process would produce enough material to treat 90% (17,580) of these patients each year.
- Viral titer is assumed to be $1.6x10^{11}$ pfu/L based on the following assumptions (Simaria et al. 2014):
    - Microcarrier surface area (Mc) = 2,530 cm^2/g
    - Microcarrier seeding density (Md) = 6.3 g/L
    - Total cells per microcarrier surface area (Cm) = $1x10^5$ $cells/cm^2$
    - Total viral particles produced per cell (VPc) = 100 pfu/cell
- The cost of microcarriers has not been taken into account in the model but is assumed to be constant as bioreactor volume is fixed.
- The model does not take into account the bioreactor seed train, but starts from 100L.
- All prices have been converted to USD using exchange rates described in the Appendix.
- All media and buffers are made up on a per batch basis.
- Single use systems are used for the following:
    - Bioreactor
    - All filtration systems
    - Media, buffer and product hold tanks
- A campaign is designed to last 12 months with 21 days of maintenance and 14 days set aside for validation.
- Each shift is 9 hours long.

- The base case batch duration for the monolith-based process is 11 days. The ultracentrifugation process takes 10 days.
- The number of batches produced per year for each base case is estimated to be 30.
- Batch failure rate is set to 5%.
- The final formulation buffer is assumed to be Tris-HCL plus sugars such as sucrose (Ungerechts et al. 2016).

The default model parameters set out in BioSolve in terms of capital breakdown, waste management, solution preparation time, cleaning, facility and maintenance costs are kept as default and are all shown in the Appendix.

7.3.2 Process Flow and Facility Design

The model compares two proposed processes. The first has two chromatographic steps, both of which are CIM monoliths; the other has two ultracentrifugation steps. The two ultracentrifugation steps, as discussed in Section 7.3.1, are assumed to be carried out using a KII Alfa Wasserman ultracentrifuges fitted with a K3 rota. Proposed process flow diagrams are shown in Figure 7.1. Each process is the same, except for the two purification steps. The whole process sequence has not yet been tested, and so it is partially conceptual, nevertheless has been assumed to work.

The model has been designed without specific costs associated with a full seed train in order to reduce complexity. As the main questions asked in the analysis are focused on determining the operational feasibility of using a chromatography-based purification process as opposed to ultracentrifugation, it was decided that accurate determination of exact costs per dose were not the primary concern. What was important was to accurately determine comparative trends and trade-offs associated with critical process

parameters known to be variable in both ultracentrifugation and chromatographic processes.

The primary recovery steps in the processes described are based on unit operations being designed at UCL (Personal Communication 2016). The process uses a tangential flow filtration step to concentrate and lyse CV-1 cells (grown on microcarriers) in the presence of TritonX-100, a non-ionic surfactant commonly used to chemically lyse cells (Giard et al. 1977;Wang and Ouyang 1999). The model assumes that an average transmembrane flux of 50 LMH is achievable, the harvest is concentrated 20 times and then diafiltered 7 times in buffer containing TritonX-100. After the diafiltration step, the retentate is passed through a depth filter to remove the microcarriers and cell debris. Depth filtration is used in many processes to remove whole cells, and has been used for clinical grade vaccinia virus to remove cell debris in the past (Ungerechts, Bossow, Leuchs, Holm, Rommelaere, Coffey, Coffin, Bell, & Nettelbeck 2016). The primary recovery steps have been kept the same for each process so that any trends seen are known to be resulting from changes made to the purification steps.

It is assumed that the first TFF step will buffer exchange the feed stream into the appropriate load buffer for the first chromatography step. The elution from the first chromatography step is then diluted 1:5 before the second column. Monoliths run at high flow rates (1 CV/min) so this increase in volume is not a limiting factor in the process, as it will only marginally increase the overall processing time of the second step. The reason why an additional UFDF step was not preferred over an inline dilution is that it was considered unnecessary. An additional UFDF step would likely reduce the overall process recovery and increase the processing time. This would decrease productivity and increase costs. The final TFF step is designed to concentrate and then buffer exchange the virus into its final formulation buffer.

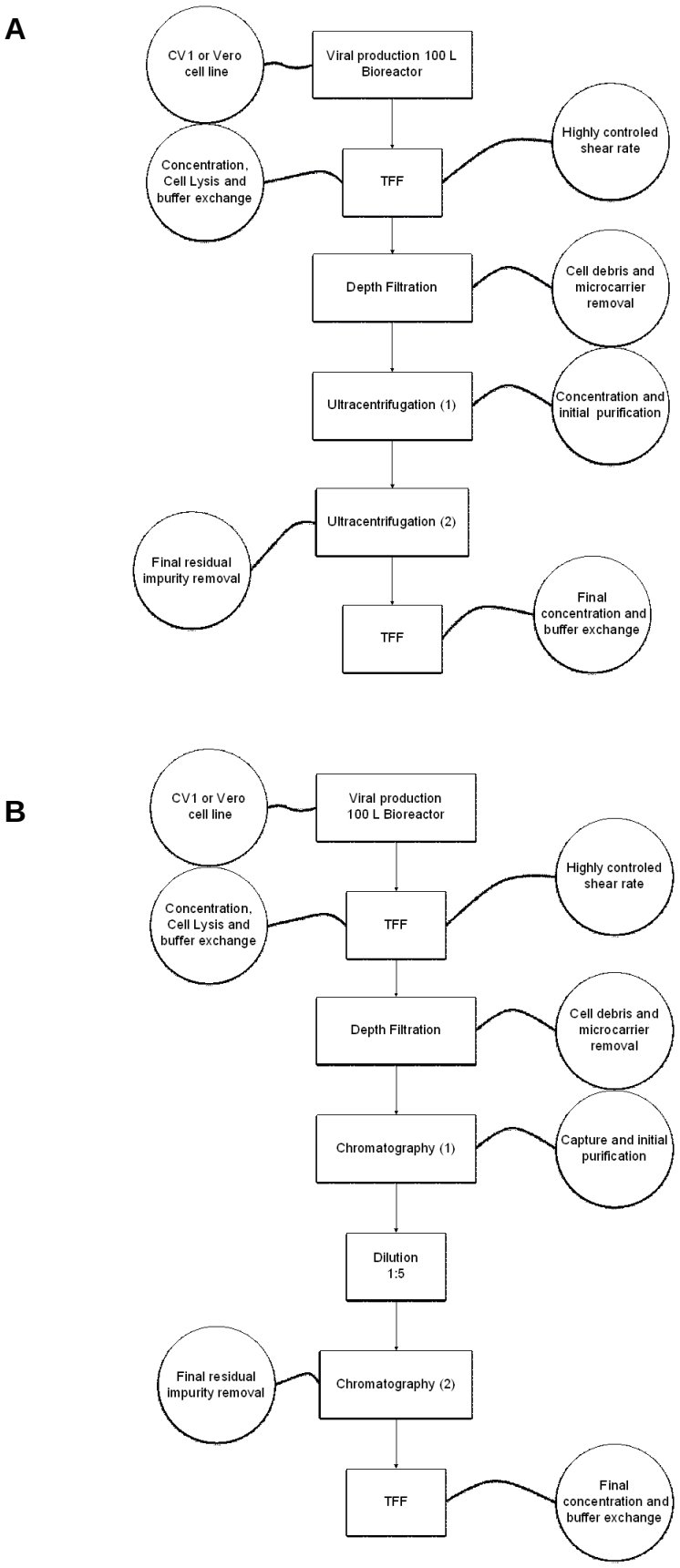

Figure 7.1 A) Proposed ultracentrifugation process flow diagram B) Proposed CIM monolith process flow diagram

One of the main process assumptions is that ultracentrifuges cannot be cycled in the same way as chromatography columns. The reason for this is that system setup and shut down is a very manual process and takes most of a 9-hour shift. It is assumed that an operator would need to leave the system running overnight for approximately 12 hours, although some viruses can take longer than 24 hours to band. Shutting the system down and fractionating the bed, not to mention cleaning and sterilising the system ready for reuse, is assumed to take at least a day. This would imply a considerably long holding time for this labile viral product at 2-8 °C. Vaccinia would likely start to lose infectivity. Instead, a batch is split and run in multiple machines in parallel. The downsides of this option are an increase in process equipment costs and an overall higher investment due to the requirement of larger facilities. The option of running ultracentrifuges in parallel needs to be taken into account in the design stage of the facility because a process change of this calibre cannot be easily retrofitted into an existing facility unless enough extra space existed into the DSP suite. Two example fit outs are shown for the ultracentrifugation process in Figure 7.2. As the majority of closed process DSP products are handled in grade C clean rooms, this would be very expensive and hence is unlikely. BioSolve Process Enterprise does not take the added design change into account when adding new equipment but calculates the total clean room space requirements based on equipment size.

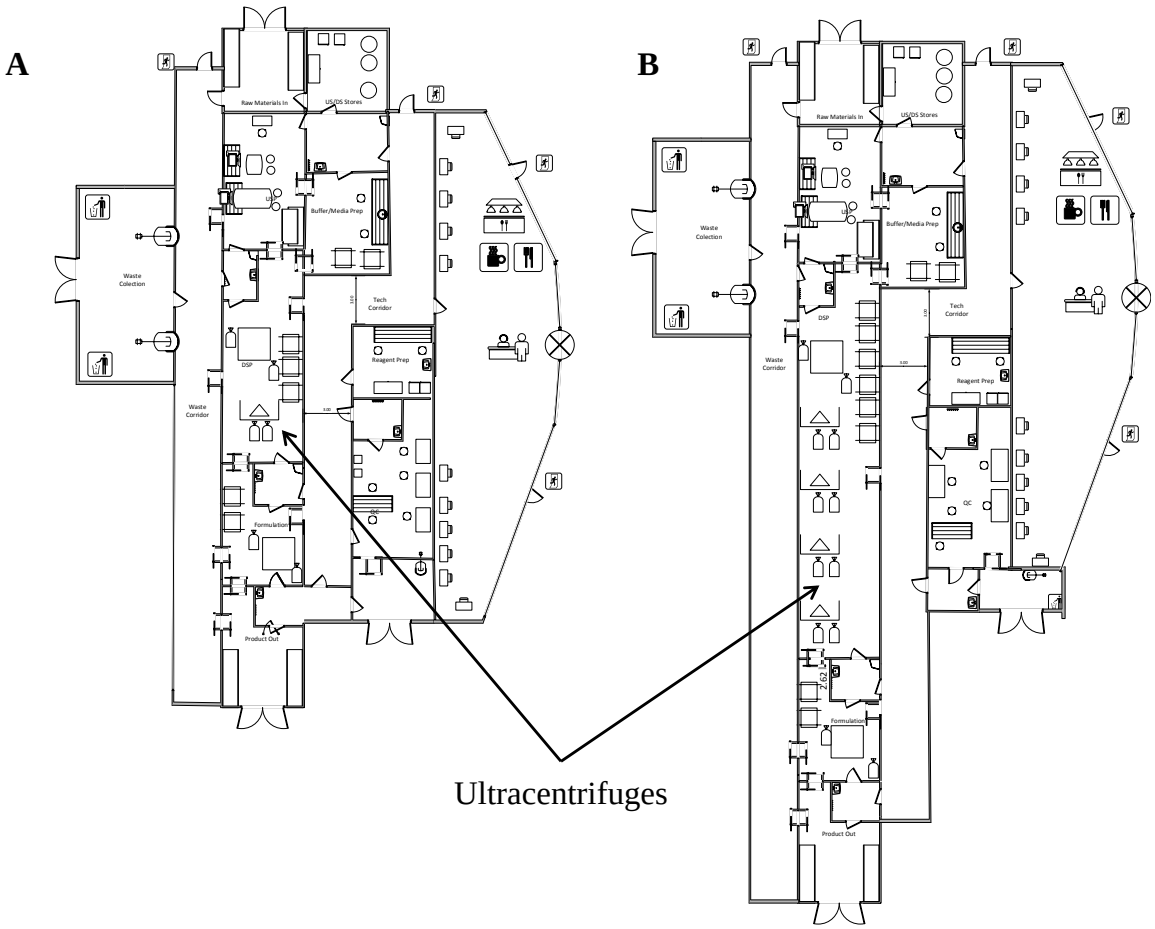

Figure 7.2 A) Facility fit out with a single ultracentrifuge B) Facility fit out with four ultracentrifuges running in parallel.

7.4 Comparison between Chromatography using CIM Monoliths and Ultracentrifugation

7.4.1 CIM Monolith and Ultracentrifugation Base Case Process Costs Breakdown

The ultracentrifugation and chromatography base case processes described above have been modelled and compared against each other. Figure 7.3 shows a cost breakdown for the ultracentrifugation and monolith processes in terms of total annual cost of goods. It is immediately obvious that the overall costs are similar. The ultracentrifugation process is estimated to cost $8.3 million per year, while the monolith process is estimated to cost $8.2 million per year.

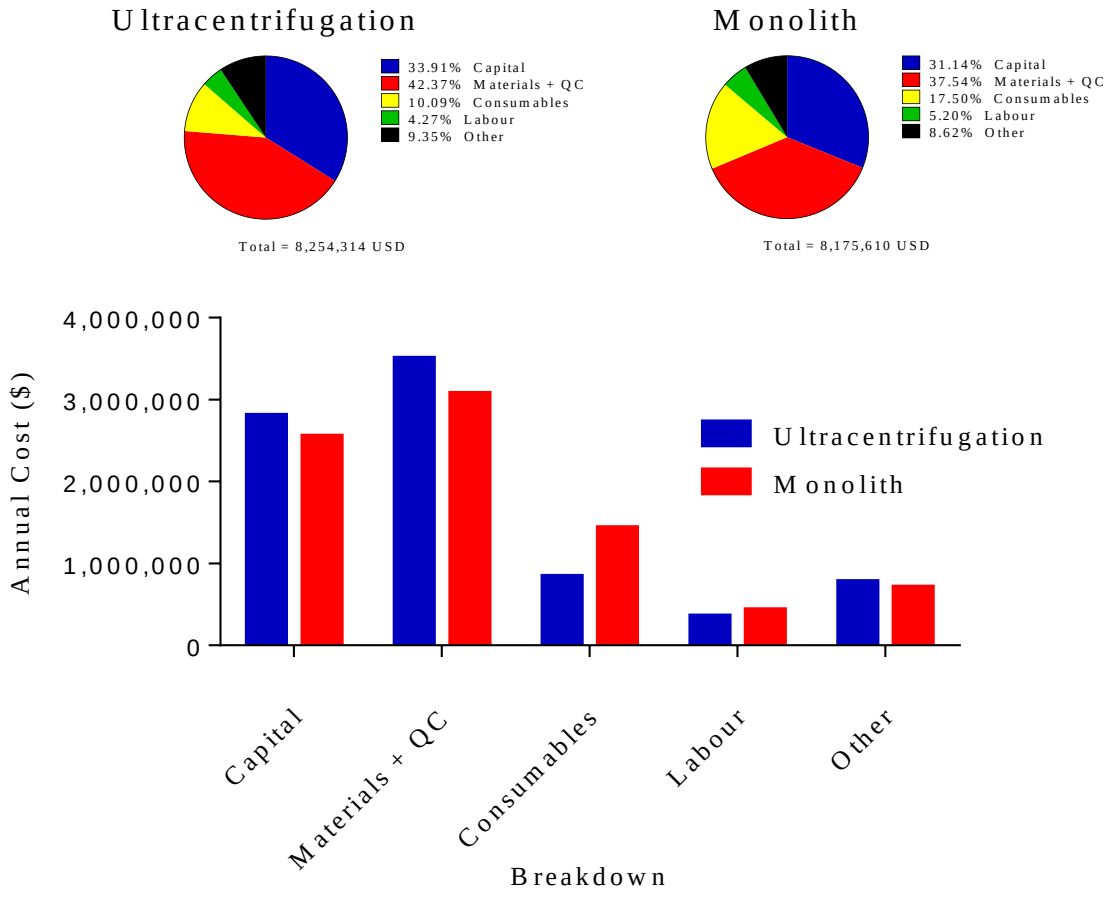

Figure 7.3 Costs breakdown of base case chromatographic and ultracentrifugation-based processes

Capital is seen to be a major cost in both processes, a breakdown of which can be seen in Figure 7.3. The reason for this is that both base case processes require a similar amount of equipment so costs associated with build, purchase, fit out, installation and validation do not vary much between processes, but are in each case significant. The ultracentrifugation process requires an additional centrifuge whilst the monolith process design assumes the requirement of two chromatography rigs, therefore the capital cost of the former process is only slightly higher than that of the monoliths process.

Materials and QC (which BioSolve groups together) is shown to be the other major cost. The majority of this cost comes from the QC. In vitro virus testing is required for each

in process product fraction, and is estimated by BioSolve to cost 13,000 USD per assay. Buffer and media costs are not particularly large as the bioreactor volume and total buffer volume requirements are relatively small.

As the ultracentrifugation process splits the batch if the percentage utilisation of a single rota reaches over 100%, extra infectivity assays (one for each product fraction) are assumed to be required. For this reason, the materials and QC costs are slightly higher for the ultracentrifugation process than for the monolith process. Labour costs are shown to be slightly higher when using monoliths as 13 cycles are required in order to process all the material. A monolith process also results in a higher consumable cost as the resins are expensive. The most expensive consumable costs associated with the ultracentrifugation process are the TFF filters, the total surface area requirement of which being the same for both base case processes.

As shown in Table 7.1, the costs labelled ‘other’ include insurance, waste management, maintenance and utilities. The reason why these are slightly higher for ultracentrifugation than for chromatography is the slightly higher capital cost.

7.4.2 CIM Monolith and Ultracentrifugation Process Sensitivity Analysis

In order to test the assumptions made in the base case model, Section 7.3.1, a sensitivity analysis was run for a number of general and purification technology specific factors thought likely to influence the cost of goods. The rational here was to gain understanding of the significance of the effects the fluctuation of these factors have on CoGs. The factors tested are presented in Table 7.5. The results are shown in Figure 7.4.

Table 7.5 Factors changed in the Ultracentrifugation and Monolith sensitivity analysis. Best case, base case and worst case scenario values are shown

Factors Changed	Range and Base Case Values					
	Ultracentrifugation Process			Monolith process		
	Low	Base	High	Low	Base	High
Capacity	1 L	20 L	200 L	$5x10^{11}$ pfu/L	$1x10^{12}$ pfu/L	$3x10^{12}$ pfu/L
Flow Rate	1 L/h	12 L/h	60 L/h	1 CV/min		
Number of Reuses	cannot be recycled			1	20	40
Percentage Virus Recovery	20%	60%	100%	20%	60%	100%
Bioreactor Volume	10 L	100 L	200 L	10 L	100 L	200 L

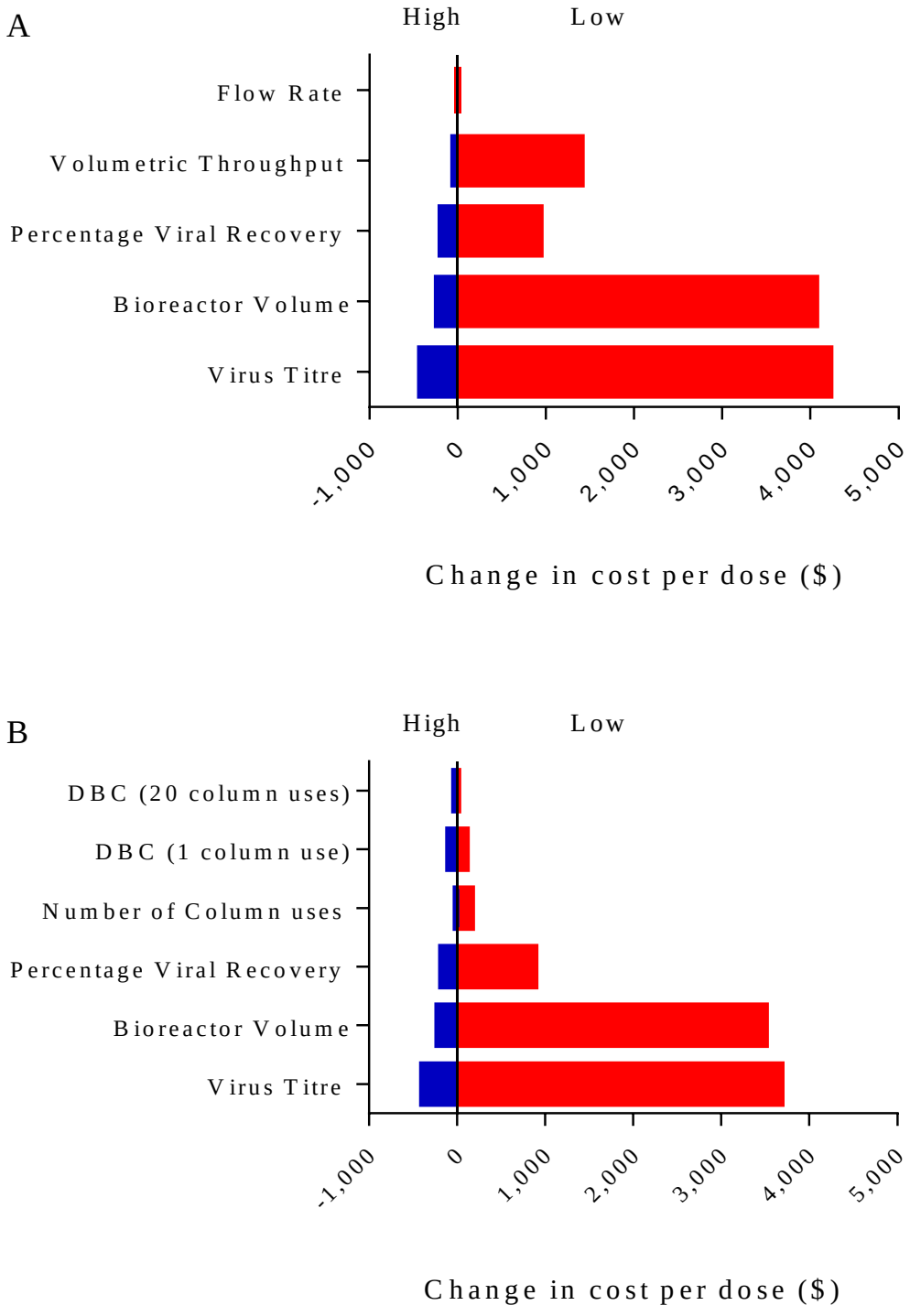

Figure 7.4 Tornado diagrams showing the effects of changes in the base case variables shown in Table 7.5 on the overall costs per dose. A) Shows factors affecting CoGs for ultracentrifugation processes. B) Show factors affecting CoGs for monolith processes. All factors were changed independently with all other conditions remaining the same as in the base case. Blue bars represent a reduction in costs per dose while red bars represent an increase.

There were a number of reasons for choosing the factors shown in Table 7.5. Firstly, it was thought that they would have a significant effect on the CoGs. Secondly, they are all parameters that can theoretically be optimised during process development. Should trade-offs that include any of the factors analysed arise during process development, an understanding of their effects on the CoG relative to each other can also help when making process development decisions. A hypothetical example of this might be a trade-off between loading capacity and the number of possible reuses of a monolith column. The results of a sensitivity analysis can be used to set priorities in terms of which parameter to favour.

The capacity achievable when developing ultracentrifugation or monoliths-based processes is likely to be one of the first major questions asked in process development (Hilfenhaus et al. 1976a;Hilfenhaus, Kohler, & Gruschkau 1976b). The ranges shown in Table 7.5 are based on both literature and vaccinia process development data. In terms of flow rate, large-scale monoliths can be run at a maximum flow rate of 1 CV/min. As mass transfer is not limited by diffusion, comparison studies looking at the effects of different flow rates on binding and resolution are unlikely to be on the critical path, therefore the decision was made not to include any variation on flow rate into the sensitivity analysis for monoliths. The range and base case values chosen for the ultracentrifugation process come from values specified by the manufacturer, and would need to be confirmed experimentally. The number of reuses possible when using monoliths are, again, based on the manufacturers best case assumptions. As described in Section 7.3.1, the model assumes that ultracentrifuges cannot be cycled. For this reason, ultracentrifugation cycling is also not included in the model. Percentage recovery of virus particles was assumed to have a large impact on CoGs for both processes. While results vary from virus to virus and from process to process, it is difficult to conclude that either one of the processes being compared would likely be superior to the other in

general terms when it came to percentage recovery. Data in the literature, as well as data generated for this thesis, shows that virus yield is extremely variable on both systems. Between 20-100% recovery of infectious virus is recorded in the literature (Gerster, Kopecky, Hammerschmidt, Klausberger, Krammer, Grabherr, Mersich, Urbas, Kramberger, Paril, Schreiner, Nobauer, Razzazi-Fazeli, & Jungbauer 2013b), therefore this range was used with a base case recovery in each case set at 60%. Bioreactor volume and virus titre were included in the analysis for two reasons. Firstly, for completeness but secondly, to act as a reference point in terms of relative impact. It is well known that titre has a massive impact on the overall CoGs per dose when varied, so the effects of other factors can be compared to this change to enable a thorough evaluation of potentiation impact.

7.4.2.1 Factors Identified in the Sensitivity Analysis to Affect Cost of Goods

As expected, changes in viral titre and bioreactor volume have the most significant effects on the CoGs as seen in Figure 7.4. The reason for this is that the number of viral particles produced per unit volume, as well as the total volume of starting material available per batch if the titre remains constant, directly affects the number of doses produced annually. This outweighs any increases in cost associated with handling the extra material.

The cost of an ultracentrifugation process is significantly affected by the volumetric capacity of the machine. Batch ultracentrifuges have significant load volume limitations as each rota has a fixed volume and this cannot be surpassed. Continuous flow ultracentrifuges are designed to be continuously loaded at a pre-defined flow rate until a maximum capacity is reached. The machine is then typically left for periods of time

ranging from several hours to several days to allow virus to band. The overall volumetric throughput is dependent on the total mass of impurities with a similar size and buoyant density to the virus. When capacity is reached, the purification factor starts to drop off quickly as banded virus and impurities start to overlap. The reason why the volumetric throughput has such a significant impact on the CoGs is directly related to one of the primary assumptions being made about ultracentrifugation in the base case model. This is that an ultracentrifuge cannot be cycled when run at large-scale. One of the main reasons for this is that viral stability would become a limiting factor as the process would take a long time to run. If this assumption is acceptable, and a centrifuge is unable to process the whole volume in a single cycle, then a batch would need to be split and run in multiple machines in parallel. Consequently, in the case of low achievable volumetric throughput, this would result in a significant increase in the capital cost of the process.

Depending on the stability of the virus being processed and the total cycle time of each ultracentrifugation step, the supposition that ultracentrifuges are not able to be cycled may become debatable. In order to evaluate the potential costs per dose of running an ultracentrifugation step in multiple cycles a scenario analysis was run assuming different processing times with and without cycling. The output was plotted as a function of volumetric throughput. This data is presented in Figure 7.5.

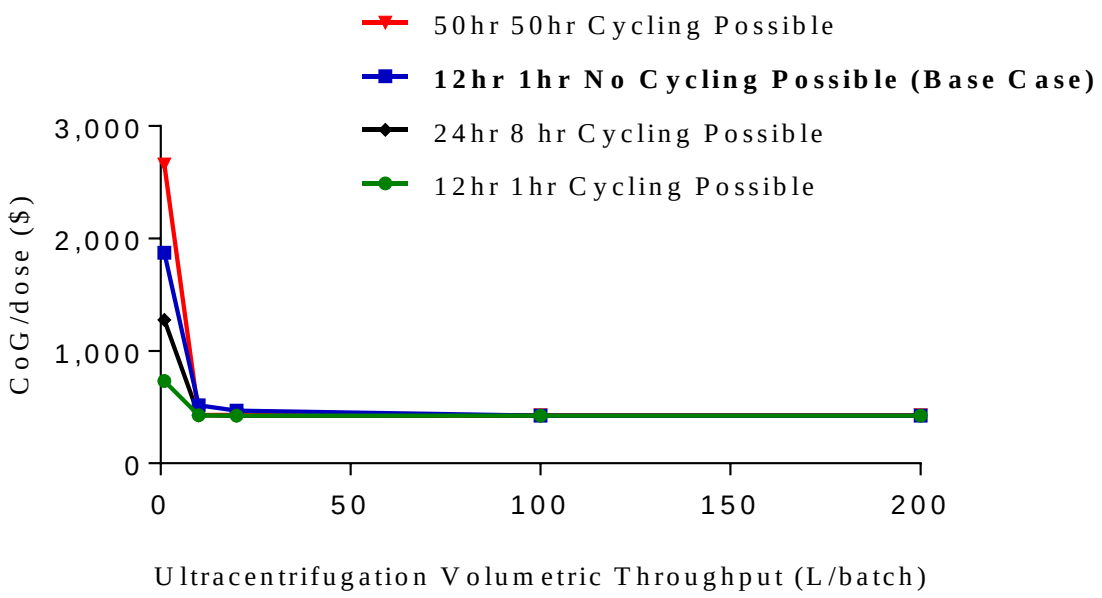

Figure 7.5 Effects of Ultracentrifugation cycling and process time on the CoGs per dose. Time periods represent the first and second ultracentrifuge step process times. Cycling Possible = batches are cycled on one machine. No Cycling Possible = batches are split and run on multiple machines if required. Base case is assuming a 20 L vol. throughput for 12hr in the first system and 1hr in the second and cannot be cycled (Blue line in bold type script).

In reference to the base case ultracentrifugation process (as shown in Figure 7.3) cycle times used in the model were taken as reported in the literature (Hilfenhaus, Kohler, & Gruschkau 1976b). In this paper virus was loaded into the KII ultracentrifuge at 12 L/h and left to band overnight. The next day virus was fractionated and processed once again but this time left to band for an hour only. 50 hours as an assumption is an exaggeration, but shows the effects of cycling on the cost of goods as the banding time increases. Other sources suggest that viruses such as Rabies will band in as little as 8 hours (Kumar et al. 2002).

The costs are shown to increase exponentially (Figure 7.5) when the volumetric throughput of an ultracentrifuge is low. This is seen to be the case even if the machines can be cycled, although the negative impact on cost is lower. This is illustrated when

comparing ultracentrifugation banding times of 12 hours followed by 1 hour with and without cycling (green and blue lines Figure 7.5). If an ultracentrifuge can be cycled, then the additional capital of purchasing multiple machines would not need to be spent, however, the downstream process would take significantly longer, and this would become a bottleneck (Morenweiser 2005). This point is emphasised when the volumetric throughout is below 20 L/batch.

It can be seen in all cases that when volumetric throughput increases above ~25 L per batch (Figure 7.5) the costs become very similar. The reason for this is that a single ultracentrifuge is able to process all the material, therefore it makes little difference whether it can be cycled or not. As only a single bioreactor is used in the model, BioSolve schedules the campaign by taking the total number of weeks the facility is in operation and dividing that number by the total time taken to complete the longest stage of the process. This is then multiplied by the percentage facility utilisation. In most cases the bottleneck in terms of time is in the upstream process (197 h). The campaign is scheduled by running the time bottle neck unit operations in series. Even if the ultracentrifugation process takes 50 hours, this unit operation would not become the bottleneck unless the volumetric throughput was lower than 20 L. At high volumetric throughput, the only significant impact compared to base case assumptions would be labour. However, labour as shown in Figure 7.3, does not make up a significant proportion of the CoGs. Capital and raw material costs remain the same as a single ultracentrifuge is run once to purify all the material. The impact of cycling the ultracentrifugation step assuming a 50-h run time on whole process timelines is shown in Figure 7.6. All other base case assumptions are kept constant.

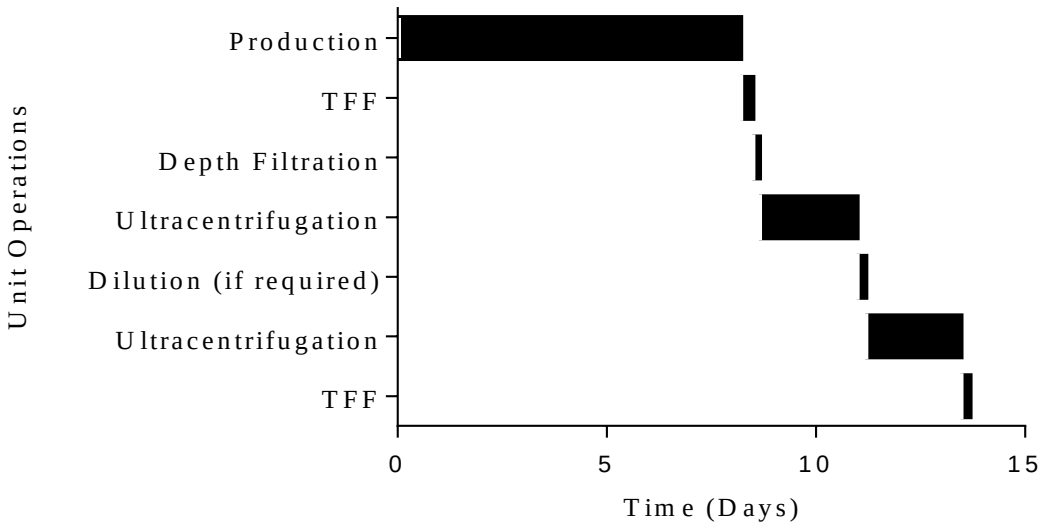

Figure 7.6 Production Gantt chart to show time requirement for each unit operation in days. This assumes each ultracentrifuge requires 50 h to band vaccinia.

Variations in the infectious virus recovery have, as expected, a significant effect on the cost of goods per dose for both chromatographic and ultracentrifugation-based processes. In a similar way to the effects seen on costs when viral titre and reactor volume are increased, more doses are produced per batch when recovery increases. Interestingly, as shown in Figure 7.7, when costs are analysed as cost of goods per batch rather than per dose for the monolith process, the trends seen are reversed. This is because the lower recovery reduces the number of particles needing to be processed, which results in less media being required, or fewer cycles of a given amount of resin per batch being needed. This reduces both the consumable and labour costs. This is not the case for ultracentrifugation as throughput is based on volume, and therefore assumed not to be affected by the number of infectious viral particles in the load.

The reason why the increase in recovery still leads to a drastic decrease in the CoG/dose is that the increase in CoG/batch is fairly marginal. An increase in percentage recovery from 20-100% elevates the CoG/batch by approximately 10%.

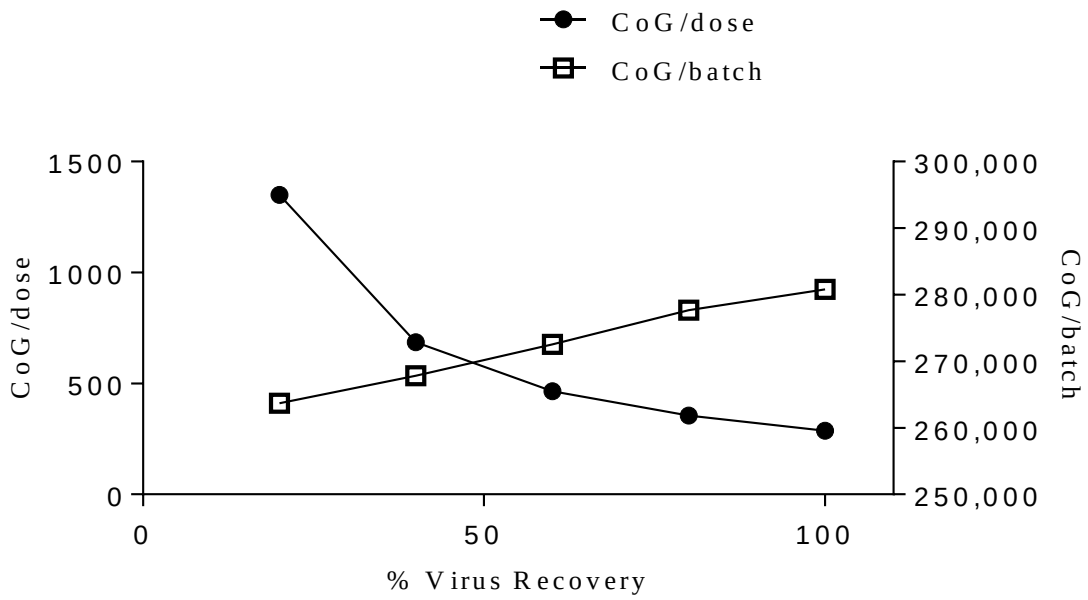

Figure 7.7 Effects of percentage virus recovery from the first of the two chromatography steps analysed as total cost per dose and costs per batch

Labile viruses have a tendency to lose infectivity during chromatographic processing, especially at extremes of salt concentration. The recovery of infectious virus from chromatographic systems is therefore an important performance attribute requiring attention during process development.

One of the disadvantages of using chromatography is that resins are expensive, especially if a large volume is required in order to process the material required. Factors that influence this cost other than the amount of material required, which is often fixed, is how much material can be loaded onto the resin before its capacity is reached, and how many times the resin can be re-used. As shown in Figure 7.8, the effects of each

factor on the cost of goods are related. There is an inversely proportional relationship between the number of reuses and the cost of goods. This is shown under base case assumptions in Figure 7.8A. There are three cGMP compliant commercially available CIM monoliths, these include 0.08 L, 0.8 L, and 8 L units. The cost of goods model was designed to pick the smallest column that will process the whole batch. Figure 7.8B shows the effects of increasing DBC on the cost of goods per dose. The graph shows 3 different values as the DBC is increased. An 8 L column is required for the lowest DBC tested; this then changes to an 0.8 L and eventually to an 0.08 L monolith.

What can also be seen when analysing Figure 7.8B is that these values are also dependant on the number of times the monoliths can be recycled. The effect of a column's inability to be recycled on the CoGs is much greater when the DBC is low, as significantly more resin is required. The data also suggests that when the columns can be recycled more than 10 times the DBC has little effect on the CoGs. This is because all the material can be purified using a single small 0.08 L monolith column. Moreover, the base case process requires 13 cycles on a 0.08 L monolith, however, as monoliths are run at high flow rates this has minimal impact on the overall batch processing time and so does not impact the total number of batches produced during a 12-month campaign. Based on this data it can be concluded that the number of reuses is more important than the relatively small changes in the DBC in reducing overall CoGs/dose. The cheapest processing option is to cycle smaller columns 10 or 20 times rather than run a single large column to capacity.

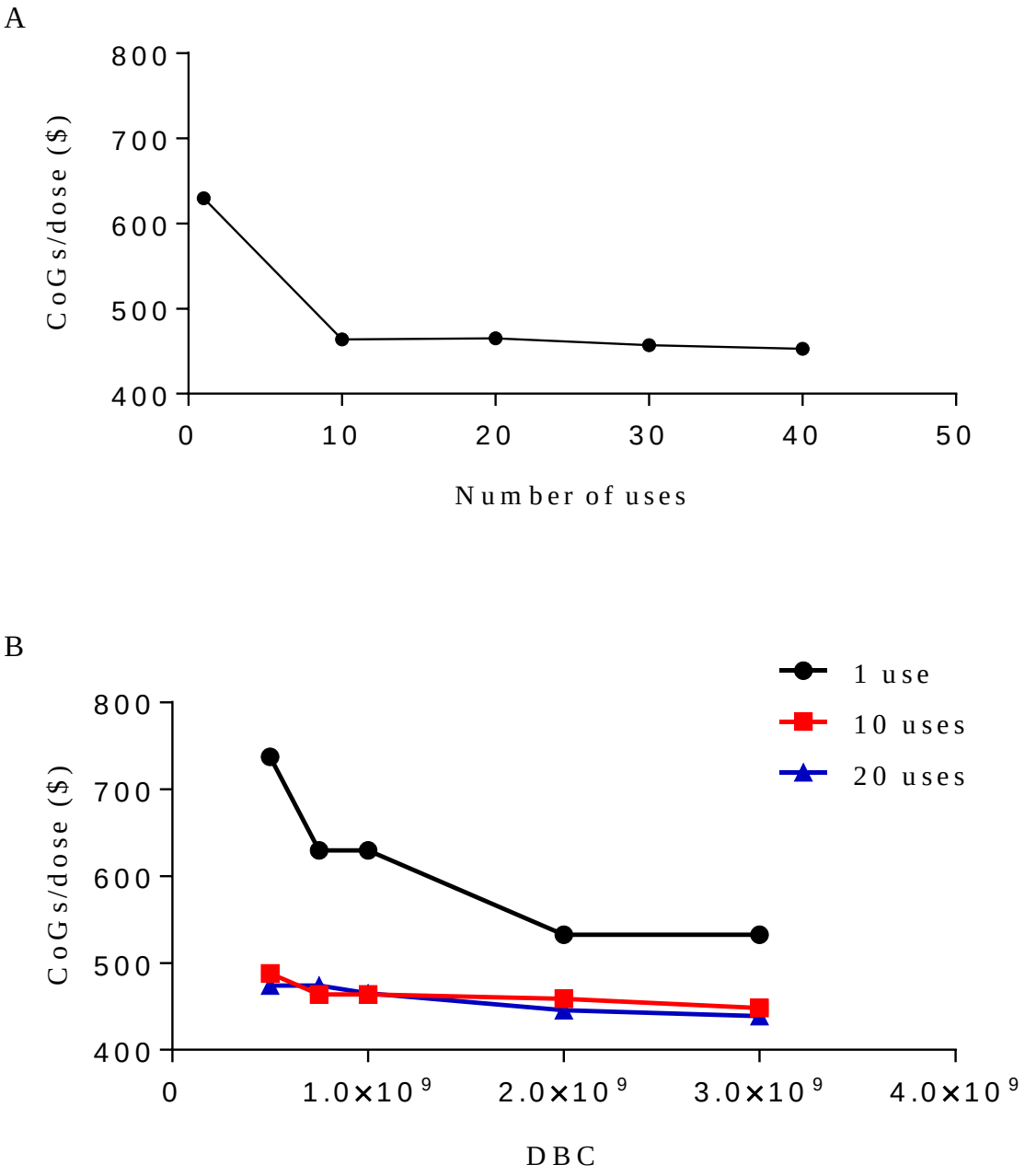

Figure 7.8 Effects of DBC and reusability of CIM Monoliths on CoG per dose.

The experimental data in this thesis suggests that CIM SO3 monoliths may yield less infectious virus in the elution fraction after multiple uses. This might be the result of monolith fouling, and may be linked to the amount of total DNA in the load as described in Section 5.5.2. CIM OH monoliths by comparison do not appear to be

affected by the number of previous uses and yield a purer viral prep than CIM SO3, as described in Section 6.7. Both monoliths have similar DBCs for vaccinia virus, although CIM SO3 shows more variability in this respect with potential DBC values ranging from $1x10^9$ to $3x10^9$ pfu/mL, (Figure 4.6). In the event that either chemistry is assessed as an initial capture step for vaccinia virus, this cost data can be combined with the experimental data obtained in order to identify drivers for future process development. An example of this might be the decision to work on increasing the binding capacity and yield of CIM SO3 but accepting that this type of monolith might only give robust and reliable results once and will therefore need to be used as a single use resin.

7.5 An Economic Comparison between Chromatography using CIM Monoliths and Ultracentrifugation.

The data in Table 7.6 summarises the advantages and disadvantages of ultracentrifugation and chromatography in comparison to each other. Both systems are able to remove impurities so purity is not generally a bottleneck. The reason percentage yield has been placed as an advantage for ultracentrifugation is that particles do not have anywhere to go. It has been reported that infectivity can be lost in some instances depending on the stationary phase used (Gias, Nielsen, Morgan, & Toms 2008), but recoveries equivalent to optimised chromatographic systems have been reported for many years (Hilfenhaus, Kohler, & Gruschkau 1976b).

Table 7.6 Advantages and disadvantages of ultracentrifugation and chromatography and filtration as purification unit operations for viral vaccines. Yield has been coloured red as the recovery of infectious virus from each unit operation is dependent on the type of virus.

	Ultracentrifugation	Chromatography
Advantages	□ Purity □ Yield	□ Purity □ Scalability (DBC)
Disadvantages	□ Cost □ **Scalability (Throughput)**	□ Cost □ **Yield (requires optimisation, trade-offs exist)**

One of the major differences between chromatography and ultracentrifugation is the trade-off between ultracentrifugation throughput and chromatography percentage yield versus product purity. During chromatographic development conditions that maximise product recovery tend to also maximise the recovery of impurities which limits the purification factor achievable. Ultracentrifugation percentage recovery is dependent on banding efficiency. The separation of product from contaminating impurities is often high if there is a significant difference in buoyant density between the different components. When the difference is small, the bands can overlap which reduces the purification factor achievable. In practical terms, this will impact the amount of material that can be loaded onto the bed as increasing the loading capacity reduces the separation efficiency. The data in Figure 7.9 shows a direct comparison between the trends in CoGs/dose from the ultracentrifugation and monolith-based processes when the volumetric throughput of the ultracentrifuge, and the recovery of infectious virus from a monolith is varied. The graph shows that the costs overlap assuming that 60% recovery of infectious virus can be achieved without optimisation from a large-scale ultracentrifuge. This would need to be amended if not the case. When the percentage

recovery is below 50% from the monolith, the ultracentrifugation process is cheaper unless the volumetric throughput decreases below ~5 L. The cost increases exponentially when additional machines need to be purchased. This makes even lower yielding chromatography processes more cost effective than ultracentrifugation processes. A monolith process is shown to become less expensive than ultracentrifugation when percentage recovery increases above 50% regardless of the volumetric throughput achievable using an ultracentrifuge. It should of course be noted that the percentage recovery achievable from the ultracentrifuge will impact where the two graphs intersect.

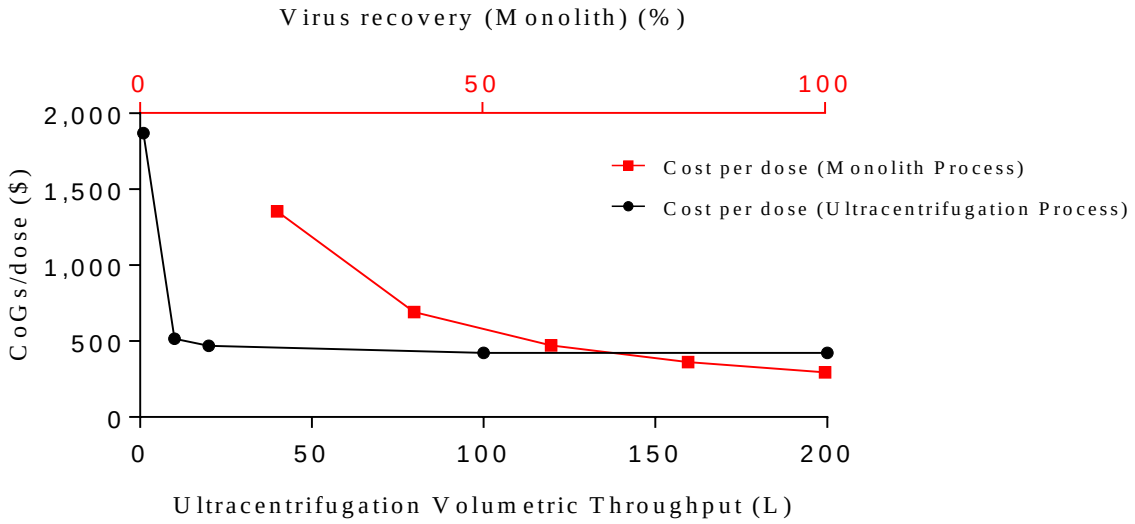

Figure 7.9 Overlay in overall CoG per dose to show how trade-offs in critical process parameters can shift the balance from chromatography to ultracentrifugation. Monolith percentage recovery is varied as trade-offs exist between virus recovery and purity. In continuous flow ultracentrifugation the trade-offs are likely to be between purity and volumetric throughput.

7.6 Conclusions

Both ultracentrifugation and chromatography can become prohibitively expensive. Depending on the critical process performance attributes, which are likely to be highly specific to the virus in question, both could be the cheaper option. As a result, it is not possible to conclude that one technology should be used preferentially over another in general terms. Ultracentrifugation is a tried and tested technique, and with the advances in continues flow systems, it has become easier in theory to scale up. Chromatography is currently the work horse in the bio pharma sector and is increasingly becoming the method of choice to purify viruses and other large macromolecules. A major issue when using chromatography, however, is the large number of experiments required in order to generate optimal separation performance. This is also true when purifying proteins, except that there are significant analytical challenges associated with quantifying viral particles. This makes process development extremely time consuming and expensive with robust processes difficult to generate. Ultracentrifugation does not have this issue as there are fewer independent variables that affect the separation and that can be used to optimise the process.

In many ways, a decision as to what technology to use will depend on the equipment already available, especially if manufacturing in house is preferred, as well as the time available for process development prior to cGMP material needing to be available.

In an ideal world, optimised processes for chromatography and ultracentrifugation would be developed in parallel and then compared before a decision is taken, however in practice this is unlikely to happen due to bottlenecks in both time and resources. Decisions will therefore need to be made with incomplete data based on the specific project requirements at the time and estimated for the life of the facility in question.

Chapter 8

Challenges associated with the development and manufacture of infectious vaccinia virus

8.1 Introduction[1]

There are a number of challenges that need to be addressed if vaccinia virus is to be licenced and validated as an oncolytic viral therapy. According to ICH guideline Q11, process validation involves "the collection and evaluation of data, from the process design stage throughout production, that establish scientific evidence that a process is capable of consistently delivering a quality drug substance" (EMA 2011). For this to be possible it is important to identify the critical quality attributes (CQAs) early on in process development. The ICH guidelines acknowledge that when dealing with complex biological material this is a challenge. They state that risk management strategies should be implemented to account for the lack of knowledge and characterisation related to the safety and efficacy of each CQA during the lifecycle of the product.

Two of the specific challenges when dealing with infectious viral products are analytical sensitivity and variability (Darling, Boose, & Spaltro 1998;Sullivan et al. 2012). These characteristics make quantifying the CQAs challenging. The relative standard deviations across each unit operation are cumulative leaving the potential variation across a process to be as high as 60% based on the research presented in this thesis. The CQAs and associated analytical challenges for vaccinia virus are discussed below.

[1] This chapter is included as part of the UCL requirements for the award of Doctor of Engineering

- **Vaccinia virus concentration**

  Physical techniques such as NTA, TRPS, TEM and flow cytometry will quantify the total number of particles of a given size, shape or physical characteristic but are nonspecific and therefore are unable to give accurate concentration data unless the sample is pure.

  Specific assays include ELISAs, qPCR-based techniques, and Western Blots. Some ELISAs claim to be able to identify whole viral particles from associated viral proteins, but this is difficult to validate. qPCR-based techniques require extensive sample pre-treatment to remove non-encapsulated viral DNA which reduces the accuracy and precision of the measurement. Both ELISAs and qPCR require reliable reference standards, which are often difficult to source, and suffer from high variability and relatively low sensitivity. ELISA reference standards are validated using protein sequence data and TEM.

- **Vaccinia virus potency**

  The potency of a virus relates to its biological activity. For vaccinia virus licenced as an oncolytic therapy, the simplest measure of potency is infectivity. The reason for this is that oncolytic viruses such as vaccinia need to be replication competent. In this thesis infectivity was measured by $TCID_{50,}$ however, there are a number of other cell-based approaches as outlined in Chapter 2. All suffer from relatively low sensitivity and high variability.

  Infectivity determines the ability of a virus to infect a cell but not necessarily to genetically modify it. If a therapy is required to transduce a cell and insert a gene of interest into the nucleus then transduction assays will need to be performed.

Transduction assays tend to be more specific than infectivity assays although variability associated with both techniques prevents robust conclusions from being generated for either in isolation.

- **Product related impurities such as:**
    - **Levels of vaccinia virus aggregation**

      Presence of aggregates can be tested using physical techniques previously discussed, however, there is currently no way of measuring the origin, infectivity and quantity of viral aggregates.
    - **Levels of vaccinia virus degradation**

      Degraded viral particles can sometimes be visualised using TEM although quantification using this approach is challenging. It also requires specialist equipment which is likely to be too expensive to bring in-house. It may be possible to use a combination of ELISAs to quantify non-encapsulated viral coat proteins, but this capability would need to be developed and would be very difficult to validate in terms of accuracy.
- **Process related impurities such as**
    - **Concentration of contaminating DNA**

      Florescence-based assays such as Quant-iT PicoGreen can be used for total DNA quantification but they are non-specific. The LLOQ of PicoGreen is 250 pg/mL, which may become limiting for some applications.

      qPCR can also be used, but this will quantify specific genes known to be conserved in the genome of the host cell. This will therefore require assumptions to be made regarding the total estimated mass of DNA in a sample based on the mass of DNA

used as a standard. High variability in impure fractions is also common when using qPCR.

- **Concentration of contaminating protein**
  - Absorbance-based techniques such as a BCA assay or similar can be used to quantify the total concentration of protein in a sample. This is not specific to host cell proteins (HCPs) however. The reason why this could be a problem is that BCA assay also detects the proteins on the surface of viruses. Consequently, this assay tends to overestimate the total mass of protein in a sample especially if the concentration of HCPs is low and the concentration of virus is high. Furthermore, these assays also suffer from low sensitivity.
  - Specific HCP ELISA can be purchased for some cell lines, although these assays only quantify specific proteins species in a sample. If a specific HCP is defined as a CQA then this could work well as long as the ELSIA used is able to identify the concentration of the specific impurity in question. In the case of the process developed in this thesis for vaccinia, there are no commercial ELISA kits available for CV-1 cells, however there are for Vero cells which also support vaccinia virus production.
- **Contamination from media components such as serum, phenol red, and antifoam.**

  If contaminants such as phenol red are defined as CQAs the easiest way of ensuring safe concentrations of these substances in the final material is to not use them. Commercial kits for the analysis of residuals such as phenol red are not commercially

available hence these would need to be developed at a cost and in-house using technologies such as mass spectrometry or reverse phase HPLC.

- **Concentration of common additives such as levels of residual Benzonase, or detergents**

  The majority of process additives, Benzonase being a good example, come with an associated specific assay. Residual Benzonase can be quantified using an ELISA which is relatively sensitive. These assays can be expensive, however the advantages of adding materials such as Benzonase to ensure the removal of DNA, can often outweigh the negative implications such as cost.

- **Levels of contaminating endotoxin, mycoplasma**

  Endotoxins are quantified using ELISAs.

  Mycoplasma can be semi-quantified using luminescence-based assays. A more sensitive technique used to quantify mycoplasma is qPCR. Mycoplasma can also be grown in culture and quantified by counting associated colonies although this is time consuming and variable.

- **Removal of adventitious viruses**

  The removal of adventitious viruses is a challenge as common techniques used in the biopharma sector such as nanofiltration and low pH hold steps will remove and destroy vaccinia virus as well as any adventitious agents.

  Viral validation can still be performed on each unit operations in the process to test for viral clearance, but processes without

specific capture steps will be optimised to recover viruses and so the log removal of contaminating virus (LRV) will likely be low.

- **Concentration of leachables from process consumables such as chromatography columns and plastics.**

  Manufactures will test and validate consumables for leachables prior to release. If leachables are biological in nature, analytical assays, often in the form of ELISAs, will likely be supplied from vendors. If the leachables are small molecules than gas chromatography/mass spectrometry (GC/MS) is often used. There is a validation challenge associated with ensuring that leachables are within safe limits, however, this is not a problem specific to viral therapies and hence, well developed best practices and guidelines are available.

8.2 Process development

From the offset of process development, probably amongst the most important challenges to be addressed for process validation of infectious virus processes generally (not specific to vaccinia) is the scalability and productivity of the presently used purification unit operations, arguably the most common being density gradient ultracentrifugation. It has been suggested that chromatography using monoliths could present an attractive alternative to ultracentrifugation namely owing to their high binding capacity, high flow rate independent binding and resolution, and scalability stated by the manufacturers of commercially available monoliths.

From a validation perspective it is likely that variation in the upstream process will affect both the purity and yield of chromatographic unit operations (Wolff & Reichl 2011). Therefore it is difficult to determine robust operation parameters even when

using response service factorial designs such as DoE. Such tools are becoming more and more common when approaching the submission of QbD filings, being stipulated in the International Conference on Harmonisation of Technical Requirements for Registration of Pharmaceuticals for Human Use (ICH) guidelines as good practice for developing both process knowledge and process understanding.

One of the other major considerations when using chromatography is sanitization validation, whether fixed or packed bed. Columns are not sold as sterile units, and the vast majority of chromatography matrices cannot be autoclaved or steam sterilised. It is for this reason that the regulators recommend a 0.2 μm sterile filter to be used up and down stream of each chromatographic step for all buffers and product fractions. While this is not a new hurdle in the world of chromatography, this will become more challenging for large viruses that cannot be sterile filtered such as vaccinia. The reason for this is that vaccinia virus is larger than 0.2 μm. To mitigate risk of batch failure, appropriate control strategies will need to be covered in a risk assessment. This will likely detail an enhanced in-process testing for endotoxin after each unit operation, as well as reduced cycling of monoliths between batches in order to ensure the process remains as closed as possible. Such risk assessment will increase costs upfront but will reduce the risk of batch failures.

The reason why this has not been an issue up to now is that large viruses such as vaccinia for use in the vaccine industry have been purified using ultracentrifugation, which can be sterilised in place.

Facilities are currently being designed for processing of viral therapies that utilise single use technologies with a 100% disposable flow paths in closed processes.

The primary recovery steps associated with viral bioprocesses can be a challenge to close as cells often require lysis to release the virus. Chemical lysis does have some

operational advantages compared to high shear based unit operations such as homogenisation from the point of view of single use, closed processing. The addition of lysis buffers containing reagents such as Triton X-100 into viral harvest material can be performed relatively easily in a closed system, while other cell disruption techniques generally require stainless steel due to the high pressure drops required. Material contact with stainless steel requires cleaning validation, and is more difficult to close. Other unit operations such as sonication have also been used in the past, but have the same limitations as homogenisation in terms single use functionality and ability to close. Sonication is also difficult to scale up.

It is possible to close chromatographic unit operations, and especially with the advancement of disposable flow path based systems such as the AKTA Ready (GE Healthcare Uppsala, Sweden), as well as single use columns packed and shipped by companies such as (RepliGen, Waltham MA, USA) single use chromatography is becoming common place for clinical manufacturing.

Smaller viruses such as AAV can be sterile filtered using membranes typically used in the mAb sector such as the Express SHC (0.5/0.2 µm filter) (Merck & Co. Kenilworth, New Jersey, USA). AAV has an approximate diameter of 25 nm.

Larger viruses such as vaccinia (300 nm) cannot be sterile filtered; therefore it is likely that columns will not be cycled across multiple batches, processes will need to be closed, and release testing for endotoxin and bioburden as well as other adventitious agents will be performed on selected in process samples as well as on each final bulk product prior to vialing.

8.3 Product release

Another challenge includes viral degradation and inactivation in standard processing conditions (such as pH and salt) likely to be encountered during chromatography, filtration or ultracentrifugation operations. The effect of long term storage on biopharmaceuticals is an issue that has been discussed for many years. As well as putting samples on long term stability studies, it has become increasingly common to partake in accelerated stability studies in an attempt to identify drug candidates that are particularly prone to degradation or oxidation causing the formation of product related impurities such as aggregates and fragments leading to loss of potency. Arguably, however, this is unlikely to effectively predict infectious viral stability as harsh conditions often encountered during accelerated stability may give variable and unrepresentative results, especially owing to the high levels of variability in infectivity assays. While accelerated stability studies cannot be a substitution for long term stability studies, it is useful when comparing a single product or process intermediate at different conditions for likely effects of an environmental stimulant.

8.4 Consumables

As a column supplier, BIA Separations produces a number of chromatography columns which need to be cGMP compliant. In order for this to be achieved, an array of batch testing prior to release is required. This includes batch testing of column performance by methods such as pulse response to measure HETP as well as integrity tests using pressure drop and visual inspection as indicators of any damage. BIA Separations also validates the nominal pore diameter of each batch of monolith prior to release to ensure the specifications meet their in house quality standards. The appropriate paper work,

preferably electronic versions, is also expected to be produced on request. Batch records from the production process will make up a large part of the data.

The aim of process validation is to demonstrate that the product is what the manufacturer says it is, and, if undamaged during transport, the product behaves in the way the process predicts when it arrives at the manufacturing site.

Chapter 9

Conclusions and Future Work

9.1 Conclusions

Two capture steps have been developed and analysed using a range of orthogonal analytical methods.

In order to achieve robust clearance of the required levels of dsDNA it is likely that a second purification step will be required before direct injection of vaccinia virus into patients. It is also likely that Benzonase endonuclease will need to be added to mitigate the risk of higher than acceptable dsDNA levels being recovered in the final product resulting in batch failure. As the likely specification of dsDNA is 10 ng/dose, the requirement of a second step will ultimately depend on the dosing requirements, which will depend on the therapeutic indication being targeted.

In summary, the developed process using CIM OH does present a reasonably robust and saleable option for Vaccinia virus capture from crude cell lysate post clarification. CIM OH was shown to be able to remove all quantifiable protein loaded to LLOQ levels. Up to 99% of the total dsDNA loaded can be removed without nuclease treatment and Vaccinia virus recovery, although variable due to cell based assay precision, was as high as 90%.

Vaccinia virus holds great potential as an oncolytic and immunotherapeutic vaccine against a broad spectrum of cancers. Purification of vaccinia virus, however, remains a

challenge. This is due to its large size, complex physicochemical properties, and highly variable starting material that often contains cell debris, DNA, proteins and aggregate.

The overall aim of this EngD project was to evaluate, understand, and work to reduce the current challenges faced by process scientists and engineers when developing vaccinia virus for vaccines and oncolytic therapies.

The scalability and productivity of presently used purification unit operations were identified early on as challenges.

The stability of vaccinia virus in commonly used processing buffers was evaluated, subsequent to which, a monolith process was developed and analysed using a variety of orthogonal analytical techniques. These included $TCID_{50}$ to measure infectivity, NTA and qPCR to measure the total number of particles and total number of viral genomes in solution, TEM and SEM to analyse viral integrity and levels of aggregation, TRPS to measure zeta potential, and BCA and PicoGreen to quantify total protein and DNA.

Vaccinia virus was shown to be able to adsorb to both CIEX and AIEX monoliths. When loading CIM SO3 with crude vaccinia harvest, and after eluting in 50 mM sodium phosphate 300 mM NaCl pH 7, DNA and total protein purification factors of up to 4.3 and 4 respectively were demonstrated, as shown in Chapter 5. Large viral aggregates were also shown to be removed after analysing load and elution fractions using TEM. The trade-off when using CIM SO3 is that the recovery of infectious virus drops from 84% to 35% when the NaCl concentration in the elution is reduced from 500 mM to 300 mM pH 7. The DNA purification factor is slightly lower when eluted at 500 mM NaCl, dropping from 4.3, to between 2.8 and 3.5. A reduction in step recovery from 84% to 35% is shown in Section 7.5 to increase the CoG/dose by approximately three fold.

DNA and total protein purification factors achievable when using CIM OH monoliths were higher than those achieved using CIM SO3. A 90% recovery of infectious virus is achieved when vaccinia harvest is loading in 50 mM sodium phosphate 1 M ammonium sulfate 2 M NaCl pH 8. All quantifiable protein is removed, and a DNA purification factor of up to 88 is achievable. Levels of polydispersity are reduced, when analysed using NTA, and large aggregates, imaged using SEM, are removed. The trade-off when using CIM OH, is the recovery of infectious virus across the pre-filter. Ammonium sulfate appears to cause vaccinia to aggregate significantly in the load, which results in a recovery of approximately 35% across the filter. This reduces the overall recovery to 32%.

Throughout this work, multiple in-process samples were taken and kept at room temperature for the duration of each experiment. All samples collected, were then frozen together at the end of each chromatography run to insure that no systematic errors would arise as a result of sample handling. It cannot be concluded with certainty that changes in either sodium chloride concentration or pH have a significant effect on vaccinia virus stability in sodium phosphate buffer due to the RSD in $TCID_{50}$ measurements. Mean averaged values, shown in Figure 4.5, suggest that initial increases in salt concentration reduced infectivity. The data also suggests that over time, at room temperature, vaccinia virus appears to lose infectivity in DMEM, although once again, robust conclusions are difficult to make with confidence due to the low precision of the $TCID_{50}$ assay.

Vaccinia titre, concentration of DNA and total protein, and levels of polydispersity varied significantly from batch to batch and with increasing concentration of ammonium sulfate. This had an impact on both the HIC and CIEX monolith performance.

It is clear that the upstream, primary recovery and pre-filtration steps still need work. In particular the primary recovery step used would be very difficult to scale up. Detergents were not used in this study as there was concern that vaccinia would lose infectivity post lysis therefore reducing viral yield. In the interest of time, a freeze thaw method, which involved freezing and then thawing pelleted cells over 3 consecutive cycles, as described in Section 3.2.2, was used. Some background on options available for cell disruption is given in Chapter 2. Mechanical lysis may be an option for future work; however, due to the risk category of the virus (Cat II) it was not possible to explore this option.

Previously published work on vaccinia virus purification (Jordan et al. 2012;Wolff, Siewert, Hansen, Faber, & Reichl 2010a;Wolff, Siewert, Lehmann, Hansen, Djurup, Faber, & REICHL 2010b), suggests that CIM monoliths may perform slightly better than membrane adsorbers, however, as previous studies were performed on a different strain of vaccinia produced in a different cell line and measured predominantly with an ELISA rather than $TCID_{50,}$ this conclusion should be taken with caution.

In comparison to ultracentrifugation, it is difficult to know how monoliths compare in terms of impurity removal. Previous literature shows that large scale continuous ultracentrifuges can recovery around 60% of infectious vaccinia virus from a crude harvest. The industry is moving away from ultracentrifugation, although there remain some advantages to the technology. Ultracentrifugation is a well-established technique which makes process development relatively straightforward in comparison to adsorption-based methods such as IEX or HIC. Using gradient media such as caesium chloride, Iodixanol or sucrose, efficient separation of a number of viral vectors has been documented (Dormond et al. 2010;Gias, Nielsen, Morgan, & Toms 2008;Otto-Wilhelm

Merten 2014). There are also significant disadvantages to using ultracentrifugation technologies. Initial capital is high, and if volumetric throughput is low, or banding time is high, then manufacturing costs, as shown in Section 7.4.2, increase exponentially.

CIM monoliths appear to offer some unique selectivity when purifying vaccinia virus. Both CIM OH and CIM SO3 show potential as being valuable stationary phases in the purification of oncolytic vaccinia viral constructs, and should be evaluated when developing clinical and commercial processes. Variations in analytical measurements make overall conclusions on process performance challenging, however, the use of multiple orthogonal analytics allows for a qualitative and semi-quantitative picture of a complex system to be built. This is critically important early on in process development in order to build up levels of process knowledge and understanding.

In conclusion, the monolith-based purification process proposed in this thesis has the enormous potential to produce oncolytic viral products in a more economically viable, scalable and robust manner than previously possible. This will impact both academia and industry by adding to the toolbox of unit operations that are able to purify vaccinia virus. For academic groups it will lead to the production of more commercially representative virus material for pre-clinical and proof of concepts studies. It will also add value by enhancing our understanding of vaccinia stability, aggregation profiles and binding kinetics. In an industrial setting it will facilitate the progression of a new and potentially life changing class of viral products to treat cancer.

In this work, the recorded dynamic binding capacity of infectious vaccinia virus was 1-3x10^9 particles/mL of monolith.

However, Based on NTA data shown in Figure 5.6 the number of particles between 250 nm and 350 nm able to adsorb to CIM SO3 from the clarified viral harvest material post 0.8 µm filtration was 1.1x10^{11}/mL. The total number of particles between 0.5 and 1000 nm able to adsorb to the monolith was 2.3x10^{11} particles/mL.

It is unlikely that the theoretical capacity of 1.15x10^{13} is achievable.

A binding capacity of ~1x10^{11} capsids per mL may be a better estimate of maximum achievable adsorption capacity; however both numbers should be used with caution.

It is known from this study that vaccinia virus aggregates and forms large complexes especially in the presence of salt (Figure 4.12). The assumption, therefore, that particles are able to adsorb in ordered monolayers is likely to be incorrect.

Monoliths have an open channel structure, however, as the channels are cross linking it is possible that some of the monolith surface is unavailable for vaccinia adsorption, in other words not in contact with the convective flow of the mobile phase. Mass transfer into these regions would be limited by diffusion, which, due to the relatively large size of vaccinia, would be very slow. It is also likely that charge repulsion and steric effects would reduce the binding capacity of vaccinia particles onto the monolith surface.

The pressure drop measured across the load step was measure to 0.02 MPa on average.

Based on work by (Andrejcic and Podgornik 2017), and assuming a porosity of 60% for 1 mL 6 µm channel monoliths (Mao, Cernigoj, Zalokar, Strancar, & Kulozik 2017), the deposited layer was calculated to be approximately 80 nm.

Based on the NTA data the majority of the adsorbed particles are not made up of infectious virus, therefore a deposited layer of 80 nm seems reasonable based on the average size of particles in the load.

9.2 Future work

9.2.1 Pre-filtration Yield Optimisation

Pre-filtration performance is one of the key areas of further work that is required to tech transfer a cost effective vaccinia process into the clinic. In order to solve this problem, there are a number of additional experiments that could be performed.

As shown in Figure 3.3, virus is diluted 1:5 in process buffer and then filtered through a 0.8µm cellulose acetate syringe filter prior to loading onto CIM monoliths. The recovery of infectious virus across the filter without the presence of ammonium sulfate in the diluent is approximately 60%. Switching the order of the dilution and filtration steps around, as shown in Figure 9.1A, may solve the problem as ammonium sulfate would be added to the feed stream after filtration. Whether this will work or not will depend on the nature of the fouling material, and the impact of its removal on CIM OH performance. It is possible that this approach could lead to high back pressures across the monolith due to the presence of large viral aggregates in the feed steam; however, as aggregates are still present in the harvest post filtration prior to column loading, fouling as a result of viral aggregation seems unlikely.

A

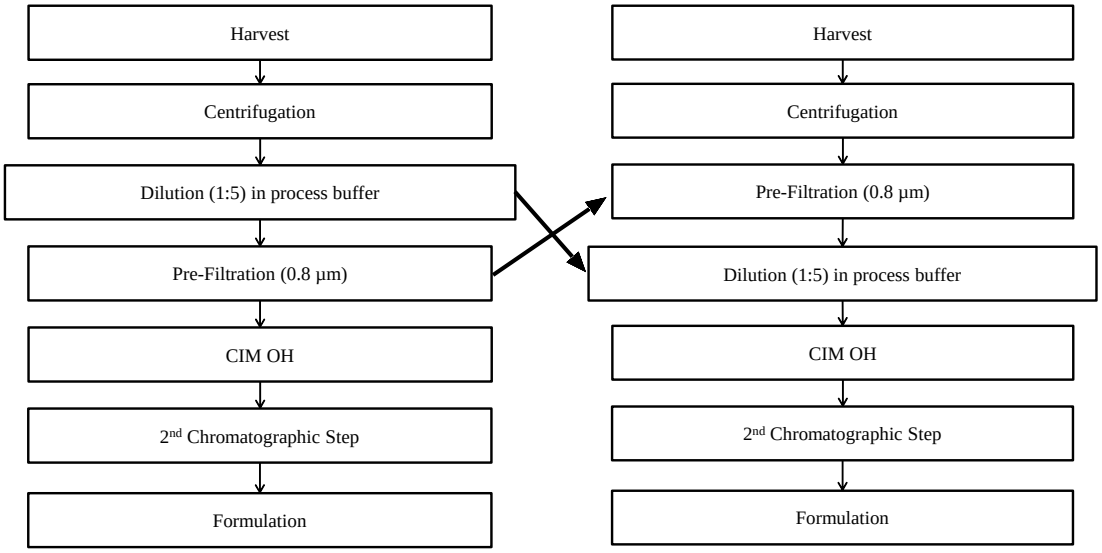

B

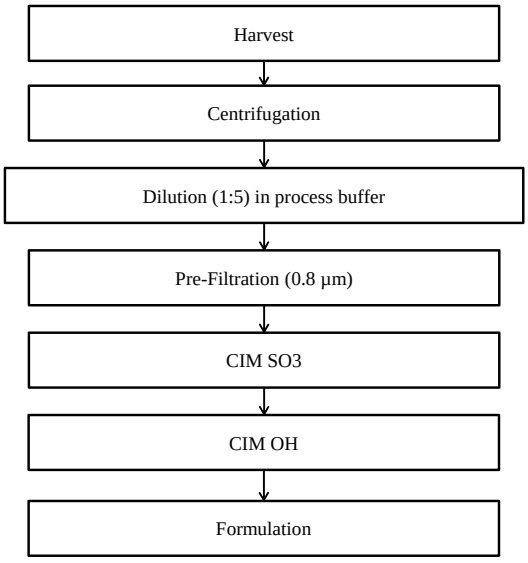

Figure 9.1 A) Proposed future study involving switching the order of the dilution and pre-filtration steps B) Proposed order of monolith steps assuming CIM OH pre-filtration continues to generate a low yield of infectious virus.

If back pressures are too high, or column performance is significantly reduced, an alternative approach would be to trial a number of different pre-filters. Due to the size of vaccinia virus (approximately 300 nm) a limited number of filters are available as many have a nominal pore size below 0.3 µm. A non-exhaustive list of commercially available filters is shown in Table 9.1.

Maximum throughput studies on normal flow membrane and depth filters would need to be performed in triplicate. A typical pressure cut-off used is 20 psig. The filtrate would need to be fractionated at regular intervals to analyse virus and impurity breakthrough. Samples may also be measured for turbidity as this can signal breakthrough of contaminants leading to fouling. P_{max} studies can be used to predict the maximum volume throughput achievable from large scale filters (van Reis and Zydney 2007) by using models that assume either pore restriction or resistance build up from cake layer formation. These can be useful when harvest volumes are limited, and time resources are stretched, however, infectious virus recovery would be the main aim of these initial studies.

Flux vs TMP studies can be performed on TFF membranes, to ensure TMP set points operate within pressure dependant regions. The cross-flow can also be optimised to ensure that sheer stress doesn't cause viral capsid degradation resulting in membrane fouling.

Table 9.1 Commercially available pre-column filters potentially applicable for vaccinia virus prior to CIM

Types of filter	Filter Name	Chemistry	Attributes	Manufacturer
Depth filters				
	Polygard CR	Polypropylene	0.1 - 100 µm pore size Designed for low fouling applications	EMD Millipore
	Millistak+Pod	Cellulose fibres and Diatomaceous Earth	Slight positive charged Designed for primary recovery and aggregate removal	EMD Millipore
Membrane filters (normal flow)				
	PolySep II	Polypropylene	Multi-layer membrane First layer 1-2 µm Second layer 0.1-1.2 µm Designed for fouling lipid feed streams	EMD Millipore
	Polygard CN	Polypropylene	0.3 - 30 µm pore size Slightly hydrophobic	EMD Millipore
Membrane filter (cross flow)				
	KrosFlow hollow fibre range	Modified Polyethersulfone (mPES), Polysulfone (PS), Mixed Ester (ME)	1KD to 0.65um UF/DF/MF	Spectrum Labs

If none of these strategies work, then CIM OH may need to be used as a second step. The recovery of infectious virus from CIM SO3 is 60 – 70% when eluted in 500 mM NaCl. Ammonium sulfate would need to be added to the CIM SO3 elution prior to loading onto CIM OH, however, as the majority of the impurities would have been removed by CIEX there may be no need for a pre-filtration step. This modified process flow is shown in Figure 9.1B. In all experiments described, CIM OH pressure drop, column lifetime and process performance will need to be monitored.

9.2.2 Development of an additional purification step to remove dsDNA

It would also be interesting to trial alternative chromatography columns such as SC-MA, discussed in the literature (Wolff, Siewert, Hansen, Faber, & Reichl 2010a). CIM monoliths are able to remove the majority of the DNA, however, depending on the dose and the variability in DNA concentration in the harvest, an additional step may be required. Depending on the percentage recovery achievable when SC-MA is challenged with infectious vaccinia virus Lister strain; this may be a good option as a capture step. CIM OH could then be trialled as a polishing step to remove DNA and protein, but without the need for a pre-filtration step. When developed using MVA, SC-MA has a DBC of approximately 6.42×10^9 pfu/capsule. If this is the same as for Lister strain, SC-MA may provide better productivity than a monolith capture step as long as the percentage recovery was comparable.

The challenge to developing a second step will be material availability. Vaccinia will need to be produced, purified and then analysed before being available for polishing

step optimisation studies. Analytical throughput will also be a bottleneck as the number of samples requiring analysis will double.

9.2.3 Qualification of assays to measure residual impurities

PicoGreen is routinely cited in the literature as a rapid, precise and accurate measure of total dsDNA. However, some concerns have been recently raised as there is a possibility that the PicoGreen reagent is able to pass through the viral envelope and protein capsid and access the viral DNA. If this occurs then the assay may give misleading results as it would overestimate the concentration of dsDNA in a sample. The magnitude of this error would be dependent on viral concentration.

Due to resource limitations the assay was not fully qualified prior to use. A number of attributes would therefore need to be assessed before PicoGreen could be used to measure dsDNA contamination in either in-process samples or final drug substance during a GMP manufacturing campaign.

ICH guidelines suggest the following are assessed.

- Precision
- Accuracy
- Sensitivity
- Specificity
- Range
- Linearity
- Robustness

PicoGreen reagent transport through the viral envelope would affect both specificity and accuracy of the assay.

In order to assess specificity and accuracy, DNA spiking studies would need to be performed. This would require the use of a fully characterised primary reference standard. This standard would need to have a known concentration of intact viral particles as well as an accurate concentration of dsDNA contamination, ideally estimated using an orthogonal assay to PicoGreen such as qPCR.

Accuracy and specificity could then be determined by spiking lambda DNA into the reference standard and measuring spike recovery using PicoGreen. This would assess the ability of the assay to quantify the spike, as well as determine whether the virus was interfering with the known concentration of dsDNA in the sample.

9.2.4 Further development of assays to quantify vaccinia virus

Analytical equipment known to be able to resolve vaccinia virus is limited.

The following list of analytical solutions were each evaluated during the project, showed some promise but could not be extensively tested or included in the battery of assays due to capital budget restrictions. Each has been covered in detail in Section 2.5.

- AIEX-HPLC, analytical monoliths (BIA Separations)
- HIC-HPLC, analytical monoliths (BIA Separations)
- TRPS, Tunable Resistive Pulse Sensing, measurements are based on individual particle impedance as virus is passed through a stretchable nanopore (IZON)
- VirusCounter 3100 based on multi-channel flow cytometry detecting presence of protein and DNA (ViroCyt, Sartorius)

Future work should include a thorough evaluation of these analytical techniques.

Chapter 10

Appendix A

10.1 Residual Assay standard curves

As detailed in the materials and methods section of this thesis BCA and Quant-iT PicoGreen assays were used to analyse total protein and dsDNA in vaccinia in process samples.

The following graphs are copies of typical standard curves generated for each assay

BCA standard curves were generated using Bovine Serum Albumin (BSA)

Quant-iT PicoGreen standard curves were generated using λ DNA (isolated from is *E. coli* bacteriophage)

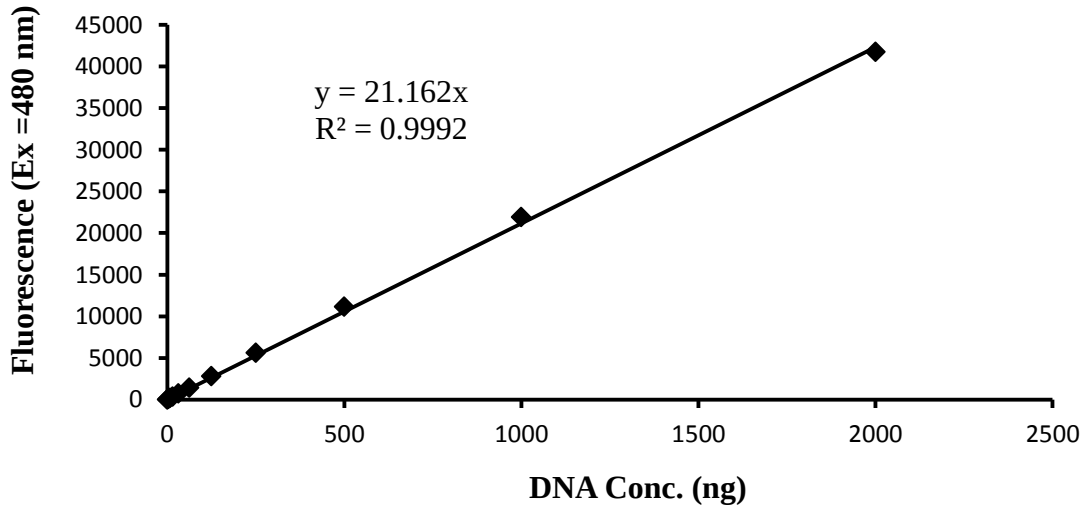

Figure 10.1 Typical λ DNA standard curve.

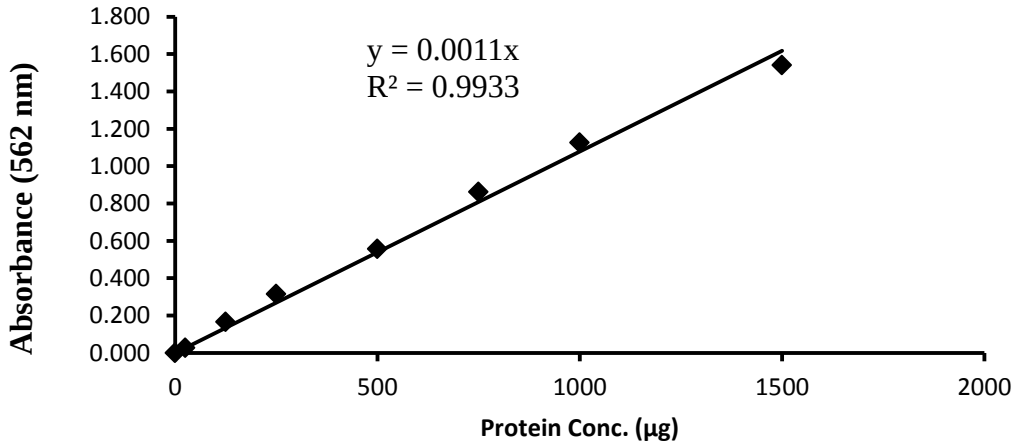

Figure 10.2 Typical BSA standard curve.

10.2 CoGs Model Parameters

WFI System

Effective Utilisation	60%
Percent Still Blowdown	10%
Storage Tank Fill Time Sizing (hr)	10
Bought-in WFI	Yes

PW System

Effective Utilisation	60%
Storage Tank Fill Time Sizing (hr)	10

Cost of Works Breakdown

Installation	38%
Minor items	0%
Pipework	20%
HVAC	34%
Control	15%
Electrical Power	25%
Plant Utilities	3%
Building	65%
Fit out	14%

Exchange Rates

	EU€	GB£	US$	CHF
EU€	1.00	0.86	1.32	1.52
GB£	1.16	1.00	1.50	1.76
US$	0.76	0.67	1.00	1.08
CHF	0.66	0.57	0.93	1.00

Other Capital Breakdown

Validation	15%
Design Fee	16%
Construction Management	4%

Internal Capitalisation Costs

Validation engineering support	0%
Engineering indirects	0%
Other support	0%
User definable add-on	0%

Cleaning & Solution Prep

Flow rate (L/min/m)	50
L:D ratio for vessels	2

CIP Cycle Timings

PW rinse (min)	5
WFI rinse (min)	5
Caustic rinse (min)	5
Acid rinse(min)	5

Cleaning

CIP time (full)	1
CIP time (rinse)	0.2
CIP/SIP Personnel (#)	2

CIP Cycles per Day

Upstream	3
Media prep and hold	5
Downstream	5
Buffer prep and hold	10

Aqueous Waste	Per m^3	Adj Cost
Non-Contaminated	US$	0.20
Contaminated	US$	0.86

Water Treatment Costs	Per L	Adj Cost
PW Treatment	US$	0.05
Bought WFI Cost	US$	1.00

Contaminated Plastics Disposal	Per T	Adj Cost
Incineration	US$	800.00
Landfill	US$	150.00

10.3 Publications by the Author

Vincent, D., Kramberger, P., Hudej, R., Štrancar, A., Wang, Y., Zhou, Y., & Velayudhan, A. 2017. The development of a monolith-based purification process for Orthopoxvirus vaccinia virus Lister strain. *Journal of Chromatography A*, 1524, (Supplement C) 87-100 available from: http://www.sciencedirect.com/science/article/pii/S0021967317313067

References

Aboud, M., Wolfson, M., Hassan, Y., & Huleihel, M. 1982. Rapid purification of extracellular and intracellular Moloney murine leukemia virus. *Archives of Virology*, 71, (3) 185-195 available from: http://dx.doi.org/10.1007/BF01314870

Ales Strancar. Basics about CIM technology and key applications. 2011.
Ref Type: Slide

Alfa Wassermann. KII & PKII Continuous Flow Ultracentrifuges. KII-PKII System Brochure . 2013. Alfa Wassermann Inc. 2013.
Ref Type: Electronic Citation

Andreadis, S.T., Roth, C.M., Le Doux, J.M., Morgan, J.R., & Yarmush, M.L. 1999. Large-Scale Processing of Recombinant Retroviruses for Gene Therapy. *Biotechnology Progress*, 15, (1) 1-11 available from: http://dx.doi.org/10.1021/bp980106m

Andrejcic, M. & Podgornik, A. 2017. Effect of pressure drop model implemented for description of pressure drop on chromatographic monolith on estimated adsorbed layer thickness. *Chemical Engineering Science*, 161, (Supplement C) 370-381 available from: http://www.sciencedirect.com/science/article/pii/S0009250916306637

Ausubel, L.J., Hall, C., Sharma, A., Shakeley, R., Lopez, P., Quezada, V., Couture, S., Laderman, K., McMahon, R., Huang, P., Hsu, D., & Couture, L. 2012. Production of CGMP-Grade Lentiviral Vectors. *BioProcess international*, 10, (2) 32-43 available from: http://www.ncbi.nlm.nih.gov/pmc/articles/PMC3374843/

Bak, H., Thomas, O.R.T., & Abildskov, J. 2007. Lumped parameter model for prediction of initial breakthrough profiles for the chromatographic capture of antibodies from a complex feedstock. *Journal of Chromatography B*, 848, (1) 131-141 available from: http://www.sciencedirect.com/science/article/pii/S1570023206005848

Bandeira, V., Peixoto, C., Rodrigues, A.F., Cruz, P.E., Alves, P.M., Coroadinha, A.S., & Carrondo, M.J.T. 2012. Downstream Processing of Lentiviral Vectors: Releasing Bottlenecks. *Human Gene Therapy Methods*, 23, (4) 255-263 available from: http://dx.doi.org/10.1089/hgtb.2012.059 Accessed 30 April 2017.

Banjac, M., Roethl, E., Gelhart, F., Kramberger, P., Jarc, B.L., Jarc, M., Strancar, A., Muster, T., & Peterka, M. 2014. Purification of Vero cell derived live replication deficient influenza A and B virus by ion exchange monolith chromatography. *Vaccine*, 32, (21) 2487-2492 available from: http://www.sciencedirect.com/science/article/pii/S0264410X14003132

Baxby, D. 1999. Edward Jenner's Inquiry; a bicentenary analysis. *Vaccine*, 17, (4) 301-307 available from: http://www.sciencedirect.com/science/article/pii/S0264410X98002072

BIA separations. CIM Convective Interaction Media Liquid Chromatography Redesigned. 2010.
Ref Type: Pamphlet

Blankenstein, T., Coulie, P.G., Gilboa, E., & Jaffee, E.M. 2012. The determinants of tumour immunogenicity. *Nat Rev Cancer*, 12, (4) 307-313 available from: http://dx.doi.org/10.1038/nrc3246

Blotta, I., Prestinaci, F., Mirante, S., & Cantafora, A. 2005. Quantitative assay of total dsDNA with PicoGreen reagent and real-time fluorescent detection. *ANNALI-ISTITUTO SUPERIORE DI SANITA*, 41, (1) 119

Bourquain, D., Dabrowski, P.W., & Nitsche, A. 2013. Comparison of host cell gene expression in cowpox, monkeypox or vaccinia virus-infected cells reveals virus-specific regulation of immune response genes. *Virology Journal*, 10, 61 available from: http://www.ncbi.nlm.nih.gov/pmc/articles/PMC3599072/

Burden, C.S., Jin, J., Podgornik, A., & Bracewell, D.G. 2012. A monolith purification process for virus-like particles from yeast homogenate. *J.Chromatogr.B Analyt.Technol.Biomed.Life Sci.*, 880, (1) 82-89 available from: PM:22134039

Chen, G.Y., Chen, C.Y., Chang, M.D.-T., Matsuura, Y., & Hu, Y.C. 2009. Concanavalin a affinity chromatography for efficient baculovirus purification. *Biotechnology Progress*, 25, (6) 1669-1677 available from: http://dx.doi.org/10.1002/btpr.253

Cheng, Y.S., Lee, M.S., Lai, S.Y., Doong, S.R., & Wang, M.Y. 2001. Separation of Pure and Immunoreactive Virus-Like Particles Using Gel Filtration Chromatography Following Immobilized Metal Ion Affinity Chromatography. *Biotechnology Progress*, 17, (2) 318-325 available from: http://dx.doi.org/10.1021/bp000155a

Chiu, W.L., Lin, C.L., Yang, M.H., Tzou, D.L., & Chang, W. 2007. Vaccinia Virus 4c (A26L) Protein on Intracellular Mature Virus Binds to the Extracellular Cellular Matrix Laminin. *Journal of Virology*, 81, (5) 2149-2157 available from: http://jvi.asm.org/content/81/5/2149.abstract

Chung, S.Y., Hill, W.E., & Doty, P. 1978. Characterization of the histone core complex. *Proceedings of the National Academy of Sciences of the United States of America*, 75, (4) 1680-1684 available from: http://www.ncbi.nlm.nih.gov/pmc/articles/PMC392402/

Cosma, A., Buhler, S., Nagaraj, R., Staib, C., Hammarin, A.L., Wahren, B., Goebel, F.D., Erfle, V., & Sutter, G. 2004. Neutralization Assay Using a Modified Vaccinia Virus Ankara Vector Expressing the Green Fluorescent Protein Is a High-Throughput Method To Monitor the Humoral Immune Response against Vaccinia Virus. *Clinical and Diagnostic Laboratory Immunology*, 11, (2) 406-410 available from: http://cvi.asm.org/content/11/2/406.abstract

Cunha, T. & Aires-Barros, R. 2000, "36 Large-Scale Extraction of Proteins," *In Aqueous Two-Phase Systems: Methods and Protocols: Methods and Protocols*, R. Hatti-Kaul, ed., Totowa, NJ: Humana Press, pp. 391-409.

Dainiak, M.B., Galaev, I.Y., & Mattiasson, B. 2006. Affinity cryogel monoliths for screening for optimal separation conditions and chromatographic separation of cells. *Journal of Chromatography A*, 1123, (2) 145-150 available from: http://www.sciencedirect.com/science/article/pii/S0021967306010922

Darling, A.J., Boose, J.A., & Spaltro, J. 1998. Virus Assay Methods: Accuracy and Validation. *Biologicals*, 26, (2) 105-110 available from: http://www.sciencedirect.com/science/article/pii/S1045105698901348

Doran, P.M. 2005. *Bioprocess Engineering Principles* Academic Press Elsevier Ltd.

Dormond, E., Chahal, P., Bernier, A., Tran, R., Perrier, M., & Kamen, A. 2010. An efficient process for the purification of helper-dependent adenoviral vector and removal of helper virus by iodixanol ultracentrifugation. *Journal of Virological Methods*, 165, (1) 83-89 available from: http://www.sciencedirect.com/science/article/pii/S0166093410000091

EMA 2011, *ICH Guidline Q11 on development and manufacture of drug substances*.

EMD Millipore. Generic process of cell culture
based influenza vaccine. USD Millipore application note . 2014. Merk Millipore.
Ref Type: Electronic Citation

Ettre, L.S. & Sakodynskii, K.I. 1993a. M. S. Tswett and the discovery of chromatography I: Early work (1899-1903). *Chromatographia*, 35, (3-4) 223-231 available from: http://dx.doi.org/10.1007/BF02269707

Ettre, L.S. & Sakodynskii, K.I. 1993b. M. S. Tswett and the discovery of chromatography II: Completion of the development of chromatography (1903-1910). *Chromatographia*, 35, (5-6) 329-338 available from: http://dx.doi.org/10.1007/BF02277520

Fenner, F., Henderson, D. A., Arita, I., Jezek, Z., & Ladnyi, I. D. 1988, *Smallpox and Its Eradication*, Geneva: World Health Organisation.

Ferguson, M.S., Lemoine, N.R., & Wang, Y. 2012. Systemic delivery of oncolytic viruses: hopes and hurdles. *Adv.Virol.*, 2012, 805629 available from: PM:22400027

Flint, S. J., Enquist, L. W., Racaniello, V. R., & Skalka, A. M. 2004, "Virus Cultivation, Detection, and Genetics," *In Principles of Virology Molecular Biology, Pathogenesis, and Control of Animal Viruses*, 2 ed. ASM Press, ed., ASM Press, American Society for Microbiology, 1752 N St. NW, Washington, DC 20036-2904, pp. 27-62.

Floyd, R. & Sharp, D.G. 1979. Viral aggregation: buffer effects in the aggregation of poliovirus and reovirus at low and high pH. *Applied and Environmental Microbiology*, 38, (3) 395-401 available from: http://www.ncbi.nlm.nih.gov/pmc/articles/PMC243506/

Gagnon, P. The Emerging Generation of Chromatography Tools for Virus Purification. BioProcess International 6[S6], 24-30. 2008.

Galasso, G.J. & Sharp, D.G. 1965. Effect of Particle Aggregation on the Survival of Irradiated Vaccinia Virus. *Journal of Bacteriology*, 90, (4) 1138-1142 available from: http://www.ncbi.nlm.nih.gov/pmc/articles/PMC315784/

Garber, K. 2006. China approves world's first oncolytic virus therapy for cancer treatment. *J.Natl.Cancer Inst.*, 98, (5) 298-300 available from: PM:16507823

Gerster, P., Kopecky, E.M., Hammerschmidt, N., Klausberger, M., Krammer, F., Grabherr, R., Mersich, C., Urbas, L., Kramberger, P., Paril, T., Schreiner, M., Nobauer, K., Razzazi-Fazeli, E., & Jungbauer, A. 2013a. Purification of infective baculoviruses by monoliths. *Journal of Chromatography A*, 1290, 36-45 available from: http://www.sciencedirect.com/science/article/pii/S0021967313005128

Giard, D.J., Thilly, W.G., Wang, D.I., & Levine, D.W. 1977. Virus production with a newly developed microcarrier system. *Applied and Environmental Microbiology*, 34, (6) 668-672 available from: http://aem.asm.org/content/34/6/668.abstract

Gias, E., Nielsen, S.U., Morgan, L.A.F., & Toms, G.L. 2008. Purification of human respiratory syncytial virus by ultracentrifugation in iodixanol density gradient. *Journal of Virological Methods*, 147, (2-2) 328-332 available from: http://www.ncbi.nlm.nih.gov/pmc/articles/PMC2486346/

Greenberg, R.N. & Kennedy, J.S. 2008. ACAM2000: a newly licensed cell culture-based live vaccinia smallpox vaccine. *Expert Opinion on Investigational Drugs*, 17, (4) 555-564 available from: http://dx.doi.org/10.1517/13543784.17.4.555

Gritti, F., Piatkowski, W., & Guiochon, G. 2003. Study of the mass transfer kinetics in a monolithic column. *Journal of Chromatography A*, 983, (1-2) 51-71 available from: http://www.sciencedirect.com/science/article/pii/S0021967302016485

Hahn, R., Panzer, M., Hansen, E., Mollerup, J., & Jungbauer, A. 2002. Mass transfer properties of monoliths. *Separation Science and Technology*, 37, (7) 1545-1565 available from: http://www.tandfonline.com/doi/abs/10.1081/SS-120002736 Accessed 12 February 2013.

Hammar, L.E.N.A. & GILLJAM, G.U.S.T. 1990. Extraction of HIV-1 in Aqueous Two-Phase Systems To Obtain a High Yield of gp120. *AIDS Research and Human Retroviruses*, 6, (12) 1379-1388 available from: http://dx.doi.org/10.1089/aid.1990.6.1379 Accessed 19 July 2016.

Heo, J., Reid, T., Ruo, L., Breitbach, C.J., Rose, S., Bloomston, M., Cho, M., Lim, H.Y., Chung, H.C., Kim, C.W., Burke, J., Lencioni, R., Hickman, T., Moon, A., Lee, Y.S., Kim, M.K., Daneshmand, M., Dubois, K., Longpre, L., Ngo, M., Rooney, C., Bell, J.C., Rhee, B.G., Patt, R., Hwang, T.H., & Kirn, D.H. 2013. Randomized dose-finding clinical trial of oncolytic immunotherapeutic vaccinia JX-594 in liver cancer. *Nat Med*, 19, (3) 329-336 available from: http://dx.doi.org/10.1038/nm.3089

Hilfenhaus, J., Kohler, R., Barth, R., Majer, M., & Mauler, R. 1976a. Large-scale purification of animal viruses in the RK-model zonal ultracentrifuge. *Journal of Biological Standardization*, 4, (4) 263-271 available from: http://www.sciencedirect.com/science/article/pii/S009211577680011X

Hilfenhaus, J., Kohler, R., & Gruschkau, H. 1976b. Large-scale purification of animal viruses in the RK-model zonal ultracentrifuge: III. Semliki Forest virus and vaccinia virus. *Journal of Biological Standardization*, 4, (4) 285-293 available from: http://www.sciencedirect.com/science/article/pii/S0092115776800133

Hung, C.F., Tsai, Y.C., He, L., Coukos, G., Fodor, I., Qin, L., Levitsky, H., & Wu, T.C. 2006. Vaccinia virus preferentially infects and controls human and murine ovarian tumors in mice. *Gene Ther*, 14, (1) 20-29 available from: http://dx.doi.org/10.1038/sj.gt.3302840

J.Michael Lane. Smallpox Vaccine. 2003.
Ref Type: Slide

Johnson, L., Gupta, A.K., Ghafoor, A., Akin, D., & Bashir, R. 2006. Characterization of vaccinia virus particles using microscale silicon cantilever resonators and atomic force microscopy. *Sensors and Actuators B: Chemical*, 115, (1) 189-197 available from: http://www.sciencedirect.com/science/article/pii/S0925400505007859

Joklik, W.K. 1962. The purification of four strains of poxvirus. *Virology*, 18, 9-18 available from: PM:14036977

Jordan, I., Bernhardt, H., & Hartmann, S. Depletion of host cell components from live vector vaccines. 31-5-2012. Google Patents.

Jordan, I., Weimer, D., Iarusso, S., Bernhardt, H., Lohr, V., & Sandig, V. 2015. Purification of modified vaccinia virus Ankara from suspension cell culture. *BMC Proceedings*, 9, (Suppl 9) O13 available from: http://www.ncbi.nlm.nih.gov/pmc/articles/PMC4685402/

Jungbauer, A. 2005. Chromatographic media for bioseparation. *Journal of Chromatography A*, 1065, (1) 3-12 available from: http://www.sciencedirect.com/science/article/pii/S0021967304015274

Jungbauer, A. & Hahn, R. 2008. Polymethacrylate monoliths for preparative and industrial separation of biomolecular assemblies. *Journal of Chromatography A*, 1184, (1-2) 62-79 available from: http://www.sciencedirect.com/science/article/pii/S0021967307022509

Kim, K.S. & Sharp, D.G. 1966. Electron Microscopic Observations on the Nature of Vaccinia Virus Particle Aggregation. *The Journal of Immunology*, 97, (2) 197-202 available from: http://www.jimmunol.org/content/97/2/197.abstract

Kirn, D.H. & Thorne, S.H. 2009. Targeted and armed oncolytic poxviruses: a novel multi-mechanistic therapeutic class for cancer. *Nat.Rev.Cancer*, 9, (1) 64-71 available from: PM:19104515

Konstantinidis, S., Welsh, J.P., Roush, D.J., & Velayudhan, A. 2016. Application of simplex-based experimental optimization to challenging bioprocess development problems: Case studies in downstream processing. *Biotechnology Progress*, 32, (2) 404-419 available from: http://dx.doi.org/10.1002/btpr.2234

Kramberger, P., Honour, R.C., Herman, R.E., Smrekar, F., & Peterka, M. 2010. Purification of the Staphylococcus aureus bacteriophages VDX-10 on methacrylate monoliths. *Journal of Virological Methods*, 166, (1-2) 60-64 available from: http://www.sciencedirect.com/science/article/pii/S0166093410000595

Kramberger, P., Peterka, M., Boben, J., Ravnikar, M., & Strancar, A. 2007. Short monolithic columns-A breakthrough in purification and fast quantification of tomato mosaic virus. *Journal of Chromatography A*, 1144, (1) 143-149 available from: http://www.sciencedirect.com/science/article/pii/S0021967306020358

Kramberger, P., Petrovic, N., Strancar, A., & Ravnikar, M. 2004. Concentration of plant viruses using monolithic chromatographic supports. *Journal of Virological Methods*, 120, (1) 51-57 available from: http://www.sciencedirect.com/science/article/pii/S0166093404001223

Kumar, A.A.P., Rao, Y.U.B., Joseph, A.L.W., Mani, K.R., & Swaminathan, K. 2002. Process standardization for optimal virus recovery and removal of substrate DNA and bovine serum proteins in Vero cell-derived rabies vaccine. *Journal of bioscience and bioengineering*, 94, (5) 375-383 available from: http://europepmc.org/abstract/MED/16233321;http://dx.doi.org/10.1016/S1389-1723(02)80212-2

Lettner, H.P., Kaltenbrunner, O., & Jungbauer, A. 1995. HETP in Process Ion-Exchange Chromatography. *Journal of Chromatographic Science*, 33, (8) 451-457 available from: http://dx.doi.org/10.1093/chromsci/33.8.451

Levy, O., Oron, C., Paran, N., Keysary, A., Israeli, O., Yitzhaki, S., & Olshevsky, U. 2010. Establishment of cell-based reporter system for diagnosis of poxvirus infection. *Journal of Virological Methods*, 167, (1) 23-30 available from: http://www.sciencedirect.com/science/article/pii/S0166093410000856

Liu, S., Ruban, L., Wang, Y., Zhou, Y., & Nesbeth, D.N.N. 2016. Establishing elements of a synthetic biology platform for Vaccinia virus production: BioBrickTM design, serum-free virus production and microcarrier-based cultivation of CV-1 cells. *bioRxiv* available from: http://biorxiv.org/content/early/2016/03/03/042275.abstract

Lock, M., Alvira, M.R., & Wilson, J.M. 2012. Analysis of Particle Content of Recombinant Adeno-Associated Virus Serotype 8 Vectors by Ion-Exchange Chromatography. *Human Gene Therapy Methods*, 23, (1) 56-64 available from: http://www.ncbi.nlm.nih.gov/pmc/articles/PMC4015067/

Luker, K.E., Hutchens, M., Schultz, T., Pekosz, A., & Luker, G.D. 2005. Bioluminescence imaging of vaccinia virus: effects of interferon on viral replication and spread. *Virology*, 341, (2) 284-300 available from: PM:16095645

Lutz, A., Dyall, J., Olivo, P.D., & Pekosz, A. 2005. Virus-inducible reporter genes as a tool for detecting and quantifying influenza A virus replication. *Journal of Virological Methods*, 126, (1-2) 13-20 available from: http://europepmc.org/abstract/MED/15847914

Mao, Y., Cernigoj, U., Zalokar, V., Strancar, A., & Kulozik, U. 2017. Production of b-Lactoglobulin hydrolysates by monolith based immobilized trypsin reactors. *ELECTROPHORESIS* n/a available from: http://dx.doi.org/10.1002/elps.201700188

Maybury, J.P., Hoare, M., & Dunnill, P. 2000. The use of laboratory centrifugation studies to predict performance of industrial machines: Studies of shear-insensitive and shear-sensitive materials. *Biotechnology and Bioengineering*, 67, (3) 265-273 available from: http://dx.doi.org/10.1002/(SICI)1097-0290(20000205)67:3<265::AID-BIT2>3.0.CO;2-J

McCart, J.A., Ward, J.M., Lee, J., Hu, Y., Alexander, H.R., Libutti, S.K., Moss, B., & Bartlett, D.L. 2001. Systemic Cancer Therapy with a Tumor-selective Vaccinia Virus Mutant Lacking Thymidine Kinase and Vaccinia Growth Factor Genes. *Cancer Research*, 61, (24) 8751-8757 available from: http://cancerres.aacrjournals.org/content/61/24/8751.abstract

McGrath, M., Witte, O., Pincus, T., & Weissman, I.L. 1978. Retrovirus purification: method that conserves envelope glycoprotein and maximizes infectivity. *Journal of Virology*, 25, (3) 923-927 available from: http://www.ncbi.nlm.nih.gov/pmc/articles/PMC525988/

Meryman, H.T. 1976. Historical recollections of freeze-drying. *Dev.Biol.Stand.*, 36, 29-32 available from: PM:801137

Michen, B. & Graule, T. 2010. Isoelectric points of viruses. *Journal of Applied Microbiology*, 109, (2) 388-397 available from: http://dx.doi.org/10.1111/j.1365-2672.2010.04663.x

Mihelic, I., Krajnc, M., Koloini, T., & Podgornik, A. 2001. Kinetic Model of a Methacrylate-Based Monolith Polymerization. *Industrial & Engineering Chemistry Research*, 40, (16) 3495-3501 available from: http://dx.doi.org/10.1021/ie010146m Accessed 20 February 2013.

Monath, T. P., Caldwell, J. R., Mundt, W., Fusco, J., Johnson, C. S., Buller, M., Liu, J., Gardner, B., Downing, G., Blum, P. S., Kemp, T., Nichols, R., & Weltzin, R. ACAM2000 clonal Vero cell culture vaccinia virus (New York City Board of Health strain) – a second-generation smallpox vaccine for biological defense. International journal of infectious diseases : IJID : official publication of the International Society for Infectious Diseases 8, 31-44. 1-10-2004.

Morenweiser, R. 2005. Downstream processing of viral vectors and vaccines. *Gene Ther*, 12, (S1) S103-S110 available from: http://dx.doi.org/10.1038/sj.gt.3302624

Negrete, A., Pai, A., & Shiloach, J. 2014. Use of hollow fiber tangential flow filtration for the recovery and concentration of HIV virus-like particles produced in insect cells. *Journal of Virological Methods*, 195, 240-246 available from: http://www.sciencedirect.com/science/article/pii/S0166093413004217

Opitz, L., Zimmermann, A., Lehmann, S., Genzel, Y., Lubben, H., Reichl, U., & Wolff, M.W. 2008. Capture of cell culture-derived influenza virus by lectins: Strain independent, but host cell dependent. *Journal of Virological Methods*, 154, (1-2) 61-68 available from: http://www.sciencedirect.com/science/article/pii/S016609340800325X

Otto-Wilhelm Merten, M.S.P.C.A.K. 2014. Manufacturing of viral vectors: part II. Downstream processing and safety aspects. *Pharmaceutical Bioprocessing*

Peixoto, C., Ferreira, T.B., Sousa, M.F.Q., Carrondo, M.J.T., & Alves, P.M. 2008. Towards purification of adenoviral vectors based on membrane technology. *Biotechnology Progress*, 24, (6) 1290-1296 available from: http://dx.doi.org/10.1002/btpr.25

Peterka, M., Kramberger, P. & Strancar., A. 2010. "Convective Interaction Media Monoliths For Separation and Purification of pDNA and Viruses.," *In Monolith chromatography and its modern applications*, Perry G Wang, ed., ILM publications.

Pol, J., Kroemer, G., & Galluzzi, L. 2016. First oncolytic virus approved for melanoma immunotherapy. *OncoImmunology*, 5, (1) e1115641 available from: http://dx.doi.org/10.1080/2162402X.2015.1115641

Pradeu, T. & Carosella, E.D. 2006. On the definition of a criterion of immunogenicity. *Proceedings of the National Academy of Sciences*, 103, (47) 17858-17861 available from: http://www.pnas.org/content/103/47/17858.abstract

Public Health England 2015, *National Cancer Intelligence Network Rare and less common cancers*.

Reed, L.J. & Muench, H. 1938. A simple method of estimating fifty per cent endpoints. *American Journal of Epidemiology*, 27, (3) 493-497 available from: http://aje.oxfordjournals.org/content/27/3/493.short

Rippe, K., Mazurkiewicz, J., Kepper, N., & Lindman, B. 2008. Interactions of histones with DNA: nucleosome assembly, stability, dynamics, and higher order structure. *DNA interactions with polymers and surfactants* 135-172

Rodriguez-Collazo, P., Leuba, S.H., & Zlatanova, J. 2009. Robust methods for purification of histones from cultured mammalian cells with the preservation of their native modifications. *Nucleic Acids Research*, 37, (11) e81 available from: http://www.ncbi.nlm.nih.gov/pmc/articles/PMC2699528/

Rouiller, Y., Solacroup, T., Deparis, V., Barbafieri, M., Gleixner, R., Broly, H., & Eon-Duval, A. 2012. Application of Quality by Design to the characterization of the cell culture process of an Fc-Fusion protein. *European Journal of Pharmaceutics and Biopharmaceutics*, 81, (2) 426-437 available from: http://www.sciencedirect.com/science/article/pii/S0939641112000744

Rupar, M., Ravnikar, M., Tusek-Znidaric, M., Kramberger, P., Glais, L., & Gutierrez-Aguirre, I. 2013. Fast purification of the filamentous Potato virus Y using monolithic chromatographic supports. *Journal of Chromatography A*, 1272, (0) 33-40 available from: http://www.sciencedirect.com/science/article/pii/S0021967312017918

Sandra Merino. Ultracentrifugation: Probably the best downstream processing tool for Large Scale Viral Vaccines. 2015.
Ref Type: Online Source

SAS JMP 12. Multivariate methods. 2017a.
Ref Type: Computer Program

SAS JMP 12. Regression Reports. 2017b.
Ref Type: Computer Program

Scappaticci, F.A., Contreras, A., Smith, R., Bonhoure, L., Lum, B., Cao, Y., Engleman, E.G., & Nolan, G.P. 2001. Statin-AE: a novel angiostatin-endostatin fusion protein with enhanced antiangiogenic and antitumor activity. *Angiogenesis.*, 4, (4) 263-268 available from: PM:12197471

Segura, M. a. M., Kamen, A. A., & Garnier, A. 2011, "Overview of Current Scalable Methods for Purification of Viral Vectors
Viral Vectors for Gene Therapy," 737 ed. O. W. Merten & M. Al-Rubeai, eds., Humana Press, pp. 89-116.

Shayakhmetov, D.M., Li, Z.Y., Ni, S., & Lieber, A. 2002. Targeting of adenovirus vectors to tumor cells does not enable efficient transduction of breast cancer metastases. *Cancer Res.*, 62, (4) 1063-1068 available from: PM:11861383

Simaria, A.S., Hassan, S., Varadaraju, H., Rowley, J., Warren, K., Vanek, P., & Farid, S.S. 2014. Allogeneic Cell Therapy Bioprocess Economics and Optimization: Single-Use Cell Expansion Technologies. *Biotechnology and Bioengineering*, 111, (1) 69-83 available from: http://www.ncbi.nlm.nih.gov/pmc/articles/PMC4065358/

Smith, G.L., Vanderplasschen, A., & Law, M. 2002. The formation and function of extracellular enveloped vaccinia virus. *J.Gen.Virol.*, 83, (Pt 12) 2915-2931 available from: PM:12466468

Smrekar, F., Ciringer, M., Strancar, A., & Podgornik, A. 2011. Characterisation of methacrylate monoliths for bacteriophage purification. *Journal of Chromatography A*, 1218, (17) 2438-2444 available from: http://www.sciencedirect.com/science/article/pii/S0021967310017942

Soema, P.C., Kompier, R., Amorij, J.P., & Kersten, G.F.A. 2015. Current and next generation influenza vaccines: Formulation and production strategies. *European Journal of Pharmaceutics and Biopharmaceutics*, 94, 251-263 available from: http://www.sciencedirect.com/science/article/pii/S0939641115002556

Stoffel, C.L., Kathy, R.F., & Rowlen, K.L. 2005. Design and characterization of a compact dual channel virus counter. *Cytometry Part A*, 65A, (2) 140-147 available from: http://dx.doi.org/10.1002/cyto.a.20145

Sullivan, K., Kloess, J., Qian, C., Bell, D., Hay, A., Lin, Y.P., & Gu, Y. 2012. High throughput virus plaque quantitation using a flatbed scanner. *J.Virol.Methods*, 179, (1) 81-89 available from: PM:22044905

Svec, F. 2008. Stellan Hjerten's contribution to the development of monolithic stationary phases. *ELECTROPHORESIS*, 29, (8) 1593-1603 available from: http://dx.doi.org/10.1002/elps.200700569

Tartaglia, J., Perkus, M.E., Taylor, J., Norton, E.K., Audonnet, J.C., Cox, W.I., Davis, S.W., van der Hoeven, J., Meignier, B., Riviere, M., & . 1992. NYVAC: a highly attenuated strain of vaccinia virus. *Virology*, 188, (1) 217-232 available from: PM:1566575

Thorne, S.H., Hwang, T.H., O'Gorman, W.E., Bartlett, D.L., Sei, S., Kanji, F., Brown, C., Werier, J., Cho, J.H., Lee, D.E., Wang, Y., Bell, J., & Kirn, D.H. 2007. Rational strain selection and engineering creates a broad-spectrum, systemically effective oncolytic poxvirus, JX-963. *J.Clin.Invest*, 117, (11) 3350-3358 available from: PM:17965776

Townsley, A.C., Senkevich, T.G., & Moss, B. 2005. Vaccinia Virus A21 Virion Membrane Protein Is Required for Cell Entry and Fusion. *Journal of Virology*, 79, (15) 9458-9469 available from: http://www.ncbi.nlm.nih.gov/pmc/articles/PMC1181583/

Tysome, J.R., Briat, A., Alusi, G., Cao, F., Gao, D., Yu, J., Wang, P., Yang, S., Dong, Z., Wang, S., Deng, L., Francis, J., Timiryasova, T., Fodor, I., Lemoine, N.R., & Wang, Y. 2009. Lister strain of vaccinia virus armed with endostatin-angiostatin fusion gene as a novel therapeutic agent for human pancreatic cancer. *Gene Ther.*, 16, (10) 1223-1233 available from: PM:19587709

Tysome, J.R., Wang, P., Alusi, G., Briat, A., Gangeswaran, R., Wang, J., Bhakta, V., Fodor, I., Lemoine, N.R., & Wang, Y. 2011. Lister vaccine strain of vaccinia virus armed with the endostatin-angiostatin fusion gene: an oncolytic virus superior to dl1520 (ONYX-015) for human head and neck cancer. *Hum.Gene Ther.*, 22, (9) 1101-1108 available from: PM:21361787

Ungerechts, G., Bossow, S., Leuchs, B., Holm, P.S., Rommelaere, J., Coffey, M., Coffin, R., Bell, J., & Nettelbeck, D.M. 2016. Moving oncolytic viruses into the clinic: clinical-grade production, purification, and characterization of diverse oncolytic viruses. *Molecular Therapy - Methods & Clinical Development*, 3, available from: http://dx.doi.org/10.1038/mtm.2016.18 Accessed 14 May 2017.

Urbas, L., Jarc, B.L., Barut, M., Zochowska, M., Chroboczek, J., Pihlar, B., & Szolajska, E. 2011. Purification of recombinant adenovirus type 3 dodecahedric virus-like particles for biomedical applications using short monolithic columns. *Journal of Chromatography A*, 1218, (17) 2451-2459 available from: http://www.sciencedirect.com/science/article/pii/S0021967311000793

Van Reis, R. & Zydney, A. 2007. Bioprocess membrane technology. *Journal of Membrane Science*, 297, (1-2) 16-50 available from: http://www.sciencedirect.com/science/article/pii/S0376738807001159

Wang, F., Richardson, D. & Shameem, M. 2015. Host-Cell Protein Measurement and Control. *BioPharm International*, 28, (6) 32-38

Wang, L., Niamke, J., Veres, G. & Knop, D. Two-Step Chromatography purification of rAAV1 Vectors Porduced by Suspension BHK cells rHSV Co-Infection. 2009.
Ref Type: Unpublished Work

Wang, Y. & Ouyang, F. 1999. Bead-to-bead transfer of Vero cells in microcarrier culture. *Cytotechnology*, 31, (3) 221-224 available from: http://www.ncbi.nlm.nih.gov/pmc/articles/PMC3449546/

WHO 2004, *Guidelines on viral inactivation and removal procedures intended to assure the viral safety of human blood plasma products*, World Heath Organization.

Wickramasinghe, S.R., Kalbfuß, B., Zimmermann, A., Thom, V., & Reichl, U. 2005. Tangential flow microfiltration and ultrafiltration for human influenza A virus concentration and purification. *Biotechnology and Bioengineering*, 92, (2) 199-208 available from: http://dx.doi.org/10.1002/bit.20599

Wittek, R. 1994, "Vaccinia Virus," *In Encyclopedia of Virology*, vol. 3 Webster and Granoff, ed., Academic Press Limited, pp. 1507-1513.

Wolff, M.W. & Reichl, U. 2011. Downstream processing of cell culture-derived virus particles. *Expert Reviews Vaccines*, 10, 1451-1475 available from: www.expert-reviews.com

Wolff, M.W. & Reichl, U. 2008. Downstream Processing: From Egg to Cell Culture-Derived Influenza Virus Particles. *Chemical Engineering & Technology*, 31, (6) 846-857 available from: http://dx.doi.org/10.1002/ceat.200800118

Wolff, M.W., Siewert, C., Hansen, S.P., Faber, R., & Reichl, U. 2010a. Purification of cell culture-derived modified vaccinia ankara virus by pseudo-affinity membrane adsorbers and hydrophobic interaction chromatography. *Biotechnology and Bioengineering*, 107, (2) 312-320 available from: http://dx.doi.org/10.1002/bit.22797

Wolff, M.W., Siewert, C., Lehmann, S., Hansen, S.P., Djurup, R., Faber, R., & REICHL, U. 2010b. Capturing of cell culture-derived modified Vaccinia Ankara virus by ion exchange and pseudo-affinity membrane adsorbers. *Biotechnology and Bioengineering*, 105, (4) 761-769 available from: http://dx.doi.org/10.1002/bit.22595

Wong, H.H., Lemoine, N.R., & Wang, Y. 2010. Oncolytic Viruses for Cancer Therapy: Overcoming the Obstacles. *Viruses.*, 2, (1) 78-106 available from: PM:20543907

World Health Organisation. Recommendations for the production and quality control of smallpox vaccine, revised 2003. [WHO Technical Report Series, No. 926, 2004]. 2004. Ref Type: Online Source

World Health Organization 1998, *WHO Expert committee on biological standardization technical report series*.

Wung, N., Acott, S.M., Tosh, D., & Ellis, M.J. 2014. Hollow fibre membrane bioreactors for tissue engineering applications. *Biotechnology Letters*, 36, (12) 2357-2366 available from: http://dx.doi.org/10.1007/s10529-014-1619-x

Yamamoto, S. & Ishihara, T. 1999. Ion-exchange chromatography of proteins near the isoelectric points. *Journal of Chromatography A*, 852, (1) 31-36 available from: http://www.sciencedirect.com/science/article/pii/S0021967399005932

Yang, H. 2013. Establishing Acceptable Limits of Residual DNA. *PDA Journal of Pharmaceutical Science and Technology*, 67, (2) 155-163 available from: http://journal.pda.org/content/67/2/155.abstract

Zou, H., Huang, X., Ye, M., & Luo, Q. 2002. Monolithic stationary phases for liquid chromatography and capillary electrochromatography. *Journal of Chromatography A*, 954, (1-2) 5-32 available from: http://www.sciencedirect.com/science/article/pii/S0021967302000729

Zwartouw, H.T., Westwood, J.C., & Appleyard, G. 1962. Purification of pox viruses by density gradient centrifugation. *J.Gen.Microbiol.*, 29, 523-529 available from: PM:14004140